



Universidade do Estado do Rio de Janeiro

Centro de Tecnologia e Ciências

Faculdade de Geologia

Thais Mothé Maia

**Petrogenetic relationship between the Abrolhos Volcanic Complex (AVC)
and the Vitória-Trindade Ridge (VTR) magmatism, Southeast Brazilian
Margin, South Atlantic Ocean**

Rio de Janeiro

2022

Thais Mothé Maia

Petrogenetic relationship between the Abrolhos Volcanic Complex (AVC) and the Vitória-Trindade Ridge (VTR) magmatism, Southeast Brazilian Margin, South Atlantic Ocean

Dissertation presented as partial requirement for obtaining the title of Master, by the *Programa de Pós-Graduação em Geociências*, of the *Universidade do Estado do Rio de Janeiro*. Area of focus: *Geologia e Geofísica de Margens tipo Atlântico*.

Advisor: Prof. Dr. Anderson Costa dos Santos (UERJ)

Co-advisor: Prof. Dr. Sérgio de Castro Valente (UFRRJ)

Prof. Dr. Eduardo Reis Viana Rocha-Júnior (UFBA)

Rio de Janeiro

2022

CATALOGAÇÃO NA FONTE
UERJ / REDE SIRIUS / BIBLIOTECA CTC/C

M217 Maia, Thais Mothé.

Relação petrogenética entre os magmatismos do Complexo Vulcânico de Abrolhos (CVA) e da Cadeia Vitória-Trindade (CVT), margem sudeste brasileira, Oceano Atlântico Sul / Thais Mothé Maia. – 2022.

137 f. : il.

Título original: Petrogenetic relationship between the Abrolhos Volcanic Complex (AVC) and the Vitória-Trindade Ridge (VTR) magmatism, Southeast Brazilian Margin, South Atlantic Ocean.

Orientador: Anderson Costa dos Santos.

Coorientadores: Sérgio de Castro Valente, Eduardo Reis Viana Rocha-Júnior

Dissertação (Mestrado) - Universidade do Estado do Rio de Janeiro, Faculdade de Geologia.

1. Vulcanismo – Abrolhos, Arquipélago dos (BA) – Eoceno – Teses. 2. Solos vulcânicos – Abrolhos, Arquipélago dos (BA) – Teses. 3. Petrografia – Caravelas (BA) – Teses. 4. Geoquímica – Isótopos – Teses. 5. Magmatismo – Abrolhos, Arquipélago dos (BA) – Teses. 6. Modelagem Geológica – Teses. I. J Santos, Anderson Costa dos. II. Valente, Sérgio de Castro. III. Rocha-Júnior, Eduardo Reis Viana IV. Universidade do Estado do Rio de Janeiro. V. Faculdade de Geologia. VI. Título.

CDU 551.21(813.8)

Bibliotecária responsável: Fernanda Lobo / CRB-7:5265

Autorizo, apenas para fins acadêmicos e científicos, a reprodução total ou parcial desta dissertação, desde que citada a fonte.

Assinatura

Data

Thais Mothé Maia

Petrogenetic relationship between the Abrolhos Volcanic Complex (AVC) and the Vitória-Trindade Ridge (VTR) magmatism, Southeast Brazilian Margin, South Atlantic Ocean

Dissertation presented as partial requirement for obtaining the title of Master, by the *Programa de Pós-Graduação em Geociências*, of the *Universidade do Estado do Rio de Janeiro*. Area of focus: *Geologia e Geofísica de Margens tipo Atlântico*.

Approved on July 8, 2022.

Advisor: Prof. Dr. Anderson Costa dos Santos

Faculdade de Geologia – UERJ

Co-advisor: Prof. Dr. Sérgio de Castro Valente

Universidade Federal Rural do Rio de Janeiro (UFRRJ)

Prof. Dr. Eduardo Reis Viana Rocha-Júnior

Universidade Federal da Bahia (UFBA)

Evaluation Committee: _____

Prof. Dr. João Mata

Universidade de Lisboa (UA)

Prof. Dr. Artur Corval

Universidade Federal Rural do Rio de Janeiro (UFRRJ)

Dr. Andres Gordon

Universidade do Estado do Rio de Janeiro (UERJ)

Rio de Janeiro

2022

ACKNOWLEDGMENTS

I thank my mentor, Prof. Dr. Anderson Costa, who has always been an example of a teacher and researcher, whose scientific and academic enthusiasm contagious me years ago and continues to inspire me. Thank you for always encouraging me. To my co-adviser Prof. Dr. Sergio Valente for all the support, sharing, and encouragement throughout the development of this project. Thank you for always being helpful and for being an incredible mentor, without whom this work would not have been accomplished. And to my second advisor Prof. Dr. Eduardo Reis, whose wisdom is inspiring. Thank you for all the debates, exchanges, and learning.

To the members of the evaluation committee, Prof. Dr. João Mata, Prof. Dr. Artur Corval, and Dr. Andres Gordon for being available to evaluate me in this work, so important for the next steps of my career. A special thanks to Prof. Dr. Leila Marques and Prof. Dr. João Mata, who assisted me since the first seminar of the master's program and who contributed so much to the development of my project.

To the technical team of the *Laboratório de Geocronologia e Isótopos Radiogênicos* (LAGIR), Carla Neto, Gilberto Vaz and João Barcellos, for the isotopic analyses carried out even during the COVID-19 pandemic, and to Professor Dr. Claudio Valeriano for the support in the isotopic data.

To the faculty of the *Programa de Pós Graduação em Geociências* (PPGG) of the *Universidade do Estado do Rio de Janeiro* (UERJ), who taught and mentored me exceptionally even during the COVID-19 pandemic. I also thank Marianni and Juçara for all their helpfulness and usual availability.

To the *Universidade do Estado do Rio de Janeiro*, it is an honor to be able to follow my academic journey in this second home and to carry its name in my formation.

And to all my geologist friends who made my journey as a graduate student a little less lonely and arduous. In special, to Gabriela Quaresma, Giovanni Oliveira, Letícia Muniz, Lucas Monteiro, Fabiano Vasconcelos, Pedro Miranda, Vanderson Ribeiro, Milena Barcelos, Guilherme Watson, and Luisa Guerra.

RESUMO

MAIA, Thais Mothé. *Relação petrogenética entre os magmatismos do Complexo Vulcânico de Abrolhos (CVA) e da Cadeia Vitória-Trindade (CVT), Margem Sudeste Brasileira, Oceano Atlântico Sul*. 2022. 137 f. Dissertação (Mestrado em Geociências) – Faculdade de Geologia, Universidade do Estado do Rio de Janeiro, Rio de Janeiro, 2022.

O Complexo Vulcânico de Abrolhos (CVA) é uma província ígnea localizada na Margem Sudeste Brasileira no limite Continente-Oceano. O CVA emerge em cinco ilhas (Santa Bárbara, Redonda, Siriba, Sueste e Guarita) que compõem o Arquipélago de Abrolhos, localizado a sudeste (cerca de 55 km) da cidade de Caravelas (BA). A Cadeia Vitória-Trindade (CVT), localizada cerca de 110 km a Sul do CVA, corresponde a uma cadeia ígnea de cerca de 1.200 km de extensão composta por edifícios vulcânicos que se estendem desde a costa brasileira até as águas profundas do Atlântico, latitude 20°S (Vitória, ES). O CVA e a CVT mostram um vulcanismo com ligeira progressão de idade consistente com o movimento da placa sul-americana em direção a Oeste, apoiando, assim, a origem a partir do hotspot de Trindade. Neste contexto, após trinta anos sem uma descrição petrológica detalhada publicada sobre o magmatismo do CVA, este estudo visa apresentar uma nova descrição de campo, petrografia, dados litogeoquímicos e composições isotópicas Sr-Nd das ilhas de Abrolhos. Também são apresentados novos dados de modelagem para alguns montes submarinos da CVT. As rochas do Arquipélago de Abrolhos compreendem uma série transicional de afinidade alcalina do Paleoceno-Eoceno com rochas relativamente evoluídas com elevado teor de TiO₂, enquanto que as rochas dos edifícios vulcânicos da CVT compreendem uma série de afinidade alcalina do Mioceno-Pleistoceno fortemente subsaturada em SiO₂ com amostras menos evoluídas. As rochas magmáticas mapeadas nas ilhas de Abrolhos são intrusões pouco profundas, em maioria *sills*, e devem ser agrupadas em unidades de diabásio. Os diagramas de elementos maiores e traço das ilhas de Abrolhos mostram uma grande dispersão de dados quando plotados em função de índices de fracionamento (MgO e Zr), sugerindo assim um envolvimento de um processo evolutivo complexo, possivelmente o RTF (*magma replenishment, tapping, and fractionation*) ligado à evolução do *plumbing system*. As composições de elementos traço dos montes submarinos da CVT (Vitória, Montague, Jaseur, Dogaressa, Davis e Colúmbia) são consistentes com uma taxa de $\leq 4\%$ de fusão parcial da fonte no campo de estabilidade da granada. Os dados isotópicos novos e compilados do CVA sugerem uma fonte mantélica astenosférica empobrecida (representada pelo DMM) metasomatizada por um componente enriquecido (EMI), e possivelmente um constituinte do tipo HIMU. Nossos cálculos de mistura sugerem uma mistura de 75% de DMM, com $<15\%$ de EMI, e possivelmente até 10% de HIMU na fonte do CVA. Para os montes e ilhas da CVT a mistura seria 90% de DMM com $<10\%$ de EMI, e para o Monte Vitória e Banco Davis as contribuições do EMI variam entre 20% e 25% no DMM. O alinhamento vulcânico entre o CVA e a CVT, em conjunto com a sobreposição dos dados litogeoquímicos e isotópicos de suas rochas, não pode ser uma característica aleatória, mas sim representar a amostragem de reservatórios semelhantes de um manto raso, sugerindo assim uma relação cogenética. Finalmente, uma possível ligação petrogenética entre os magmatismos do CVA e da CVT é discutida.

Palavras-chave: Vulcanismo de Abrolhos. Cadeia Vitória-Trindade. Vulcanismo do Eoceno-Pleistoceno. Modelagem Geoquímica. Características isotópicas de Sr-Nd.

ABSTRACT

Maia, Thais Mothé. *Petrogenetic relationship between the Abrolhos Volcanic Complex (AVC) and the Vitória-Trindade Ridge (VTR) magmatism, Southeast Brazilian Margin, South Atlantic Ocean*. 2022. 137 f. Dissertação (Mestrado em Geociências) – Faculdade de Geologia, Universidade do Estado do Rio de Janeiro, Rio de Janeiro, 2022.

The Abrolhos Volcanic Complex (AVC) is an igneous province (63,000 km²), located at the Southeast Brazilian Margin. The AVC emerges as five islands called Santa Bárbara, Redonda, Siriba, Sueste, and Guarita, which compose the Abrolhos Archipelago, located *ca.* 55 km southeast of Caravelas city (BA). The Vitória-Trindade Ridge (VTR), *ca.* 110 km south, corresponds to a *ca.* 1200 km long west-east direction ridge composed of volcanic edifices that extend from the Brazilian eastern bank to the deep-water portion of the Atlantic, latitude *ca.* 20°S, in the city of Vitória (ES). The AVC and the VTR show slight age-progressive volcanism from the older *ca.* 60 Ma Abrolhos Complex to the younger Martin Vaz and Trindade Islands, consistent with the motion of the South American plate toward the west and thus supporting a Trindade hotspot origin for these magmatism. After almost thirty years without any detailed published article for the petrology of the Abrolhos magmatism, this work presents new field work mapping, petrographic, lithochemical, and Sr-Nd isotopic data for the Abrolhos Islands. We also present a possible petrogenetic link between the AVC and VTR magmatism, and some new modeling data for some VTR seamounts. Abrolhos Archipelago rocks comprise a Paleocene-Eocene transitional basalt series of alkaline affinity with relatively evolved rocks with high TiO₂ contents, while VTR volcanic edifices rocks comprise a Miocene-Pleistocene strongly undersaturated alkaline affinity series with the less evolved samples. Mapped magmatic rocks in the Abrolhos Islands are shallow intrusions, mostly sills, and should be grouped into diabase units. Major and trace element diagrams of the Abrolhos Islands show a large data dispersion when plotted as a function of fractionation index (*e.g.*, MgO and Zr) thus suggesting a complex evolution. Differentiation by magma replenishment, tapping, and fractionation (RTF) seems to have been the predominant process, potentially linked to the subvolcanic plumbing system evolution. Trace element compositions of VTR Seamounts (Vitória, Montague, Jaseur, Dogaressa, Davis, and Colúmbia) are consistent with $\leq 4\%$ partial melting of the mantle source in the garnet stability field. New and compiled isotope AVC data suggest a peridotitic mantle source (represented by depleted MORB mantle – DMM) metasomatized by an enriched mantle I (EMI) component and a HIMU-type constituent. Our model mixing calculations suggest a mixture with 75% of DMM, <15% of EMI, and possibly up to 10% of HIMU in the AVC source. For VTR seamounts and islands the mixture would be 90% of DMM with <10% of EMI, and for Vitória Seamount and Davis Bank the EMI contributions vary from 20% to 25% in the DMM. The volcanic alignment between the VTR and AVC, along with the overlap of geochemical and isotopic data of their different igneous rocks, cannot be a random feature but instead represent the sampling of similar shallow mantle reservoirs, thus suggesting a cogenetic relationship. Finally, a possible petrogenetic link between the AVC and VTR magmatism is discussed.

Keywords: Abrolhos volcanism. Vitória-Trindade Ridge. Eocene-Pleistocene Volcanism. Geochemical Modeling. Sr-Nd isotope characteristics.

SUMMARY

	INTRODUCTION.....	7
1	OBJECTIVES.....	8
2	GEOLOGICAL BACKGROUND.....	9
2.1	Neocretaceous to Paleocene Magmatism.....	9
2.2	Paleocene-Eocene magmatism: Abrolhos Volcanic Complex (AVC).....	11
2.3	Eocene-Pleistocene Magmatism: Vitória-Trindade Ridge (VTR).....	17
2.4	Relation of Brazilian Southeast Margin magmatism to global tectonic events.....	23
3	MATERIAL AND METHODS.....	26
3.1	Literature review and data compilation.....	26
3.2	Petrographic study.....	26
4	RESULTS.....	27
5	CONCLUDING REMARKS.....	28
	REFERENCES.....	30
	APPENDIX A – First petrologic data for Vitória Seamount, Vitória-Trindade Ridge, South Atlantic: a contribution to the Trindade Mantle Plume Evolution (published paper on August/2021 in Journal of South American Earth Sciences - DOI: https://doi.org/10.1016/j.jsames.2021.103304).....	39
	APPENDIX B – Abrolhos Volcanic Complex petrogenesis and its link with the Vitória-Trindade Ridge, Southeast Brazilian Margin, South Atlantic Ocean.....	78
	APPENDIX C – Abrolhos Volcanic Complex petrography compilation.....	137

INTRODUCTION

This master's degree work presents the petrogenetic study about two Cenozoic magmatic processes located in the Brazilian Southeast Margin: the Abrolhos Volcanic Complex (AVC) and the Vitória-Trindade Ridge (VTR). After almost thirty years without any detailed published article for the petrology of the Abrolhos magmatism, this work presents new field work mapping, petrographic, lithogeochemical, and Sr-Nd isotopic data for the Abrolhos Islands (Santa Bárbara, Siriba, Sueste and Redonda). A petrogenetic relationship between the VTR and AVC magmatic processes is also debated with detailed interpretation of petrography, geochemistry and isotopic data. Particularly about the VTR, new data from the seamounts (Vitória Smt., Montague Smt., Jaseur Smt., Davis Bank, and Dogaressa Bank) are reported.

This dissertation will be structured according to the "dissertation-article" model, with the articles attached in the appendices as the results of the dissertation. The appendix A display the first article (First petrologic data for Vitória Seamount, Vitória-Trindade Ridge, South Atlantic: a contribution to the Trindade Mantle Plume Evolution), which is already published at the Journal of South American Earth Sciences (<https://doi.org/10.1016/j.jsames.2021.103304>). The appendix B display the second article (Abrolhos Volcanic Complex petrogenesis and its link with the Vitória-Trindade Ridge, Southeast Brazilian Margin, South Atlantic Ocean) which was submitted to the special volume "Atlantic Evolution" at Journal of South American Earth Science.

1 OBJECTIVE

On the basis of new field work mapping, petrographic and whole-rock chemistry data, and Sr-Nd isotope signatures, the present dissertation aims to identify different source components present in the petrogenesis of Abrolhos and VTR magmatism, as well as the differentiation processes involved in the AVC evolution. This study also aims to recognize a possible petrogenetic link between the AVC and VTR magmatism.

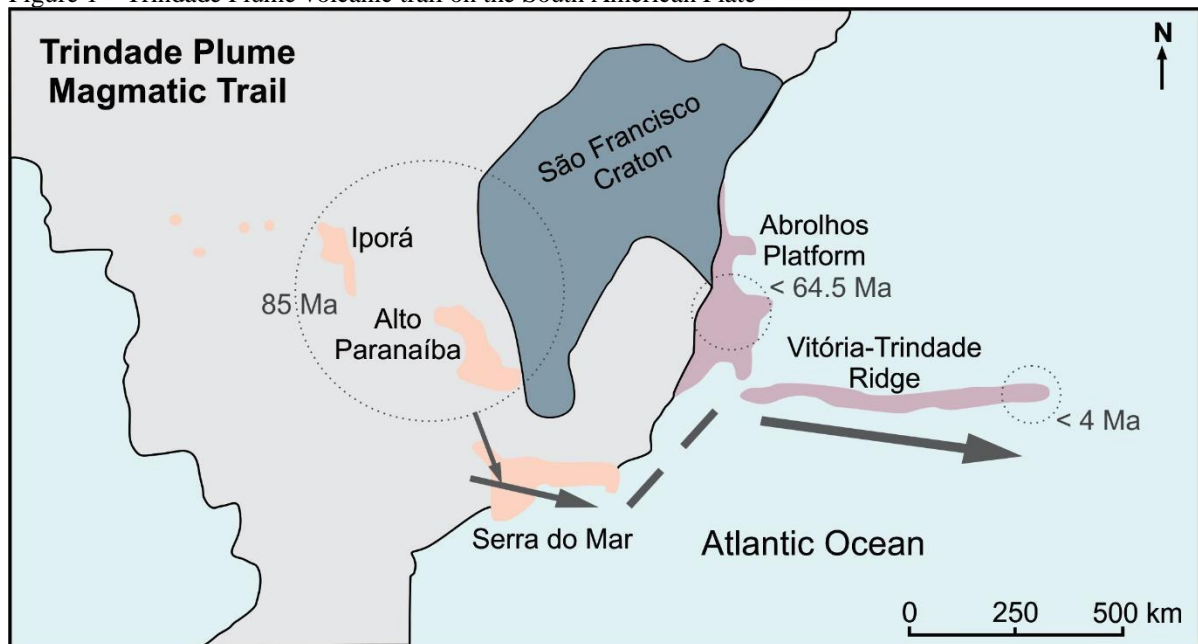
2 GEOLOGICAL BACKGROUND

The evolution of the Brazilian East Margin and its marginal basins is part of the Mesozoic-Cenozoic tectonic reactivation phase, known as Wealdenian reactivation (ALMEIDA, 1967). This phase is marked by the break-up of the supercontinent Gondwana and the split between the South American and African plates, which took place from the Neojurassic to the Eocretaceous and culminated in the opening of the South Atlantic Ocean. This event comprises reactivations of previous tectonic structures and several basic and alkaline magmatic events recorded in the South American shelf, both on the continent and in the newly formed South Atlantic Ocean. These magmatic activities range from the Neocretaceous, in the central-southeastern portion of Brazil, to the Pleistocene, in deep waters of the Atlantic Ocean.

2.1 Neocretaceous to Paleocene Magmatism

Once the rifting process shaped the Brazilian East Margin, the South American Plate passed over a thermal anomaly known as the Trindade Plume. The plume activity caused an epeirogenetic uplift of the continental crust and an alkaline and basaltic magmatism in the Brazilian central-western and southeastern regions between 89 and 65 Ma (ZALÁN; OLIVEIRA, 2001; 2005). The igneous provinces of Iporá and Alto Paranaíba would be the first surface expression of the plume, which magmatism had its peak at *ca.* 85 Ma (GIBSON et al., 1995, 1997). Afterward, the upwelling mantle of the Trindade Plume would have deflected from the thick lithosphere beneath the São Francisco craton, changing its path southward until it reached a thinner lithosphere that allowed its decompression (HILL, 1991; THOMPSON; GIBSON, 1991; SLEEP, 1996, 1997; THOMPSON et al., 1998). Thus, the extension of plume activity would have been the magmatism of the Serra do Mar province, dated between 84 and 49 Ma (Ar-Ar, K-Ar e Rb-Sr methods; RIBEIRO FILHO; CORDANI, 1966; AMARAL et al., 1967; CORDANI, 1970; SADOWSKI; DIAS NETO, 1981; SONOKI; GARDA, 1988; THOMAZ-FILHO; RODRIGUES, 1999; RICCOMINI et al., 2004), and located *ca.* 500 km south of the São Francisco craton (Figure 1; THOMPSON et al., 1998).

Figure 1 – Trindade Plume volcanic trail on the South American Plate



Subtitle – The Iporá and the Alto Paranaíba magmatism (highlighted by the circle) are considered to be the first expression of the Trindade Plume on the South American Plate at *ca.* 85 Ma (GIBSON et al., 1995, 1997). The arrows are the calculated and inferred track of the passage of the South American Platform over the Trindade Plume. The path is deflected to the southeast due to the presence of a thick lithosphere beneath the São Francisco craton, giving rise to the Serra do Mar Province magmatism. The Abrolhos magmatism would be the first expression of the plume on the continental margin and is linked to the Vitória-Trindade Ridge (VTR), which also belongs to the plume track.

Source: Modified from Thompson et al. (1998)

Then, during the Cenozoic, alkaline and basaltic magmatism occurred in the Brazilian passive continental margin, *e.g.*, the Abrolhos Volcanic Complex (AVC) and the Vitória-Trindade Ridge (VTR) magmatism. They have also been interpreted as part of the Trindade Plume volcanic trail on the South American Plate (O'CONNOR; DUNCAN, 1990; CONCEIÇÃO et al., 1996; THOMPSON et al., 1998; FERRARI; RICCOMINI, 1999; GIBSON et al., 1999; FODOR; HANAN, 2000; SIEBEL et al., 2000, SOBREIRA et al., 2004; ALVES et al., 2006; MOHRIAK, 2006; SKOLOTNEV et al., 2011; SANTOS, 2013; BONGIOLO et al., 2015; PIRES et al., 2016; SANTOS, 2016; SANTOS et al., 2018a, 2018b, 2022a, 2022b; OLIVEIRA et al., 2021; MAIA et al., 2021; SANTOS; HACKSPACHER, 2021). The apparent eastward decrease in the VTR radiometric and paleontological ages and the presence of a low-velocity anomaly down to 200-260 km in the VTR and AVC regions (CELLI et al., 2020) point out an influence of a shallow thermochemical mantle anomaly in their magmatic processes. Moreover, the presence of a linear positive geoid anomaly beneath the São Francisco craton that links the Alto Paranaíba Province to the Vitória-Trindade Ridge would be evidence of the plume deflection (THOMPSON et al., 1998).

2.2 Paleocene-Eocene magmatism: Abrolhos Volcanic Complex (AVC)

From the Upper Paleocene to the Upper Eocene occur the most intense volcanic activity recorded in the Espírito Santo sedimentary basin, marked by tholeiitic to alkaline basalts and volcanoclastic rocks interbedded with turbiditic sandstones, shales, and carbonates. The Abrolhos Volcanic Complex (AVC) took place during this phase of intense magmatic manifestations. The AVC (ALMEIDA et al., 1996; CONCEIÇÃO et al., 1996; FRANÇA et al., 2007; STANTON et al., 2021; 2022) is located at the Continent-Ocean Boundary (COB) of the Southeast Brazilian Margin (STANTON et al., 2021; 2022), in the area of the marginal Espírito Santo, Mucuri, and Cumuruxatiba sedimentary basins (ALMEIDA et al., 1996; MOHRIAK, 2006; SOBREIRA; FRANÇA, 2006; FRANÇA et al., 2007; STANTON et al., 2021; Figure 2). The AVC has a roughly circular geometry with an estimated area of about 63,000 km² (STANTON et al., 2021; Figure 2), and corresponds to an igneous province composed of transitional basalts interbedded with sedimentary layers (FODOR et al., 1989; SOBREIRA; SZATMARI, 2002; ARENA, 2008). Its volcanism has been attributed to eruptions from central conduits over a thin and stretched continental platform and oceanic crust (ALMEIDA et al., 1996; SOBREIRA; FRANÇA, 2006; STANTON et al., 2021). The AVC volcanism displays two deep central igneous bodies (R1 and R2) that feed radially the smaller shallow elongated bodies (E1-E7) formed by different magmatic pulses (Figure 2; STANTON et al., 2021; see text for discussions). These two larger buildings coincide with the possible magmatic chambers presented in the work of Sobreira and França (2006). Besides the large buildings and elongated ones, there are also two anomalies located in the oceanic crust (O1 and O2; STANTON et al., 2021).

The AVC emerges into five small islands (Santa Bárbara, Redonda, Siriba, Sueste, and Guarita) that compose the Abrolhos Archipelago, located *ca.* 55 km southeast of Caravelas city (Bahia; Figure 2). The Santa Bárbara Island reaches the highest height above sea level (27 m) and has the most extensive surface area of *ca.* 0.44 km². The Abrolhos Archipelago rocks comprise a Paleocene-Eocene (69-32 Ma; Table 1; CORDANI, 1970; CORDANI; BLAZEKOVIC, 1970; FODOR; MCKEE; ASMUS, 1983; SOBREIRA; SZATMARI, 2002, 2003; SOBREIRA et al., 2004) transitional basalt series of alkaline affinity. In studied islands, basalts, diabases, and cumulatic rocks (CORDANI, 1970; FODOR et al., 1989; GOMES; BORBA; CUNHA, 1992; ARENA, 2008 – Appendix C) crop out interbedded with sedimentary rocks, mainly turbiditic sandstones, and marine shales (CORDANI, 1970; FODOR et al., 1989;

SOBREIRA; FRANÇA, 2006; MOHRIAK, 2006; ARENA, 2008; MATTE, 2013; OLIVEIRA; OLIVEIRA; PEREIRA, 2018).

Table 1 – Compiled radiometric ages from the Abrolhos Volcanic Complex (AVC)

Reference	Lithotype	Site	Code	Method	Material	Age (Ma)
2	Diabase	St Bárbara Isl.	AB-9	K/Ar	Whole Rock	32.2 ± 1.9
	Diabase	St Bárbara Isl.	AB-16	K/Ar	Whole Rock	42.1 ± 3.8
	Diabase	St Bárbara Isl.	AB-17	K/Ar	Plagioclase	37.3 ± 2.2
	Diabase	St Bárbara Isl.	AB-17	K/Ar	Whole Rock	37.1 ± 4.8
	Diabase	St Bárbara Isl.	AB-19	K/Ar	Whole Rock	60.7 ± 9.1
1, 2	Diabase	St Bárbara Isl.	SB-1-BA (620 m)	K/Ar	Plagioclase	41.4 ± 1.2
	Diabase	St Bárbara Isl.	SB-1-BA (709 m)	K/Ar	Whole Rock	43.3 ± 1.3
3	Wherfite	St Bárbara Isl.	BAS33	K/Ar		57.8 ± 2.2
5	Basalt	St Bárbara Isl.		Ar/Ar		46.8 ± 2.5
	Basalt	St Bárbara Isl.		Ar/Ar		44 ± 0.4
	Basalt	St Bárbara Isl.		Ar/Ar		42.6 ± 0.3
6		St Bárbara Isl. and Siriba Isl.		Ar/Ar		50-42
1, 2	Diabase (Sill)	Siriba Isl.	AB-29	K/Ar	Whole Rock	47.6 ± 1.5
5	Diabase	Siriba Isl.		Ar/Ar		50 ± 0.3
2	Diabase	Siriba Isl.	AB-31	K/Ar	Whole Rock	43.5 ± 2.5
1	Diabase (Sill)	Sueste Isl.	AB-26	K/Ar	Whole Rock	46.6 ± 4.7
1, 2	Diabase (Sill)	Sueste Isl.	AB-23	K/Ar	Whole Rock	50.3 ± 2.0
2	Diabase	Sueste Isl.	AB-26	K/Ar	Whole Rock	46.6 ± 3.7
1	Diabase (Sill)	Redonda Isl.	AB-5	K/Ar	Whole Rock	52.4 ± 1.6
2	Diabase	Redonda Isl.	AB-3	K/Ar	Plagioclase	38.9 ± 2.3
	Diabase	Redonda Isl.	AB-3	K/Ar	Whole Rock	46.2 ± 6.5
	Diabase	Redonda Isl.	AB-3	K/Ar	Whole Rock	43.4 ± 3.5
	Diabase	Redonda Isl.	AB-5	K/Ar	Whole Rock	52.4 ± 1.7
	Diabase	Guarita Isl.	AB-1	K/Ar	Plagioclase	44.1 ± 3.5
	Diabase	Guarita Isl.	AB-1	K/Ar	Whole Rock	63.6 ± 7
4	Basalt	Abrolhos Platform		Ar/Ar		53-64
3	Diabase	Abrolhos Platform	ESS9	K/Ar		43.2 ± 2.1
1	Diabase	Caravelas (BA)	Cst-1-BA	K/Ar	Whole Rock	46.5 ± 1.4
6			Petrobras Well	Ar/Ar		61
7, 8	Ignibrite	São Mateus River (Onshore)		Ar/Ar	Mafic grain	69.4 ± 1.3
1	Gabbro	Curaçá (Onshore)	OB/PF/F-1	K/Ar	Plagioclase	73.2 ± 4.4

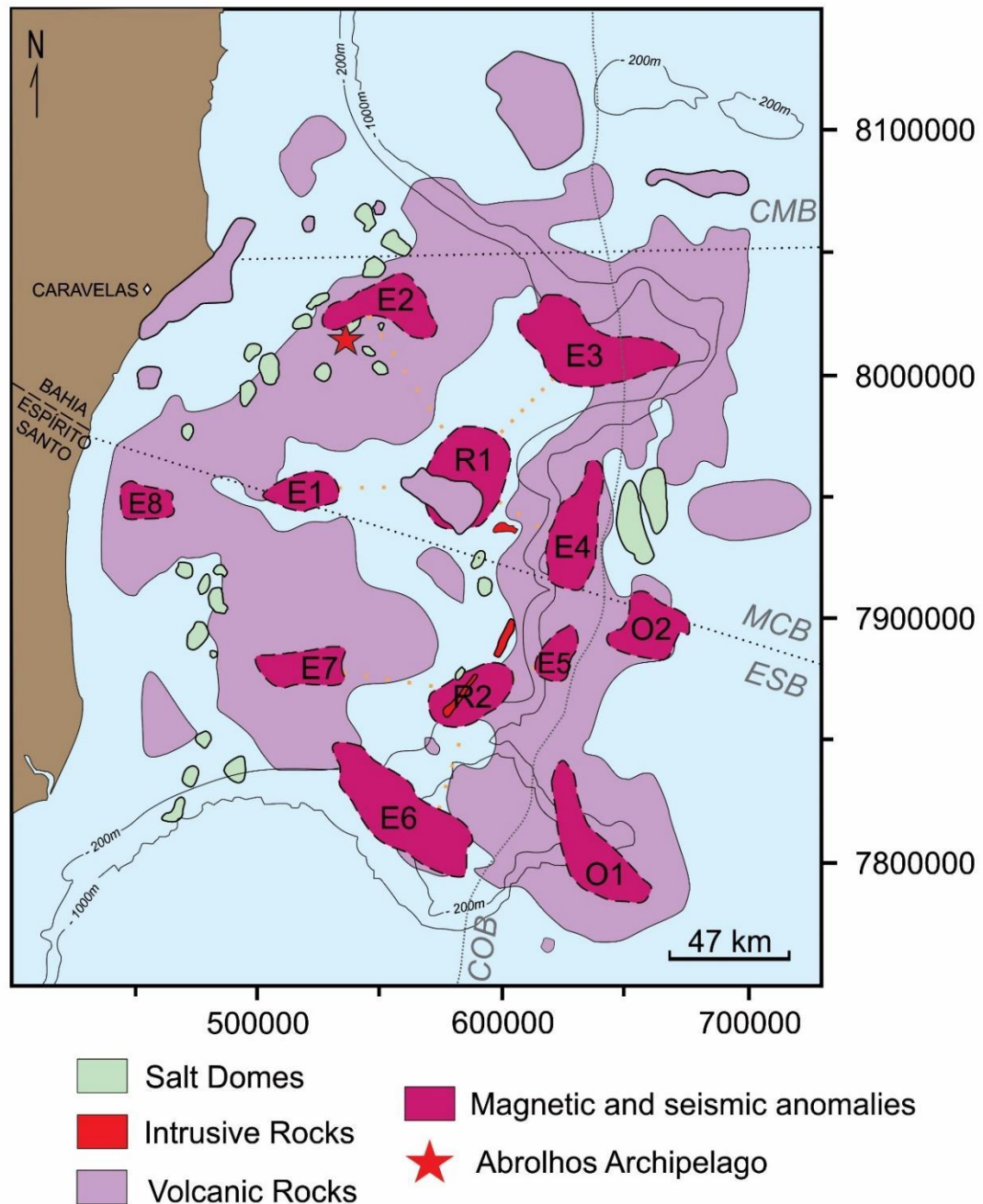
Subtitle - 1 – Cordani (1970); 2 – Cordani and Blazekovic (1970); 3 – Fodor, McKee and Asmus (1983); 4 – Sobreira and Szatmari (2002); 5 – Sobreira and Szatmari (2003); 6 – Sobreira et al. (2004); 7 – Gomes and Suita (2010); 8 – Vieira et al. (2014).

Source: THE AUTHOR, 2022

The Abrolhos Archipelago region uplift has been associated with regional compressional tectonic forces and salt tectonics (MOHRIAK et al., 2003; MOHRIAK, 2006, 2020; STANTON et al., 2022). Apatite fission-track analyses pointed to an apex of the Abrolhos uplift around 50 Ma, *i.e.*, within the radioisotopic ages' interval of the Abrolhos magmatism. Furthermore, compressional features are demarcated in the Neogene, which would

be related to the uplift of the Santa Barbara Island (MOHRIAK et al., 2003; MOHRIAK, 2006). The presence of angular unconformities in the seismic profiles corroborated this later Neogene uplift (SOBREIRA, 1996, SOBREIRA et al., 2004; MOHRIAK, 2006). The presence of dykes and sills that have intruded intervals containing older volcanic rocks suggested a late Neogene to Quaternary magmatic reactivation (SOBREIRA, 1996, SOBREIRA et al., 2004).

Figure 2 – Magmatic framework model of the Abrolhos Volcanic Complex (AVC) region.



Subtitle – R1, R2, E1-E7, O1 and O2 are magnetic and seismic anomalies interpreted as igneous bodies (STANTON et al., 2021). ESB = Espírito Santo Sedimentary Basin; MCB = Mucuri Sedimentary Basin; CMB = Cumuruxatiba Sedimentary Basin; COB = Continent-Ocean Boundary.

Source: Modified from Sobreira and França (2006) and Stanton et al. (2021)

About the igneous rocks that outcrop on the Abrolhos Archipelago, Fodor et al. (1989) described pyroxene-olivine-plagioclase basalts collected from Santa Bárbara, Sueste, and Siriba Islands. Intergranular and porphyritic textures prevail among the studied samples. The groundmass is composed of plagioclase, clinopyroxene, and Fe-Ti oxides and may contain olivine (some altered to smectite). Grain sizes vary from 0.1 to 0.5 mm. Olivines, clinopyroxenes, and plagioclase also occur as microphenocrysts about 1 mm. In some samples, Fe-Ti oxide grains (1 mm) enclose grains of plagioclase and clinopyroxene from the groundmass, indicating *subsolidus* growth.

Arena (2008) analyzed pyroxene-plagioclase basalt samples from the Santa Bárbara Island, pyroxene-plagioclase-olivine basalt from Siriba Island, and olivine-plagioclase basalt from Sueste Island. The former is hypocrystalline and the others are holocrystalline. All lithotypes have inequigranular and porphyritic textures. The pyroxene-plagioclase basalt is composed of plagioclase (20%) and clinopyroxene (80%) phenocrysts varying from 1 to 2.5 mm in size. The latter shows poikilitic texture, compositional zoning, and corrosion. The groundmass is composed of clinopyroxene, plagioclase, and opaque minerals smaller than 1 mm. Chlorite, saussurite, biotite, and carbonate occur as secondary phases. One sample of a chilled margin was described and it presents plagioclase, opaque minerals and glass in the groundmass, and plagioclase phenocrysts about 0.2-0.3 mm in size. The pyroxene-plagioclase-olivine basalt has plagioclase, clinopyroxene, and olivine in the groundmass and as phenocrysts, varying from 0.1 to 0.5 mm and 0.5 to 1 mm, respectively. Apatite and opaque minerals appear as accessory phases. Plagioclase phenocrysts are described with poikilitic texture, compositional zoning, fractures, and opaque minerals inclusions. Lastly, the olivine-plagioclase basalt groundmass has clinopyroxene, plagioclase, olivine, and opaque minerals varying from 0.1 to 0.3 mm. The fractionating assemblage is composed of olivine (80%) and plagioclase (20%) crystals about 0.5 to 3 mm, which occur fractured and zoned. The olivine grains are altered to iddingsite. Apatite is an accessory mineral.

Fodor et al. (1989) analyzed diabase samples from the Petrobras drill holes SB-1-BA from the Santa Bárbara Island (620 and 670 m below the surface) and ESS9 within the Abrolhos Platform. Cordani (1970) also described samples from the Petrobras drill hole SBST-1-BA (620 and 709 m below the surface), as well as Gomes, Borba and Cunha (1992). Fodor et al. (1989) described diabase rocks composed of clinopyroxene phenocrysts (27-43%) with irregular and jagged margins and Fe-Ti oxide phenocrysts (11-14%) with resorption features. Both are generally 0.5-4 mm in size. The groundmass comprises plagioclase laths of *ca.* 0.5-1 mm and alteration phases such as biotite, chlorite, and sericite. The ESS9 sample has intergranular

altered plagioclase (58%), clinopyroxene grains of 1-3 mm (26%), Fe-Ti oxides of 1 mm (6.5%), smectite (8%) and minor quartz (1.5%). The diabase described by Cordani (1970) from the drill hole SBST-1-BA is holocrystalline and porphyritic and could have ophitic or subophitic textures. It has augite phenocrysts and the groundmass is composed of labradorite, magnetite, apatite, and alteration minerals. At last, the diabase analyzed by Gomes, Borba and Cunha (1992) are holocrystalline (some samples are hypocrySTALLINE), inequigranular, seriate, and have ophitic, subophitic, and poikilitic textures. The groundmass comprises anorthite, clinopyroxenes (augite or diopside), olivine, opaque minerals, titanite and biotite, and apatite occur as an accessory mineral. Prehnite, biotite, amphiboles, chlorite, and epidote occur and are mineral phases typically found in metabasalts, suggesting a small degree of metamorphism (GOMES; BORBA; CUNHA, 1992).

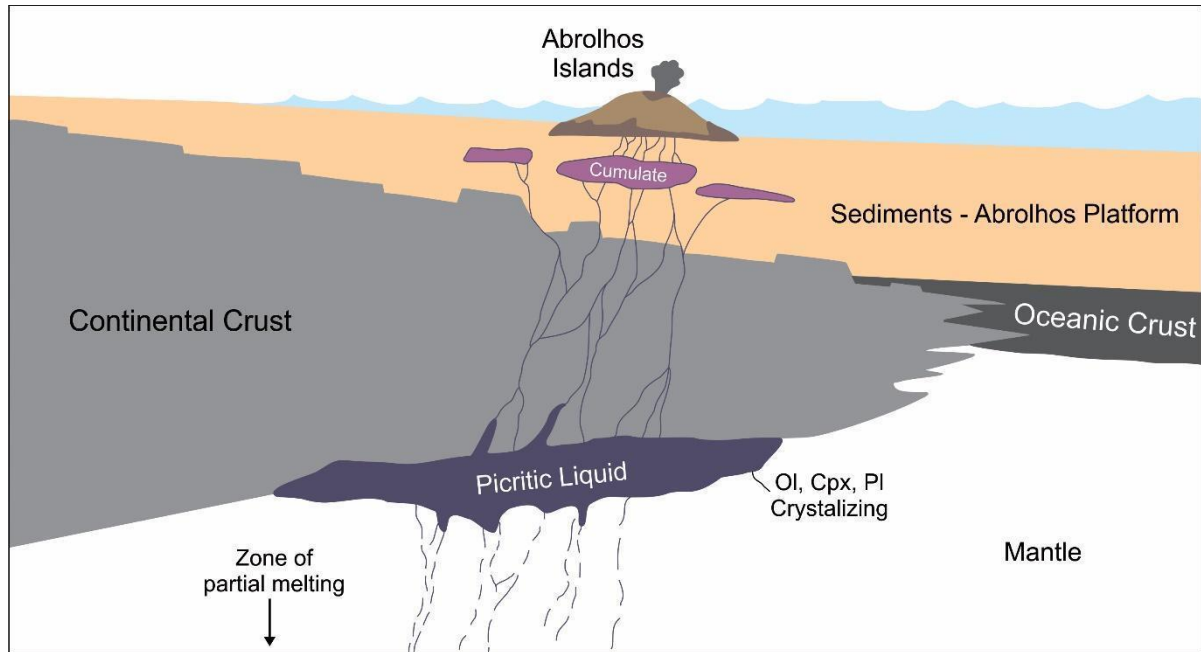
The cumulated rocks of the AVC are from the Petrobras drill hole SB-1-BA (573 m below the surface; FODOR et al., 1989) and also outcrops in the western portion of the Santa Bárbara Island (ARENA, 2008). They have inequigranular and porphyritic textures and are composed of plagioclase and clinopyroxene phenocrysts 1-5 mm long, and intergranular ilmenite grains (1-2 mm). Arena (2008) reported a groundmass with plagioclase, clinopyroxenes, and opaque minerals with 0.1 to 1 mm in size. The clinopyroxene phenocrysts have compositional zoning and corrosion (ARENA, 2008) and are altered to smectite and chlorite. Plagioclase grains are altered to saussurite.

Some volcanic acid deposits have been associated with de Abrolhos magmatism. Novais et al. (2008) and Vieira et al. (2014) reported ignimbrites nearby the São Mateus River margin, located in the onshore portion of the Espírito Santo Basin. Gomes and Suita (2010) studied rhyolites and trachytes from the top of the Abrolhos Formation located in the Mucuri Basin. Motoki et al. (2007) reported rocks of rhyolitic pyroclastic nature in the Espírito Santo Basin.

The genesis of the Abrolhos Archipelago basaltic rocks was attributed to the crystallization of a picritic parental liquid with a relatively rapid cooling (FODOR et al., 1989). This picritic liquid would have emplaced at the base of or into cold crystalline continental crust in the Eocene (Figure 3). On the other hand, based on the analyses of variation diagrams for major and trace elements and trace element ratios, Arena (2008) and Arena et al. (2008) pointed out that fractional crystallization without changing in the fractionating assemblage would be a possible evolutionary process for the basalts of the Abrolhos Archipelago. However, the inconsistency between the fractionating assemblage and the phenocryst assemblage identified in the petrography, and features pointing to crystal-liquid disequilibrium require a more complex evolutionary model than just the fractional crystallization process itself. Thus, Arena

(2008) and Arena et al. (2008) have considered a more complex evolutionary model, *i.e.*, fractional crystallization associated with the RTF process. The latter is a geochemical evolutionary process proposed for magmatic chambers with slightly variable eruption rates and which are periodically **R**eplenished by new pulses of parental magmas, periodically **T**apped (erupted), and continuously **F**ractionated (O'HARA; MATHEWS, 1981; COX, 1988).

Figure 3 - Schematic of proposed genesis for Abrolhos Archipelago rocks



Subtitle – Schematic model for the genesis of Abrolhos Archipelago rocks. Its generation would be from the crystallization of a picritic parent liquid, which occupies deep crustal levels. Olivines, clinopyroxenes, and plagioclase are possible mineral phases that can be crystallized from this liquid. After an intense crystallization process, more evolved and less dense residual liquids would ascend to shallow crustal levels (FODOR et al., 1989).

Source: Modified from Fodor et al. (1989)

Regarding the melting regime, $La/Yb_{(N)}$ e $La/Nb_{(N)}$ ratios (*ca.* 6.0-9.3 and 0.4-1.0, respectively) from diverse basalts can be explained by different degrees of partial melting from the same fertile mantle source (plume-type; Arena, 2008). Fodor et al. (1989) also proposed a mixture between compositions of a mantle plume and a depleted component to explain the AVC trace-element ratios (*e.g.*, Zr/Y *avg.* 7.9; Zr/Nb *avg.* 5.4) and isotopic compositions (*e.g.*, $^{87}Sr/^{86}Sr$ *ca.* 0.70382; $^{143}Nd/^{144}Nd$ *ca.* 0.512807). This plume involvement was proposed by some authors (*e.g.* THOMPSON et al., 1998), who suggested that the Abrolhos Volcanic Complex is part of the volcanic trail left by the passage of the South American Plate over the Trindade Plume, being its first expression in the passive continental margin (O'CONNOR; DUNCAN, 1990; CONCEIÇÃO et al., 1996; THOMPSON et al., 1998; FERRARI;

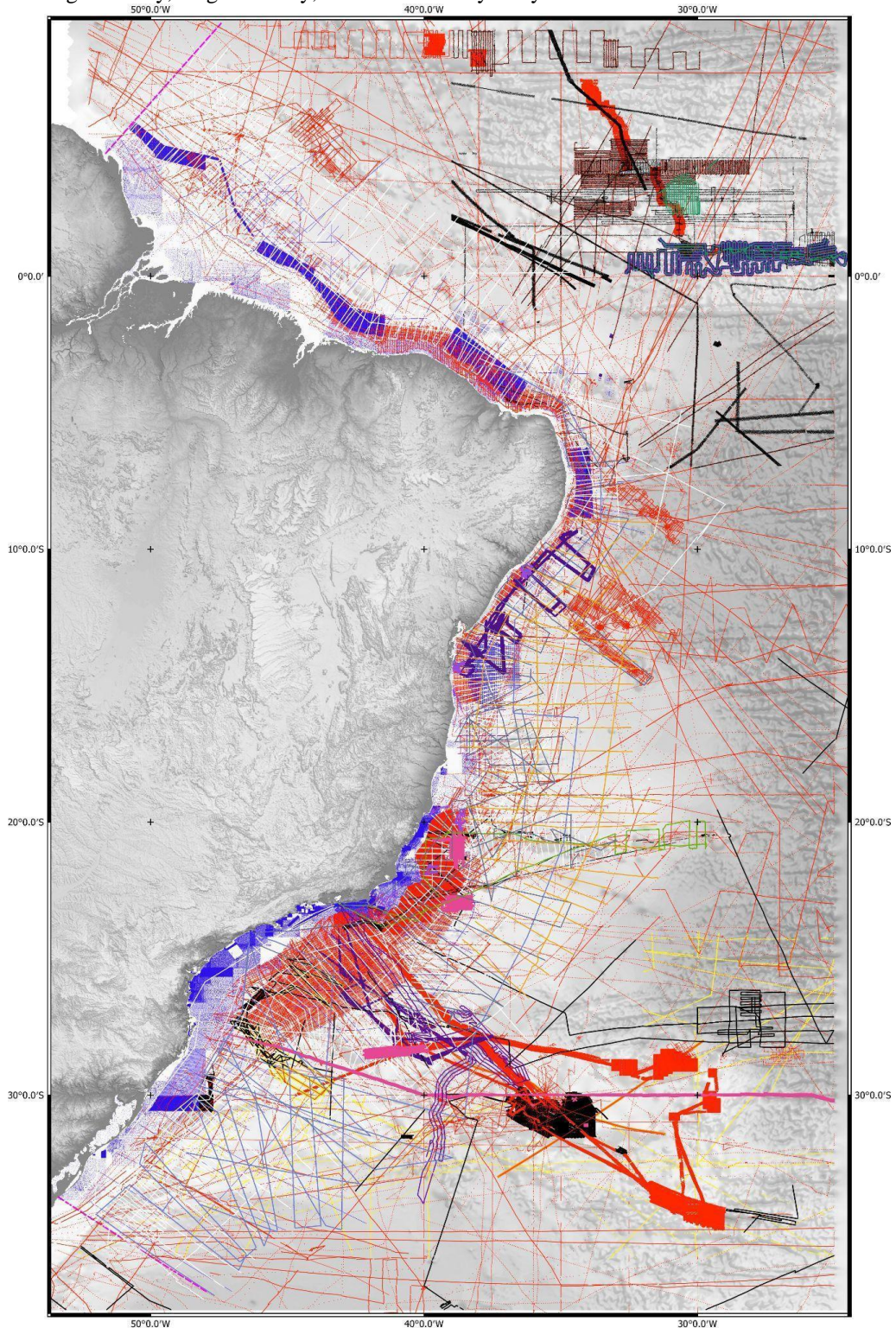
RICCOMINI, 1999; SOBREIRA et al., 2004; ALVES et al., 2006; MOHRIAK, 2006; ARENA, 2008).

Previous isotopic data from the Abrolhos Volcanic Complex basalts show $^{87}\text{Sr}/^{86}\text{Sr}_{(m)}$ ratios ranging from 0.70372 to 0.70390 (FODOR; MCKEE; ASMUS, 1983; FODOR et al., 1989). The diabase samples have more radiogenic measured $^{87}\text{Sr}/^{86}\text{Sr}$ ratios (0.704110 to 0.704670), and the cumulated rock show an even more radiogenic Sr measured ratio (0.707330), probably due to sea water contamination. The measured $^{143}\text{Nd}/^{144}\text{Nd}$ ratios range from 0.512636 to 0.512841 among all lithotypes. The $^{206}\text{Pb}/^{204}\text{Pb}_{(m)}$, $^{207}\text{Pb}/^{204}\text{Pb}_{(m)}$ and $^{208}\text{Pb}/^{204}\text{Pb}_{(m)}$ isotope ratios range from 18.90 to 19.33, 15.54 to 15.63 and 38.73 to 39.07, respectively. These depleted isotopic compositions do not suggest any mantle metasomatism, according to Fodor et al. (1989).

2.3 Eocene-Pleistocene Magmatism: Vitória-Trindade Ridge (VTR)

The Vitória-Trindade Ridge extends *ca.* 110 km southeast of the AVC from the Brazilian continental slope to *ca.* 1200 km in deep waters of the Atlantic Ocean (ALMEIDA, 2006), forming a west-east-trending volcanic aseismic ridge composed mainly of more than 30 seamounts and banks. VTR's morphology studies date back to the 1950s. During the 1972-78 period, an agreement between several Brazilian institutions gave rise to the REMAC project (*Programa de Reconhecimento Global da Margem Continental Brasileira, in English - free translation: Brazilian Continental Margin Global Recognition Program*). Hereafter, LEPLAC Program (Brazilian Continental Shelf Survey Program – 1987-2020) started and carried out several surveys along the Brazilian margin, especially in the last decade, when additional multibeam bathymetric data were acquired in the VTR region so that all banks and seamounts could be better described (Figure 4).

Figure 4 - Brazilian offshore area showing diverse colored lines from several geological surveys such as gravimetry, magnetometry, seismic and bathymetry.



Source: LEPLAC-DHN - Brazilian Navy.

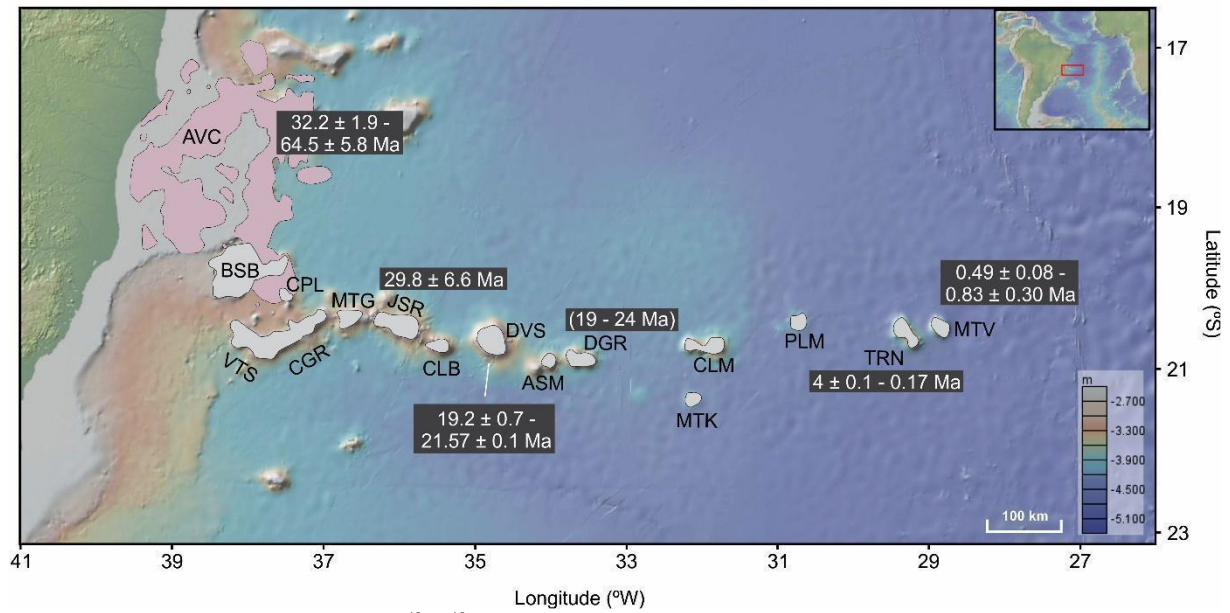
The most expressive submerged volcanic edifices (Figure 5) and their depths related to the sea level correspond to the Besnard Bank (55 m), southeast of the Abrolhos Volcanic Complex (AVC), the Vitória Seamount (52 m), Congress Bank (63 m), the Champlain

Seamount (62 m), the Jaseur Seamount (54 m), the Montague Seamount (57 m), the Colúmbia Bank (60 m), the Davis Bank (61 m), the Asmus Bank, the Dogaressa Bank (54 m), the Colúmbia Seamount (96 m), as well as the Trindade Island and the Martin Vaz Archipelago, which represent the easternmost and emerged segment of the ridge (ALMEIDA, 2006; SANTOS et al., 2015; 2018a, 2018b, 2022a, 2022b; SANTOS; HACKSPACHER, 2021; MONTEIRO et al., 2022).

As aforementioned, some authors interpreted the VTR as the Trindade Plume volcanic trail on the South American Plate (GIBSON et al., 1999; FODOR; HANAN, 2000; SIEBEL et al., 2000, SANTOS, 2013; BONGIOLO et al., 2015; PIRES et al., 2016; SANTOS, 2016; SANTOS et al., 2018a, 2018b; JESUS et al., 2019; MAIA et al., 2021; OLIVEIRA et al., 2021; REGO et al., 2021). Notwithstanding the plume hypotheses, other models were also brought up in the literature. Marques et al. (1999) suggested that Trindade Island's extrusive materials could come from stratified magma chambers that might be periodically replenished with ultrabasic magmas in the late stages of magmatic activity. Quaresma et al. (*in press*) further highlighted the lack of convincing evidence for the Trindade Plume hypothesis, emphasizing the need for diverse and accurate geochronological data. In addition, as there is no geochemical and geophysical evidence linking the VTR genesis to the deep mantle plume, these last authors proposed that the VTR petrogenesis would be associated with the presence of detached SCLM fragments and different proportions of recycled oceanic crust (MORB-eclogite) and lithosphere in the upper mantle (*ca.* 250 km) beneath the South Atlantic Ocean.

Other models that dispute the origin of intraplate magmatism to deep mantle plumes suggest that the locations of melting anomalies are controlled by stress, since volcanic chains or lineations are expected to develop along extensional structures, such as fissures, faults or cracks (*e.g.*, FAIRHEAD; WILSON, 2005). In this way, the VTR is believed to be associated with the Vitória-Trindade Fracture Zone, which acted as a conduit for this enriched mantle-derived magmatism (VELOSO; MACHADO, 1986; SZATMARI; MOHRIAK, 1995; CONCEIÇÃO et al., 1996; FERRARI; RICCOMINI, 1999; ALMEIDA, 2006; ALVES et al., 2006, 2022).

Figure 5 - The Vitória-Trindade Ridge (VTR) and the Abrolhos Volcanic Complex (AVC)



Subtitle – AVC – Abrolhos Volcanic Complex ($^{40}\text{K}/^{40}\text{Ar}$ ages from Cordani, 1970; Cordani and Blazekovic, 1970; Fodor et al., 1983; $^{40}\text{Ar}/^{39}\text{Ar}$ ages from Sobreira and Szatmari, 2003; Sobreira et al., 2004); BSB – Besnard Bank; CPL – Champlain Seamount; VTS – Vitória Seamount; CGR – Congress Seamount; MTG – Montague Seamount; JSR – Jaseur Seamount ($^{238}\text{U}/^{206}\text{Pb}$ ages from Skolotnev et al., 2011); CLB – Colúmbia Bank; DVS – Davis Bank ($^{40}\text{Ar}/^{39}\text{Ar}$ ages from Santos, 2016; Skolotnev and Peive, 2017, Quaresma et al., *in press*); ASM – Asmus Bank; DGR – Dogaressa Bank (paleontological ages obtained from recrystallized limestones in parentheses; Skolotnev et al., 2011); CLM – Colúmbia Seamount; MTK – Motoki Hill; PLM – Palma Seamount; TRN – Trindade Island ($^{40}\text{Ar}/^{39}\text{Ar}$ ages from Geraldés et al., 2013; Pires et al., 2016); MTV – Martin Vaz Archipelago ($^{40}\text{Ar}/^{39}\text{Ar}$ ages from Santos, 2013; 2016; Santos et al., 2015; 2021; Santos and Hackspacher, 2021; Monteiro et al., 2022; Santos et al., 2022a).

Source: Modified from Maia et al. (2021)

In general, the VTR seamounts and banks display ultrabasic rocks with alkaline affinity, such as ankaramites from the Colúmbia Seamount (FODOR; HANAN, 2000) and the Dogaressa Bank (SKOLOTNEV et al., 2010), melanephelinites from the Montague and the Jaseur Seamounts (SANTOS, 2016) and alkaline basalt from the Vitória Seamount (MAIA et al., 2021). On the other hand, basic rocks occur on the Davis Bank, as basanites and olivine basalts (SKOLOTNEV et al., 2010; JESUS et al., 2019). The VTR volcanic rocks show a strong enriched mantle signature based on normalized REE ratios, strongly undersaturated alkaline affinity ranging lithologically from basanites and nephelinites to more evolved rocks, such as tephri-phonolites and (nosean-)phonolites (MARQUES et al., 1999; SANTOS, 2013, 2016; BONGIOLO et al., 2015; PIRES; BONGIOLO, 2016; SANTOS et al., 2015; 2018a, 2018b, 2021, 2022a, 2022b; OLIVEIRA et al., 2021; MAIA et al., 2021; REGO et al., 2021; SANTOS; HACKSPACHER, 2021; MONTEIRO et al., 2022).

Only a few ages obtained from samples dredged and collected from the volcanic edifices from the VTR have been reported in the literature, but the ages of the seamounts, banks, and island seem to become progressively younger eastwards (Figure 5): U-Pb zircon dating yielded

ages of 29.8 ± 6.6 Ma for Jaseur Seamount (SKOLOTNEV et al., 2011 - see text for details regarding data reliability); based on $^{40}\text{Ar}/^{39}\text{Ar}$ dating of whole-rock and plagioclase and pyroxene minerals, 19.2 ± 0.7 to 21.57 ± 0.1 Ma for Davis Bank (SANTOS 2016; SKOLOTNEV; PEIVE, 2017, QUARESMA et al., *in press*); an age range close to Davis Bank (19-24 Ma) was suggested for the Dogaressa Bank, based on recrystallized limestones that may have been formed during the period of time closest to the end of the volcanic activity of these edifices (SKOLOTNEV et al., 2011). Finally, Trindade Island has $^{40}\text{Ar}/^{39}\text{Ar}$ ages ranging from 4 ± 0.1 Ma to 0.17 Ma (GERALDES et al., 2013; PIRES et al., 2016; SANTOS; HACKSPACHER, 2021; MONTEIRO et al., 2022) and $^{40}\text{K}/^{40}\text{Ar}$ ages ranging from 6.4 ± 3.5 Ma to < 0.17 Ma (CORDANI, 1970; VALENCIO; MENDÍA, 1974) and the Martin Vaz Archipelago exhibited $^{40}\text{Ar}/^{39}\text{Ar}$ ages ranging from 0.49 ± 0.08 Ma to 0.64 ± 0.08 Ma (SANTOS, 2013; 2016; SANTOS et al., 2015, 2021, 2022a; SANTOS; HACKSPACHER, 2021).

No geochronological ages are available for the other VTR volcanic edifices, such as the Besnard Bank, the Vitória, Montague, and Colúmbia Seamounts. The Besnard Bank is located just southeast of the Abrolhos Volcanic Complex and is considered coeval to its magmatism (FAINSTEIN; SUMMERHAYES, 1982), but lacks geochronological data to confirm the aforementioned assumption. However, exploratory drilling on the top of the structure penetrated Cenozoic sediments above the volcanic rocks (MOHRIAK, 2006). Maia et al. (2021) suggested that the Vitória Seamount should have around 34 Ma considering an approximately 5 cm/year rate of South Atlantic velocity motion (COLLI et al., 2014; MÜLLER et al., 2016) and assuming a hotspot origin. Thus, it is somehow also correlated with the final volcanic events in the South Abrolhos Bank. Fodor and Hanan (2000) also considered the hotspot trail, but based on a 3 cm/year rate of plate motion (GRIPP; GORDON, 1990), estimated the age of about 10 Ma for the Colúmbia Seamount.

The least evolved compositions from the VTR (alkaline basalts, melanephelinites, tephrites, anakamites, basanites, and nephelinites; MARQUES et al., 1999; FODOR; HANAN, 2000; SIEBEL et al., 2000; PEYVE; SKOLOTNEV, 2014; BONGIOLO et al., 2015; SANTOS, 2016; SANTOS et al., 2018a, 2022a, 2022b; JESUS et al., 2019; MAIA et al., 2021; REGO et al., 2021; OLIVEIRA et al., 2021; SANTOS; HACKSPACHER, 2021; MONTEIRO et al., 2022) have 30–47 wt.% in SiO_2 (lower values in Dogaressa and Colúmbia ankaramites), 5–12 wt.% in FeO (lower values from Trindade Island basanites; SIEBEL et al., 2000), high MgO (avg. 9.08 wt.%) and TiO_2 contents (avg. 4.31 wt.%) and $\text{Ti}/\text{Y} = 869$, with higher Ti values in Trindade Island and Montague Seamount. Based on Marques et al. (1999), Siebel et al. (2000),

Bongiolo et al. (2015), Santos (2016), Santos et al. (2018a) data, Santos and Hackspacher (2021), Monteiro et al. (2022) and Santos et al. (2022a), the more evolved compositions in Trindade and Martin Vaz (phonotephrites, tephriphonolites, and phonolites) have SiO₂ contents ranging from 46.0 to 57.3 wt.%, FeO* vary from 0.97 to 10.32 wt.% (avg. 4.6 wt.%), with higher values in the Trindade Island phonotephrites and lower values in phonolite plugs of both islands, and show low MgO and TiO₂ contents (avg. 1.2 and 0.9 wt.%, respectively).

The VTR rocks show low Zr/Nb (avg. 3.8 to 6.7) and Y/Nb (avg. 0.2 to 0.4) ratios. They indicate geochemically enrichment (LE ROEX et al., 2010) and are typically found in OIB-type intraplate magmatic settings, being typical of alkaline magmas (PEARCE; NORRY, 1979; NIU et al., 2012; XIA; LI, 2019). In general, the VTR shows high to moderate values of HFSE (high-field strength elements) such as Nb, Ta, and Th, and high concentrations of LILE (large ion-lithophile elements) such as Ba and Sr. The Martin Vaz basanites and melanephelinites and Trindade basanites are more enriched in rare-earth elements (REE, mostly light ones; La/Yb_N avg. 26) than the rest of the Vitória-Trindade seamounts (La/Yb_N avg. 18). The seamounts located closer to the Brazilian coastline and southeastwards the Abrolhos Bank (e.g., Vitória, Montague, and Jaseur seamounts) present the same patterns in light rare-earth elements (La/Sm_N ca. 2.6; SANTOS, 2006; PEYVE; SKOLOTNEV, 2014; MAIA et al., 2021, SANTOS et al., 2022b) with variably heavy rare-earth elements: La/Yb_N avg. 7.7 in Abrolhos (FODOR et al., 1989; ARENA, 2008) basalts and in the aforementioned seamounts ranging from 16.6 to 21. These VTR geochemical characteristics and the melting model suggest that its rocks were generated by a low-variable-degree of partial melting (0.1 to 7%) in the stability field of garnet-spinel(-phlogopite) lherzolite with minor amount of CO₂ (0.25 wt.%) with or without TiO₂ (SIEBEL et al., 2000; SANTOS; MARQUES, 2007; PEYVE; SKOLOTNEV, 2014; BONGIOLO et al., 2015; SKOLOTNEV; PEIVE, 2017; SANTOS et al., 2018a, 2022a, 2022b; MAIA et al., 2021; SANTOS; HACKSPACHER, 2021; MONTEIRO et al., 2022).

The Vitória-Trindade Ridge has ⁸⁷Sr/⁸⁶Sr_(m) ratios ranging from 0.703607 to 0.704251 and ¹⁴³Nd/¹⁴⁴Nd_(m) ratios ranging from 0.512622 to 0.512879 (Table 2; HALLIDAY et al., 1992; MARQUES et al., 1999; FODOR; HANAN, 2000; SIEBEL et al., 2000; SKOLOTNEV et al., 2011; PEYVE; SKOLOTNEV, 2014; BONGIOLO et al., 2015; SANTOS, 2016; SANTOS et al., 2018a, 2022a, 2022b; MAIA, 2019; QUARESMA, 2019; MAIA et al., 2021; SANTOS; HACKSPACHER, 2021; MONTEIRO et al., 2022; QUARESMA et al., *in press*). The Vitória Seamount (MAIA et al., 2021) and Davis Bank (SKOLOTNEV et al., 2011; SANTOS, 2016; QUARESMA, 2019; QUARESMA et al., *in press*) samples have the more radiogenic ⁸⁷Sr/⁸⁶Sr_(m) ratios (0.7040) and the less radiogenic ¹⁴³Nd/¹⁴⁴Nd_(m) ratios (0.5126)

among the VTR (Table 2). Dogaressa Bank shows anomalous radiogenic $^{87}\text{Sr}/^{86}\text{Sr}_{(m)}$ ratios (0.70869 and 0.70775) which probably originated from seawater contamination (PEYVE; SKOLOTNEV, 2014). The $^{206}\text{Pb}/^{204}\text{Pb}_{(m)}$, $^{207}\text{Pb}/^{204}\text{Pb}_{(m)}$ and $^{208}\text{Pb}/^{204}\text{Pb}_{(m)}$ isotope ratios of the VTR range from 19.01 to 19.50, 15.05 to 15.62 and 38.82 to 39.51, respectively (Table 2). These VTR geochemical and isotopic signatures suggest a mixture between a depleted mantle component (DMM) and enriched components such as EMI and HIMU (MARQUES et al., 1999; SIEBEL et al., 2000; SANTOS, 2013; 2016; PEYVE; SKOLOTNEV, 2014; BONGIOLO et al., 2015; SKOLOTNEV; PEIVE, 2017; MAIA et al., 2021; SANTOS; HACKSPACHER, 2021; SANTOS et al., 2022a, 2022b; MONTEIRO et al., 2022; QUARESMA et al., *in press*).

Table 2 - Compiled Sr-Nd-Pb isotopic data from the Vitória-Trindade Ridge (VTR)

Reference	Lithotype	Site	$^{87}\text{Sr}/^{86}\text{Sr}_{(m)}$	$^{143}\text{Nd}/^{144}\text{Nd}_{(m)}$	$^{206}\text{Pb}/^{204}\text{Pb}_{(m)}$	$^{207}\text{Pb}/^{204}\text{Pb}_{(m)}$	$^{208}\text{Pb}/^{204}\text{Pb}_{(m)}$
1	Alkaline Basalt	Vitória Smt.	0.704031	0.512635			
2	Melanepheinite	Montague Smt.	0.703727	0.512806			
3	Melanepheinite	Jaseur Smt.	0.70405	0.51277	19.20	15.57	39.37
4	Basanite	Davis Bank	0.70391	0.51275	19.26	15.60	39.42
3	Nephelinite	Dogaressa Smt.	0.70413	0.51272	19.01	15.59	39.08
5	Ankaramite	Columbia Smt.	0.7039	0.512786	19.19	15.05	39.24
6	Nephelinite	Trindade Isl.	0.703837	0.512799	19.15	15.52	39.02
7	Phonolite	Trindade Isl.	0.70386	0.512787	19.27	15.58	39.22
7	Basanite	Martin Vaz Arch.	0.703607	0.512788	19.28	15.6	39.25
7	Phonolite	Martin Vaz Arch.	0.704207	0.512785	19.24	15.6	39.34

Subtitle - 1 – Maia et al. (2021); 2 – Santos (2016); 3 – Peyve and Skolotnev (2014); 4 – Skolotnev et al. (2011); 5 – Fodor and Hanan (2000); 6 – Halliday et al. (1992); 7 – Siebel et al. (2000).

Source: THE AUTHOR, 2022

2.4 Relation between the Brazilian Southeast Margin magmatism and global tectonic events

Tectonic events of global and local magnitude that took place during the Cenozoic may have played an important role in the volcanism of the Vitória-Trindade Ridge edifices (COLLI et al., 2018; CELLI et al., 2020 and references therein). The Andean uplift started in the Middle Eocene with a slow initial stage, developing and reaching its first culmination in the Oligocene-Early Miocene (Figure 6; SEMPERE; FOLGUERA; GERBAULT, 2008; CELLI et al., 2020). The compressive forces resulting from subduction at the Andean margin and the spreading of the Meso-Atlantic Dorsal may have affected the AVC and VTR magmatism (SZATMARI;

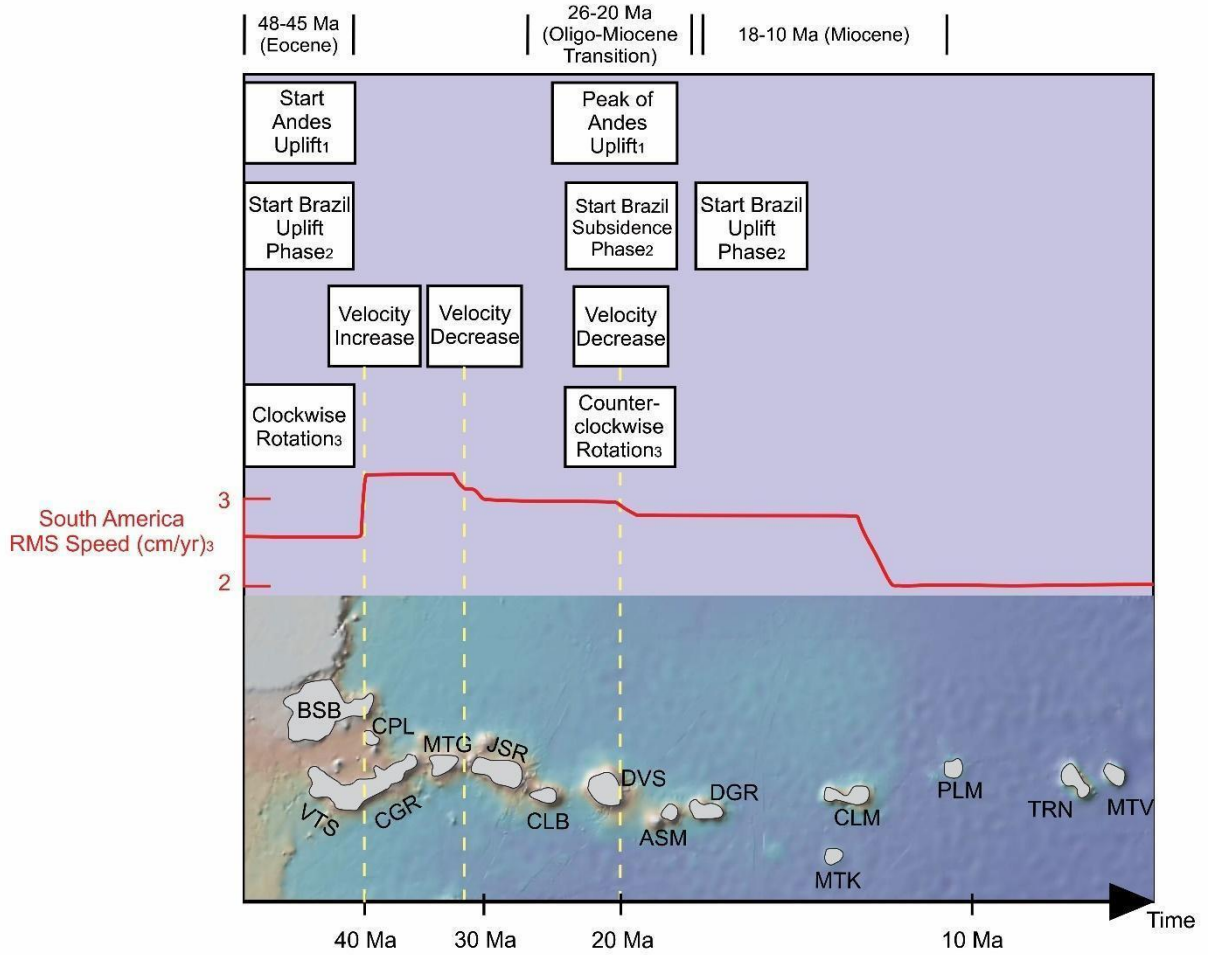
MOHRIAK, 1995). In this way, the Abrolhos Archipelago uplift is associated with regional compressional tectonic forces (MOHRIAK et al., 2003; MOHRIAK, 2006, 2020). The stair-step seafloor formation caused by tectonic events predate the VTR development (SKOLOTNEV et al., 2010). Moreover, other events dating from the Eocene show a correlation with the AVC and the VTR magmatism. A global heat flow increase and reorganization of tectonic plates (56-48 Ma) marked the Eocene (GORDON; JURDY, 1986; CONCEIÇÃO et al., 1996), *i.e.*, within the radiometric ages' interval of the Abrolhos magmatism, and would have resulted in intense global volcanic activity. An uplift event in Northeast Brazil is observed between 48 and 45 Ma (Figure 6; JAPSEN et al., 2012). A clockwise rotation of the South American continent is reported during the Middle Eocene (Figure 6; ERNESTO, 1996; THOMAZ-FILHO; RODRIGUES, 1999; THOMAZ-FILHO et al., 2005; MÜLLER et al., 2016), further evidence for a possible link between the path of the Trindade Plume, the Serra do Mar Province and the VTR magmatic processes. In addition, there is a clockwise rotation of about 40° from the axis of the Chile mountain range recorded during the Oligocene-Miocene interval (TEBBENS; CANDE, 1997; SOMOZA, 1998), nearly coeval to the VTR magmatic events. Santos and Campos sedimentary basins present important turbiditic generation during these periods, indicating instability in the continental shelf, which is possibly correlated with both magmatic and tectonic events (MOHRIAK, 2006).

Some authors (*e.g.*, FERRARI; RICCOMINI, 1999; ALMEIDA, 2006; ALVES et al., 2006, BARÃO et al., 2020, STANTON et al., 2021; ALVES et al., 2022) advocate the control of structural features in the VTR and AVC emplacement and evolution process. The Vitória-Trindade Fracture Zone acts as a conduit for VTR magmatism (VELOSO; MACHADO, 1986; SZATMARI; MOHRIAK, 1995; CONCEIÇÃO et al., 1996; FERRARI; RICCOMINI, 1999; ALMEIDA, 2006; ALVES et al., 2006, BARÃO et al., 2020, ALVES et al., 2022) and Precambrian structural trends along with offshore rifting structures and the Continent-Ocean Boundary (COB) influenced the AVC emplacement (FAINSTEIN; SUMMERHAYS, 1982; STANTON et al., 2021).

Ferrari and Riccomini (1999) pointed out a temporal relation between the variations in the orientation of the Vitória-Trindade Ridge and the changes in velocity and direction of movement of the South American Plate. The NE-SW segment of the VTR would consist of the Besnard Bank, Vitória Seamount, and Congress Bank, begin coeval to an increase in plate velocity, which was also found by Müller et al. (2016). On the other hand, the NW-SE direction, consisting of Jaseur Seamount, Colúmbia Bank, and Davis Bank, would be contemporaneous

to a velocity decrease. Overall, the Andean uplift and other South American Plate tectonic events suggest an influence on and a relationship with the VTR volcanism.

Figure 6 - Andean uplift and South American Plate tectonic events



Subtitle – ¹Sempere, Folguera and Gerbault (2008); ²Japsen et al. (2012); ³Müller et al. (2016).

Source: QUARESMA ORAL COMMUNICATION

3 MATERIAL AND METHODS

The following phases have been developed to achieve the objectives mentioned in section 1: literature review and data compilation, sample selection and preparation, laboratory involving petrographic, lithochemical and isotopic analyses, and geochemical modeling. In order to avoid doubling of information, the methods developed for sample preparation, lithochemical and Sr-Nd isotopic analyses are described along the articles attached in the appendices A and B. Other procedures are described below.

3.1 Literature review and geological background data

Published data about the Vitória-Trindade Ridge and Abrolhos Volcanic Complex have been gathered in this phase. From the detailed reading of the bibliography, it was possible to structure a summary about the geological background of the studied area, elaborating and comparing hypotheses about the possible processes involved in the genesis of these magmatism.

3.2 Petrographic study

Thin slides were analyzed using AXIO Zeiss polarizing microscope from the Petrography Laboratory (LPETRO) of the *Faculdade de Geologia* (FGEL) of the *Universidade Estadual do Rio de Janeiro* (UERJ).

4 RESULTS

The results are exposed in the articles attached in the appendices A and B. The Appendix A display the first article published at the Journal of South American Earth Sciences, titled “First petrologic data for Vitória Seamount, Vitória-Trindade Ridge, South Atlantic: a contribution to the Trindade Mantle Plume Evolution” (<https://doi.org/10.1016/j.jsames.2021.103304>). The Appendix B display the second article that was submitted to the special volume “Atlantic Evolution” at Journal of South American Earth Science, title “Abrolhos Volcanic Complex petrogenesis and its link with the Vitória-Trindade Ridge, Southeast Brazilian Margin, South Atlantic Ocean”.

5 CONCLUDING REMARKS

Throughout the work, several similarities among the geochemistry and isotopic signatures of the VTR and the AVC magmatism have been pointed out. The VTR shows a much wider range of litho-geochemical signatures than the Abrolhos samples. The AVC rocks comprise a discrete and different group when compared with the VTR on the basis of incompatible, immobile trace elements. Abrolhos Archipelago rocks comprise a Paleocene-Eocene transitional basalt series of alkaline affinity with relatively evolved rocks with high TiO_2 contents, while VTR volcanic edifices comprise a Miocene-Pleistocene strongly undersaturated alkaline affinity series with the less evolved samples. Yet, at the spidergram and REE diagrams, the Abrolhos Islands signatures overlap the VTR field, with less enrichment in AVC contents for most of the elements. Both magmatism show geochemical signatures typical from OIB intraplate magmatic settings, such as absence of negative Nb and Ta anomalies, and low Zr/Nb and Y/Nb ratios. The Abrolhos islands rocks show lower contents of the REE_L and slightly higher values of the middle and heavy REE when compared with the VTR. These differences in La/Yb_N ratios must have resulted from the different degrees of partial melting from the same mantle source. Trace element compositions of VTR Seamounts (Vitória, Montague, Jaseur, Dogressa, Davis, and Colúmbia) are consistent with $\leq 4\%$ partial melting of the mantle source in the garnet stability field, while the bibliography suggests a degree of partial melting ranging from 10% to 15% for AVC lavas derived from a garnet-lherzolite. AVC litho-geochemical data points to an involvement of a complex evolutionary process, possibly the magma replenishment, tapping, and fractionation (RTF) process that is probably related to a plumbing system with interconnected dykes, sills, and other structures shapes. The VTR magmatism is also potentially related to a multiple-stage plumbing system.

Most Sr-Nd-Pb isotope signatures of the Abrolhos Islands overlap the main VTR range and modeling of the Nd-Sr isotopic data points out to a common mantle source for the AVC and VTR magmatism. The model proposed in this work for explaining the AVC isotopic signatures comprises a depleted asthenospheric mantle (DMM) enriched by fragments of metasomatized subcontinental lithospheric mantle (SCLM; EMI component) detached during the Gondwana break up and/or with a delamination of the South American subcontinental lithospheric mantle caused by edge-driven convection. The presence of a recycled subducted oceanic crust related to a HIMU-type endmember is necessary to explain the AVC and the VTR Pb signatures. The assimilation of these oceanic crust slabs is linked to the Brasiliano Event

due to the Nd modal ages from AVC and VTR ranging from 407 Ma to 767 Ma, and 420 Ma to 640 Ma, respectively. The slight differences in the VTR and AVC isotopic ratios would be associated with different proportions in the mixture of these three mantle components (DMM, EMI and HIMU). The petrogenetic model aforementioned was also proposed for VTR, thus pointing to a cogenetic relationship between these magmatism. Model mixing calculations performed here suggest a mixture with 75% of DMM, <15% of EMI, and possibly up to 10% of HIMU in the AVC source. For VTR seamounts and islands the mixture would be 90% of DMM with <10% of EMI, and for Vitória Seamount and Davis Bank the EMI contributions vary from 20% to 25% in the DMM. Finally, the volcanic alignment between the VTR and AVC, along with the overlap of geochemical and isotopic data of their different igneous rocks, cannot be a random circumstance but instead represent the sampling of a common shallow mantle source, thus suggesting a cogenetic relationship.

REFERENCES

- ALMEIDA, F.F.M. As ilhas oceânicas brasileiras e suas relações com a tectônica do Atlântico Sul. *Terræ didática*, v. 2, p. 3-18, 2006.
- ALMEIDA, F.F.M. Origem e Evolução da Plataforma Brasileira. *Bol. Div. Geol. Min. DNPM*, Rio de Janeiro, n. 241, p. 1-36, 1967.
- ALMEIDA, F.F.M.; CARNEIRO, C.D.R.; MIZUSAKI, A.M.P. Correlação do magmatismo das bacias da margem continental Brasileira com o das áreas emersas adjacentes. *Revista Brasileira de Geociências*, v. 26, p. 125-138, 1996.
- ALVES, E.C.; MAIA, M.; SICHEL, S.E.; CAMPOS, C.M.P. Zona de Fratura de Vitória-trindade no Atlântico Sudeste e suas implicações tectônicas. *Revista Brasileira de Geofísica*, v. 24, p. 117–127, 2006.
- ALVES, E.C.; ARAUJO, R.S.; RAMOS, E.C.; MAIA, M.; SANTOS, A.C.; HACKSPACHER, P.C. Chapter 2 - Ocean fracture zones: their evolution and impact on tectonic and magmatism of the South and Southeast Brazilian continental margin. 2022. In: SANTOS, A.C.; HACKSPACHER, P.C. Meso-Cenozoic Brazilian Offshore Magmatism: Geochemistry, Petrology and Tectonics. Elsevier Inc., 2021, p. 47-94.
- AMARAL, G.; BUSHEE, J.; CORDANI, U.G.; KAWASHITA, K.; REYNOLDS, J.H. Potassium–argon ages of alkaline rocks from southern Brasil. *Geochimica et Cosmochimica Acta*, v. 31, p. 117–142, 1967.
- ARENA, Michele Correia. Petrologia da Sucessão Magmática do Arquipélago de Abrolhos. 2008. 113 fl. Dissertação (Mestrado em Geologia) – Faculdade de Geologia, Universidade do Estado do Rio de Janeiro, Rio de Janeiro, 2008.
- ARENA, M.C.; VALENTE, S.; VALLADARES, C.S.; DUARTE, B. P.; HEILBRON, M.; CORVAL, A.; SZATMARI, P. Petrologia da Sucessão Magmática do Arquipélago de Abrolhos. In: IV SIMPÓSIO DE VULCANISMO E AMBIENTES ASSOCIADOS, 2008, Foz do Iguaçu. Anais... São Paulo: Acquacon, 2008.
- BARÃO, L.M.; TRZASKOS, B.; ANGULO, R.J.; DE SOUZA, M.C.; DAUFENBACH, H.F.; SANTOS, F.A.; VASCONCELLOS, E.M.G. Deformational structures developed in volcanic sequences as a product of tectonic adjustments in the South Atlantic Ocean. *Journal of South American Earth Sciences*, v. 104, 102812, 2020.
- BONGIOLO, E.M.; PIRES, G.L.C.; GERALDES, M.C.; SANTOS A.C.; NEUMANN R. Geochemical modeling and Nd-Sr data links nephelinite-phonolite successions and xenoliths of Trindade Island (South Atlantic Ocean, Brazil). *Journal of Volcanology and Geothermal Research*, v. 306, p. 58–73, 2015.
- CELLI, N.L.; LEBEDEV, S.; SCHAEFFER, A.J.; RAVENNA, N.; GAINA, C. The upper mantle beneath the South Atlantic Ocean. South America and Africa from waveform

tomography with massive data sets. *Geophysical Journal International*, v. 221, p. 178–204, 2020.

COLLI, L.; GHELICHKHAN, S.; BUNGE, H.-P.; OESER, J. Retrodictions of Mid Paleogene mantle flow and dynamic topography in the Atlantic region from compressible high resolution adjoint mantle convection models: Sensitivity to deep mantle viscosity and tomographic input model. *Gondwana Research*, v. 53, p. 252–272, 2018.

COLLI, L.; STOTZ, I.; BUNGE, H.P.; SMETHURST, M.; CLARK, S.; IAFFALDANO, G.; TASSARA, A.; GUILLOCHEAU, F.; BIANCHI, M.C. Rapid South Atlantic spreading changes and coeval vertical motion in surrounding continents: evidence for temporal changes of pressure-driven upper mantle flow. *Tectonics*, v. 33, 1304–21, 2014.

CONCEIÇÃO, J.C.J.; MISUZAKI, A.M.P.; ALVES, D.B.; SZATMARI, P. Controle tectônico do magmatismo do Complexo Vulcânico de Abrolhos, Bacia do Espírito Santo. In: CONGRESSO BRASILEIRO DE GEOLOGIA, 39, 1996, Camboriu, Anais... Camboriu: SBG. v. 5, p. 384-387, 1996.

CORDANI, U.G. Idade do vulcanismo do Oceano Atlântico Sul. *Boletim do Instituto de Geociências e Astronomia (IGA-USP)*, v. 1, p. 9-75, 1970.

CORDANI, U.G.; BLAZEKOVIC, A. Idades radiométricas das rochas vulcânicas dos Abrolhos. In: 24º CONGRESSO BRASILEIRO DE GEOLOGIA, 1970, Brasília. Anais... Brasília. p. 265-270, 1970.

COX, K.G. Numerical Modelling of a Randomized RTF Magma Chamber: A Comparison with Continental Flood Basalt Sequences. *Journal of Petrology*, v. 29, n. 3, p. 681-697, 1988.

ERNESTO, M. Determinação da curva de deriva polar aparente para o Mesozóico da América do Sul, Thesis, IAG/USP, 56 pp, 1996.

FAINSTEIN, R.; SUMMERHAYS, C. P. Structure and origin of marginal banks off eastern Brazil. *Marine Geology*, v. 46, p. 199-215, 1982.

FAIRHEAD, M.J.; WILSON, M. Plate tectonic processes in the south Atlantic ocean: do we need deep mantle plumes? In: FOULGER, G.R.; NATLAND, J.H.; PRESNALL, D.C.; ANDERSON, D.L. (Eds.), *Plates, Plumes, and Paradigms*. Geological Society of America, p. 537–554, 2005.

FERRARI, A.; RICCOMINI, C. Campo de esforços Plio Pleistocênico na Ilha de Trindade (Oceano Atlântico Sul, Brasil) e sua relação com a tectônica regional. *Revista Brasileira de Geociências*, v. 29, n. 2, p. 195-202, 1999.

FODOR, R.V.; HANAN, B.B. Geochemical evidence for the Trindade Hotspot trace: Columbia seamount ankaramite. *Lithos*, v. 51, p. 293–304, 2000.

FODOR, R.V.; MCKEE, E.H.; ASMUS, H.E. K-Ar ages and the opening of the South Atlantic Ocean: basaltic rock from the Brazilian margin. *Marine Geology*, v. 54, M1-M8, 1983.

FODOR, R.V.; MUKASA, S.B.; GOMES, C.B.; CORDANI, U.G. Ti-rich eocene basaltic rocks, abrolhos platform, Offshore Brazil, 18°S: Petrology with respect to South Atlantic magmatism. *Journal of Petrology*, v. 30, p.763–786, 1989.

FRANÇA, R.L.; DEL REY, A.C.; TAGLIARI, C.V.; BRANDÃO, J.R.; FONTANELLI, P.R. Bacia do Espírito Santo. In: MILANI, E.J.; RANGEL, H.D.; BUENO, G.V.; STICA, J.M.; WINTER, W.R.; CAIXETA, J.M.; PESSOA NETO, O.C. (eds.). Bacias Sedimentares Brasileiras - Cartas Estratigráficas. *Boletim de Geociências da Petrobras*, Rio de Janeiro, v. 15, p.501-509, 2007.

GERALDES, M.C.; MOTOKI, A.; COSTA, A.; MOTA, C.E.; MOHRIAK, W.U. Geochronology (Ar/Ar and K-Ar) of the South Atlantic post-break-up magmatism. *Geological Society London Special Publications*, v. 369, n. 1, p. 41-74, 2013.

GIBSON, S.A.; THOMPSON, R.N.; LEONARDOS, O.H.; DICKIN, A.P.; MITCHELL, J.G. The Late Cretaceous impact of the Trindade mantle plume: Evidence from large-volume; mafic, potassic magmatism in SE Brazil. *Journal of Petrology*, v. 36, p. 189-229, 1995.

GIBSON, S.A.; THOMPSON, R.N.; LEONARDOS, O.H.; DICKIN A.P., MITCHELL J.G. The limited extent of plume-lithosphere interactions during continental flood-basalt genesis: Geochemical evidence from Cretaceous magmatism in southern Brazil. *Contributions to Mineralogy and Petrology*, v. 137, p. 147–169, 1999.

GIBSON, S.A.; THOMPSON, R.N.; WESKA, R.K.; DICKIN, A.P.; LEONARDOS, O.H. Late Cretaceous rift-related upwelling and melting of the Trindade starting mantle plume head beneath western Brazil. *Contributions to Mineralogy and Petrology*, v. 126, p. 303-314, 1997.

GOMES, N.S.; BORBA, R.P.; CUNHA, E.M. Alteração hidrotermal em diabásios do Banco de Abrolhos, Bacia do Espírito Santo, Brasil: Resultados preliminares. In: XXXVII CONGRESSO DE GEOLOGIA, 1992, São Paulo. Boletim de Resumos Expandidos... São Paulo: Sociedade Brasileira de Geologia, p. 60-61, 1992.

GOMES, N.S.; SUITA, M.T.F. Ocorrência de vulcanismo bimodal de idade terciária na Bacia de Mucuri. *Boletim de Geociências da Petrobras*, v. 18, n. 2, p. 232–248, 2010.

GORDON, R.G.; JURDY, D.M. Cenozoic global plate motions. *Journal of Geophysical Research*, v. 91, p. 12.389-12.406, 1986.

GRIPP, A.E.; GORDON, R.G. Current plate velocities relative to the hotspot incorporating the NUVEL1 global plate motion model. *Geophysical Research Letters*, v. 17, p. 1109–1112, 1990.

HALLIDAY, A.N.; DAVIES, G.R.; LEE, D.C.; TOMMASINI, S.; OASLICK, C.R.; FITTON, J.G.; JAMES D.E. Lead isotope evidence for young trace element enrichment in the oceanic upper mantle. *Nature*, v. 359, p. 623-627, 1992.

HILL, R.I. Starting plumes and continental break-up. *Earth and Planetary Science Letters*, v. 104, p. 398–416, 1991.

JAPSEN, P.; BONOW, J.M.; GREEN, P.F.; COBBOLD, P.R.; CHIOSSI, D.; LILLETVEIT, R.; MAGNAVITA, L.P.; PEDREIRA, A. Episodic burial and exhumation in NE Brazil after opening of the South Atlantic. *Geological Society of America Bulletin*, v. 124, n. 5/6, p. 800-816, 2012.

JESUS, J.V.M.; SANTOS, A.C.; MENDES, J.C.; SANTOS, W.H.; REGO, C.A.Q.; GERALDES, M.C. Petrogênese do Banco Davis, Cadeia Vitória-Trindade, Atlântico Sul: o Papel de Voláteis (H₂O e CO₂) na Evolução Magmática do Banco Davis. *Anuário do Instituto de Geociências*, v.42, p. 237–253, 2019.

LE ROEX, A.P.; CLASS, C.; O’CONNOR, J.; JOKAT, W. Shona and Discovery Aseismic Ridge Systems, South Atlantic: Trace Element Evidence for Enriched Mantle Sources. *Journal of Petrology*, v. 51, p. 2089–2120, 2010.

MAIA, T.M. Petrologia inédita das rochas do Monte Submarino Vitória, Cadeia Vitória Trindade, Atlântico Sul. 2019. 2019, 92 p. Monography Geology Bsc. Course, Rio de Janeiro State University, Rio de Janeiro, Brazil, 2019.

MAIA, T.M.; SANTOS, A.C.; ROCHA-JÚNIOR, E.R.V.; VALERIANO, C.M.; MENDES, J.C.; JECK, I.K.; SANTOS, W.H.; OLIVEIRA, A.L.; MOHRIAK, W.U. First petrologic data for Vitória Seamount, Vitória-Trindade Ridge, South Atlantic: a contribution to the Trindade mantle plume evolution. *Journal of South American Earth Sciences*, v. 109, 103304, 2021.

MARQUES, L.S.; ULBRICH, M.N.C.; RUBERTI, E.; TASSINARI, C.G. Petrology, geochemistry and Sr-Nd isotopes of the Trindade and Martin Vaz volcanic rocks (Southern Atlantic Ocean). *Journal of Volcanology and Geothermal Research*, v. 93, p.191–216, 1999.

MATTE, R.R. Sedimentologia e estratigrafia das ilhas de Santa Bárbara e Redonda, Arquipélago dos Abrolhos, sul da Bahia. *Boletim de Geociências da Petrobras*, v. 21, n. 2, p. 369-384, 2013.

MOHRIAK, W.U. Interpretação geológica e geofísica da Bacia do Espírito Santo e da região de Abrolhos: petrografia, datação radiométrica e visualização sísmica das rochas vulcânicas. *Boletim de Geociências da Petrobras*, v. 14, n. 1, p. 133-142, 2006.

MOHRIAK, W.U. Genesis and evolution of the South Atlantic volcanic islands offshore Brazil. *Geo-Marine Letters*, v. 40, p. 1–33, 2020.

MOHRIAK, W. U.; PAULA, O.; SZATMARI, P.; SOBREIRA, J. F.; PARSONS, M.; MACQUEEN, J.; UNDLI, T. H.; BERSTAD, S.; WEBER, M.; HORSTAD, I. Volcanic provinces in the Eastern Brazilian margin: geophysical models and alternative geodynamic interpretations. In: INTERNATIONAL CONGRESS OF THE BRAZILIAN GEOPHYSICAL SOCIETY, 8., 2003, Rio de Janeiro. Rio de Janeiro: Sociedade Brasileira de Geofísica, 2003. 1 CD-ROM, 4f

MONTEIRO, L.G.P.; SANTOS, A.C.; PIRES, G.L.C.; BARÃO, L.M.; ROCHA-JÚNIOR, E.R.V.; BIANCINI, J.R.C.; HACKSPACHER, P.C.; JÚNIOR, H.I.A.; JECK, I.K.; SANTOS, J.F. Chapter 10 - Trindade Island: evolution of the geological knowledge. 2022. In: SANTOS, A.C.; HACKSPACHER, P.C. Meso-Cenozoic Brazilian Offshore Magmatism: Geochemistry, Petrology and Tectonics. Elsevier Inc., 2021, p. 337-390.

MOTOKI, A.; NOVAIS, L.C.C.; SICHEL, S.E.; NEVES, J.L., AIRES, J.R. Felsic pyroclastic rock originated from subaqueous eruption in the Espírito Santo sedimentary basin: an association with the tectonic-sedimentary model. *Geociências*, v. 26, n. 2, p. 151–160, 2007.

MÜLLER, R.D.; SETON, M.; ZAHIROVIC, S.; WILLIAMS, S.E.; MATTHEWS, K.J.; WRIGHT, N.M.; SHEPHARD, G.E.; MALONEY, K.T.; BARNETT-MOORE, N.; HOSSEINPOUR, M.; BOWER, D.J.; CANNON, J. Ocean Basin Evolution and Global-Scale Plate Reorganization Events Since Pangea Breakup. *Annual Review of Earth and Planetary Sciences*, v. 44, p. 107–138, 2016.

NIU, Y.; WILSON, M.; HUMPHREYS, E.R.; O'HARA, M.J. A trace element perspective on the source of ocean island basalts (OIB) and fate of subducted ocean crust (SOC) and mantle lithosphere (SML). *Episodes*, v. 35, p. 310-327, 2012.

NOVAIS, L.C.C.; ZELENKA, T.; SZATMARI, P.; MOTOKI, A.; AIRES, J.R.; TAGLIARI, C.V. Ocorrência de rochas vulcânicas ignimbríticas na porção norte da Bacia do Espírito Santo: evolução do modelo tectono-sedimentar. *Boletim de Geociências da Petrobras*, v. 16, n. 1, p. 139–156, 2008.

O'CONNOR, J.M.; DUNCAN, R.A. Evolution of the Walvis Ridge–Rio Grande Rise hot spot system: implications for African and South American plate motions over plumes. *Journal of Geophysical Research*, v. 95, p. 17475–17502, 1990.

De OLIVEIRA, A.L.; DOS SANTOS, A.C.; NOGUEIRA, C.C.; MAIA, T.M.; GERALDES, M.C. Green core clinopyroxenes from Martin Vaz Archipelago Plio-Pleistocene alkaline rocks, South Atlantic Ocean, Brazil: A magma mixing and polybaric crystallization record. *Journal of South American Earth Sciences*, 102951, 2021.

O'HARA, M.J.; MATHEWS, R.E. Geochemical evolution in an advancing, periodically replenished, periodically tapped, continuously fractionated magma chamber. *Journal of the Geological Society*, v. 138, p. 237-277, 1981.

OLIVEIRA, L.C.; OLIVEIRA R.M.A.G., PEREIRA; E. Seismic characteristics of the onshore Abrolhos magmatism, East-Brazilian continental margin. *Marine and Petroleum Geology*, v. 89, p. 488-499, 2018.

PEARCE, J.A.; NORRY, M.J. Petrogenetic implications of Ti, Zr, Y and Nb variations in volcanic rocks. *Contributions to Mineralogy and Petrology*, v. 69, p. 33–47, 1979.

PEYVE, A.A.; SKOLOTNEV, S.G. Systematic variations in the composition of volcanic rocks in tectono-magmatic seamount chains in the Brazil Basin. *Geochemistry International*, v. 52, p. 111–130, 2014.

PIRES, G.L.C.; BONGIOLO, E.M. The nephelinitic–phonolitic volcanism of the Trindade Island (South Atlantic Ocean): Review of the stratigraphy, and inferences on the volcanic styles and sources of nephelinites. *Journal of South American Earth Sciences*, v. 72, p. 49-62, 2016.

PIRES, G.L.C.; BONGIOLO, E.M.; GERALDES, M.C.; RENAC, C.; SANTOS, A.C.; JOURDAN, F.; NEUMANN, R. New $^{40}\text{Ar}/^{39}\text{Ar}$ ages and revised $^{40}\text{K}/^{40}\text{Ar}^*$ data from

nephelinitic–phonolitic volcanic successions of the Trindade Island (South Atlantic Ocean). *Journal of Volcanology and Geothermal Research*, v. 327, p. 531-538, 2016.

QUARESMA, G.O.A. Geoquímica Isotópica Sr-Nd-Pb e Geocronologia $^{40}\text{Ar}/^{39}\text{Ar}$ do Banco Submarino Davis, Cadeia Vitória-Trindade: Possíveis Implicações com a Movimentação da Placa Sul-Americana durante o Mioceno. 121 p. Monography Geology Bsc. Course, Rio de Janeiro State University, Rio de Janeiro, Brazil, 2019.

QUARESMA, G.O.A.; SANTOS, A.C.; ROCHA-JÚNIOR, E.R.V.; BONIFÁCIO, J.; REGO, C.A.Q.; MATTIELLI, N.; MATA, J.; JOURDAN, F.; GERALDES, M.C. Isotopic Constraints on Davis Bank, Vitória-Trindade Ridge: A Revisited Petrogenetic Model. *Journal of South American Earth Sciences*, in press.

REGO, C.A.Q.; QUARESMA, G.O.; SANTOS, A.C.; MOHRIAK, W.U.; JESUS, J.V.M.; RODRIGUES, S.W.O. Davis Bank geodynamic context, South Atlantic Ocean: Insights into the Vitória-Trindade Ridge evolution. *Journal of South American Earth Sciences*, v. 112, 103620, 2021.

RIBEIRO FILHO, E.; CORDANI, U.G. Contemporaneidade das intrusões de rochas alcalinas do Itatiaia, Passa Quatro e Morro Redondo. Publ. 1, Núcleo do Rio de Janeiro. Sociedade Brasileira de Geologia, v. 1, 6263, 1996.

RICCOMINI, C.; SANT'ANNA, L.G.; FERRARI, A.L. Evolução geológica do rift continental do sudeste do Brasil. In: MANTESSO-NETO, V.; BARTORELLI, A.; CARNEIRO, C.D.R.; BRITO-NEVES, B.B. (Eds.). Geologia do continente Sul-Americano: Evolução da obra de Fernando Flávio Marques de Almeida. São Paulo, Editora Beca, 673p, 2004.

SADOWSKI, G.R.; DIAS NETO, C.M. O lineamento sismotectônico de Cabo Frio. *Revista Brasileira de Geociências*, v. 11, p. 209–21, 1981.

SANTOS, A.C. Petrography, Litho geochemistry and $^{40}\text{Ar}/^{39}\text{Ar}$ dating of the seamounts and Martin Vaz Islands -Vitoria-Trindade Ridge. Dissertation, Universidade do Estado do Rio de Janeiro, Brazil, 2013.

SANTOS, A.C. Petrology of Martin Vaz Island and Vitoria-Trindade Ridge seamounts: Montague, Jaseur, Davis, Dogaressa and Columbia. Trace elements, $^{40}\text{Ar}/^{39}\text{Ar}$ dating and Sr and Nd isotope analysis related to the Trindade Plume evidence. Ph. D. Thesis, Universidade do Estado do Rio de Janeiro, Brazil, 2016.

SANTOS, A.C.; GERALDES, M.C.; VARGAS, T.; WILLIAMS, S. Geology of Martin Vaz, South Atlantic, Brazil. *Journal of Maps*, v. 11, p. 314–322, 2015.

SANTOS, A.C.; GERALDES, M.C.; SIEBEL, W.; MENDES, J.; BONGIOLO, E.; SANTOS, W.H.; GARRIDO, T.C.V., RODRIGUES S.W.O. Pleistocene alkaline rocks of Martin Vaz volcano, South Atlantic: low-degree partial melts of a CO_2 -metasomatized mantle plume. *International Geology Review*, v. 61, p. 296–313, 2018a.

SANTOS, A.C.; HACKSPACHER, P.C. Meso-Cenozoic Brazilian Offshore Magmatism: Geochemistry, Petrology and Tectonics. Elsevier Inc., 2021.

SANTOS, A.C.; MATA, J.; JOURDAN, F.; RODRIGUES, S.W. DE O.; MONTEIRO, L.G.P.; GUEDES, E.; BENEDINI, L.; GERALDES, M.C. Martin Vaz island geochronology: Constraint on the Trindade Mantle Plume track from the youngest and easternmost volcanic episodes. *Journal Of South American Earth Sciences*, v. 106, 103090, 2021.

SANTOS, A.C.; MOHRIAK, W.U.; GERALDES, M.C.; SANTOS, W.H.; PONTE-NETO, C.F.; STANTON, N. Compiled potential field data and seismic surveys across the Eastern Brazilian continental margin integrated with new magnetometric profiles and stratigraphic configuration for Trindade Island, South Atlantic, Brazil. *International Geology Review*, v. 61, p. 1728-1744, 2018b.

SANTOS, A.C.; OLIVEIRA, O.L.; BEVILAQUA, L.A.; ROCHA-JÚNIOR, E.R.V.; RODRIGUES, S.W.O.; MENDES, J.C.; JECK, I.K. Chapter 11 - Martin Vaz Archipelago: the youngest magmatism in the Brazilian Territory. 2022a. In: SANTOS, A.C., HACKSPACHER, P.C. Meso-Cenozoic Brazilian Offshore Magmatism: Geochemistry, Petrology and Tectonics. Elsevier Inc., 2021, p. 391-432.

SANTOS, A.C.; ROCHA-JÚNIOR, E.R.V.; QUARESMA, G.O.A.; MAIA, T.M.; JESUS, J.V.M.; REGO, C.A.Q.; JECK, I.K. Chapter 9 - Vitória-Trindade seamounts: undersaturated alkaline series evolution from an enriched metasomatized source. 2022b. In: SANTOS, A.C., HACKSPACHER, P.C. Meso-Cenozoic Brazilian Offshore Magmatism: Geochemistry, Petrology and Tectonics. Elsevier Inc., 2021, p. 293-336.

SEMPERE, T.; FOLGUERA, A.; GERBAULT, M. New insights into Andean evolution: An introduction to contributions from the 6th ISAG symposium (Barcelona, 2005). *Tectonophysics*, 459, p. 1–13, 2008.

SIEBEL, W.; BECCHIO, R.; VOLKER, F.; HANSEN, M.A.F.; VIRAMONTE, J.; TRUMBULL, R.B.; HAASE, G.; ZIMMER, M. Trindade and Martin Vaz Islands, South Atlantic: Isotopic (Sr, Nd, Pb) and trace element constraints on plume related magmatism. *Journal of South American Earth Science*, v. 13, p. 79–103, 2000.

SKOLOTNEV, S.G.; BYLINSKAYA, M.E.; GOLOVINA, L.A.; IPATEVA, I.S. First Data on the Age of Rocks from the Central Part of the Vitória–Trindade Ridge (Brazil Basin, South Atlantic). *Doklady Earth Sciences*, v. 437, p. 316–322, 2011.

SKOLOTNEV, S.G.; PEIVE, A.A. Composition, structure, origin, and evolution of off-axis linear volcanic structures of the Brazil Basin, South Atlantic. *Geotectonics*, v. 51, p. 53–73, 2017.

SKOLOTNEV, S.G.; PEYVE, A.A.; TURKO, N.N. New Data on the Structure of the Vitoria Trindade Seamount Chain (Western Brazil Basin, South Atlantic). *Doklady Earth Sciences*, v. 431, n. 2, p. 435-440, 2010.

SLEEP, N.H. Lateral flow of hot plume material ponded at sublithospheric depths. *Journal of Geophysical Research*, v. 101, p. 28065–28083, 1996.

SLEEP, N.H. Lateral flow and ponding of starting plume material. *Journal of Geophysical Research*, v. 102, p. 10001–10012, 1997.

SOBREIRA, J.F.F. Complexo Vulcânico de Abrolhos: proposta de modelo tectono-magmático. In: CONGRESSO BRASILEIRO DE GEOLOGIA, 1996, Salvador, Anais... São Paulo: Sociedade Brasileira de Geologia, v. 5, p. 387-391, 1996.

SOBREIRA, J.F.F.; FRANÇA R.L. Um modelo tectono-magmático para a região do Complexo Vulcânico de Abrolhos. *Boletim de Geociências da Petrobras*, v. 14, p. 143-147, 2006.

SOBREIRA, J.F.F.; SZATMARI, P.; MOHRIAK, W.U.; VALENTE, S.C.; YORK, D. Recorrência, em diferentes escalas, do magmatismo paleogênico no Arquipélago de Abrolhos, Complexo Vulcânico de Abrolhos. XLII CONGRESSO BRASILEIRO DE GEOLOGIA, 2004, Araxá, Minas Gerais. Anais... Araxá, 2004.

SOBREIRA, J.F.F.; SZATMARI, P. Datações Ar-Ar Das Rochas Vulcânicas De Abrolhos E Implicações para a Evolução da Margem Continental Leste Brasileira No Terciário. XLI CONGRESSO BRASILEIRO DE GEOLOGIA, 2002, João Pessoa, Pernambuco, Anais... João Pessoa, p. 395, 2002.

SOBREIRA, J.F.F.; SZATMARI, P. Idades Ar-Ar para as rochas ígneas do Arquipélago de Abrolhos, margem sul da Bahia. In: SIMPÓSIO NACIONAL DE ESTUDOS TECTÔNICOS, 9, 2003, Búzios. Boletim de Resumos... Búzios. p. 382-383, 2003.

SOMOZA, R. Updated Nazca (Farallon)-South America relative motions during the last 40 My: Implications for mountain building in the central Andean region. *Journal of South American Earth Sciences*, v. 11, p. 211-215, 1998.

SONOKI, I.K.; GARDA, G.M. Idades K/Ar de rochas alcalinas do Brasil Meridional e Paraguai Oriental: compilação e adaptação às novas constantes de decaimento. Boletim IG-USP, Série Científica 19, p. 63-85, 1988.

STANTON, N.; GORDON, A.; CARDOZO, C.; KUSZNIR, N. Morphostructure, emplacement and duration of the Abrolhos Magmatic Province: A geophysical analysis of the largest post-breakup magmatism of the South-Eastern Brazilian Margin. *Marine and Petroleum Geology*, v. 133, 105230, 2021.

STANTON, N.; GORDON, A.C.; VALENTE, S.C.; MOHRIAK, W.U.; MAIA, T.M.; ARENA, M. Chapter 6 - The Abrolhos Magmatic Province, the largest postbreakup magmatism of the Eastern Brazilian margin: a geological, geophysical, and geochemical review. 2022. In: SANTOS, A.C.; HACKSPACHER, P.C. Meso-Cenozoic Brazilian Offshore Magmatism: Geochemistry, Petrology and Tectonics. Elsevier Inc., 2021, p. 189-230.

SZATMARI, P.; MOHRIAK, W.U. Plate model of post-breakup tectono-magmatic activity in the adjacent Atlantic. In: SIMPÓSIO NACIONAL DE ESTUDOS TECTÔNICOS, 5, 1995, Gramado. Anais... Gramado: SBG/Núcleo Rio grande do Sul, p. 213-214, 1995.

TEBBENS, S.; CANDE, S. Southeast Pacific tectonic evolution from Early Oligocene to present. *Journal of Geophysical Research*, v. 102, p. 12061-12084, 1997.

THOMAZ-FILHO, A.; CESERO, P.; MARIA, A.; LEA, J.G. Hot spot volcanic tracks and their implications for south American plate motion, Campos basin (Rio de Janeiro state), Brazil. *Journal of South American Earth Sciences*, v. 18, p. 383–389, 2005.

THOMAZ-FILHO, A.; RODRIGUES, A.L. O alinhamento de rochas alcalinas Poços de Caldas-Cabo Frio (RJ) e sua continuidade na Cadeia Vitória-Trindade. *Revista Brasileira de Geociências*, v. 29, n. 2, p. 189-194, 1999.

THOMPSON, R.N.; GIBSON, S.A. Subcontinental mantle plumes, hot spots and pre-existing thinspots. *Journal of the Geological Society*, v. 148, p. 973–977, 1991.

THOMPSON, R.N.; GIBSON, S.A.; MITCHELL, J.G.; DICKIN, A.P.; LEONARDOS, O.H.; BROD, J.A.; GREENWOOD, J.C. Migrating Cretaceous – Eocene Magmatism in the Serra do Mar Alkaline Province, SE Brazil: Melts from the Deflected Trindade Mantle Plume? *Journal of Petrology*, v. 39, p. 1493–1526, 1998.

VALENCIO, D.A.; MENDÍA, J.E. Palaeomagnetism and K/Ar Ages of Some Igneous Rocks Of The Trindade Complex And The Valado Formation, From Trindade Island, Brazil. *Revista Brasileira de Geociências*, v. 4, p. 124-132, 1974.

VELOSO, J.A.V.; MACHADO, D.L. Estudos sismológicos na ilha da Trindade desenvolvidos pela estação sismológica da UnB. In: CONGRESSO BRASILEIRO DE GEOLOGIA, 34, 1986, Goiânia. Anais... Goiânia: SBG, 6, p. 2.608-2.613, 1986.

VIEIRA, V.S.; NOVAIS, L.C.C.; SILVA, M.A.; CORRÊA, T.R.; LOPES, N.H.B. Caracterização geoquímica das rochas ignimbríticas no noroeste do estado do Espírito Santo. In: CONGRESSO BRASILEIRO DE GEOLOGIA, 47., 2014, Salvador. Anais... Salvador: SBG Núcleo Bahia, 2014. 1CD-ROM.

XIA, L.; LI, X., 2019. Basalt geochemistry as a diagnostic indicator of tectonic setting. *Gondwana Research*, v. 65, p. 43–67, 2019.

ZALÁN, P.V.; OLIVEIRA, J.A. Origem e evolução estrutural do sistema de riftes cenozóicos do sudeste do Brasil. In: SIMPÓSIO DO CRETÁCEO DO BRASIL, 7, 2001, Serra Negra. Boletim... Serra Negra: SBG, p. 24-27, 2001.

ZALÁN, P.V.; OLIVEIRA, J.A.B. Origem e evolução estrutural do Sistema de Riftes Cenozóicos do Sudeste do Brasil. *Boletim de Geociências da Petrobras*, v. 13, n. 2, 2005.

APPENDIX A – First petrologic data for Vitória Seamount, Vitória-Trindade Ridge, South Atlantic: a contribution to the Trindade mantle plume evolution (published paper on August/2021 in Journal of South American Earth Sciences - DOI: <https://doi.org/10.1016/j.jsames.2021.103304>)

First petrologic data for Vitória Seamount, Vitória-Trindade Ridge, South Atlantic: a contribution to the Trindade Mantle Plume evolution

Thais Mothé Maia^{1a}; Anderson Costa dos Santos^{1b}; Eduardo Reis Viana Rocha Júnior²; Claudio de Morisson Valeriano^{3a}; Julio Cezar Mendes⁴; Izabel King Jeck⁵; Werlem Holanda dos Santos¹; André Leite de Oliveira^{1c}; Webster Ueipass Mohriak³

¹Universidade do Estado do Rio de Janeiro (UERJ), Faculdade de Geologia, Departamento de Mineralogia e Petrologia Ígnea (DMPI). Rua São Francisco Xavier, 524 - 4º e 2º andar. Maracanã, 20550-900, Rio de Janeiro, RJ, Brasil. ^{1a}Orcid: 0000-0002-5956-6362. ^{1b} Tektos Group, UERJ - Brazil / GeoBioTec Group, Aveiro University - Portugal. Orcid: 0000-0003-2526-8620. ^{1c}Orcid: 0000-0001-6340-5679

²Universidade Federal da Bahia (UFBA), Instituto de Física, Departamento de Física da Terra e do Meio Ambiente. Rua Barão de Jeremoabo, s/n, 40170-115, Salvador (BA), Brasil. Orcid: 0000-0003-1853-015X

³Universidade do Estado do Rio de Janeiro (UERJ), Faculdade de Geologia, Departamento de Geologia Regional e Geotectônica (DGRG). Rua São Francisco Xavier, 524 - 4º e 2º andar/bloco A, 20550-900, Rio de Janeiro, RJ, Brasil. ^{3a}Orcid: 0000-0002-9341-2615

⁴Universidade Federal do Rio de Janeiro, Instituto de Geociências, Departamento de Geologia. Av. Athos da Silveira Ramos, 274, 21941-916, Rio de Janeiro (RJ), Brasil. Orcid: 0000-0002-4332-8802

⁵LEPLAC (Brazilian Continental Shelf Survey Program), Directorate of Hydrography and Navigation, Brazilian Navy, Barão de Jaceguai s/n. Ponta da Armação, Niterói, RJ, Brazil.

Emails: thais_mothe@hotmail.com; andcostasantos@gmail.com; eduardo.junior@ufba.br; valeriano.claudio@gmail.com; julio@geologia.ufrj.br; izabelkj@hotmail.com; werlem.santos@uerj.br; andre.leite.quatis@gmail.com; webmohr@gmail.com

Abstract

The Vitória Seamount (VTS), distant *ca.* 300 km from the Brazilian coastline at latitude 20°S, is the second closest offshore volcanic complex of the Vitória-Trindade Ridge (VTR) which corresponds to a *ca.* 1200 km long ridge of seamounts and islands composed of SiO₂-undersaturated magmatic rocks commonly considered to be the volcanic track of the Trindade mantle plume in the South American Plate. Based on the first sample dredged from Vitória Seamount, new petrographic and electron microprobe analyses from its rock show an alkaline basalt with pseudo trachytic texture consisting of bytownite and salite phenocrysts, labradorite microliths, anhedral titanomagnetite, and a yellowish green pseudomorphous phase composed of MgO-Al₂O₃-SiO₂-FeO. The fine-grained groundmass is mainly composed of strongly oriented lath-shaped labradorite microliths, opaque minerals, and vesicles filled by a yellowish green

pseudomorph phase. Whole-rock analyses of the Vitória Seamount rock reveal its SiO₂ undersaturation (SiO₂ *ca.* 40 wt.%; normative nepheline = 13.8), enrichment in Cr, Co, Ni, V and Sc, along with depletion in Zr, La and Nd contents compared to the other seamounts of the VTR. VTS show a strong enrichment in light-REE (La/Sm_N *ca.* 2.68) compared to heavy-REE (La/Yb_N = 20.79). Major and trace element evidence indicate that the melting of an enriched mantle source to generate the Vitória Seamount magma occurred dominantly in the garnet stability field. Trace element composition of VTS is consistent with $\leq 3\%$ partial melting of the mantle source. Neodymium and Sr isotopic data suggest that the mantle source of the Vitória Seamount had been variably metasomatized by melts derived from enriched mantle component, which may have developed approximately 600 Ma, reconciling with the Brasiliano Orogeny, according to Nd age model. Modeling of the Nd-Sr isotope systematics points out that the primary melt was formed from an asthenospheric mantle (DMM – Depleted MORB [Mid-Ocean Ridge Basalts] Mantle) that underwent mixing with a continentally derived material (represented by EMI [Enriched Mantle I] component). This process can be explained by the mixing of melts from these mantle components during magma genesis.

Keywords: Aseismic Volcanic Ridge, Eocene-Pleistocene Volcanism, Geochemical Modeling, Mantle Reservoirs.

1 Introduction

The Vitória Seamount (*ca.* 4700 km³) located offshore Brazil at *ca.* 20°S, south of the Besnard Bank, is the second closest offshore volcanic edifice of the Vitória-Trindade Ridge (VTR), which some authors interpreted as the Trindade Plume volcanic trail on the South American Plate (Fig. 1) (see references for details - Gibson et al., 1999; Fodor & Hanan, 2000; Siebel et al., 2000, Santos, 2013; Bongiolo et al., 2015; Pires et al., 2016; Santos, 2016; Santos et al., 2018a, 2018b). Marques et al. (1999) also brought up the hypotheses that the Trindade Island's extrusive materials could come from stratified magma chambers that might be periodically replenished with ultrabasic magmas in the late stages of magmatic activity. The VTR is believed to be associated with the Vitória-Trindade Fracture Zone, that acted as a conduit for this enriched mantle-derived magmatism (Veloso & Machado, 1986; Szatmari & Mohriak, 1995; Conceição et al., 1996; Ferrari & Riccomini, 1999; Almeida, 2006; Alves et al., 2006).

The VTR is a west-east-trending alkaline igneous province that extends from the Brazilian eastern shelf to the deep-water portion of the southern Atlantic Ocean, towards the Trindade Archipelago located *ca.* 1200 km away from the coastline. This aseismic ridge is composed of several alkaline seamounts, banks, guyots, and islands. VTR's morphology studies date back to the 1950s and during the period 1972-78 an agreement between several Brazilian institutions gave rise to the REMAC project, which is a global reconnaissance of the Brazilian

Continental Margin project. Hereafter, LEPLAC Program (Brazilian Continental Shelf Survey Program – 1987-2020) was started and carried out several surveys along the Brazilian margin, especially in the last decade, when additional multibeam bathymetric data were acquired in the VTR region, so that all banks and seamounts could be better described.

The most expressive submerged volcanic edifices (Fig. 2) correspond to the Besnard Bank (55 m), southeast of the Abrolhos Volcanic Complex (AVC), the Vitória Seamount (52 m), Congress Bank (63 m), the Champlain Seamount (62 m), the Jaseur Seamount (54 m), the Montague Seamount (57 m), the Colúmbia Bank (60 m), the Davis Bank (61 m), the Asmus Bank, the Dogaressa Bank (54 m), the Colúmbia Seamount (96 m), the Motoki Hill, and the Palma Seamount, as well as the Trindade Island and the Martin Vaz Archipelago, which represent the easternmost and emerged segment of the ridge (Almeida, 2006; Santos et al., 2018a, 2018b). The magmatic rocks of this aseismic ridge have typical oceanic island basalts (OIBs) geochemical signatures, since they are characterized by the occurrence of alkaline rocks enriched in titanium (mean $\text{TiO}_2 = 4.1$ wt. %) and other incompatible lithophile trace elements (*e.g.*, enrichment in light rare earth elements [LREE]). Some geochemical and isotopic studies (*e.g.*, Marques et al., 1999; Siebel et al., 2000; Santos, 2013, 2016) carried out at the VTR indicate that these rocks were derived from magmas that originated from an asthenosphere-like source (DMM) metasomatized by recycled component (represented by EMI).

This work presents the first petrographic, mineralogical, geochemical, and isotopic data of the Vitória Seamount (VTS) magmatic rock, since it is the first sample dredged from this seamount. The goal of this study is to further characterize the mantle source(s) and the processes involved in the genesis of the Vitória Seamount using the first data of this magmatism, as well as comparing these data with the other VTR magmatic rocks and Abrolhos Volcanic Complex.

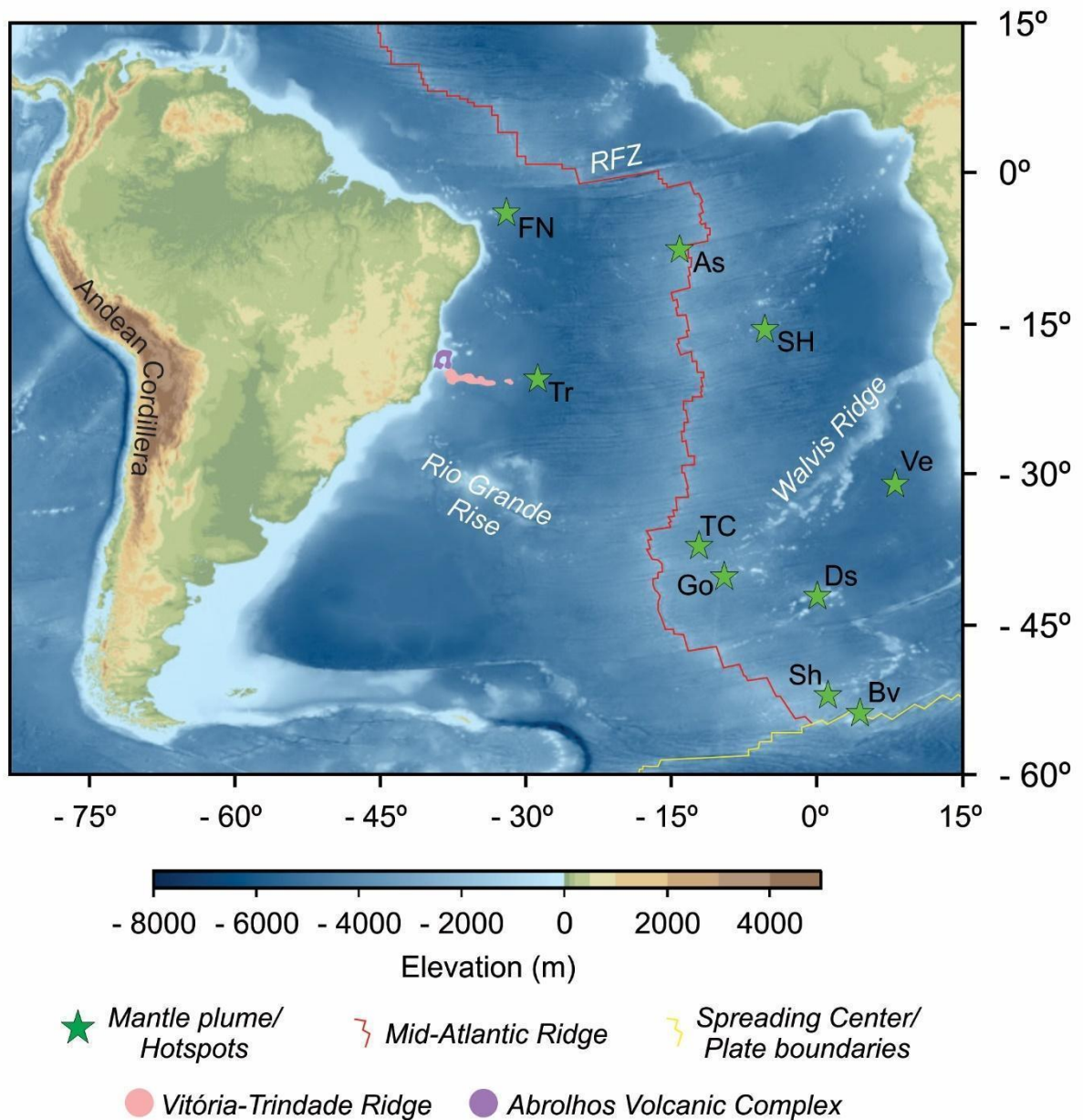


Fig. 1 Topographic map of the South Atlantic region (modified from Celli et al., 2020). Vitória-Trindade Ridge is shown in light pink and Abrolhos Volcanic Complex is shown in light purple. Mantle plumes/Hotspots are shown as green stars: As – Ascension; Bv – Bouvet; Ds – Discovery; FN – Fernando de Noronha; Go – Gough; Sh – Shona; SH – Saint Helena; TC – Tristan da Cunha; Tr – Trindade; Ve – Vema. Oceanic features: RFZ, Romanche Fracture Zone. Spreading centers/plate boundaries are shown in yellow lines and the Mid-Atlantic Ridge is shown in red lines.

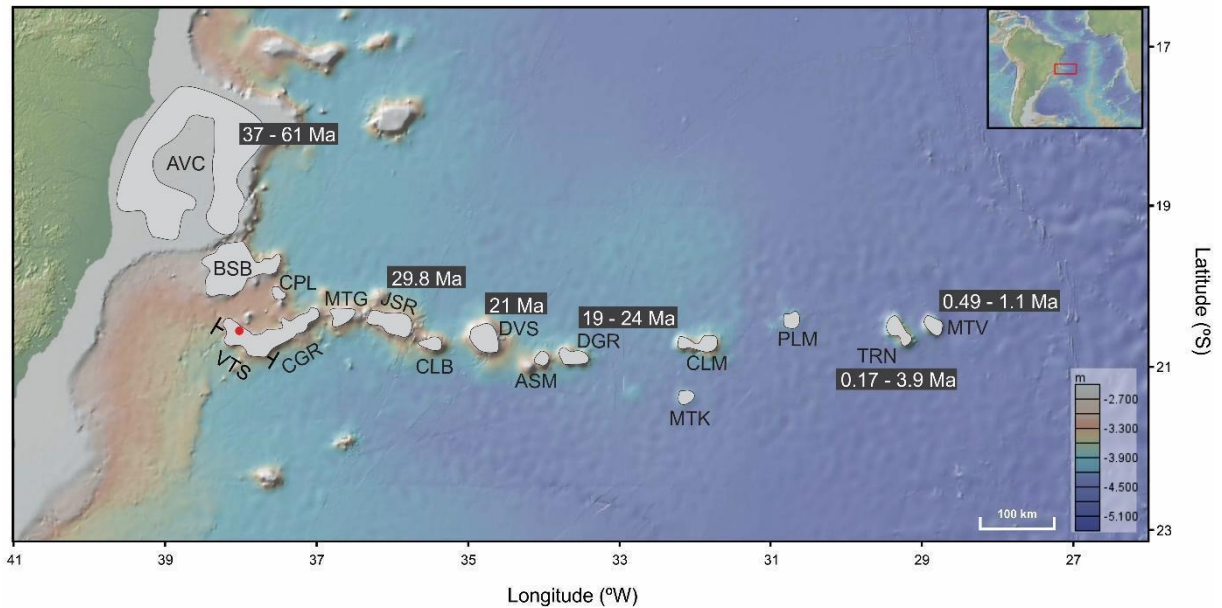


Fig. 2 Regional bathymetric map of the Brazilian southeastern continental margin. Dredged sample location is shown by the red point over the Vitória Seamount (VTS). The bathymetric profile of the VTS is shown in Figure 3. Sources: AVC – Abrolhos Volcanic Complex (ages from Cordani, 1970; Cordani and Blazekovic, 1970; Fodor et al., 1983; Mizusaki et al., 1994; Sobreira et al., 2004); BSB – Besnard Bank; CPL – Champlain Seamount; VTS – Vitória Seamount; CGR – Congress Seamount; MTG – Montague Seamount; JSR – Jaseur Seamount (ages from Skolotnev et al., 2011); CLB – Colúmbia Bank; DVS – Davis Bank (ages from Santos, 2016; Skolotnev & Peive, 2017, Quaresma, 2019); ASM – Asmus Bank; DGR – Dogaressa Bank (ages from Skolotnev et al., 2011); CLM – Colúmbia Seamount; MTK – Motoki Hill; PLM – Palma Seamount; TRN – Trindade Island (ages from Cordani, 1970; Pires et al., 2016); MTV – Martin Vaz Archipelago (ages from Mizusaki et al., 1998; Santos, 2013; Santos et al., 2015; Santos et al., 2021).

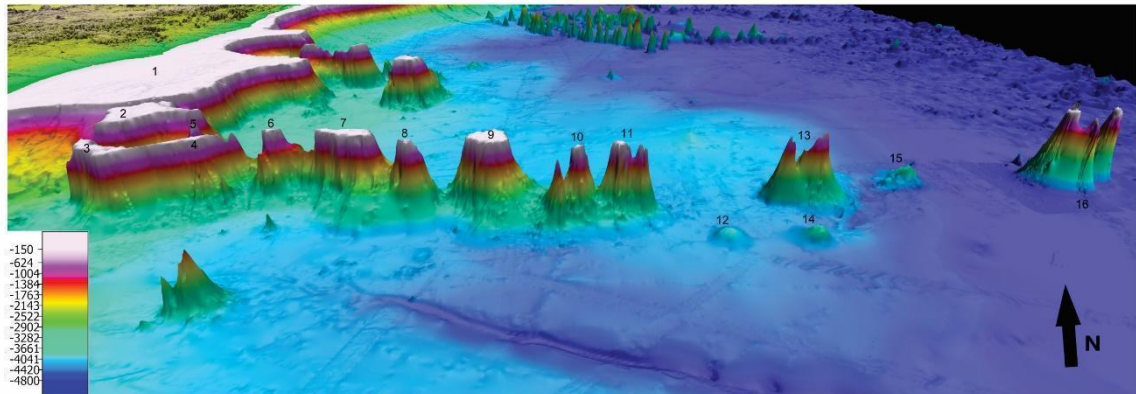
2 Geological background

The VTS is located 300 km eastwards of the Brazilian coastline. It lies between 52 m and 70 m water depth, similar to the Jaseur, Davis, and Congress edifices (Gorini, 1969). Its flat top reaches a width of 48 km due to an erosional process related to the last Pleistocenic ice age marine transgression. The VTS is connected to the Congress Bank, forming an elongated and inflected bank in its middle portion, being 30 km wide with a total extension of 150 km. It is characterized by a planar top with a total area of 1420 km², incomparably larger than the other seamounts and volcanic buildings along the VTR (Fig. 3).

The Vitória Seamount and the Congress Bank were described as part of the continental shelf fragment, which was detached from Abrolhos Platform and transported during the early stages of Gondwana break-up to their present position (Motoki et al., 2012). Considering that

this hypothesis was based only on geomorphological observations, the origin of the Vitória Seamount will be discussed in this paper based on petrological data.

(a)



(b)

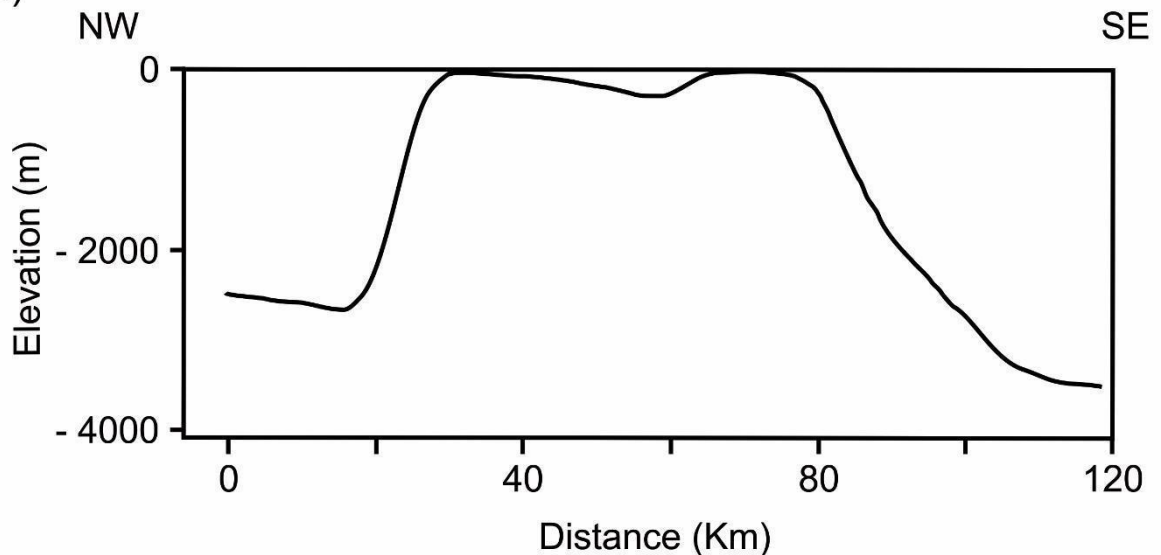


Fig. 3 (a) 3D color DTM view over the Vitória-Trindade Ridge from Abrolhos Shelf to Trindade and Martin Vaz Islands. 1 – Abrolhos Shelf, 2 – Besnard Bank, 3 – Vitória Seamount, 4 – Congress Bank, 5 – Champlain Seamount, 6 – Montague Seamount, 7 – Jaseur Seamount, 8 – Colúmbia Bank, 9 – Davis Bank, 10 – Asmus Bank, 11 – Dogaressa Bank, 12 – Gilberto Amado Hill, 13 – Columbia Seamount, 14 – Motoki Hill, 15 – Palma Seamount, 16 – Trindade and Martin Vaz Islands. It is possible to see the connection between Vitória Seamount and Congress Bank, and the inflection in the middle. (b) Simplified NW-SE bathymetric profile of the VTS, displaying the geometry of the volcanic edifice showing its flat top that reaches a width of 48 km (see Figure 2 for identification of the profile localization).

The Vitória-Trindade Ridge is composed of undersaturated and saturated alkaline lavas (Marques et al., 1999; Fodor and Hanan, 2000; Siebel et al., 2000; Santos, 2013; Peyve & Skolotnev, 2014; Bongioiolo et al., 2015; Pires et al., 2016; Santos, 2016; Santos et al., 2018a, 2018b). Its lavas are characterized by ultrabasic to intermediate signatures ($\sim 36\text{-}57$ SiO₂ wt. %)

with high MgO contents (~10-15 wt. %). Davis Bank are basic and characterized by a more evolved rock composed of basanite from a high fractionated liquid (MgO *ca.* 4 wt.%; Jesus et al., 2019), which is an exception among the VTR seamounts and banks. Besides that, those rocks are characterized by a strong enrichment in LREE typical of alkaline OIBs. Isotopically, the VTR samples have slightly radiogenic Sr isotopes ($^{87}\text{Sr}/^{86}\text{Sr}$ ratios ranging from 0.703607 to 0.703946), and slightly radiogenic Nd isotopes ($^{143}\text{Nd}/^{144}\text{Nd}$ ratios varying between 0.512752 to 0.512837) (Marques et al., 1999; Fodor and Hanan, 2000; Siebel et al., 2000; Halliday et al., 1992; Santos 2013, 2016; Santos et al., 2018a; Supplementary Table 7). In contrast, the Davis Bank has a slightly more radiogenic $^{87}\text{Sr}/^{86}\text{Sr}$ ratio of *ca.* 0.704025, and more unradiogenic $^{143}\text{Nd}/^{144}\text{Nd}$ ratio of *ca.* 0.512629 when compared to the other VTR rocks (Santos 2013, 2016; Quaresma 2019).

Few ages for VTR rocks have been reported in the literature, but the ages of the seamounts, banks and island seem to become progressively younger eastwards, as such (Fig. 2): U-Pb zircon dating yielded ages of 29.8 ± 6.6 Ma for Jaseur Seamount (Skolotnev et al., 2011); based on $^{40}\text{Ar}/^{39}\text{Ar}$ dating of whole-rock and plagioclase and pyroxene minerals, Davis Bank average age of *ca.* 21 Ma was yielded (Santos 2016; Skolotnev & Peive, 2017, Quaresma 2019); Dogaressa Bank yielded ages ranging between 19 and 24 Ma from U-Pb dating in zircon (Skolotnev et al., 2011 - see text for details). Finally, Trindade Island has $^{40}\text{Ar}/^{39}\text{Ar}$ ages and revised $^{40}\text{K}/^{40}\text{Ar}$ ages ranging from 3.9 Ma to 0.17 Ma (Cordani, 1970; Pires et al., 2016) and the Martin Vaz Archipelago exhibited $^{40}\text{K}/^{40}\text{Ar}$ ages of 1.1 ± 0.5 Ma (Mizusaki et al., 1998) and $^{40}\text{Ar}/^{39}\text{Ar}$ ages ranging from 0.49 ± 0.08 Ma to 0.64 ± 0.08 Ma (Santos 2013; Santos et al., 2015; Santos et al., 2021) and a $^{40}\text{K}/^{40}\text{Ar}$ age of 0.83 ± 0.30 Ma (Brazilian Navy internal report – personal communication).

No geochronological ages are available for the Vitória Seamount. The VTS should have around 34 Ma considering an approximately 5 cm/year rate of South Atlantic velocity motion (Colli et al., 2014; Müller et al., 2016) and assuming a hotspot origin. Thus, it is somehow correlated with the final volcanic events in the South Abrolhos Bank, also possibly related to the Trindade plume (Fodor et al., 1989). Fodor and Hanan (2000) also considered the hotspot trail but based on a 3 cm/year rate of plate motion (Gripp and Gordon, 1990), estimated an age of about 10 Ma for the Colúmbia Seamount.

The Abrolhos Volcanic Complex (AVC - Fodor et al., 1989), located offshore Brazil at 18°S, northwest of the VTR, is also thought to be part of the aforementioned hotspot volcanic track, as the Trindade Plume's first expression in the passive continental margin (O'Connor & Duncan, 1990; Conceição et al., 1996; Ferrari & Riccomini, 1999; Thompson et al., 1998;

Sobreira et al., 2004; Alves et al., 2006; Mohriak, 2006). It is characterized by Paleocene-Eocene (37-61 Ma, $^{40}\text{K}/^{40}\text{Ar}$ and $^{40}\text{Ar}/^{39}\text{Ar}$ ages; Cordani, 1970; Cordani and Blazekovic, 1970; Fodor et al., 1983; Mizusaki et al., 1994; Sobreira et al., 2004) igneous rocks interbedded with sedimentary rocks. The volcanic sequences in the subsurface are composed of alkaline and tholeiitic basalts interbedded with sedimentary rocks and salt domes (Fodor et al., 1989; Sobreira and França, 2006; Mohriak, 2006) that occur in the middle/distal portion of the Espírito Santo, Mucuri and Cumuruxatiba sedimentary basins (Almeida et al., 1996; Mohriak, 2006; Sobreira & França, 2006; França et al., 2007). The Besnard Bank is considered coeval to the Abrolhos magmatism (Fainstein & Summerhayes, 1982) but lacks geochronological data to confirm the aforementioned assumption. However, exploratory drilling on top of the structure penetrated Cenozoic sediments above the volcanic rocks (Mohriak, 2006).

3 Material and methods

3.1 Sampling and preparation

The investigated rock was collected at lat. 20°35'58" S and long. 38°1'19" W (Fig. 2) from a depth of 1995 m by the Vitória-Trindade Ridge dredging project "Deep Sea Dredging, Offshore Brazil" hired by FEMAR and supported by the Brazilian Navy in 2010. The objective of this survey was to collect rock samples from seamounts throughout the Brazilian coast. The results of the analyses have been used to support the Brazilian Continental Shelf beyond 200 nautical miles Submission. Operations on the coordinates comprised three sub-bottom profile lines and five bags of samples, of which one fresh rock fragment was analyzed, being the first Vitória Seamount sample to be studied.

The sample was prepared at the Laboratório Geológico de Preparação de Amostras (LGPA) of the Universidade do Estado do Rio de Janeiro (UERJ) to obtain the powder for geochemical and isotopic analyses. The crushed sample was leached in HCl solution, hand-picked to eliminate clay-filled vesicles and grounded (200 mesh) with a tungsten ball Spex mill-mixer.

3.2 Whole-rock element composition analyses

Abundances of Al, Ca, Fe, K, Mg, Mn, Na, P, Ti, Ba, Cr, Sr, V, Y and Zn were determined by Inductively Coupled Plasma Atomic Emission Spectrometry (ICP-AES); and

Co, Cs, Ga, Mo, Nb, Pb, Rb, Sb, Th, U, W, Zr and Rare Earth Elements (REE) were analyzed by ICP-MS (Mass Spectrometry) at Activation Laboratories, Canada, following the procedures described by Hofmann (1992). Only one sample was analyzed due to the small volume of dredged rock.

3.3 Mineral element composition analyses

Mineral chemistry was determined at the Laboratório de Difração de Raios X e Microsonda Eletrônica (LABSONDA) of the Universidade Federal do Rio de Janeiro, Brazil, using a JEOL JXA-8230 five-spectrometer electron microprobe. Wavelength-Dispersive analyses were carried out using an accelerating voltage of 15 kV and beam current of 20 nA for silicate minerals, and 20 kV and 20 nA for opaque minerals. Quantitative analyses were obtained based on chemical data of Smithsonian Microbeam Standards (pyroxene and opaque mineral - Jarosewich, 2002) and Astimex pattern collection MINM25-53 (plagioclase).

3.4 Thermobarometry

Thermobarometer data were obtained with Putirka's geothermobarometry excel spreadsheets, available at <http://www.fresnostate.edu/csm/ees/faculty-staff/putirka.html>. Clinopyroxene estimates were based on Neave and Putirka (2017) model, plagioclase estimates were based on Putirka (2005) model. These models consider a temperature of 1100°C and one logarithmic unit above the quartz-fayalite-magnetite (QFM) buffer of oxygen fugacity and can be used for crystal-liquid equilibrium based on predicted and observed DiHd components approaches zero (Supplementary Table 6).

3.5 Sr and Nd isotopic analyses

The Sm-Nd (ID-TIMS) and Sr isotope analyses were performed in the Laboratório de Geocronologia e Isótopos Radiogênicos (LAGIR) at Universidade do Estado do Rio de Janeiro (UERJ) Brazil, using a multi-collector TRITON thermal ionization mass spectrometer (TIMS) (see Valeriano et al., 2003). The measured isotope ratios were normalized to $^{147}\text{Sm}/^{152}\text{Sm} = 0.56083$, $^{146}\text{Nd}/^{144}\text{Nd} = 0.7219$ and $^{86}\text{Sr}/^{88}\text{Sr} = 8.3752$. Repeated analyses (n=140) of $^{86}\text{Sr}/^{88}\text{Sr}$ for the NBS-987 (NIST) standard gave a mean value of $0.710239 \pm 0.000007(2\sigma)$. And the analyses (n=214) of the JNd1 (Tanaka et al., 2000) standard reference materials yielded mean

ratios $^{143}\text{Nd}/^{144}\text{Nd} = 0.512100 \pm 0.000006$ (2σ). The blanks recorded during the analyses were below 200 pg for Nd and less than 70 pg for Sm, while the Sr value had not been obtained. The results gave a variance in the penultimate decimal place (10^{-5}).

3.6 X-ray diffraction analyses (XRD)

The mineralogy was identified in the $< 63 \mu\text{m}$ fraction using the interplanar distances (d) of the minerals. The X-rays diffraction analysis were done in a Bruker-AXS D2 Advance Eco equipment in the Laboratório de Estratigrafia Química e Geoquímica Orgânica (LGQM), at the Universidade do Estado do Rio de Janeiro (UERJ), Brazil. The sample was scanned at a rate of $0,01^\circ 2\theta/\text{min}$ from 5° to $70^\circ 2\theta$. The qualitative interpretation of the spectrum was performed with a Bruker-AXS Diffrac.EVA software and PDF release 2014 RBDL database (ICDD, 2017). Qualitative mineralogical analysis followed the method described by Jesus et al., (2019) and Maia (2019).

3.7 Digital Terrain Model (DTM)

LEPLAC Program developed the Digital Terrain Model (DTM) on the VTR region, exhibit in Figure 3a, based on acquired single-beam and multi-beam bathymetric data (LEPLAC; Directorate of Hydrography and Navigation (DHN); Petróleo Brasileiro S.A (PETROBRAS); Brazilian National Agency of Oil, Gas, and Biocombustibles (ANP); public domain data from Brazilian and foreign institutions, among others).

In order to complement the bathymetric grid in distal regions of the margin (vicinities of Trindade and Martin Vaz Archipelago), between longitudes 29°W and 26°W , the SRTM30_PLUS data were used (data derived from the Shuttle Radar Topography Mission of National Aeronautics and Space Administration – NASA). So, with this qualified database, a DTM on the VTR region was developed with a grid cell-size varying from 1500 to 100 m, together with a detailed seafloor morphology. OASIS MONTAJ® software was used to expand and improve the data visualization capacity and FLEDERMAUS® to create the 3D views. The absence of bathymetric data in some regions, especially Trindade and Martin Vaz Islands, causes a difference in DTM resolution.

4 Results

The petrographic descriptions and whole-rock analysis were performed using only one available fresh sample. Two (duplicated) Sm-Nd (ID-TIMS) and Sr isotope analyses were obtained.

4.1 Petrography

The investigated sample is an alkaline basalt with porphyritic texture. The fine-grained pseudo trachytic groundmass is mainly composed of lath-shaped plagioclase microliths (< 0.2 mm in size; Fig. 4 A, B), opaque minerals (Fig. 4 C, D), and a yellowish green pseudomorphic phase (Fig. 4 E), similar to one described by Fodor and Hanan (2000) as greenish yellow smectite vesicles filled with a MgO-Al₂O₃-SO₃ hydrous phase. In some portions, the groundmass is slightly oxidized. The opaque minerals also occur as euhedral microphenocrysts and are 0.1-0.3 mm in size.

Pinkish-to-yellowish clinopyroxene microphenocrysts are subhedral to euhedral, generally < 0.8 mm in size and sometimes exhibit magmatic corrosion (Fig. 4 F) and hourglass twinning (Fig. 4 G, H), attesting disequilibrium with melt. Lath-shaped euhedral plagioclase crystals are enclosed by clinopyroxene, giving rise to a subophitic texture (Fig. 4 F, G, H). Plagioclase is also found as microphenocrysts. They are 0.2 – 0.5 mm in size, subhedral and have *Carlsbad* twinning, locally forming a glomeroporphyritic texture (Fig. 4 G, H).

XRD data were obtained to refine the mineralogical composition of the studied rock. Considering the principal and secondary interplanar distances (d) relative to the diffractometric reflections and their corresponding relative intensities, the following mineral phases were identified in the whole-rock analysis: labradorite, bytownite, clinopyroxene (augite), sanidine, ilmenite, and apatite (Fig. 5).

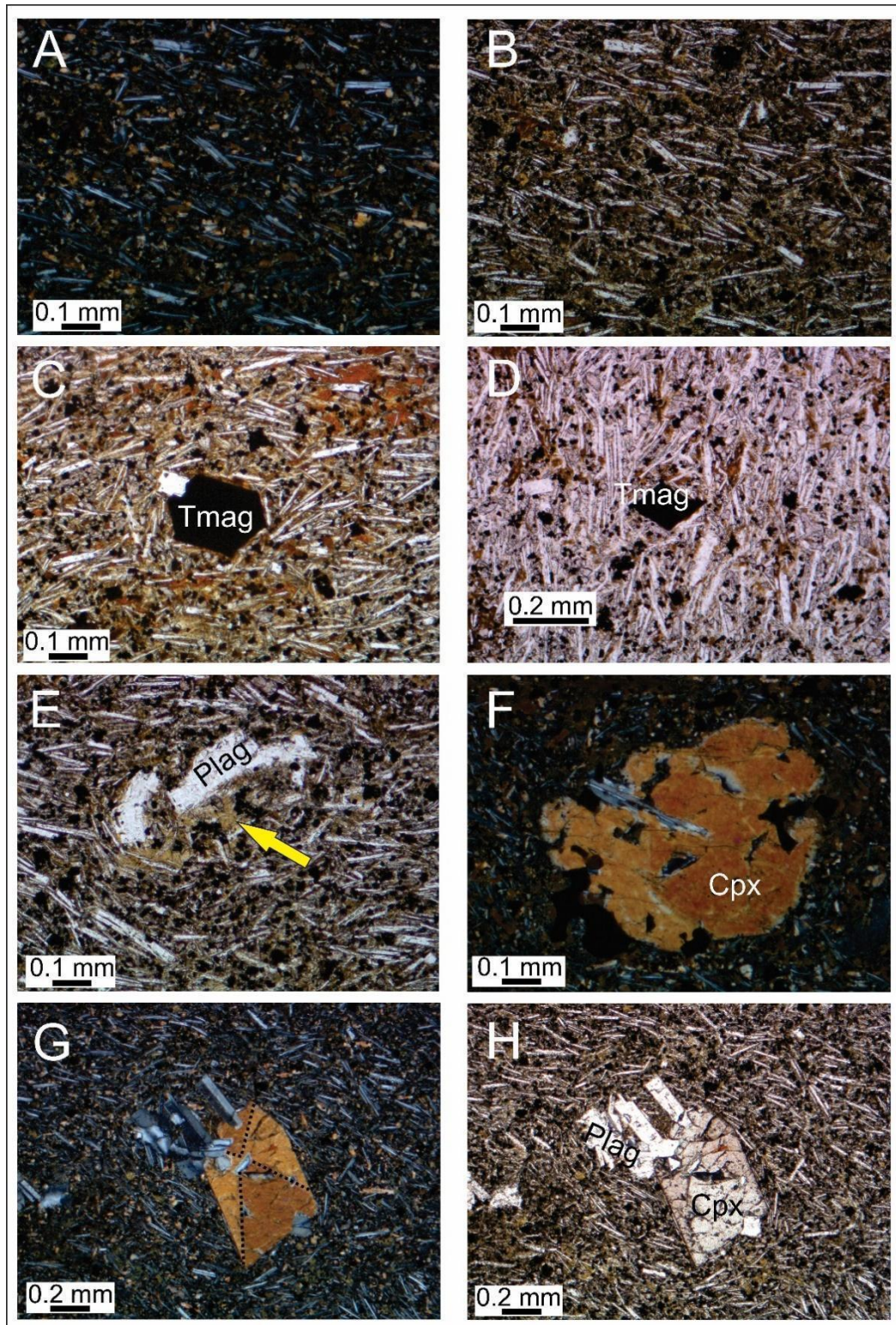


Fig. 4 Photomicrographs of the Vitória Seamount alkali basalt sample (TRIM-09B). A, F, G: crossed polarizers and B, C, D, E, H: parallel polarizers. Microlithic groundmass with plagioclase and opaque minerals. A, B: pseudo trachytic texture; C, D: euhedral opaque mineral (titanomagnetite - TMag) phenocrystal; E: greenish yellow pseudomorphic phase; F: clinopyroxene (Cpx) crystal with magmatic corrosion; G, H: hourglass-textured euhedral clinopyroxene crystal highlighted by the dotted lines; and glomeroporphyritic-textured feldspar (plagioclase - Plag) with *Carlsbad* twinning.

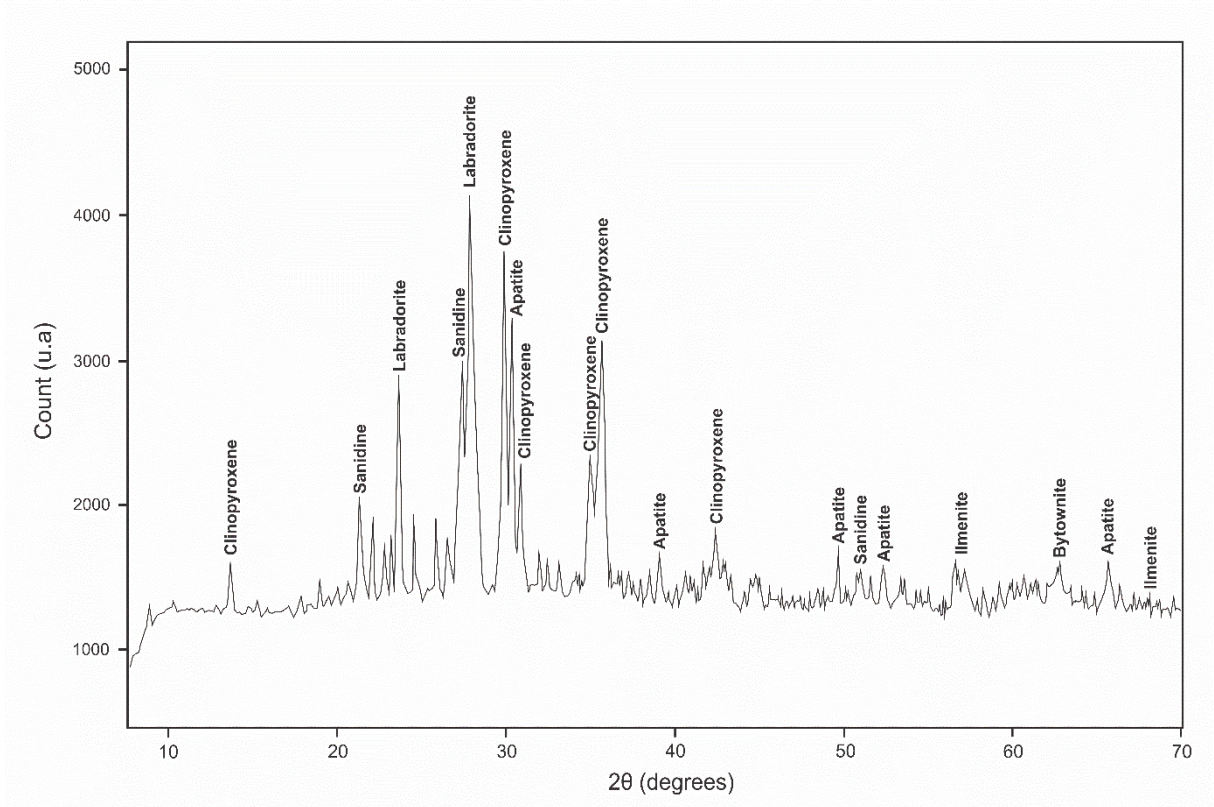


Fig. 5 X-Ray Diffractogram of the mineral composition of the alkaline basalt from the Vitória Seamount.

4.2 Mineral chemistry

4.2.1 Feldspar

The studied feldspars belong to the plagioclase group (Supplementary Table 1, Fig. 6). The microliths in the groundmass have labradorite compositions ($An_{65-66}Ab_{31-32}Or_{1-2}$), similar to the plagioclase composition in the Davis Bank rock samples (Jesus et al., 2019). The phenocrysts are homogeneous, and they did not show significant chemical variations showing bytownitic compositions ($An_{70-89}Ab_{11-29}Or_{0-1}$).

4.2.2 Clinopyroxene

The clinopyroxene phenocrysts (Supplementary Table 2, Fig. 7) are homogeneous salitic diopside ($Wo_{47-50}En_{37-42}Fs_{11-13}$). Locally show hourglass texture with slightly compositional variations. The clinopyroxene crystals are composed of more aluminous and titaniferous rims, such as the clinopyroxenes in Davis Bank (Jesus et al., 2019), and towards the cores a slightly more enrichment pattern in SiO_2 (range: 44.5 – 48.6 wt.%) and MgO (range:

12.5 – 14.2 wt.%). The CaO and Na₂O values do not show significant variations, as occur in Davis Bank (Jesus et al., 2019).

4.2.3 Opaque Minerals

The opaque minerals (Supplementary Table 3) composition is restricted to titanomagnetite. The microphenocrysts have TiO₂-rich (21.3 wt.%) rims, and also show an Al₂O₃ (15.5 wt.%), FeO (62.6 wt.%), and MgO (5.6 wt.%) enrichment towards the cores.

4.2.4 Yellowish Green Pseudomorphic Phase

The yellowish green pseudomorphic phase that occurs filling the vesicles is composed of SiO₂ (48.9 wt.%), Al₂O₃ (24.7 wt.%), CaO (16.5 wt.%), MgO (12.0 wt.%), FeO (8.9 wt.%), K₂O (4.5 wt.%) and Na₂O (1.9 wt.%), partially similar to the composition found by Fodor and Hanan (2000), except for the absence of sulfur (S) and presence of Si, Fe, K, Ca and Na.

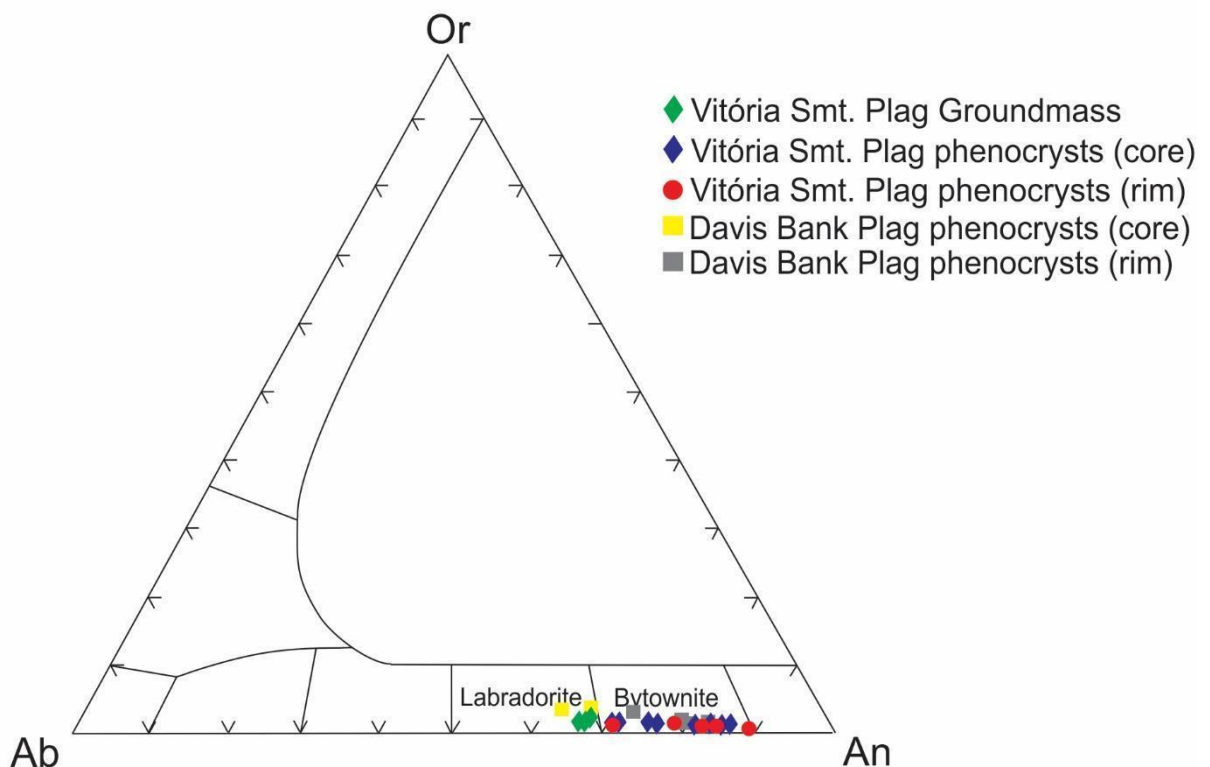


Fig. 6 Feldspars of the volcanic rock from the Vitória Seamount and Davis Bank (Jesus et al., 2019) plotted in the ternary classification diagram (Ab = albite, An = anorthite, Or = orthoclase, Plag = plagioclase).

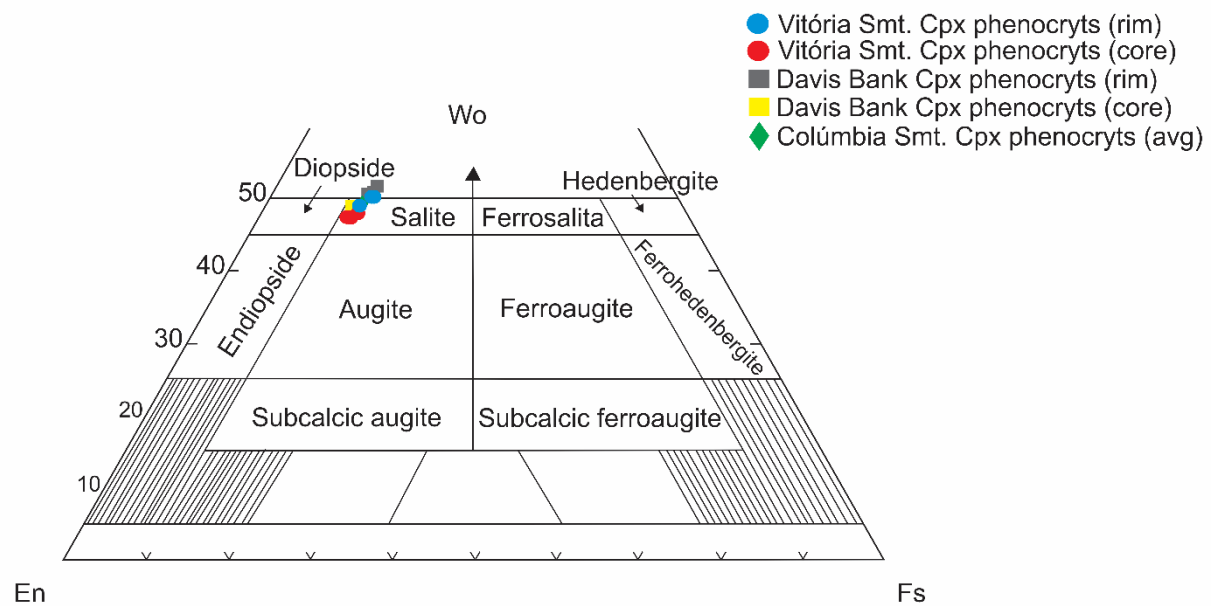


Fig. 7 Clinopyroxene of the volcanic rock from the Vitória Seamount, Davis Bank (Jesus et al., 2019) and Colúmbia Seamount (Fodor & Hanan, 2000) plotted in the ternary classification diagram (En = enstatite, Wo = wollastonite, Fs = ferrosalite, Cpx = clinopyroxene).

4.2.5 Thermobarometry

Thermobarometric data based on clinopyroxene compositions shows that phenocrysts rims are crystallized at slightly higher pressure (5.7 – 6.3 kbar) and temperature (1166.8 – 1173.5 °C) than cores (4.6 – 5.5 kbar and 1161.6 – 1170.4 °C). Unzoned phenocrysts show pressure ranging from 5.1 – 7.1 kbar and temperature from 1157.6 – 1180.3 °C.

When compared with Davis Bank thermobarometric data (Jesus et al., 2019), Vitória Seamount clinopyroxenes show a similar range of pressure and a higher temperature range. In comparison with Martin Vaz Archipelago data (Oliveira et al., 2021), Vitória Seamount clinopyroxene presents lower crystallization pressures and temperatures between the more evolved Martin Vaz member (phonolite) and the more primitive member (alkaline basalt, Fig. 8).

Plagioclase thermobarometric data indicates a similar temperature range for Vitória Seamount and Davis Bank (1065 – 1085 °C) but a lower pressure condition involved in Vitória plagioclases crystallization (*ca.* 4 kbar), while Davis Bank present *ca.* 9 kbar. But according to Putirka (2008), the plagioclase-liquid barometer is a quite questionable model because most thermometers are P sensitive. In this way, just plagioclase crystallization temperature should be considered in further discussions.

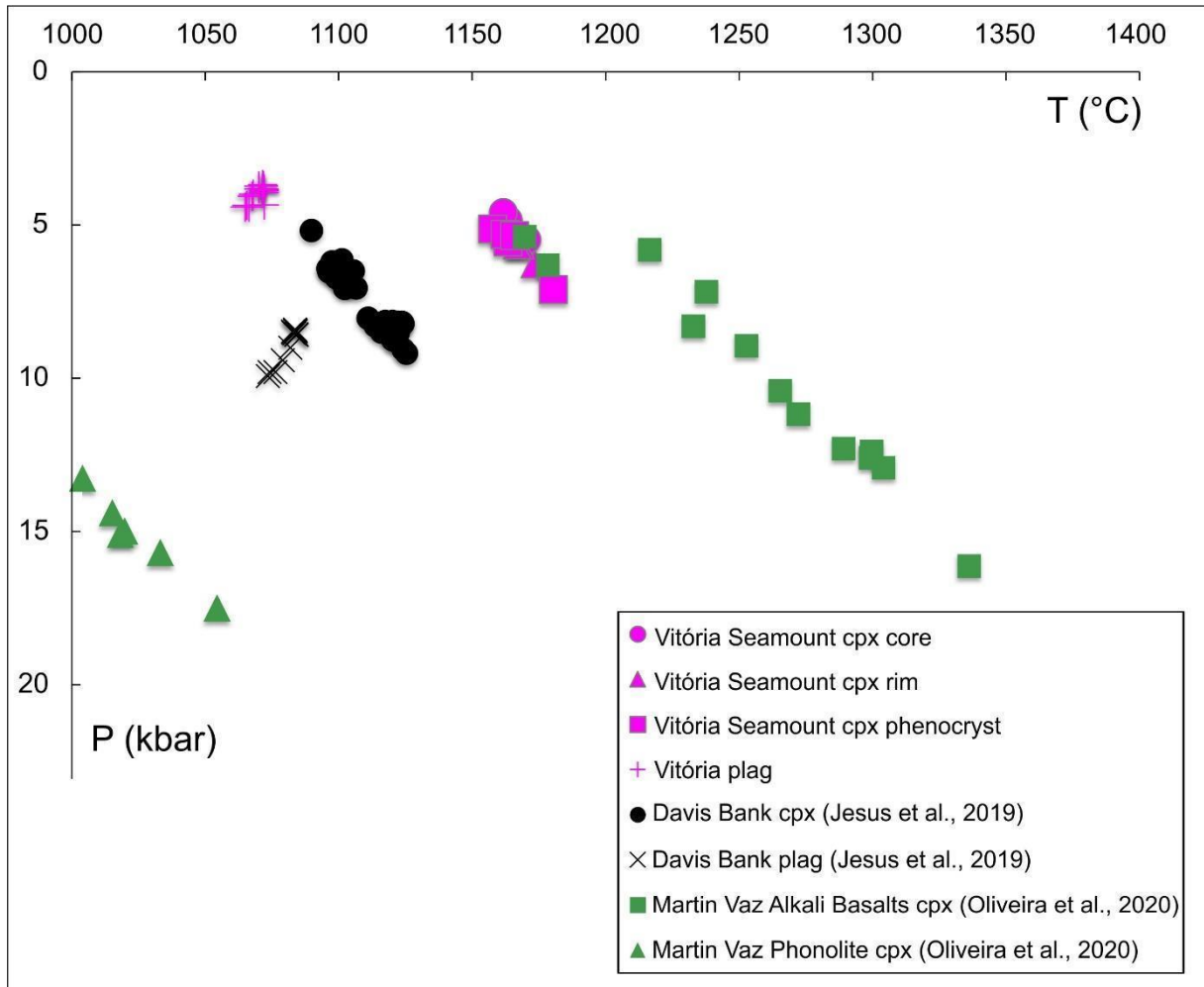


Fig. 8 P and T estimates diagrams for clinopyroxene and plagioclase crystallization, based on their compositions (Neave & Putirka, 2017; Putirka, 2005). Abbreviations: cpx – clinopyroxene; plag – plagioclase.

4.3 Whole-rock composition

One sample from Vitória Seamount was analyzed and data for major, minor and trace elements are given in Supplementary Table 4. In the geochemical and isotope diagrams further presented, the Vitória Seamount data is compared with other samples from the seamounts, banks, and islands along the Vitória-Trindade Ridge.

4.3.1 Major elements

The alkaline basalt dredged from the Vitória Seamount has a low LOI value (1 %). Based on the total alkali *versus* silica diagram (Cox et al., 1979, Fig. 9), the Vitória Seamount sample plots in the nephelinite field. As well as all the Vitória-Trindade Ridge rocks, with exception of Davis Bank, the Vitória Seamount sample has low SiO₂ (40.6 wt. %) and high MgO (11 wt. %) contents, which is expected for less evolved rocks (nephelinites and basanites).

Davis Bank, for comparison, is composed of a more evolved rock from a higher fractionated liquid (MgO *ca.* 4.0 wt. %; Jesus et al., 2019). The Vitória Seamount lava has moderate P₂O₅ (0.6 wt. %) contents and relatively high TiO₂ (5.2 wt. % - Fig. 10), which is in agreement with the other VTR seamounts and banks that show high-TiO₂ rocks (*avg.* 4.19 wt.%; Ti/Y = 869), with an TiO₂ fractionation on the more evolved ones. VTS also has high FeO content (7.7 wt. %), similar to those found in the Abrolhos Volcanic Complex. As for the alkalis content, VTS has slightly high Na₂O (4.3 wt. % - Fig. 10), and slightly low K₂O (0.9 wt. %), which are within the range of the VTR and AVC (4.8-0.7 wt. % and 3-0.4 wt. %, respectively). All VTR submerged edifices show sodic affinity and the most evolved rocks are the richest in alkalis. The Vitória Seamount CaO content is low (9.9 wt. %) compared to the other analyzed samples, resembling Davis Bank and Abrolhos Volcanic Complex.

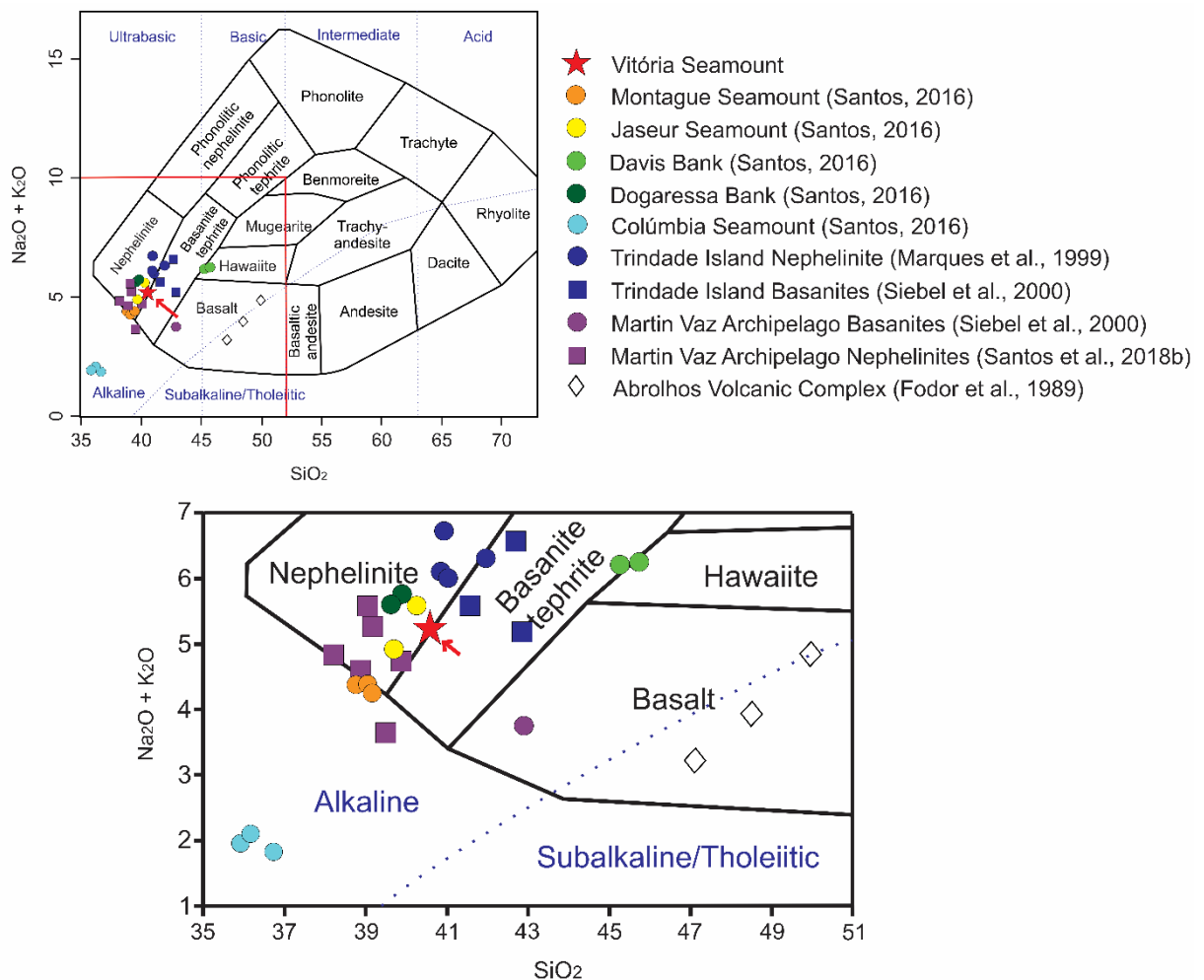


Fig. 9 Total alkali *versus* silica (TAS - Cox et al., 1979) diagram for Vitória Seamount (highlighted by the red arrow), Abrolhos Volcanic Complex and other Vitória-Trindade Ridge seamounts, banks, and islands.

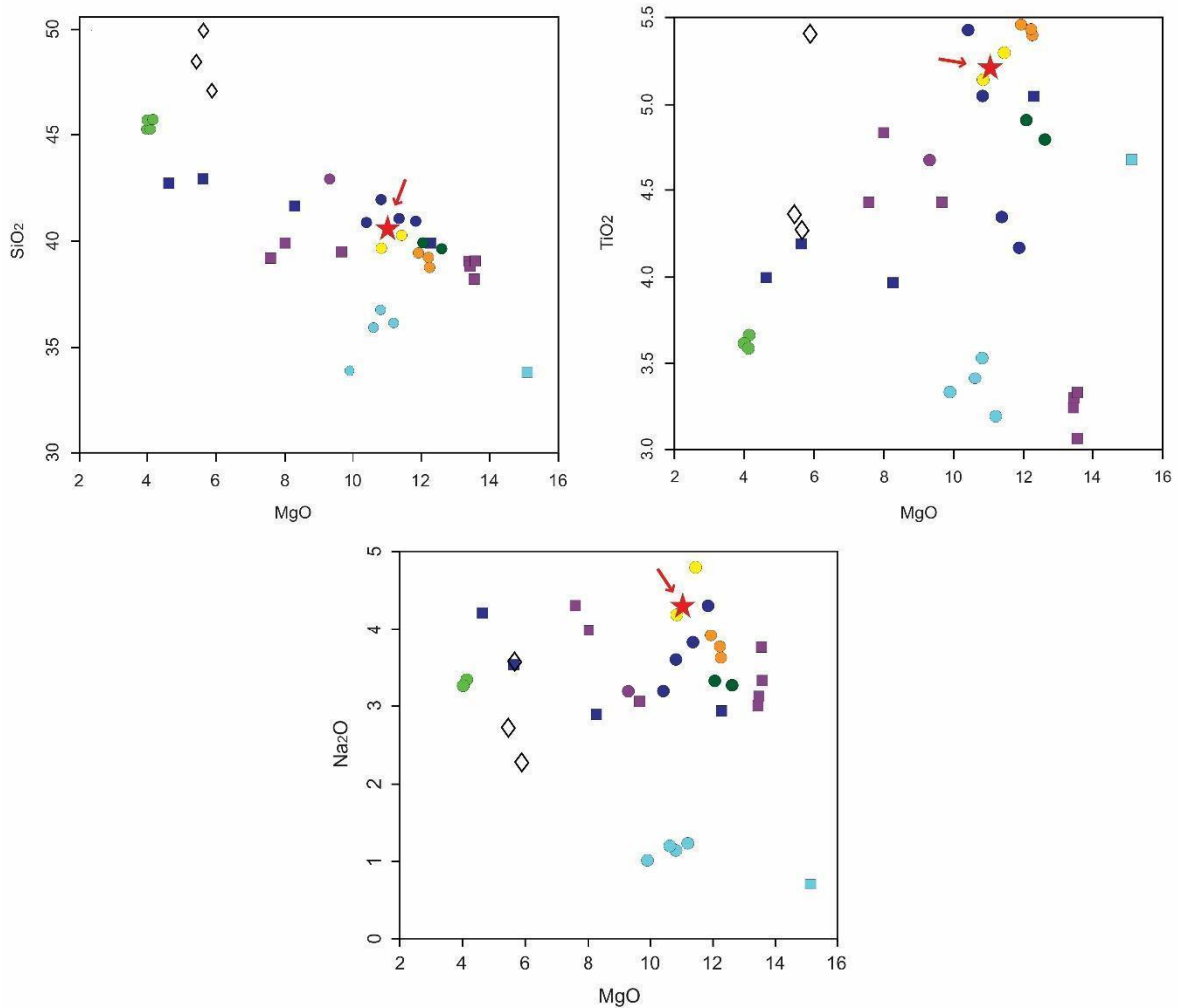


Fig. 10 MgO (wt. %) versus major and minor elements (wt. %) variation diagrams comparing Vitória Seamount alkaline basalt (highlighted by the red arrow) to Abrolhos Volcanic Complex and other Vitória-Trindade Ridge rocks. Data sources and symbols as in Fig. 9.

4.3.2 Trace elements

Trace element patterns are presented in spider diagrams (Fig. 11 a, b), where element contents are normalized to that of the Ocean Island Basalt (OIB) (Sun and McDonough, 1989) and Primitive Mantle composition (Sun and McDonough, 1989). The Vitória Seamount presents lower concentration for incompatible trace elements such as Zr (237 ppm), La (37 ppm) and Nb (68 ppm) except for Ba (*ca.* 1011 ppm) and high values of compatible trace elements such as Cr (370 ppm), Co (82 ppm), Ni (140 ppm), V (354 ppm) and Sc (22 ppm), which are typically found in primitive melts (Frey et al., 1978). Among the seamounts, Davis basanite shows the highest values of incompatible trace elements as Zr (407-419 ppm) and La (80.4-83.9 ppm) related to evolution from clinopyroxene and plagioclase fractionation.

4.3.3 Rare earth elements

Chondrite-normalized REE patterns (Boynton, 1984) for VTR and Abrolhos Volcanic Complex lavas are shown in Fig. 12. The Vitória Seamount lava is characterized by enrichment in light REE ($(\text{La}/\text{Yb})_{\text{N}} = 20.79$, $(\text{La}/\text{Sm})_{\text{N}} = 2.68$; $\text{Sm}/\text{Yb} = 7.25$), as the other lavas from Vitória-Trindade Ridge (Table 1) and Abrolhos Volcanic Complex, imprinting a common signature from alkaline magmas (Fodor and Hanan, 2000; Jung et al., 2006).

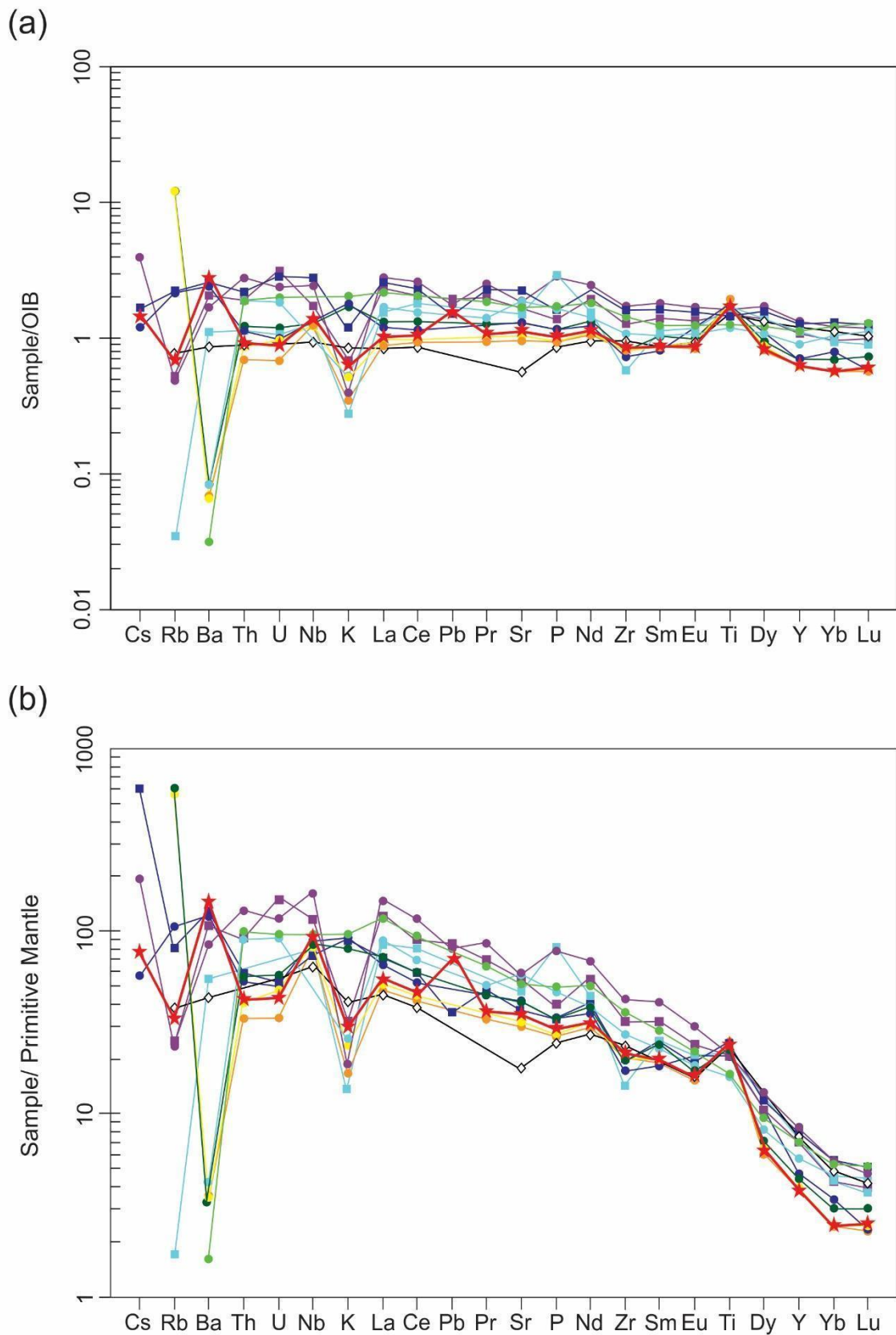


Fig. 11 Trace-element spider diagram normalized to (a) OIB (Sun and McDonough, 1989) and (b) primitive mantle (Sun and McDonough, 1989) for Vitória Seamount, Abrolhos Volcanic Complex, and other Vitória-Trindade Ridge seamounts, banks, and islands. Data sources and symbols as in Fig. 9.

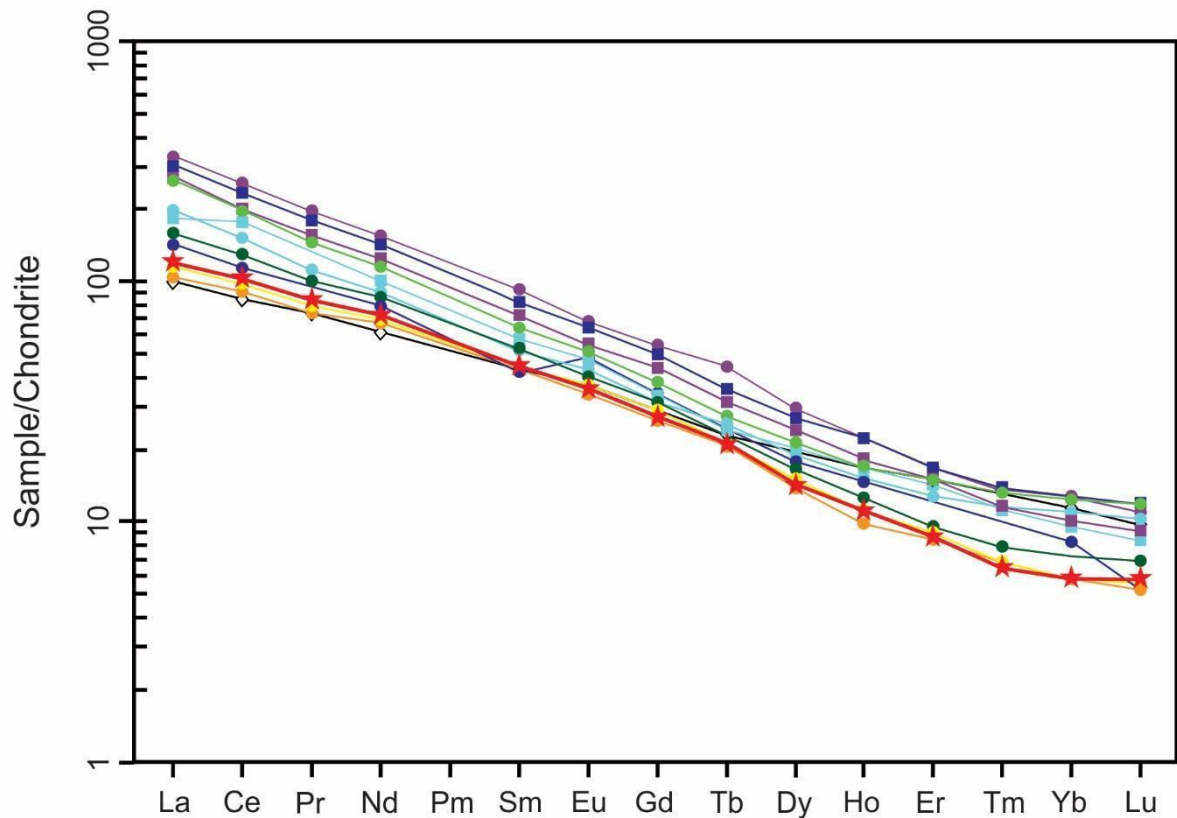


Fig. 12 Chondrite-normalized REE diagram (values from Boynton, 1984) for the different alkaline rocks of Vitória-Trindade Ridge and Abrolhos Volcanic Complex lavas. Data sources and symbols as in Fig. 9.

Table 1 REE ratios of Vitória-Trindade Ridge volcanic edifices (Marques et al., 1999; Siebel et al., 2000; Santos, 2013; Peyve & Skolotnev, 2014; Bongioiolo et al., 2015; Santos, 2016; Santos et al., 2018a) and this manuscript for the Vitória Seamount, for comparison.

	<i>Vitória Smt.</i>	<i>Montague Smt.</i>	<i>Jaseu r Smt.</i>	<i>Davis Bank</i>	<i>Dogares sa Bank</i>	<i>Colúmbia Smt.</i>	<i>Trindade Island (less evolved members)</i>	<i>Martin Vaz Archipelago (Melanephelinites)</i>
<i>MgO (avg. wt.%)</i>	11.02	12.14	8.41	5.01	12.35	10.65	9.43	12.15
$(La/Sm)_N$	2.68	2.50	2.58	4.1	3.06	3.75	3.08	2.39
$(La/Yb)_N$	20.79	18.99	20.28	21.2	22.92	17.43	28.17	18.37
(Eu/Eu^*)	1.02	1.06	1.04	1.04	1.03	1.03	0.98	0.97
<i>Sm/Yb</i>	7.25	7.08	7.30	4.80	7.00	4.30	6.81	7.16
<i>La/Gd</i>	5.21	4.82	4.81	8.30	6.20	7.20	7.05	4.74

4.4 Sr and Nd isotope compositions

The Vitória Seamount sample (duplicated) has $^{87}\text{Sr}/^{86}\text{Sr}$ ratios of 0.704054 and 0.704031; and a chondritic Nd signature ($^{143}\text{Nd}/^{144}\text{Nd} = 0.512629$ and 0.512635). The isotopic compositions are presented in Supplementary Table 5. Sr and Nd isotope data together with compiled data from Vitória-Trindade Ridge and Abrolhos Volcanic Complex (Supplementary Table 7), such as reported by Fodor et al. (1989), Halliday et al. (1992), Marques et al. (1999), Fodor and Hanan (2000), Siebel et al. (2000), Santos (2016), are plotted in the $^{87}\text{Sr}/^{86}\text{Sr}$ versus $^{143}\text{Nd}/^{144}\text{Nd}$ diagram (Fig. 13). Data from Alto Paranaíba (Gibson et al., 1995), Poxoréu (Gibson et al., 1997) and Serra do Mar provinces (Thompson et al., 1998), which are believed to represent Trindade Plume volcanic track in the onshore portion, are shown for comparison, as well data from Fernando de Noronha (Gerlach et al., 1987), Santa Helena (Chaffey et al., 1989) and Tristan da Cunha (Le Roex et al., 1990), which are other Atlantic Ocean's magmatism. The Vitória Seamount analyses plot in the bottom left quadrant similar to the Davis Bank basanite data reported by Santos (2016) but differ from the data of the other volcanic edifices from VTR, which plot in the upper left, less enriched quadrant (Fig. 13).

The Vitória Seamount and Davis Bank samples have a slightly more radiogenic $^{87}\text{Sr}/^{86}\text{Sr}$ ratio of *ca.* 0.704034, compared to the other Vitória-Trindade Ridge samples and Abrolhos Volcanic Complex samples, which have $^{87}\text{Sr}/^{86}\text{Sr}$ ratios ranging from 0.703607 to 0.703946. The Vitória Seamount Nd isotopic signature is also similar to those of Davis Bank Nd near chondritic values (Santos, 2016), and differ from the other seamounts and islands from the Vitória-Trindade Ridge, which have a bit more radiogenic $^{143}\text{Nd}/^{144}\text{Nd}$ ratio *ca.* 0.512785.

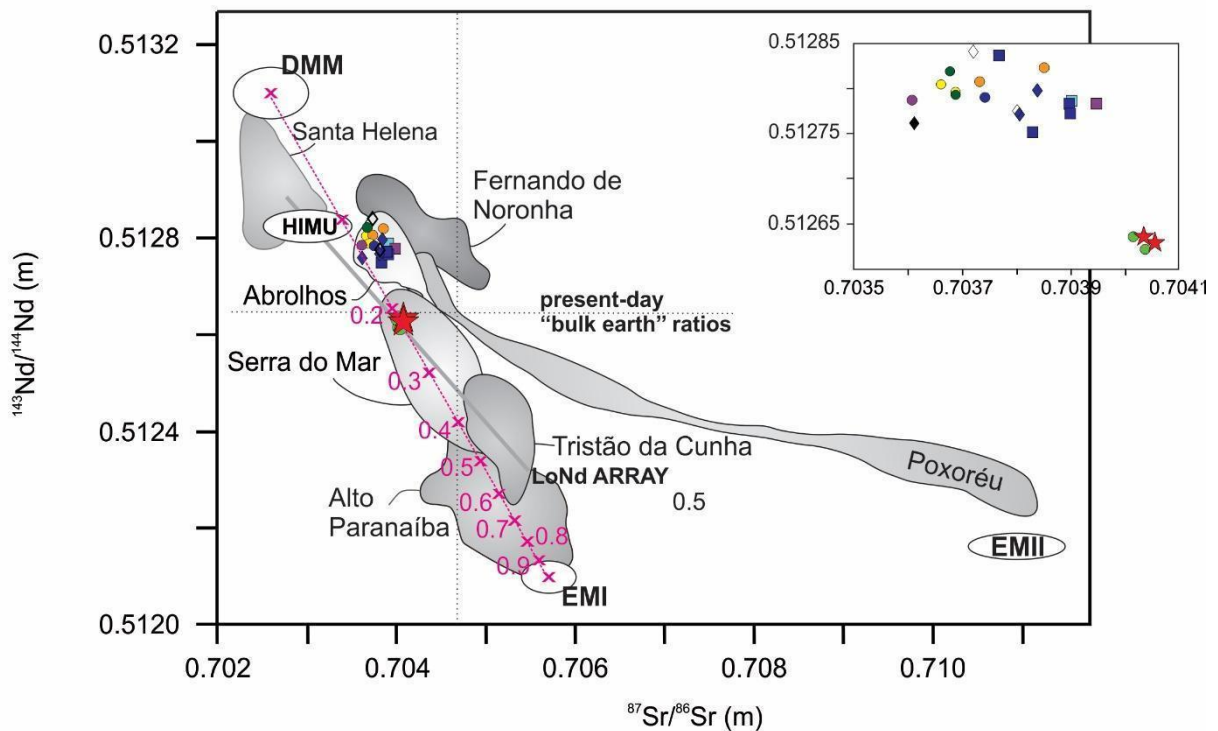


Fig. 13 Nd-Sr isotopic ratios (measured) correlation plots for VTS (duplicated), VTR and Abrolhos Volcanic Complex lavas. Data sources and symbols as in Fig. 9 and in Halliday et al. (1992) – dark blue diamonds (Trindade Island Nephelinites); Abrolhos (Fodor et al., 1989); Alto Paranaíba (Gibson et al., 1995); Alkaline rocks from Serra do Mar igneous complex (Thompson et al., 1998); Poxoréu (Gibson et al., 1997). Although data for Fernando de Noronha (Gerlach et al., 1987), Tristan da Cunha (Le Roex et al., 1990) and Santa Helena (Chaffey et al., 1989) are not on the Trindade track, they are shown for comparison as plume-related ocean island basalts. Low-Nd (LoNd) reference line (Hart et al., 1986). Mantle components: Bulk Earth (Zindler & Hart, 1986), EMI (Eisele et al., 2002; Hofmann, 2014), DMM (Zindler and Hart, 1986; Salters & Stracke, 2004; Workman & Hart, 2005), EMII (Zindler & Hart, 1986; Hart, 1988) and HIMU (Hart, 1988; Jackson & Dasgupta, 2008). Modeling assumes two-component mixing between melt DMM ($^{87}\text{Sr}/^{86}\text{Sr} = 0.7026$, $[\text{Sr}] = 160$ ppm, $^{143}\text{Nd}/^{144}\text{Nd} = 0.5131$, $[\text{Nd}] = 9.6$ ppm; Zindler & Hart, 1986; Salters & Stracke, 2004; Jackson & Dasgupta, 2008) and EMI ($^{87}\text{Sr}/^{86}\text{Sr} = 0.7057$, $[\text{Sr}] = 495$ ppm, $^{143}\text{Nd}/^{144}\text{Nd} = 0.5121$, $[\text{Nd}] = 30.6$ ppm; Zindler & Hart, 1986; Eisele et al., 2002; Hofmann, 2014). The Sr and Nd contents of the EMI end-member are based on data from the GEOROC database (<http://georoc.mpch-mainz.gwdg.de/georoc/>), whereas for the melt DMM, the Sr and Nd contents were calculated considering a partial melting degree of *ca.* 3% (as discussed in subitem 5.2; bulk DSr = 0.0185 and DNd = 0.0317). Increments of mixing (%) are shown as pink crosses.

5 Discussion

5.1 Nature of the Mantle source(s)

In the $^{143}\text{Nd}/^{144}\text{Nd}$ versus $^{87}\text{Sr}/^{86}\text{Sr}$ diagram, Vitória Seamount samples fall close to the limit between depleted and enriched source components (Fig. 13), being plotted between DMM, HIMU and EM I. $^{87}\text{Sr}/^{86}\text{Sr}$ ratios of the Vitória lavas, as well Davis Bank lavas, are slightly

higher than in DMM and HIMU while $^{143}\text{Nd}/^{144}\text{Nd}$ ratios are more unradiogenic than these mantle components. Note that the Vitória Seamount is more radiogenic in Nd isotope ratios than in EMI. Because this study lacks adequate Pb isotopic data for a comprehensive petrogenetic evaluation of these rocks (involving HIMU and FOZO components), we must leave that task to future investigations.

In this context, we observed that the Vitória Seamount lavas, as well as other VTR rocks, have chemical and isotopic signatures that indicate a contribution of an enriched mantle (EMI) in the depleted asthenospheric mantle (represented by DMM) (Marques et al., 1999; Fodor and Hanan, 2000; Siebel et al., 2000; Peyve and Skolotnev, 2014; Santos, 2016; Skolotnev and Peive, 2017; Santos et al., 2018a). On the basis of Sr and Nd isotopes there is little doubt of the involvement of a EMI mantle domain in the origin of VTR, including the Vitória Seamount (Fig. 13). The involvement of the EMI component is supported by Sr and Nd isotopic compositions, whose origin has been attributed to delamination of lower continental crust (LCC) (Tatsumi, 2000) or subcontinental lithospheric mantle (SCLM), which was also suggested as an important source component for OIB and alkaline magmas (McKenzie and O’Nions, 1995; Niu, 2009; Niu et al., 2012; Jung et al., 2006). This last mechanism was also invoked by Marques et al. (1999), where it was proposed that during the breakup of Western Gondwanaland, detached fragments of LCC and SCLM may have been left behind and later thermally remobilized by the Trindade hotspot. Note that the crustal material recycling and mantle metasomatism can result in mineralogical and compositional heterogeneities, producing a variety of mafic and ultramafic sources (*e.g.*, metasomatized peridotite, pyroxenite, hornblendite). The main features of the EMI component are: slightly radiogenic Sr isotopes ($^{87}\text{Sr}/^{86}\text{Sr}$ *ca.* 0.7055 – 0.7060; Eisele et al., 2002; Hofmann, 2014), unradiogenic Nd ($^{143}\text{Nd}/^{144}\text{Nd}$ *ca.* 0.5121; Zindler & Hart, 1986), and unradiogenic Pb isotopes ($^{206}\text{Pb}/^{204}\text{Pb}$ < 17.5; Zindler & Hart, 1986; Jackson & Dasgupta, 2008). Other models have suggested that the EMI end-member may have been generated by mantle recycling of subducted oceanic crust with pelagic sediment, thermal erosion of SCLM anomalously hotspot, subducted oceanic plateaus (*e.g.*, Eisele et al., 2002; Rocha-Júnior et al., 2012).

As discussed by Bizzi et al. (1995) and Rocha-Júnior et al. (2013), the oceanic basalts with EMI signatures in the South Atlantic are ascribed to processes by which the Brazilian Neoproterozoic continental lithosphere was delaminated, and contaminated a zone of the South Atlantic asthenosphere which is now erupting as hotspot island and nearby sections of Mid-Atlantic ridge (Hawkesworth et al., 1986). According to this model, the Walvis Ridge basalts

are mixtures of delaminated enriched subcontinental lithosphere and more typical “normal” oceanic compositions lying within the oceanic mantle array.

To assess quantitatively the relationships in Nd-Sr isotope space of the VTS rocks and to test for involvement of an enriched component (represented by EMI) embedded in the asthenospheric source (represented by DMM), we have performed mixing calculations. The melt DMM component is represented by $^{87}\text{Sr}/^{86}\text{Sr} = 0.7026$, $[\text{Sr}] = 160$ ppm, $^{143}\text{Nd}/^{144}\text{Nd} = 0.5131$ and $[\text{Nd}] = 9.6$ ppm (Zindler & Hart, 1986; Salters & Stracke, 2004; Jackson & Dasgupta, 2008), while the EMI component is characterized by $^{87}\text{Sr}/^{86}\text{Sr} = 0.7057$, $[\text{Sr}] = 495$ ppm, $^{143}\text{Nd}/^{144}\text{Nd} = 0.5121$, $[\text{Nd}] = 30.6$ ppm (Zindler & Hart, 1986; Eisele et al., 2002; Hofmann, 2014). Our modeling was carried out by mixing melts from these components. The results of the calculations are shown in Fig. 13 and indicate that EMI contributions varying from 20% to 25% can account for the observed VTS compositions. Note that the involvement of the EMI end-member can account for the more radiogenic Sr and unradiogenic Nd in the VTS. Our favored explanation is that the EM-I component associated with VTS petrogenesis derived from mixtures of eclogites or pyroxenite with peridotite since pyroxenite melts freeze and react entirely with the ambient peridotite.

The low Zr/Nb (3.5) and Y/Nb (0.26) ratios of Vitória Seamount, the LREE strong enrichment ($(\text{La}/\text{Sm})_{\text{N}} = 2.68$; $(\text{La}/\text{Yb})_{\text{N}} = 20.79$ see Table 1 for comparison) and the enrichment in the progressively more incompatible elements indicates that VTS sample is geochemically enriched (Le Roex et al., 2010). These geochemical characteristics also occur in the majority of OIB-type intraplate magmatic events (Pearce and Norry, 1979; Niu et al., 2012; Xia & Li, 2019) and are consistent with derivation from geochemically enriched mantle sources associated with low partial melting proportion, corroborating to the hypothesis of mantle metasomatism (Downes, 2001; Bianchini et al., 2007; Niu, 2009; Niu et al., 2012 and references therein; Avanzinelli et al., 2020).

The age of this metasomatism event cannot be resolved on basis of the geochemical data, but the Nd model ages, varying from 0.60 to 0.61 Ga (calculated concerning the depleted mantle; Supplementary Table 5), could reflect mantle enrichment processes by metasomatic events related to the Brasiliano orogenic event (750–450 Ma). This suggests that the continental lithosphere and oceanic subducted slabs may have influenced the composition of the VTS imprinting enriched signatures in the mantle sources. The same relationship was also suggested by Marques et al. (1999; see text for discussions) for the Trindade and Martin Vaz volcanic rocks, correlating the tectonic evolutionary settings during that time to the rock signature observed in the volcanic ridge. This is supported by the radiogenic $^{87}\text{Sr}/^{86}\text{Sr}$ and unradiogenic

$^{143}\text{Nd}/^{144}\text{Nd}$ isotopic ratios that are evidence of recycled continental crust material (Avanzinelli et al., 2020) and that point to the involvement of the EMI component. That way, the enriched signatures could also be explained by plume thermally remobilization of detached fragments of subcontinental lithospheric mantle from the opening of the South Atlantic Ocean (Gondwana breakup) that have been left behind (Hawkesworth et al., 1986; Zindler & Hart, 1986; Marques et al., 1999; Class & Le Roex, 2006).

By the way, the reason of the isotopic similarity between Vitória Seamount and Davis Bank, two distant volcanic edifices, may be related to the source, which could be associated to these aforementioned older oceanic subducted slabs (up to 1 Ga – Santos oral communication; Skolotnev & Peive, 2017) that imprint this signature. But this is the object of further and deeper discussions.

5.2 Partial Melting regime

As previously discussed, the Vitória Seamount has an MgO = 11 wt.%, indicating that it was probably little affected by the effects of fractional crystallization. Therefore, this sample can be used to infer the dynamics of melting, as well as to compare it with other seamounts and islands that occur in the VTR (only samples with MgO > 10 wt.% to minimize the effects of fractional crystallization). Major and trace elements of the VTS lavas are characterized by elevated $(\text{Dy}/\text{Yb})_{\text{N}}$, $\text{CaO}/\text{Al}_2\text{O}_3$, and Zr/Y ratios indicating that the parental magmas originated from a dominantly garnet lherzolite stability field. Note that the depletion in HREE also indicates the generation of the VTS rocks in the presence of residual garnet (Fig. 14).

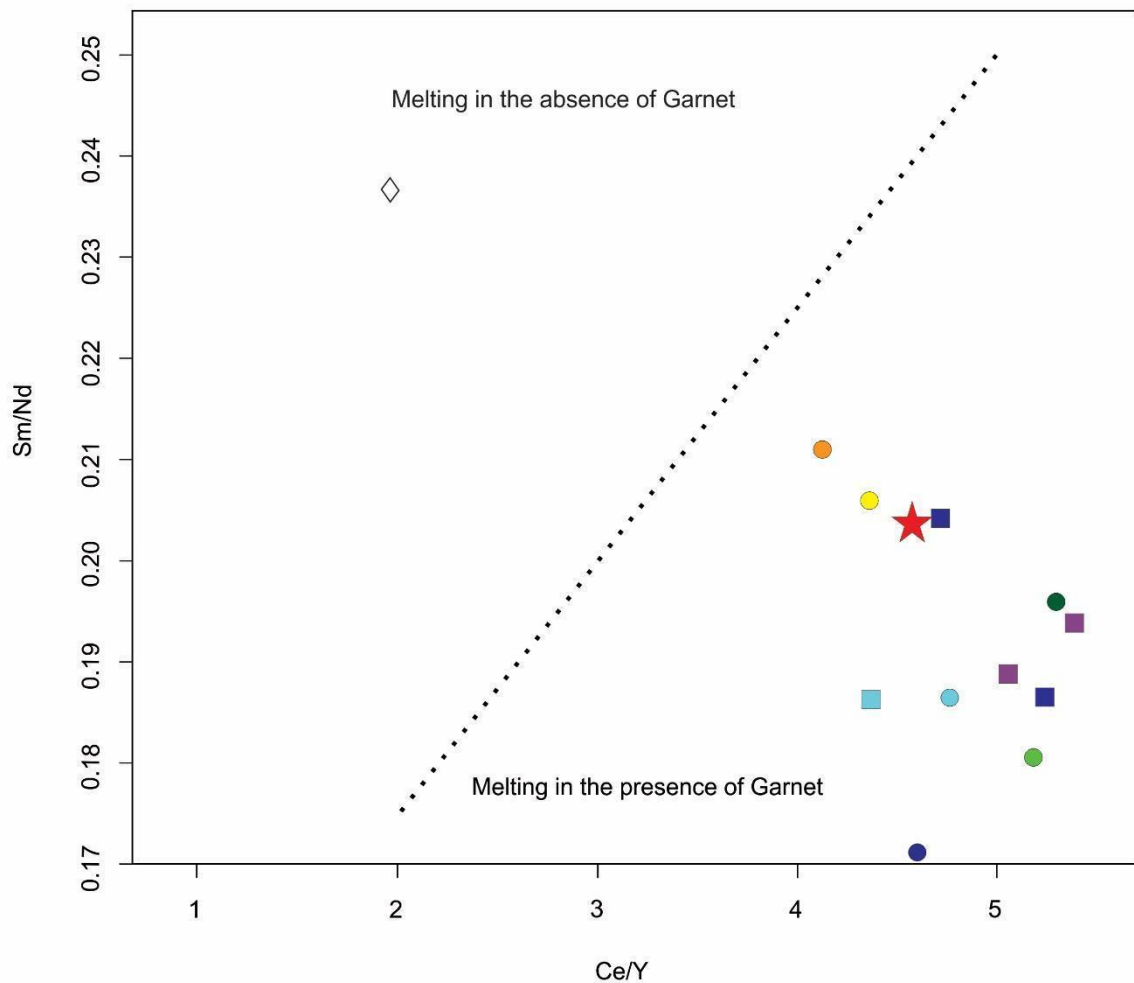


Fig. 14 Sm/Nd versus Ce/Y ratios for Vitória-Trindade rocks and from Abrolhos Volcanic Complex. Data sources and symbols as in Fig. 9. (see Ellam, 1992 and Siebel et al., 2000 for discussions).

A relatively fertile peridotite mantle source (represented by Primitive Mantle; McDonough and Sun, 1995) for the VTS is required for models of trace element ratios (Fig. 15). The melting model assumes the following modes for batch melting of volatile-free garnet peridotite (olivine = 0.598; orthopyroxene = 0.211; clinopyroxene = 0.076, and garnet = 0.115) and spinel peridotite (olivine = 0.578; orthopyroxene = 0.270; clinopyroxene = 0.119, and spinel = 0.033).

Our modeling revealed that these geochemical characteristics can be explained by relatively low-degree (less than 3%) melting of enriched peridotite in the presence of garnet (Fig. 15), which has high partition coefficients for Y and HREE. However, it is noteworthy that the VTR rocks have Dy/Yb ratios somewhat higher than the spinel-lherzolite melting curve, but lower than those of the garnet-lherzolite melting curve, indicating an enriched mantle source with variable proportions of garnet and spinel. The Vitória Seamount has Dy/Yb ratio slightly lower than the garnet-lherzolite melting curve, implying a garnet lherzolite mantle source.

Different seamounts, banks, and islands of the VTR have variable Dy/Yb and La/Yb ratios, indicating that these differences reflect different depths and degrees of partial melting. The modeling also shows that the Dogaressa Bank, Trindade Island basanites, and Colúmbia Seamount were generated at lower pressure and indicate lower extents of partial melting ($\leq 2\%$), explaining why the incompatible elements of VTS are more depleted compared to these lavas (Figs. 11 and 12). Note that different partial melting degrees alter the geochemical composition of the parental magma, but do not change the more incompatible trace element ratios or isotopic compositions. The VTR rocks have $^{143}\text{Nd}/^{144}\text{Nd}$ isotopic compositions varying from 0.51275 to 0.51284 and distinct trace element ratios (Figs. 13 and 14), suggesting that these geochemical differences reflect different degrees of partial melting, as well as may also indicate different proportions of the enriched component (EMI) embedded in the asthenospheric source (DMM).

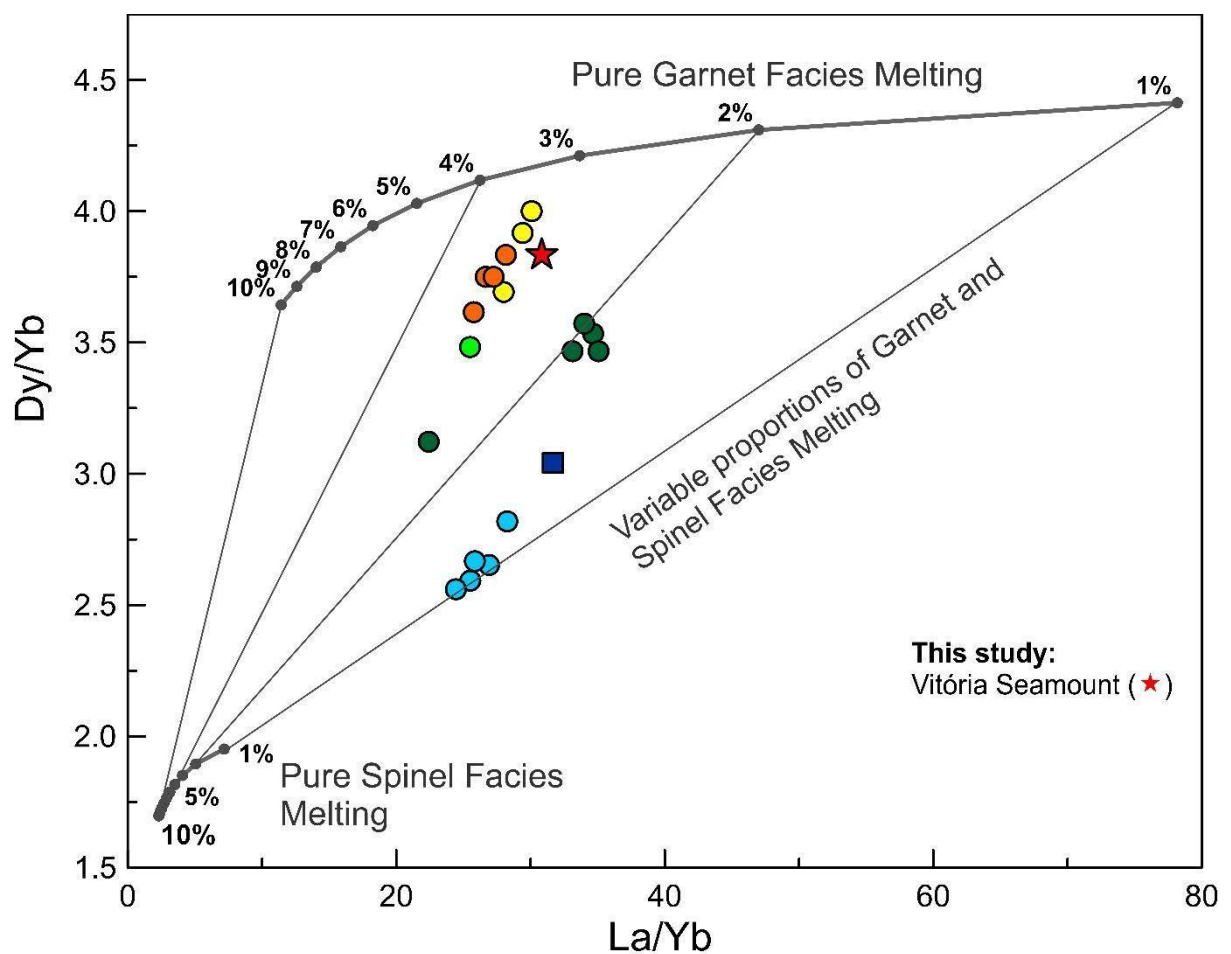


Fig. 15 Plot of La/Yb versus Dy/Yb ratios for Vitória Seamount and other VTR rocks with $\text{MgO} \geq 10$ wt.% in order to minimize the effects of fractional crystallization. Melting model are calculated for batch melting (Shaw, 1970) of volatile-free garnet (olivine = 0.598; orthopyroxene = 0.211; clinopyroxene = 0.076, and garnet = 0.115) and spinel (olivine = 0.578; orthopyroxene = 0.270; clinopyroxene = 0.119, and spinel = 0.033) peridotite (McKenzie &

O’Nions, 1991). Partition coefficients for garnet and spinel peridotite are from Salters & Stracke (2004) and Day et al. (2010). Trace element concentrations of enriched mantle source ([La] = 0.648 ppm; [Dy] = 0.674 ppm; [Yb] = 0.441 ppm) are from McDonough and Sun (1995). Data sources and symbols as in Fig. 9.

As shown above, the melting model suggests that Vitória Seamount lava was generated by less than 3% melting of a garnet-lherzolite source, which is in agreement with the range of Vitória-Trindade Ridge data and also others alkaline undersaturated magmatism: Siebel et al. (2000) considered batch melting as the melting process producing small melt fractions for Poxoréu (5-6.4%), Abrolhos (3.4-4.7%) and Trindade and Martin Vaz Islands (1-1.7%); Santos & Marques (2007) also point to a very low degree (1–2%) of partial melting for Trindade Island’s ultrabasic rocks; Bongiolo et al. (2015) show that Trindade Island’s nephelinites could be formed from 0.1 to 7% of partial melting of an enriched garnet–lherzolite source or from 1 to 5% partial melting of TiO₂-rich garnet–phlogopite lherzolite; Santos et al. (2018a) described that Martin Vaz melanephelinites were generated by 3–4% partial melting from a garnet lherzolite source; Weaver (1990) reported that Fernando de Noronha basanites were produced by about 8% melting.

5.3 Relation to tectonic events

Sr and Nd isotopic similarities between Vitória Seamount and Davis Bank, which are approximately 315 km away and are probably roughly 15 Ma apart, have been pointed out. On the other hand, these seamounts have different rates of lava evolution, which evokes a more complex evolutionary history.

Tectonic events of global and local magnitude that took place during the Cenozoic may have played an important role in the volcanism of the Vitória-Trindade Ridge edifices (Colli et al., 2018; Celli et al., 2020 and references therein). The Andean uplift started in the Middle Eocene with a slow initial development and reaching the first uplift culmination in the Oligocene-Early Miocene (Sempere et al., 2008; Celli et al., 2020). These events are contemporary to the Vitória Seamount and Davis Bank generation, respectively. Moreover, a clockwise rotation of the South American continent is reported during the Middle Eocene (Ernesto, 1996; Thomaz-Filho et al., 2005; Müller et al., 2016). In addition, there is a clockwise rotation of about 40° from the axis of the Chile mountain range registered during the Oligocene-Miocene interval (Tebbens and Cande, 1997; Somoza, 1998), which are also coeval events to the Vitória and Davis volcanism. Notwithstanding, Santos and Campos Basin present important

turbiditic generation during these epochs, indicating instability in the continental shelf, which can possibly be correlated with both magmatic and tectonics events (Mohriak, 2006).

In this way, the Andean uplift and other South American Plate tectonic events suggest an influence and a relationship to the Vitória-Trindade Ridge volcanism, interacting with shallow mantle-plume convection, as will be discussed in further studies.

6 Conclusions

The Vitória Seamount, *ca.* 300 km southeast of the Brazilian coastline, has unquestionable characteristics of alkaline basaltic magma, refuting the hypothesis that this seamount corresponds to a continental crust fragment. Its melt was generated by low-degree (less than 3%) melting of a garnet-lherzolite source and, together with Rare-Earth Elements enrichment, indicate the alkaline character and the geochemical enrichment of Vitória Seamount. These characteristics confirm the presence of a geochemically enriched mantle source region, supporting an origin from an upwelling mantle plume and mantle metasomatism. The VTS Sr-Nd isotopic signatures suggest a mixture between an enriched component (EM I) and a depleted mantle component (DMM), as was pointed out in other Vitória-Trindade Ridge rocks. Metasomatic event(s) may have occurred and, according to Nd model ages, may have taken place about 600 Ma ago, which suggests a relationship to the Brasiliano Orogeny.

Similarities between the Vitória Seamount and the Davis Bank, which are approximately 315 km away, have been pointed out and evoke a more complex evolutionary history. During the Eocene-Miocene (Vitória Seamount and Davis Bank) volcanic edifice generation an influence of Andean Orogeny in South American Platform and South American Plate tectonic events is suggested.

Acknowledgements

The authors thank the logistic support of the Brazilian Navy. We thank LAGIR staff for support and isotopes analyses. We thank program PROCiência – UERJ for cooperating with scholarship in the VTR project. Our many thanks to Dr. Ronald Fodor (North Carolina State University), Dr. José Francisco Santos (Aveiro University) and Sara Ribeiro, Carla Neto and Gilberto Vaz (LAGIR-UERJ), Amanda Tosi and Iara Déniz Ornellas (LabSonda) for their knowledge and patience to teach ICPMS and Sr-Nd methodologies. The authors thank the CNPq (2019 self-sustained project) and the logistic support of the Brazilian Navy. We thank

Universidade do Estado do Rio de Janeiro for allowing Dr. Anderson Costa dos Santos, through its PROCAD Program (Capacitation Program) and CAPES Process 88881.177228/2018-01 for the post-doctorate fellowship, to execute part of this research at Aveiro University, Portugal. We thank Geobiotec (UID/GEO/04035/2019 - Aveiro University research group) for encouraging this research. We are grateful to the LEPLAC Program for allowing the use of the bathymetric data set and to access the internal report produced by Hémond & Révillon (2012), as well to the technical group that has been studying the Brazilian Continental Margin since 1987 in order to produce the Brazilian Submission for the extension of the Continental Shelf according to Article 76 of UNCLOS. We thank in name of Rio de Janeiro State University the Captains Izabel King Jeck, Ana Angélica Ligiéro Alberoni and Luiz Carlos Torres for the partnership in our research. The second author, Dr. Anderson Costa dos Santos, thanks PROCIÊNCIA program (PR-2) from Rio de Janeiro State University for partially support and encouraging this research. We thank FAPERJ APQ1 for supporting this project under project nº 210.179/2019. We thank Dr. Keith Putirka for the assistance with the thermobarometric models. The new names of three volcanic edifices accepted by the Sub-Committee on Undersea Feature Names (SCUFN) are in honor to deceased professors Akihisa Motoki, Asmus and Jorge Palma, that contributed so much to science. We are also grateful for the critical review and illuminating suggestions and helpful comments received from the Editor and the referees.

Funding

This work was supported by the CNPq (Pro Trindade Program) [Process Nº. 557146/2009-7]; the MCT/CNPq project [nº 26/2009]; the Universidade do Estado do Rio de Janeiro for PROCAD Program (Capacitation Program) leave and CAPES [Process 88881.177228/2018-01]; and FAPERJ [APQ1 2019 n 210.179/2019].

References

- Almeida, F.F.M., 2006. As ilhas oceânicas brasileiras e suas relações com a tectônica do Atlântico Sul. *Terræ didática*, 2, 3-18.
- Almeida, F.F.M., Carneiro, C.D.R., Mizusaki, A.M.P., 1996. Correlação do magmatismo das bacias da margem continental Brasileira com o das áreas emersas adjacentes. *Rev. Bras. Geoc.*, 26, 125-138.
- Alves, E.C., Maia, M., Sichel, S.E. e Campos, C.M.P., 2006. Zona de Fratura de Vitória-trindade no Atlântico Sudeste e suas implicações tectônicas. *Revista Brasileira de Geofísica*, 24, 117–127.

Avanzinelli, R., Bianchini, G., Tiepolo, M., Jasim, A., Natali, C., Braschi, E., Dallai, L., Beccaluva, L., Conticelli, S., 2020. Subduction-related hybridization of the lithospheric mantle revealed by trace element and Sr-Nd-Pb isotopic data in composite xenoliths from Tallante (Betic Cordillera, Spain). *Lithos*, 105316. Doi: <https://doi.org/10.1016/j.lithos.2019.105316>

Bianchini, G., Beccaluva, L., Bonadiman, C., Nowell, G., Pearson, G., Siena, F., Wilson, M., 2007. Evidence of diverse depletion and metasomatic events in harzburgite–lherzolite mantle xenoliths from the Iberian plate (Olot, NE Spain): Implications for lithosphere accretionary processes. *Lithos*, 94, 25–45. Doi: <https://doi.org/10.1016/j.lithos.2006.06.008>

Bizzi, L.A., De Wit, M.J., Smith, C.B., McDonald, I., Armstrong, R.A., 1995. Heterogeneous enriched mantle materials and Dupal-type magmatism along the SW margin of the São Francisco craton, Brazil. *Journal of Geodynamics*, 20(4), 469-491. Doi: [https://doi.org/10.1016/0264-3707\(95\)00028-8](https://doi.org/10.1016/0264-3707(95)00028-8)

Bongiolo, E.M., Pires, G.L.C., Geraldés, M.C., Santos A.C., Neumann R., 2015. Geochemical modeling and Nd-Sr data links nephelinite-phonolite successions and xenoliths of Trindade Island (South Atlantic Ocean, Brazil). *Journal of Volcanology and Geothermal Research*, 306, 58–73. Doi: <https://doi.org/10.1016/j.jvolgeores.2015.10.002>

Boynton, W.V., 1984. Geochemistry of Rare Earth Elements: Meteorite Studies. In: Henderson, P. (Ed.). *Rare Earth Element Geochemistry*. Amsterdam: Elsevier Sci. Publ. Co., 2, 63-114.

Celli, N.L., Lebedev, S., Schaeffer, A.J., Ravenna, N., Gaina, C., 2020. The upper mantle beneath the South Atlantic Ocean. South America and Africa from waveform tomography with massive data sets. *Geophysical Journal International*, 221, 178–204. Doi: <https://doi.org/10.1093/gji/ggz574>

Chaffey, D.J., Cliff, R.A., Wilson, B.M., 1989. Characterization of the St. Helena source. In: Saunders, A.D. & Norry, M.J. (Eds). *Magmatism in the Ocean Basins*. Geological Society, London, Special Publications, 42, 257-276. Doi: <http://dx.doi.org/10.1144/GSL.SP.1989.042.01.16>

Class, C., le Roex, A.P., 2006. Continental material in the shallow oceanic mantle—how does it get there? *Geology*, 34, 129-132. Doi: <https://doi.org/10.1130/G21943.1>

Colli, L., Ghelichkhan, S., Bunge, H.-P., Oeser, J., 2018. Retrodictions of Mid Paleogene mantle flow and dynamic topography in the Atlantic region from compressible high resolution adjoint mantle convection models: Sensitivity to deep mantle viscosity and tomographic input model. *Gondwana Research*, 53, 252-272. Doi: <https://doi.org/10.1016/j.gr.2017.04.027>

Colli, L., Stotz, I., Bunge, H.P., Smethurst, M., Clark, S., Iaffaldano, G., Tassara, A., Guillocheau, F., Bianchi, M.C., 2014. Rapid South Atlantic spreading changes and coeval vertical motion in surrounding continents: evidence for temporal changes of pressure-driven upper mantle flow. *Tectonics*, 33, 1304–21. Doi: <https://doi.org/10.1002/2014TC003612>

Conceição, J.C.J., Misuzaki, A.M.P., Alves, D.B. & Szatmari, P., 1996. Controle tectônico do magmatismo do Complexo Vulcânico de Abrolhos, Bacia do Espírito Santo. In: SBG, Congresso Brasileiro de Geologia, 39, Camboriu, Anais, 5, 384-387

Cordani, U.G., 1970. Idade do vulcanismo do Oceano Atlântico Sul. *Boletim do Instituto de Geociências e Astronomia (IGA-USP)*, 1, 9-75.

Cordani, U.G., Blazekovic, A., 1970. Idades radiométricas das rochas vulcânicas dos Abrolhos. In: CONGRESSO BRASILEIRO DE GEOLOGIA, Brasília, Brazil.

Cox, K.G., Bell, J.D., Pankhurst, R.J., 1979. The Interpretation of Igneous Rocks. Allen and Unwin, London.

Day, J.M.D., Pearson, D.G., Macpherson, C.G., Lowry, D., Carracedo, J.C., 2010. Evidence for distinct proportions of subducted oceanic crust and lithosphere in HIMU-type mantle beneath El Hierro and La Palma, Canary Islands. *Geochimica et Cosmochimica Acta*, 74, 6565-6589. Doi: <https://doi.org/10.1016/j.gca.2010.08.021>

Downes, H., 2001. Formation and modification of the shallow sub-continental lithospheric mantle: a review of geochemical evidence from ultramafic xenolith suites and tectonically emplaced ultramafic massifs of Western and Central Europe. *J. Petrol.*, 42, 233–250. Doi: <https://doi.org/10.1093/petrology/42.1.233>

Eisele, J., Sharma, M., Galer, S.J.G., Blichert-Toft, J., Devey, C.W., Hofmann, A.W., 2002. The role of sediment recycling in EM-1 inferred from Os, Pb, Hf, Nd, Sr isotope and trace element systematics of the Pitcairn hotspot. *Earth and Planetary Science Letters*, 196, 197-212. Doi: [https://doi.org/10.1016/S0012-821X\(01\)00601-X](https://doi.org/10.1016/S0012-821X(01)00601-X)

Ellam, R.M., 1992. Lithospheric thickness as a control on basalt geochemistry. *Geology*, 20, 153-156. Doi: [https://doi.org/10.1130/0091-7613\(1992\)020<0153:LTAACO>2.3.CO;2](https://doi.org/10.1130/0091-7613(1992)020<0153:LTAACO>2.3.CO;2)

Ernesto, M., 1996. Determinação da curva de deriva polar aparente para o Mesozóico da América do Sul, Thesis, IAG/USP, 56 pp.

Fainstein, R. & Summerhays, C. P., 1982. Structure and origin of marginal banks off eastern Brazil. *Marine Geology*, 46, 199-215. Doi: [https://doi.org/10.1016/0025-3227\(82\)90080-9](https://doi.org/10.1016/0025-3227(82)90080-9)

Ferrari, A. & Riccomini, C. 1999. Campo de esforços Plio Pleistocênico na Ilha de Trindade (Oceano Atlântico Sul, Brasil) e sua relação com a tectônica regional. *Revista Brasileira de Geociências*, 29, 195-202.

Fodor, R.V., Hanan, B.B., 2000. Geochemical evidence for the Trindade Hotspot trace: Columbia seamount ankaramite. *Lithos*, 51, 293–304. Doi: [https://doi.org/10.1016/S0024-4937\(00\)00002-5](https://doi.org/10.1016/S0024-4937(00)00002-5)

Fodor, R.V., McKee, E.H., Asmus, H.E., 1983. K-Ar ages and the opening of the South Atlantic Ocean: basaltic rock from the Brazilian margin. *Marine Geology*, 54, M1-M8. Doi: [https://doi.org/10.1016/0025-3227\(83\)90002-6](https://doi.org/10.1016/0025-3227(83)90002-6)

Fodor, R.V., Mukasa, S.B., Gomes, C.B., Cordani, U.G., 1989. Ti-rich eocene basaltic rocks, abrolhos platform, Offshore Brazil, 18°S: Petrology with respect to South Atlantic magmatism. *Journal of Petrology*. 30, 763–786. Doi: <https://doi.org/10.1093/petrology/30.3.763>

França, R.L., Del Rey, A.C., Tagliari, C.V., Brandão, J.R., Fontanelli, P.R., 2007. Bacia do Espírito Santo. In: Milani, E.J., Rangel, H.D., Bueno, G.V., Stica, J.M., Winter, W.R., Caixeta, J.M., Pessoa Neto, O.C. (eds.). *Bacias Sedimentares Brasileiras - Cartas Estratigráficas*. Boletim de Geociências da Petrobras, Rio de Janeiro, 15, 501-509.

Frey, F.A., Green, D.H., Roy, S.D., 1978. Integrated Models of Basalt Petrogenesis - Study of Quartz Tholeiites to Olivine Melilities from South Eastern Australia Utilizing Geochemical and

Experimental Petrological Data. *Journal of Petrology*, 19, 463-513. Doi: <https://doi.org/10.1093/petrology/19.3.463>

Gerlach, D.C., Stormer, J.C., Mueller P.A., 1987. Isotopic geochemistry of Fernando de Noronha. *Earth and Planetary Sciences Letters*, 85, 129-144. Doi: [https://doi.org/10.1016/0012-821X\(87\)90027-6](https://doi.org/10.1016/0012-821X(87)90027-6)

Gibson, S.A., Thompson, R.N., Leonardos, O.H., Dickin, A.P., Mitchell, J.G., 1995. The Late Cretaceous impact of the Trindade mantle plume: Evidence from large-volume, mafic, potassic magmatism in SE Brazil. *Journal of Petrology*, 36, 189-229. Doi: <https://doi.org/10.1093/petrology/36.1.189>

Gibson, S.A., Thompson, R.N., Leonardos, O.H., Dickin A.P., Mitchell J. G., 1999. The limited extent of plume-lithosphere interactions during continental flood-basalt genesis: Geochemical evidence from Cretaceous magmatism in southern Brazil. *Contributions to Mineralogy and Petrology*, 137, 147–169. Doi: <https://doi.org/10.1007/s004100050588>

Gibson, S.A., Thompson, R.N., Weska, R.K., Dickin, A.P., Leonardos, O.H., 1997. Late Cretaceous rift-related upwelling and melting of the Trindade starting mantle plume head beneath western Brazil. *Contributions to Mineralogy and Petrology*, 126, 303-314. Doi: <https://doi.org/10.1007/s004100050252>

Gorini, M.A., 1969. Geologic observations on the “Comissão Oceanográfica Leste I” aboard the Research Vessel “Almirante Saldanha”. *An. Acad. brasil. Ciênc.*, 41, 642-643.

Gripp, A.E., Gordon, R.G., 1990. Current plate velocities relative to the hotspot incorporating the NUVEL1 global plate motion model. *Geophys. Res. Lett.*, 17, 1109–1112. Doi: <https://doi.org/10.1029/GL017i008p01109>

Halliday, A.N., Davies, G.R., Lee, D.C., Tommasini, S., Oaslick, C.R., Fitton, J.G., James D.E., 1992. Lead isotope evidence for young trace element enrichment in the oceanic upper mantle. *Nature*, 359, 623 627. Doi: <https://doi.org/10.1038/359623a0>

Hart, S.R., 1988. Heterogeneous mantle domains: Signatures, genesis and mixing chronologies. *Earth and Planetary Science Letters*, 90, 272–296. Doi: [https://doi.org/10.1016/0012-821X\(88\)90131-8](https://doi.org/10.1016/0012-821X(88)90131-8)

Hart, S.R., Gerlach, D.C., White, W.M., 1986. A possible new Sr Nd Pb mantle array and consequences for mantle mixing. *Geochimica et Cosmochimica Acta*, 50, 1551-1557. Doi: [https://doi.org/10.1016/0016-7037\(86\)90329-7](https://doi.org/10.1016/0016-7037(86)90329-7)

Hawkesworth, C. J., Mantovani, M. S. M., Taylor, P. N. & Palacz, Z., 1986. Evidence from the Paraná of south Brazil for a continental contribution to Dupal basalts. *Nature*, 322, 356-359. Doi: <https://doi.org/10.1038/322356a0>

Hémond, C., Révillon, S., 2012. Petrological and geochemical study of - Vitória-Trindade Ridge and Trindade and Martin Vaz Islands - North Brazilian ridge. FINAL REPORT. 56 p.– UNPUBLISHED AND INTERNAL TO LEPLAC PROJECT.

Hoffman, A.W., 2014. 3.3 - Sampling Mantle Heterogeneity through Oceanic Basalts: Isotopes and Trace Elements. H.D. Holland, K.K. Turekian (Eds.), *Treatise on Geochemistry (Second Edition)*, 3, 67-101. Doi: <https://doi.org/10.1016/B978-0-08-095975-7.00203-5>

Hoffman, E.L., 1992. Instrumental Neutron Activation in Geoanalysis. *Journal of Geochemical Exploration*, 44, 297-319. Doi: [https://doi.org/10.1016/0375-6742\(92\)90053-B](https://doi.org/10.1016/0375-6742(92)90053-B)

International Centre for Diffraction Data (ICDD), International Centre for Diffraction Data-Pdf4+ Relational Powder Diffraction File. Available online: <http://www.icdd.com/products/pdf4.htm>. Accessed 20 March 2020

Jackson, M.G., Dasgupta, R., 2008. Compositions of HIMU, EM1, and EM2 from global trends between radiogenic isotopes and major elements in ocean island basalts. *Earth and Planetary Science Letters*, 276, 175–186. Doi: <https://doi.org/10.1016/j.epsl.2008.09.023>

Jarosewich, E., 2002. Smithsonian Microbeam Standards. *Journal of Research of the National Institute of Standards and Technology*, 107, 681-687. Doi: 10.6028/jres.107.054

Jesus, J.V.M., Santos, A.C., Mendes, J.C., Santos, W.H., Rego, C.A.Q., Geraldês, M.C., 2019. Petrogênese do Banco Davis, Cadeia Vitória-Trindade, Atlântico Sul: o Papel de Voláteis (H₂O e CO₂) na Evolução Magmática do Banco Davis. *Anuário do Instituto de Geociências*, 42, 237–253. Doi: http://dx.doi.org/10.11137/2019_3_237_253

Jung, C., Jung, S., Hoffer, E., Berndt, J., 2006. Petrogenesis of Tertiary Mafic Alkaline Magmas in the Hocheifel, Germany. *Journal of Petrology*, 47, 1637-1671. Doi: <https://doi.org/10.1093/petrology/egl023>

Le Roex, A.P., Cliff, R.A., Adair, B.J.I., 1990. Tristan da Cunha, South Atlantic: Geochemistry and Petrogenesis of a Basanite-Phonolite Lava Series. *Journal of Petrology*, 31, 779-812. Doi: <https://doi.org/10.1093/petrology/31.4.779>

Le Roex, A.P., Class, C., O'Connor, J., Jokat, W., 2010. Shona and Discovery Aseismic Ridge Systems, South Atlantic: Trace Element Evidence for Enriched Mantle Sources, *Journal of Petrology*, 51, 2089–2120. Doi: <https://doi.org/10.1093/petrology/egq050>

Maia, T.M., 2019. Petrologia inédita das rochas do Monte Submarino Vitória, Cadeia Vitória Trindade, Atlântico Sul. 2019, 92 p. Monography Geology Bsc. Course, Rio de Janeiro State University, Rio de Janeiro, Brazil.

Marques, L.S., Ulbrich, M.N.C., Ruberti, E., Tassinari, C.G., 1999. Petrology, geochemistry and Sr-Nd isotopes of the Trindade and Martin Vaz volcanic rocks (Southern Atlantic Ocean). *Journal of Volcanology and Geothermal Research*, 93, 191–216. Doi: [https://doi.org/10.1016/S0377-0273\(99\)00111-0](https://doi.org/10.1016/S0377-0273(99)00111-0)

McDonough, W.F., Sun, S.S., 1995. The composition of the Earth. *Chemical Geology*, 120, 223-253. Doi: [https://doi.org/10.1016/0009-2541\(94\)00140-4](https://doi.org/10.1016/0009-2541(94)00140-4)

Mckenzie, D., O'Nions, R.K., 1991. Partial melt distributions from inversion of rare earth element concentrations. *Journal of Petrology*, 32, 1021-1091. Doi: <https://doi.org/10.1093/petrology/32.5.1021>

Mckenzie, D., O'Nions, R.K., 1995. The source regions of oceanic island basalts. *Journal of Petrology*, 36, 133-159. Doi: <https://doi.org/10.1093/petrology/36.1.133>

Mizusaki, A.M.P., Alves, D.B., Conceição, J.C.J., 1994. Eventos magmáticos nas bacias do Espírito Santo, Mucuri e Cumuruxatiba. Cong. Brasil. Geol. XXXVIII, Anais. SBG, Camboriú (SC) 1994, p. 566–568.

Mizusaki, A.M.P., Thomaz, F.A., de Césero, P., 1998. Age of the magmatism and the opening of the South Atlantic Ocean. *Inst. Geoc., UFRGS, Porto Alegre: Pesquisas*, 25, 47–57.

Mohriak, W.U., 2006. Interpretação geológica e geofísica da Bacia do Espírito Santo e da região de Abrolhos: petrografia, datação radiométrica e visualização sísmica das rochas vulcânicas. *Boletim de Geociências da Petrobras*. 14, 133–142.

Motoki, A., Motoki, K.F., Melo, D.P., 2012. Submarine morphology characterization of the Vitória-Trindade Chain and the adjacent areas, state of Espírito Santo, Brazil, based on the predicted bathymetry of the TOPO version 14.1. *Revista Brasileira de Geomorfologia*, 13, 151–170. Doi: <http://dx.doi.org/10.20502/rbg.v13i2.195>

Müller, R.D., Seton, M., Zahirovic, S., Williams, S.E., Matthews, K.J., Wright, N.M., Shephard, G.E., Maloney, K.T., Barnett-Moore, N., Hosseinpour, M., Bower, D.J., Cannon, J., 2016. Ocean Basin Evolution and Global-Scale Plate Reorganization Events Since Pangea Breakup. *Annu. Rev. Earth Planet. Sci.*, 44, 107–138. Doi: <https://doi.org/10.1146/annurev-earth-060115-012211>

Neave, D.A., Putirka, K.D., 2017. A new clinopyroxene-liquid barometer, and implications for magma storage pressures under Icelandic rift zones. *Am. Mineral*, 102 (4), 777–794. Doi: [10.2138/am-2017-5968](https://doi.org/10.2138/am-2017-5968)

Niu, Y., 2009. Some basic concepts and problems on the petrogenesis of intra-plate ocean island basalts. *Chinese Science Bulletin*, 54, 4148–4160. Doi: <https://doi.org/10.1007/s11434-009-0668-3>

Niu, Y., Wilson, M., Humphreys, E.R., O'Hara, M.J., 2012. A trace element perspective on the source of ocean island basalts (OIB) and fate of subducted ocean crust (SOC) and mantle lithosphere (SML). *Episodes*, 35, 310–327. Doi: <https://doi.org/10.18814/epiugs/2012/v35i2/002>

O'Connor, J.M., Duncan, R.A., 1990. Evolution of the Walvis Ridge–Rio Grande Rise hot spot system: implications for African and South American plate motions over plumes. *Journal of Geophysical Research*, 95, 17475–17502. Doi: <https://doi.org/10.1029/JB095iB11p17475>

Oliveira, A.L., dos Santos, A.C., Nogueira, C.C., Maia, T.M., Geraldés, M.C., 2021. Green core clinopyroxenes from Martin Vaz archipelago Plio-Pleistocene alkaline rocks, south Atlantic ocean, Brazil: A magma mixing and polybaric crystallization record. *Journal of South American Earth Sciences*, 102951. Doi: <https://doi.org/10.1016/j.jsames.2020.102951>

Pearce, J.A., Norry, M.J., 1979. Petrogenetic implications of Ti, Zr, Y and Nb variations in volcanic rocks. *Contributions to Mineralogy and Petrology*, 69, 33–47. Doi: <https://doi.org/10.1007/BF00375192>

Peyve, A.A., Skolotnev, S.G., 2014. Systematic variations in the composition of volcanic rocks in tectono-magmatic seamount chains in the Brazil Basin. *Geochem. Int.*, 52, 111–130. Doi: <https://doi.org/10.1134/S0016702914020062>

Pires, G.L.C., Bongiolo, E.M., Geraldés, M.C., Renac, C., Santos, A.C., Jourdan, F., Neumann, R., 2016. New $^{40}\text{Ar}/^{39}\text{Ar}$ ages and revised $^{40}\text{K}/^{40}\text{Ar}^*$ data from nephelinitic–phonolitic volcanic successions of the Trindade Island (South Atlantic Ocean). *Journal of Volcanology and Geothermal Research*, 327, 531–538. Doi: <https://doi.org/10.1016/j.jvolgeores.2016.09.020>

Putirka, K. D., 2005. Igneous thermometers and barometers based on plagioclase+ liquid equilibria: Tests of some existing models and new calibrations. *American Mineralogist*, 90 (2-3), 336-346. Doi: <https://doi.org/10.2138/am.2005.1449>

Putirka, K.D., 2008. Thermometers and barometers for volcanic systems. *Rev. Mineral. Geochem.* 69 (1), 61–120. Doi: <https://doi.org/10.2138/rmg.2008.69.3>

Quaresma, G.O.A., 2019. Geoquímica Isotópica Sr-Nd-Pb e Geocronologia $^{40}\text{Ar}/^{39}\text{Ar}$ do Banco Submarino Davis, Cadeia Vitória-Trindade: Possíveis Implicações com a Movimentação da Placa Sul-Americana durante o Mioceno. 121 p. Monography Geology Bsc. Course, Rio de Janeiro State University, Rio de Janeiro, Brazil.

Rocha-Júnior, E.R.V., Puchtel, I.S., Marques, L.S., Walker, R.J., Machado, F.B., Nardy, A.J.R., Babinski, M., Figueiredo, A.M.G., 2012. Re-Os isotope and highly siderophile element systematics of the Paraná Continental Flood Basalts (Brazil). *Earth and Planetary Science Letters*, 337-338, 164-173. Doi: <https://doi.org/10.1016/j.epsl.2012.04.050>

Rocha-Júnior, E.R.V., Marques, L.S., Babinski, M., Nardy, A.J.R., Figueiredo, A.M.G., Machado, F.B., 2013. Sr-Nd-Pb isotopic constraints on the nature of the mantle sources involved in the genesis of the high-Ti tholeiites from Northern Paraná Continental Flood Basalts (Brazil). *Journal of South American Earth Sciences*, 46, 9-25. Doi: <https://doi.org/10.1016/j.jsames.2013.04.004>

Salters, V.J.M., Stracke, A., 2004. Composition of the depleted mantle. *Geochemistry, Geophysics, Geosystems*, 5, Q05B07. Doi: <https://doi.org/10.1029/2003GC000597>

Santos, A.C., 2013. Petrography, Lithochemochemistry and $^{40}\text{Ar}/^{39}\text{Ar}$ dating of the seamounts and Martin Vaz Islands -Vitoria-Trindade Ridge. Dissertation, Universidade do Estado do Rio de Janeiro, Brazil.

Santos, A.C., 2016. Petrology of Martin Vaz Island and Vitoria-Trindade Ridge seamounts: Montague, Jaseur, Davis, Dogoressa and Columbia. Trace elements, $^{40}\text{Ar}/^{39}\text{Ar}$ dating and Sr and Nd isotope analysis related to the Trindade Plume evidence. Ph. D. Thesis, Universidade do Estado do Rio de Janeiro, Brazil.

Santos, A.C., Geraldés, M.C., Vargas, T., Williams, S., 2015. Geology of Martin Vaz, South Atlantic, Brazil. *Journal of Maps*, 11, 314–322. Doi: <https://doi.org/10.1080/17445647.2014.936913>

Santos, A.C., Geraldés, M.C., Siebel, W., Mendes, J., Bongiollo, E., Santos, W.H., Garrido, T. C.V., Rodrigues S.W.O., 2018a. Pleistocene alkaline rocks of Martin Vaz volcano, South Atlantic: low-degree partial melts of a CO_2 -metasomatized mantle plume. *International Geology Review*, 61, 296–313. Doi: <https://doi.org/10.1080/00206814.2018.1425921>

Santos, A.C., Mata, J., Jourdan, F., Rodrigues, S.W. de O., Monteiro, L.G.P., Guedes, E., Benedini, L., Geraldés, M.C., 2021. Martin Vaz island geochronology: Constraint on the Trindade Mantle Plume track from the youngest and easternmost volcanic episodes. *Journal Of South American Earth Sciences*, 106, 103090. Doi: <https://doi.org/10.1016/j.jsames.2020.103090>

Santos, A.C., Mohriak, W.U., Geraldés, M.C., Santos, W.H., Ponte-Neto, C.F., Stanton, N., 2018b. Compiled potential field data and seismic surveys across the Eastern Brazilian continental margin integrated with new magnetometric profiles and stratigraphic configuration

for Trindade Island, South Atlantic, Brazil. *International Geology Review*, 61, 1728-1744. Doi: <https://doi.org/10.1080/00206814.2018.1542634>

Santos, R.N. & Marques, L.S., 2007. Investigation of ^{238}U – ^{230}Th – ^{226}Ra and ^{232}Th – ^{228}Ra – ^{228}Th radioactive disequilibria in volcanic rocks from Trindade and Martin Vaz Islands (Brazil; Southern Atlantic Ocean). *Journal of Volcanology and Geothermal Research*, 161, 215–233. Doi: <https://doi.org/10.1016/j.jvolgeores.2006.11.010>

Sempere, T., Folguera, A., & Gerbault, M., 2008. New insights into Andean evolution: An introduction to contributions from the 6th ISAG symposium (Barcelona, 2005). *Tectonophysics*, 459, 1–13. Doi: <https://doi.org/10.1016/j.tecto.2008.03.011>

Shaw, D.M., 1970. Trace element fractionation during anatexis. *Geochimica et Cosmochimica Acta*, 34, 237-243. Doi: [https://doi.org/10.1016/0016-7037\(70\)90009-8](https://doi.org/10.1016/0016-7037(70)90009-8)

Siebel, W., Becchio, R., Volker, F., Hansen, M.A.F., Viramonte, J., Trumbull, R.B., Haase, G., Zimmer, M., 2000. Trindade and Martin Vaz Islands, South Atlantic: Isotopic (Sr, Nd, Pb) and trace element constraints on plume related magmatism. *Journal of South American Earth Science*, 13, 79–103. Doi: [https://doi.org/10.1016/S0895-9811\(00\)00015-8](https://doi.org/10.1016/S0895-9811(00)00015-8)

Skolotnev, S.G., Bylinskaya, M.E., Golovina, L.A., Ipateva, I.S., 2011. First Data on the Age of Rocks from the Central Part of the Vitória–Trindade Ridge (Brazil Basin, South Atlantic). *Dokl. Earth Sc.*, 437, 316–322. Doi: <https://doi.org/10.1134/S1028334X11030093>

Skolotnev, S.G., Peive, A.A., 2017. Composition, structure, origin, and evolution of off-axis linear volcanic structures of the Brazil Basin, South Atlantic. *Geotectonics*, 51, 53–73. <https://doi.org/10.1134/S001685211701006X>

Sobreira, J.F.F., França R.L., 2006. Um modelo tectono-magmático para a região do Complexo Vulcânico de Abrolhos. *Boletim de Geociências da Petrobrás*, 14, 143-147.

Sobreira, J. F. F.; Szatmari, P.; Mohriak, W. U.; Valente, S. C.; York, D., 2004. Recorrência, em diferentes escalas, do magmatismo paleogênico no Arquipélago de Abrolhos, Complexo Vulcânico de Abrolhos. XLII Congresso Brasileiro de Geologia, 2004, Araxá, MG. Anais. Sociedade Brasileira de Geologia, Núcleo de Minas Gerais.

Somoza, R., 1998. Updated Nazca (Farallon)-South America relative motions during the last 40 My: Implications for mountain building in the central Andean region. *Journal of South American Earth Sciences*, 11, 211–215. Doi: [https://doi.org/10.1016/S0895-9811\(98\)00012-1](https://doi.org/10.1016/S0895-9811(98)00012-1)

Szatmari, P & Mohriak, W. U., 1995. Plate model of post-breakup tectono-magmatic activity in the adjacent Atlantic. In: SBG/Núcleo Rio grande do Sul, Simpósio Nacional de Estudos Tectônicos, 5, Gramado, Anais, 1, 213-214.

Sun, S.S., McDonough, W.F., 1989. Chemical and isotopic systematics of oceanic basalts: implications for mantle composition and processes. *Geological Society*, London, Special Publications, 42, 313-345. Doi: <https://doi.org/10.1144/GSL.SP.1989.042.01.19>

Tanaka, T., Togashi, S., Kamioka, H., Amakawa, H., Kagami, H., Hamamoto, T., Yuhara, M., Orihashi, Y., Yoneda, S., Shimizu, H., Kunimaru, T., Takahashi, K., Yanagi, T., Nakano, T., Fujimaki, H., Shinjo, R., Asahara, Y., Tanimizu, M., Dragusanu C., 2000. JNdi-1: a neodymium isotopic reference in consistency with LaJolla neodymium. *Chemical Geology*, 168, 279–281. Doi: [https://doi.org/10.1016/S0009-2541\(00\)00198-4](https://doi.org/10.1016/S0009-2541(00)00198-4)

- Tatsumi, Y., 2000. Continental crust formation by crustal delamination in subduction zones and complementary accumulation of the enriched mantle I component in the mantle. *Geochemistry, Geophysics, Geosystems*, 1. Doi: <https://doi.org/10.1029/2000GC000094>
- Tebbens, S., Cande, S., 1997. Southeast Pacific tectonic evolution from Early Oligocene to present. *Journal of Geophysical Research*, 102, 12061-12084. Doi: <https://doi.org/10.1029/96JB02582>
- Thomaz-Filho, A., Cesero, P. De, Maria, A., Lea, J.G., 2005. Hot spot volcanic tracks and their implications for south American plate motion, Campos basin (Rio de Janeiro state), Brazil. *Journal of South American Earth Sciences*, 18, 383–389. doi: <https://doi.org/10.1016/j.jsames.2004.11.006>
- Thompson, R.N., Gibson, S.A., Mitchell, J.G., Dickin, A.P., Leonardos, O.H., Brod, J.A., Greenwood, J.C., 1998. Migrating Cretaceous – Eocene Magmatism in the Serra do Mar Alkaline Province, SE Brazil: Melts from the Deflected Trindade Mantle Plume? *Journal of Petrology*, 39, 1493–1526. Doi: <https://doi.org/10.1093/petroj/39.8.1493>
- Valeriano, C.M., Ragatk, C.D., Geraldes, M.C., Heilbron, M., Valladares, C.S., Schmitt, R.S., Tupinambá, M., Palermo, N., Almeida, J.C.H., Duarte, B.P., Martins, J.R.E., Nogueira, J.R., 2003. A new TIMS laboratory under construction in Rio de Janeiro, Brazil. In IV South American Symposium on Isotope Geology, Salvador. *Short Papers IV South American Symposium on Isotope Geology*, 1, 131–133.
- Veloso, J.A.V. & Machado, D.L., 1986. Estudos sismológicos na ilha da Trindade desenvolvidos pela estação sismológica da UnB. In: Cong. Bras. Geol., 34, Goiânia. 1986. Anais Goiânia SBG, 6, 2.608-2.613.
- Xia, L., Li, X., 2019. Basalt geochemistry as a diagnostic indicator of tectonic setting. *Gondwana Research*, v. 65, p. 43–67. Doi: <https://doi.org/10.1016/j.gr.2018.08.006>
- Weaver, B.L., 1990. Geochemistry of highly-undersaturated ocean island basalt suites from the South Atlantic Ocean: Fernando de Noronha and Trindade islands. *Contributions to Mineralogy and Petrology*, 105, 502-515. Doi: <https://doi.org/10.1007/BF00302491>
- Workman, R.K., Hart, S.R., 2005. Major and trace element composition of the depleted MORB mantle (DMM). *Earth and Planetary Science Letters*, 231, 53-72. Doi: <https://doi.org/10.1016/j.epsl.2004.12.005>
- Zindler, A., Hart, S.R., 1986. Chemical geodynamics. Annual reviews: *Earth and Planetary Science Letters*, 14, 493–571. Doi: <https://doi.org/10.1146/annurev.ea.14.050186.002425>

APPENDIX B – Abrolhos Volcanic Complex petrogenesis and its link with the Vitória-Trindade Ridge, Southeast Brazilian Margin, South Atlantic Ocean

**Abrolhos Volcanic Complex petrogenesis and its link with the Vitória-Trindade Ridge,
Southeast Brazilian Margin, South Atlantic Ocean**

Thais Mothé Maia^{1a}; Anderson Costa dos Santos^{1b}; Sérgio Castro Valente²; Eduardo Reis Viana Rocha Júnior³; Guilherme Pacheco Watson de Barros¹; Mônica Heilbron^{4a}; Claudio de Morisson Valeriano^{4b}; Michele Arena⁵

¹Universidade do Estado do Rio de Janeiro (UERJ), Faculdade de Geologia, Departamento de Mineralogia e Petrologia Ígnea (DMPI). Rua São Francisco Xavier, 524 - 4º e 2º andar. Maracanã, 20550-900, Rio de Janeiro, RJ, Brasil. ^{1a}ORCID: 0000-0002-5956-6362. ^{1b}Tektos Group, UERJ - Brazil / GeoBioTec Group, Aveiro University - Portugal. ORCID: 0000-0003-2526-8620.

²Universidade Federal Rural do Rio de Janeiro (UFRRJ), Departamento de Petrologia e Geotectônica. Rodovia BR 465 Km 7, Cidade Universitária, 23890-000, Seropédica, RJ, Brasil. ORCID: 0000-0002-7467-672X

³Universidade Federal da Bahia (UFBA), Instituto de Física, Departamento de Física da Terra e do Meio Ambiente. Rua Barão de Jeremoabo, s/n, 40170-115, Salvador (BA), Brasil. ORCID: 0000-0003-1853-015X

⁴Universidade do Estado do Rio de Janeiro (UERJ), Faculdade de Geologia, Departamento de Geologia Regional e Geotectônica (DGRG). Rua São Francisco Xavier, 524 - 4º e 2º andar/bloco A, 20550-900, Rio de Janeiro, RJ, Brasil. ^{4a}ORCID: 0000-0002-3521-9251; ^{4b}ORCID: 0000-0002-9341-2615

⁵ Universidade Federal do Rio De Janeiro (UFRJ), Departamento de Geologia, Instituto de Geociências, Laboratório de Geologia Sedimentar (Lagesed). Av. Athos da Silveira Ramos, 274. CEP: 21941-916, Campus Ilha do Fundão, Rio de Janeiro, Brasil. ORCID: 0000-0002-6883-3936

Emails: thais_mothe@hotmail.com; andcostasantos@gmail.com; sergio@ufrj.br; eduardo.junior@ufba.br; w.atson@hotmail.com; monica.heilbron@gmail.com; valeriano.claudio@gmail.com; michele@geologia.ufrj.br

Abstract

The Abrolhos Volcanic Complex (AVC) is an example of a large igneous province with about 63,000 km² located at the Continent-Ocean Boundary (COB). Its magmatic rocks crop out at the offshore section of the Espírito Santo, Mucuri, and Cumuruxatiba sedimentary basins, Southeast Brazilian Margin. The AVC emerges as five small islands (Santa Bárbara, Redonda, Siriba, Sueste, and Guarita) which integrate the Abrolhos Archipelago located about 55 km offshore Brazil. The AVC and the Vitória-Trindade Ridge (VTR) show an eastward decreasing age pattern from the older *ca.* 60 Ma Abrolhos Complex to the younger Martin Vaz and Trindade Islands, located *ca.* 1200 km away from the coastline. This age pattern is consistent with the westward motion of the South American plate over the Trindade hotspot. The AVC magmatism lies northwest of the VTR (*ca.* 110 km) and extends approximately 250 km from

the stretched continental to the oceanic lithospheres. This work presents new detailed field mapping, petrographic, and whole-rock chemistry data, besides Sr-Nd isotopic compositions from rocks of the AVC. Mapped magmatic rocks in the Abrolhos Islands have been described as extrusive rocks, but we point out that they are shallow intrusions, mostly sills, and should be grouped into diabase units. The studied Paleocene-Eocene Abrolhos rocks belong to a transitional basalt series of alkaline affinity, with relatively evolved rocks with high TiO₂ contents. Major and trace element diagrams show large data dispersion when plotted versus a fractionation index (*e.g.* MgO and Zr), thus suggesting a complex evolution. Since the whole-rock samples analyzed in this study have low LOI contents (≤ 3.8 wt.%), they possibly represent fresh basic rocks with a minor post-emplacement alteration. Indeed, all the chemical and isotopic variation could be possibly attributed to original variation, and differentiation by magma replenishment, tapping, and fractionation (RTF) seems to have been the predominant process, potentially linked to the subvolcanic plumbing system evolution. New and compiled isotope data suggest a peridotitic mantle source (represented by depleted MORB mantle – DMM) metasomatized by an enriched mantle I (EMI) component and a HIMU-type constituent. Our model mixing calculations suggest a mixture with 75% of DMM, <15% of EMI, and possibly up to 10% of HIMU in the AVC source. The assimilation of subducted slabs of the oceanic crust associated with the HIMU signatures is possibly linked to the Brasiliano Event due to the range of the AVC Nd T_{DM} model ages, from 407 to 767 Ma. A viable mechanism for the EMI-like end-member rocks could either be a physical detachment of the South American subcontinental lithospheric mantle during the breakup of the Gondwana or lithospheric delamination of the South American plate caused by edge-driven convection mechanism. The volcanic alignment between the VTR and AVC, along with the overlap of geochemical and isotopic data of their different igneous rocks, cannot be a random feature but instead represent the sampling of similar shallow mantle reservoirs, thus suggesting a cogenetic relationship. Finally, a possible petrogenetic link between the AVC and VTR magmatism is discussed.

Keywords: Abrolhos volcanism, Sr-Nd isotope characteristics, Plumbing system, Eocene-Pleistocene volcanism, Vitória-Trindade Ridge

1. Introduction

The intraplate magmatism in the southern South Atlantic Ocean is often attributed to plumes of hot mantle material rising from the deep mantle based on geochemical and isotopic data, age progression of volcanic alignments, and pronounced bathymetric anomalies (Courtillot et al., 2003; Colli et al., 2013; Celli et al., 2020; Koppers et al., 2021). In this context, the Abrolhos Volcanic Complex (AVC) and the Vitória-Trindade Ridge (VTR) (Fig. 1) have been interpreted as the Trindade Plume volcanic trail at the South American Plate (*e.g.*, Thompson et al., 1998; Mohriak, 2006; Bongiolo et al., 2015; Pires et al., 2016; Santos et al., 2018a,b). The apparent eastward decrease in radiometric and paleontological ages along the AVC and the VTR (*e.g.*, Cordani, 1970; Cordani and Blazekovic, 1970; Pires et al., 2016; Skolotnev and Peive, 2017; Santos et al., 2015; 2021; Monteiro et al., 2022) and the presence of a low-velocity anomaly down to 200-260 km in the VTR and AVC regions (Celli et al., 2020)

point out the influence of a shallow thermochemical mantle anomaly in magmatic processes in both areas. Therefore, geophysical surveys don't suggest any kind of upper and lower mantle communication below the South Atlantic since low-seismic velocity anomalies have been recorded up to 260 km.

Thus, these geophysical anomalies observed exclusively in the shallow mantle have been used to challenge the need to invoke deep mantle plumes originating at the core-mantle boundary (CMB) or 670 km seismic discontinuity to explain the origin of intraplate volcanism. Instead, some authors (*e.g.*, Meibom and Anderson, 2003; Niu and O'Hara, 2003; Mallik and Dasgupta, 2012) have suggested that upper mantle processes can account for most features assigned to a mantle plume origin. For instance, Stanton et al. (2021) suggested that the sizable area and longtime duration of the AVC activity are incompatible with a fixed hotspot mechanism, as well as the lack of an eastward age progression in AVC magmatism. Quaresma et al. (*in press*) further highlighted the lack of convincing evidence for the Trindade plume participation in the VTR petrogenesis, emphasizing the need for diverse and accurate geochronological data. In addition, as there is no geochemical and geophysical evidence linking the VTR genesis to a deep mantle plume, those authors proposed that the VTR petrogenesis would be associated with the presence of detached subcontinental lithospheric mantle (SCLM) fragments and different proportions of recycled oceanic crust (MORB-eclogite) and lithosphere in the upper mantle (at 250 km) beneath the South Atlantic Ocean.

Other models that dispute the origin of intraplate magmatism from deep mantle plumes suggest that the location of melting anomalies is controlled by stress, since volcanic chains or volcanic alignments are expected to develop along extensional structures, such as fissures, faults or cracks. For instance, Fairhead and Wilson (2005) suggested that the bathymetric features observed along Walvis Ridge and the Rio Grande Rise were formed as a consequence of periodic release of intraplate stress via shear faulting, according to high-resolution gravity data. Other authors also attributed the origin and evolution of the VTR and the AVC to the control of structural features (Fainstein and Summerhays, 1982; Veloso and Machado, 1986; Szatmari and Mohriak, 1995; Conceição et al., 1996; Ferrari and Riccomini, 1999; Almeida, 2006; Alves et al., 2006, Barão et al., 2020, Stanton et al., 2021; Alves et al., 2022). As such, the Vitória-Trindade Fracture Zone (Fig. 1) may have acted as a conduit for the VTR magmatism (Veloso and Machado, 1986; Szatmari and Mohriak, 1995; Conceição et al., 1996; Ferrari and Riccomini, 1999; Almeida, 2006; Alves et al., 2006, Barão et al., 2020, Alves et al., 2022) whereas the Precambrian structural trends along with offshore rifting structures and the

Continent-Ocean Boundary (COB) may have played a role in the AVC emplacement (Fainstein and Summerhays, 1982; Stanton et al., 2021).

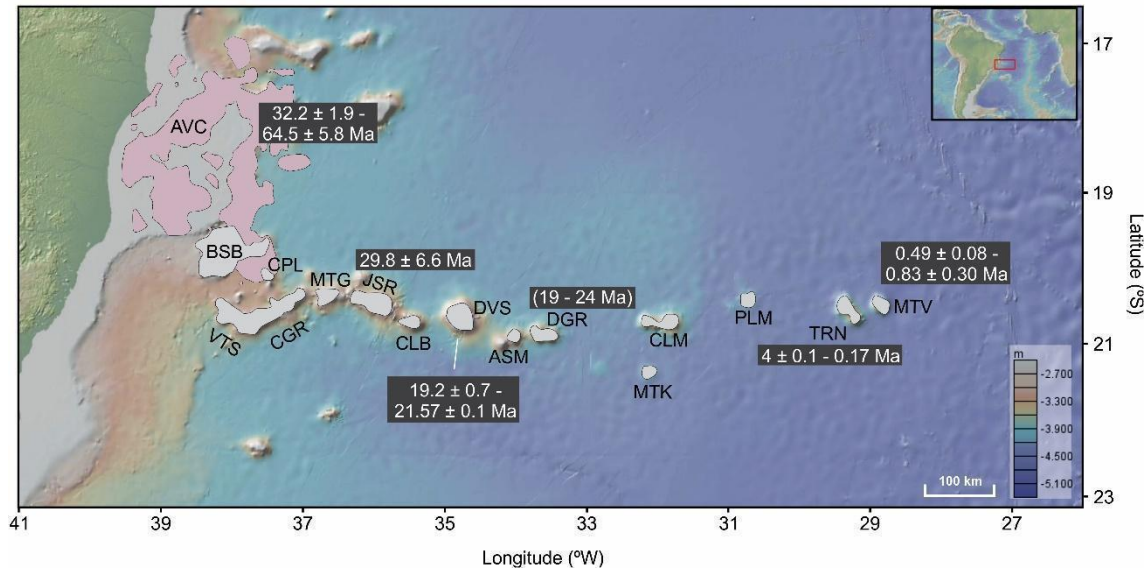


Fig. 1 – The Vitória-Trindade Ridge (VTR) and the Abrolhos Volcanic Complex (AVC) modified from Maia et al. (2021). AVC – Abrolhos Volcanic Complex ($^{40}\text{K}/^{40}\text{Ar}$ ages from Cordani, 1970; Cordani and Blazekovic, 1970; Fodor et al., 1983; $^{40}\text{Ar}/^{39}\text{Ar}$ ages from Sobreira and Szatmari, 2003; Sobreira et al., 2004); BSB – Besnard Bank; CPL – Champlain Seamount; VTS – Vitória Seamount; CGR – Congress Seamount; MTG – Montague Seamount; JSR – Jaseur Seamount ($^{238}\text{U}/^{206}\text{Pb}$ ages from Skolotnev et al., 2011); CLB – Colúmbia Bank; DVS – Davis Bank ($^{40}\text{Ar}/^{39}\text{Ar}$ ages from Santos, 2016; Skolotnev and Peive, 2017, Quaresma et al., *in press*); ASM – Asmus Bank; DGR – Dogaressa Bank (paleontological ages obtained from recrystallized limestones in parentheses; Skolotnev et al., 2011); CLM – Colúmbia Seamount; MTK – Motoki Hill; PLM – Palma Seamount; TRN – Trindade Island ($^{40}\text{Ar}/^{39}\text{Ar}$ ages from Geraldes et al., 2013; Pires et al., 2016); MTV – Martin Vaz Archipelago ($^{40}\text{Ar}/^{39}\text{Ar}$ ages from Santos, 2013; 2016; Santos et al., 2015; 2021; Santos and Hackspacher, 2021; Monteiro et al., 2022; Santos et al., 2022a).

After almost thirty years without any detailed published article for the petrology of the Abrolhos magmatism, this work presents new field work mapping, petrographic, lithogeochemical, and Sr-Nd isotopic data for the Abrolhos Islands (Santa Bárbara, Siriba, Sueste and Redonda). These new data were used to discriminate different source components associated with the petrogenesis of the Abrolhos magmatism, as well as the differentiation processes involved in the AVC evolution. This study also discusses a possible petrogenetic link between the AVC and VTR magmatism, since the AVC, along with the VTR, show broad age-progressive magmatic events from the younger Martin Vaz and Trindade Islands to AVC, supporting a Trindade hotspot origin for these magmatic events.

2. Geological background

2.1. The Abrolhos Volcanic Complex (AVC)

The AVC (Almeida et al., 1996; Conceição et al., 1996; Sobreira and França, 2006; Stanton et al., 2021; 2022) is located at the Continent-Ocean Boundary (COB) of the Southeast Brazilian Margin (Stanton et al., 2021; 2022), encompassing the Espírito Santo, Mucuri, and Cumuruxatiba marginal sedimentary basins (Almeida et al., 1996; Mohriak, 2006; Sobreira and França, 2006; França et al., 2007; Stanton et al., 2021; Fig. 2). It corresponds to an igneous province composed of transitional basalts (Fodor et al., 1989; Sobreira and Szatmari, 2002; Arena, 2008). The origin of the magmatism has been attributed to eruptions from central conduits over a thin and stretched continental platform and oceanic crust (Almeida et al., 1996; Sobreira and França, 2006; Stanton et al., 2021; 2022). It has a roughly circular geometry with an estimated area of about 63,000 km² (Stanton et al., 2021; 2022; Fig. 2) that may be even larger and not restricted just to the offshore portion of the adjoining sedimentary basins (Oliveira et al., 2018) and neither to the Abrolhos Platform (Stanton et al., 2021). The AVC volcanism displays two deep central magmatic bodies (R1 and R2) that feed radially the smaller shallow elongated bodies (E1-E7) formed by different magmatic pulses (Fig. 2; Stanton et al., 2021; see text for discussions). These two larger buildings coincide with the location of possible magma chambers as suggested by Sobreira and França (2006). Besides those two larger bodies and the elongated ones, there are also two magnetic and seismic anomalies located in the oceanic crust (O1 and O2; Stanton et al., 2021). The Abrolhos Archipelago region uplift has been associated with regional compressional tectonic forces and salt tectonics (Mohriak et al., 2003; Mohriak, 2006; 2020; Stanton et al., 2022). Apatite fission trace analyses point to an apex of the Abrolhos uplift around 50 Ma (Mohriak, 2006), *i.e.*, within the interval of the radiometric ages of the Abrolhos magmatism.

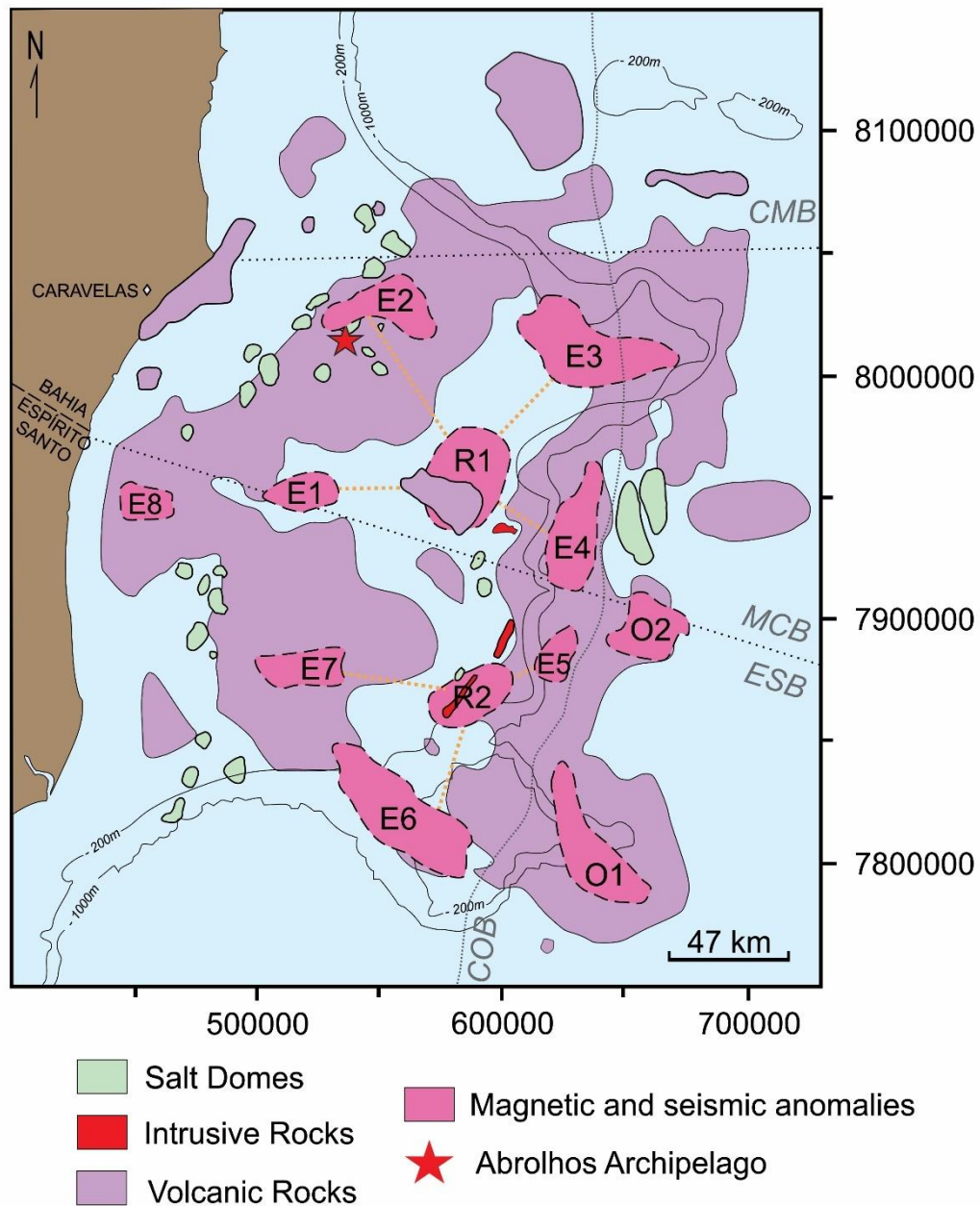


Fig. 2 – Magmatic framework model of the Abrolhos Volcanic Complex (AVC) region (modified from Sobreira and França (2006) and Stanton et al. (2021)). R1, R2, E1-E7, O1 and O2 are magnetic and seismic anomalies interpreted as igneous bodies by Stanton et al. (2021). ESB = Espírito Santo Sedimentary Basin; MCB = Mucuri Sedimentary Basin; CMB = Cumuruxatiba Sedimentary Basin; COB = Continent-Ocean Boundary.

The AVC emerges as five small islands (Santa Bárbara, Redonda, Siriba, Sueste, and Guarita) that constitute the Abrolhos Archipelago located about 55 km southeast of Caravelas city, Bahia state (Fig. 2 and 3). The Santa Bárbara Island reaches the highest altitude above sea level (27 m) and the most extensive surface area of 0.44 km². The Abrolhos Archipelago rocks comprise a Paleocene-Eocene (32-64 Ma; Cordani, 1970; Cordani and Blazekovic, 1970; Fodor et al., 1983; Sobreira and Szatmari, 2002; 2003; Sobreira et al., 2004) transitional basalt series

of alkaline affinity. In studied islands, basalts, diabases, and cumulatic rocks (Supplementary Material 1) crop out interbedded with sedimentary rocks, mainly turbiditic sandstones, and marine shales (Cordani, 1970; Fodor et al., 1989; Gomes et al., 1992; Sobreira and França, 2006; Mohriak, 2006; Arena, 2008; Matte, 2013; Oliveira et al., 2018).

The magmatic rocks in the AVC were generally described as basalts with prevailing intergranular, porphyritic, and poikilitic textures. Phenocrysts are mostly pyroxene and plagioclase and minor olivine. The groundmass is composed of plagioclase, clinopyroxene, Fe-Ti oxides, and may contain olivine and devitrified and altered glass. Chlorite, saussurite, biotite, smectite, and iddingsite are secondary phases, and apatite appears as an accessory mineral (Fodor et al., 1989; Arena, 2008). Cumulatic rocks occur in the Petrobras well SBST-1-BA drilled on Santa Bárbara (573 m below surface; Fodor et al., 1989) and also outcrop in the western portion of the Santa Bárbara Island at the top of the lithostratigraphic sequence (Arena, 2008). They have inequigranular and porphyritic textures and are composed of plagioclase and clinopyroxene phenocrysts and intergranular ilmenite grains. Diabases were also described in drill holes SBST-1-BA (620, 670 and 709 m below surface; Fodor et al., 1989; Cordani, 1970; Gomes et al., 1992) and ESS9, the latter within the Espírito Santo sedimentary basin (Fodor et al., 1989). The well samples usually show porphyritic, poikilitic, ophitic, or subophitic textures. The phenocrysts are represented by clinopyroxene, plagioclase, Fe-Ti oxide, and occasionally olivine. The groundmass comprises plagioclase, clinopyroxene, magnetite, apatite, olivine, and alteration phases such as biotite, chlorite, and sericite. Some samples also bear prehnite, biotite, amphiboles, chlorite, and epidote, which are mineral phases typically found in metabasalts, suggesting a very low degree of metamorphism (Gomes et al., 1992).

Some volcanic deposits with acid rocks onshore have been associated with the Abrolhos magmatism. Novais et al. (2008) and Vieira et al. (2014) reported ignimbrites nearby the São Matheus River margin, located on the onshore portion of the Espírito Santo Basin. Gomes and Suita (2010) placed rhyolites and trachytes located in the Mucuri Basin at the top of the Abrolhos Formation. Motoki et al. (2007) reported rocks of pyroclastic rhyolitic nature in the Espírito Santo Basin.

The genesis of the Abrolhos basaltic rocks was attributed to the crystallization of a picritic parental liquid with a relatively rapid cooling (Fodor et al., 1989). This picritic liquid would have been emplaced at the base of or into a cold crystalline continental crust in the Eocene.

The $La/Yb_{(N)}$ e $La/Nb_{(N)}$ ratios (*ca.* 6.0-9.3 and 0.4-1.0, respectively) of the different AVC rocks can be explained by different degrees of partial melting from the same fertile mantle

source (plume-type; Arena, 2008). Fodor et al. (1989) have also proposed a mixture between compositions of a mantle plume and a depleted component to explain the AVC trace-element ratios (*e.g.*, Zr/Y *avg.* 7.9; Zr/Nb *avg.* 5.4) and isotopic compositions. Some authors (*e.g.*, Thompson et al., 1998) have proposed the involvement of a plume component, suggesting that the AVC is part of the volcanic trail left by the passage of the South American Plate over the Trindade Plume. As such, the AVC would be the first plume expression in the passive continental margin (O'Connor and Duncan, 1990; Conceição et al., 1996; Thompson et al., 1998; Ferrari and Riccomini, 1999; Sobreira et al., 2004; Alves et al., 2006; Arena, 2008).

Previous isotopic data from the AVC basalts show $^{87}\text{Sr}/^{86}\text{Sr}_{(m)}$ ratios ranging from 0.703720 to 0.703900 (Fodor et al., 1983; 1989). The diabase samples have more radiogenic Sr ratios (0.704110 to 0.704670), and a wehrlite sampled in well ESS9 showed an even more radiogenic Sr measured ratio (0.707330), probably due to seawater alteration (Fodor et al., 1989). The $^{143}\text{Nd}/^{144}\text{Nd}_{(m)}$ ratios range from 0.512636 to 0.512841 among all lithotypes. The $^{206}\text{Pb}/^{204}\text{Pb}$, $^{207}\text{Pb}/^{204}\text{Pb}$ and $^{208}\text{Pb}/^{204}\text{Pb}$ isotope ratios range from 18.90 to 19.33, 15.54 to 15.63 and 38.73 to 39.07, respectively (Fodor et al., 1989).

2.2. The Vitória-Trindade Ridge (VTR)

The Vitória-Trindade Ridge (VTR) extends southeast of the AVC from the Brazilian continental slope to about 1,200 km into the deep waters of the Atlantic Ocean (Almeida, 2006). It shapes a west-east-trending volcanic aseismic ridge composed of more than 30 seamounts and banks, and the easternmost islands named Trindade and Martin Vaz, where the youngest volcanic rocks of VTR and Brazil outcrop above sea-level (Santos et al., 2015; 2018a,b; Alberoni et al., 2020; Santos and Hackspacher, 2021; Alberoni and Jeck, 2022; Monteiro et al., 2022; Santos et al., 2022a,b) (Fig. 1). The VTR volcanic rocks show a strong enriched mantle signature based on normalized REE ratios and a strongly undersaturated alkaline affinity, ranging lithologically from basanites and nephelinites to more evolved rocks, such as tephri-phonolites and (nosean-)phonolites (Santos, 2013; 2016; Bongiolo et al., 2015; Pires and Bongiolo, 2016; Santos et al., 2015; 2018a,b; 2021; 2022 a,b; Oliveira et al., 2021; Maia et al., 2021; Rego et al., 2021; Santos and Hackspacher, 2021; Monteiro et al., 2022).

In general, ultrabasic alkaline rocks comprise the VTR seamounts and banks, such as ankaramites from the Colúmbia Seamount and the Dogaressa Bank, melanephelinites from the Montague and Jaseur seamounts, and alkaline basalt from the Vitória Seamount (Fodor and Hanan, 2000; Skolotnev et al., 2010; Santos, 2013; 2016; Maia et al., 2021; Santos and

Hackspacher, 2021; Santos et al., 2022b). On the other hand, basic rocks occur on Davis Bank, which shows basanites and olivine basalts (Skolotnev et al., 2010; Jesus et al., 2019; Rego et al., 2021). Some ages obtained from samples dredged from the VTR submarine volcanic edifices have been reported in the literature (Fig. 1), such as 29.8 ± 6.6 Ma for Jaseur Seamount (U-Pb in zircon; Skolotnev et al., 2011) and 19.2 ± 0.7 to 21.57 ± 0.1 Ma for Davis Bank (whole-rock $^{40}\text{Ar}/^{39}\text{Ar}$; Santos, 2016; Skolotnev and Peive, 2017; Quaresma et al., *in press*). An age range similar to Davis (19-24 Ma) was suggested for the Dogaressa Bank based on recrystallized limestones that may have been formed during the magmatic quiescence (Skolotnev et al., 2011).

The Trindade and Martin Vaz volcanic rocks present a strong enriched mantle signature (La/Yb_N *ca.* 30) of strongly undersaturated alkaline affinity composed of nephelinitic-phonolitic successions (Marques et al., 1999; Santos, 2013; 2016; Bongiollo et al., 2015; Pires and Bongiollo, 2016; Santos et al., 2015; 2018a,b; 2021; 2022a; Oliveira et al., 2021; Santos and Hackspacher, 2021; Monteiro et al., 2022). The Trindade Island and Martin Vaz volcanic rocks have ages ($^{40}\text{Ar}/^{39}\text{Ar}$) between 4.0 ± 0.1 Ma and 0.17 Ma (Geraldés et al., 2013; Pires et al., 2016) and between 0.83 ± 0.30 Ma and 0.49 ± 0.08 Ma (Cordani, 1970; Santos, 2013; 2016; Santos et al., 2015; 2021), respectively.

The least evolved compositions of the VTR rocks (alkaline basalts, melanephelinites, tephrites, ankaramites, basanites, and nephelinites) have 30–47 wt.% in SiO_2 (lower values in Dogaressa and Colúmbia ankaramites), 5-12 wt.% in FeO (with an average value of 11.74 wt.%; lowest values from the Trindade Island basanites; Siebel et al., 2000), high MgO (*avg.* 9.1 wt.%) and TiO_2 contents (*avg.* 4.3 wt.%) and $\text{Ti}/\text{Y} = 869$, with higher Ti values in the Trindade Island and Montague Seamount (Marques et al., 1999; Fodor and Hanan, 2000; Siebel et al., 2000; Peyve and Skolotnev, 2014; Bongiollo et al., 2015; Santos, 2016; Santos et al., 2018a; 2022a,b; Jesus et al., 2019; Maia et al., 2021; Monteiro et al., 2022). The more evolved compositions in Trindade and Martin Vaz (phonotephrites, tephriphonolites, and phonolites) have SiO_2 contents ranging from 46.0 to 57.3 wt.%, an average FeO content of 3.5 wt.%, with higher values in the Trindade Island phonotephrites and lower values in phonolite plugs of both islands, and low MgO and TiO_2 contents (*avg.* 1.15 and 0.90 wt.%, respectively) (Marques et al., 1999; Siebel et al., 2000; Bongiollo et al., 2015; Santos, 2016; Santos et al., 2018a; Monteiro et al., 2022).

The VTR less and more evolved rocks show low Zr/Nb (*avg.* 3.8 and 6.7, respectively) and Y/Nb (*avg.* 0.4 and 0.2, respectively) ratios indicating a role for fertile mantle sources (Le Roex et al., 2010), typically found in OIB-type intraplate magmatic settings, being typical of alkaline magmas (Pearce and Norry, 1979; Niu et al., 2012; Xia and Li, 2019). In general, the

VTR shows high to moderate values of HFSE (high-field strength elements) as Nb, Ta, and Th, and high concentrations of LILE (large ion-lithophile elements) as Ba and Sr. The Martin Vaz and the Trindade nephelinitic-phonolitic successions are more enriched in rare earth elements (REE, mostly light ones; La/Yb_N *avg.* 26) than the rest of the Vitória-Trindade seamounts (La/Yb_N *avg.* 18). These VTR geochemical characteristics and melting models suggest that its rocks were generated by low and variable degrees of partial melting (0.1 to 7%) in the stability field of garnet-spinel(-phlogopite) lherzolite with minor amounts of CO₂ (0.25 wt.%) with or without TiO₂ (Siebel et al., 2000; Peyve and Skolotnev, 2014; Bongioiolo et al., 2015; Skolotnev and Peive, 2017; Santos et al., 2018a; 2022a,b; Maia et al., 2021; Monteiro et al., 2022).

The Vitória-Trindade Ridge has ⁸⁷Sr/⁸⁶Sr_(m) ratios ranging from 0.703607 to 0.704251 and ¹⁴³Nd/¹⁴⁴Nd_(m) ratios ranging from 0.512622 to 0.512879 (Halliday et al., 1992; Marques et al., 1999; Fodor and Hanan, 2000; Siebel et al., 2000; Skolotnev et al., 2011; Peyve and Skolotnev, 2014; Bongioiolo et al., 2015; Santos, 2016; Santos et al., 2018a; Maia et al., 2021; Quaresma et al., *in press*). The Vitória Seamount (Maia et al., 2021) and Davis Bank (Santos, 2016; Quaresma et al., *in press*) samples have the more radiogenic ⁸⁷Sr/⁸⁶Sr_(m) (0.7040) and the less radiogenic ¹⁴³Nd/¹⁴⁴Nd_(m) (0.5126) ratios among the VTR. Samples from the Dogaressa Bank show anomalously radiogenic ⁸⁷Sr/⁸⁶Sr_(m) ratios (0.70869 and 0.70775), probably due to seawater contamination (Peyve and Skolotnev, 2014). The ²⁰⁶Pb/²⁰⁴Pb, ²⁰⁷Pb/²⁰⁴Pb, and ²⁰⁸Pb/²⁰⁴Pb isotope ratios from the VTR range from 19.01 to 19.50, 15.05 to 15.62, and 38.82 to 39.51, respectively (Halliday et al., 1992; Fodor and Hanan, 2000; Siebel et al., 2000; Skolotnev et al., 2011; Peyve and Skolotnev, 2014; Quaresma et al., *in press*). These VTR geochemical and isotopic signatures suggest a mixture between a depleted mantle component (DMM) and an enriched component such as EMI (Marques et al., 1999; Bongioiolo et al., 2015; Maia et al., 2021) and HIMU (Siebel et al., 2000; Peyve and Skolotnev, 2014; Pires and Bongioiolo, 2016; Skolotnev and Peive, 2017; Santos et al., 2022a,b; Quaresma et al., *in press*).

3. Material and methods

This work presents new data from thirty-four AVC samples (Fig. 3) collected on the Santa Bárbara, Redonda, Siriba e Sueste Islands. The samples were prepared at the *Laboratório Geológico de Preparação de Amostras* (LGPA) at the *Universidade do Estado do Rio de Janeiro* (UERJ), Brazil, to obtain thin sections and to be reduced to powder for geochemical and isotopic analyses. Initially, the Abrolhos rocks were broken into small fragments, leached in 1M HCl solution, dried for 30 minutes, washed under distilled water, and dried at 110°C.

Fragments were grounded (less than 170 mesh) in an agate mortar and dried out, and 2g of the powdered sample were set apart for whole-rock geochemical analysis. About 400 mg of the powder separated for isotope analyses following acid leaching with 6M HCl. Leaching was done in PFA teflon (Savillex) screw-top beakers left to react for 2 hours under room temperature. Then, the solution was transferred to a screw-top plastic tube and centrifuged for about 10 minutes, decanting the powder using a pipette. The procedure was repeated twice from the reaction with 6M HCl, wiping between each one with reverse osmosis water. The powder was then dried down under lamps in a fume cupboard under filtered air.

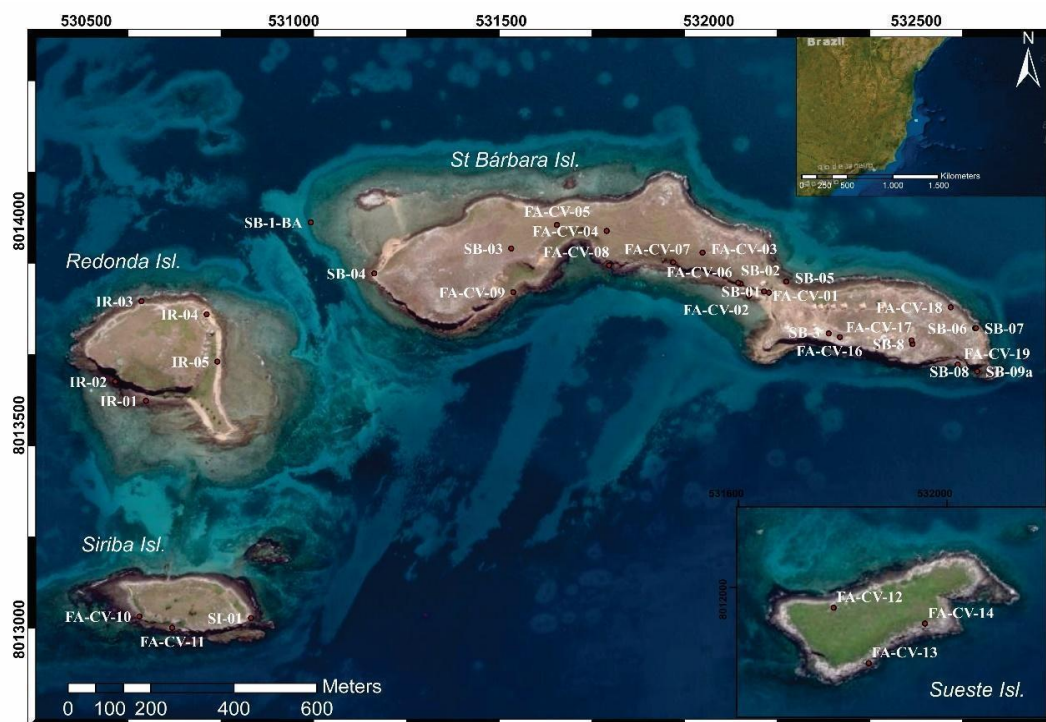


Fig. 3 – Sample locations on the Abrolhos islands.

The whole-rock geochemical analyses of the Abrolhos Volcanic Complex rocks were obtained at the ACTLABS, in Canada, and at the Australian Laboratory Services (ALS), in Brazil. Major elements (SiO_2 , TiO_2 , Al_2O_3 , Fe_2O_3^t (total iron as ferric iron), MnO , MgO , CaO , Na_2O , K_2O , P_2O_5) were measured as oxides in weight percentage (wt. %) by Inductively Coupled Plasma Atomic Emission Spectrometry (ICP-AES) after acid digestion of fused beads. Selected trace elements (Cr, V, Ba, Rb, Sr, Y, Nb, Zr, Hf, Ta, U, Th and the whole set of rare earth elements; REE) were measured in parts per million (ppm) by ICP-MS (Mass Spectrometry), except Ni, Sc, Co and Pb which were measured by ICP-AES. The loss on ignition was measured by percentual weight differences between non-ignited and ignited

samples after heating for 12 hours at 1100-1200°C. The analytical precision and accuracy of major elements were 1.2-2.6% and 0.8-7%, respectively. Precision for trace elements ranged from 1.2 to 6%, except for Sc (0%), Ba (20%), Co (18%), and Pb (38%), being below 8% (except for Ce and Lu; *ca.* 13%) for the REE. Accuracy for trace elements, including the REE, was below 10%, except for U (12%), Zr (13%), Cr (67%), Gd (15%), and Tb (13%). SY-4 was the certified material used as a reference.

The Sr and Nd isotope compositions of the Abrolhos islands samples were determined at the *Laboratório de Geocronologia e Isótopos Radiogênicos* (LAGIR) of the *Universidade do Estado do Rio de Janeiro* (UERJ), Brazil. The chemical separation procedures were carried out in separate clean rooms with positive air pressure and double HEPA air filtering. The solutions used were sub-boiled, distilled, and diluted with pure water produced by a Millipore® RiOs-5 and Millipore Milli-Q Academic® system. Sample dissolution was performed during five days cycles using HF/HNO₃ solution. ⁸⁷Sr/⁸⁶Sr and ¹⁴³Nd/¹⁴⁴Nd isotopic ratios were measured in a multi-collector TRITON thermal ionization mass spectrometer (TIMS) operating in static mode. Sm and Nd were loaded separately on degassed double Re filament arrangement, and Sr on Ta filament arrangement. The measured Sr and Nd isotopic ratios were normalized to ⁸⁸Sr/⁸⁶Sr = 8.3752 and ¹⁴⁶Nd/¹⁴⁴Nd = 0.7219, respectively, and the error was obtained at 2 sigmas. During this study, the international NBS-987 (NIST; N = 140) and JNdi-1 (N = 214) (Tanaka et al., 2000) standards gave average values of ⁸⁷Sr/⁸⁶Sr = 0.710239 ± 0.0000010 (2σ) and ¹⁴³Nd/¹⁴⁴Nd = 0.512100 ± 0.0000010 (2σ) (Valeriano et al., 2008, 2009; Neto et al., 2009). Analytical blanks for Sm and Nd are lower than 70 pg and 200 pg, respectively, while the Sr value was not obtained.

4. Results

4.1. Field data

The magmatic rocks of the Abrolhos islands can be grouped into four units that compose the Abrolhos Magmatic Succession (AMS; from bottom to top; Fig. 4): (i) Olivine-Pyroxene-Plagioclase Diabase on the Sueste island; (ii) Pyroxene-Plagioclase-Olivine Diabase on the Siriba and the Redonda islands; (iii) Pyroxene-Plagioclase Diabase and (iv) Porphyritic Diabase on the Santa Bárbara island. The Undifferentiated Igneous Rock limits were defined based on satellite images, since we were not able to map and define the lithology in the field due to tidal oscillations. The Pyroxene-Plagioclase Diabase Unit has well-defined bottom and top contacts,

so we named it the Santa Bárbara Formation. It occurs on the homonymous island under the Porphyritic Diabase Unit and above the sedimentary unit (Fig. 4). The contact between these three units is predominantly concordant, but locally discordant. The AMS units occur as fractured layers, locally altered, overlapping sandstones, mudstones, and conglomerates, setting up the typical outcrop of the Abrolhos islands (Fig. 5A). The AMS rocks are subparallel to the sedimentary rocks, bearing a northwest dip varying from 5° to 15° (Fig. 4). The sedimentary rocks that outcrop on the islands may constitute an analog of the Lower Tertiary turbiditic sedimentation on the Brazilian continental margin (Mohriak, 2006).

Equigranular fine-grained phaneritic rocks compose most of the Olivine-Pyroxene-Plagioclase Diabase, Pyroxene-Plagioclase-Olivine Diabase (Fig. 5B), and Pyroxene-Plagioclase Diabase units. They have plagioclase, pyroxene, and olivine phenocrysts up to 1 mm in size. Locally at the bottom of the layers, the rocks within the Pyroxene-Plagioclase Diabase and the Olivine-Pyroxene-Plagioclase Diabase units show an inequigranular coarse-grained texture. There is a 4 cm-thick chilled margin at the lower contact between the Pyroxene-Plagioclase Diabase Unit and the Sedimentary Unit below (Fig 5C). The rocks in the Olivine-Pyroxene-Plagioclase Diabase unit on the Redonda Island also display chilled margins. The Porphyritic Diabase Unit mapped at the top of Santa Bárbara Island is a highly porphyritic rock in which the phenocrysts make up more than 70% of the rock volume, with pyroxene phenocrysts up to 3 mm (Fig. 5D). There is columnar jointing in magmatic rocks on Siriba and Sueste islands (Fig. 5E). Faults and joints are found in rocks of all units.

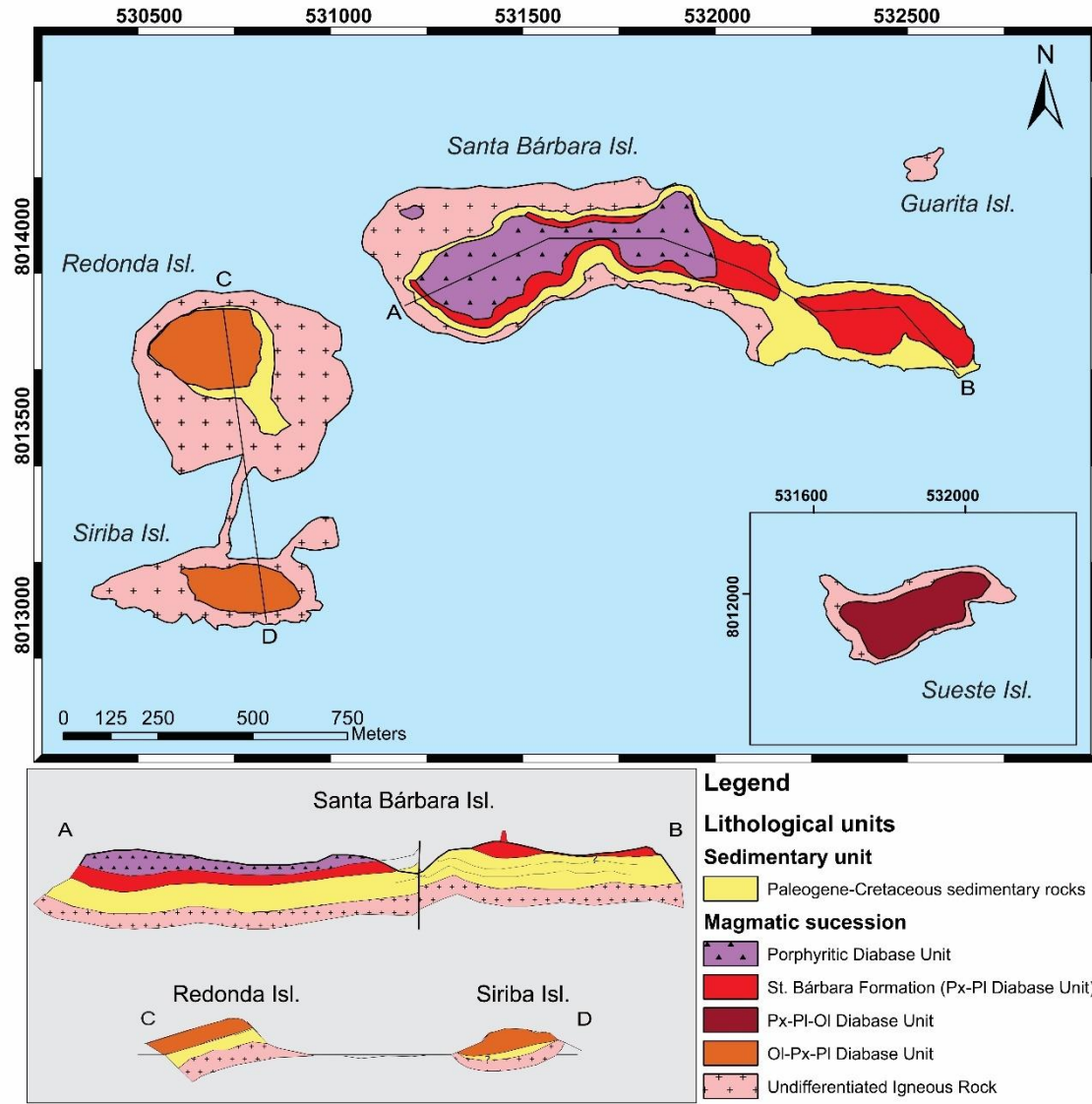


Fig. 4 – Lithological map of the Abrolhos islands and schematic cross-sections from Santa Bárbara, Redonda and Siriba Islands. Datum WGS 1984. Coordinate System UTM Zone 24S. Ol = olivine; Pl = plagioclase; Px = pyroxene.

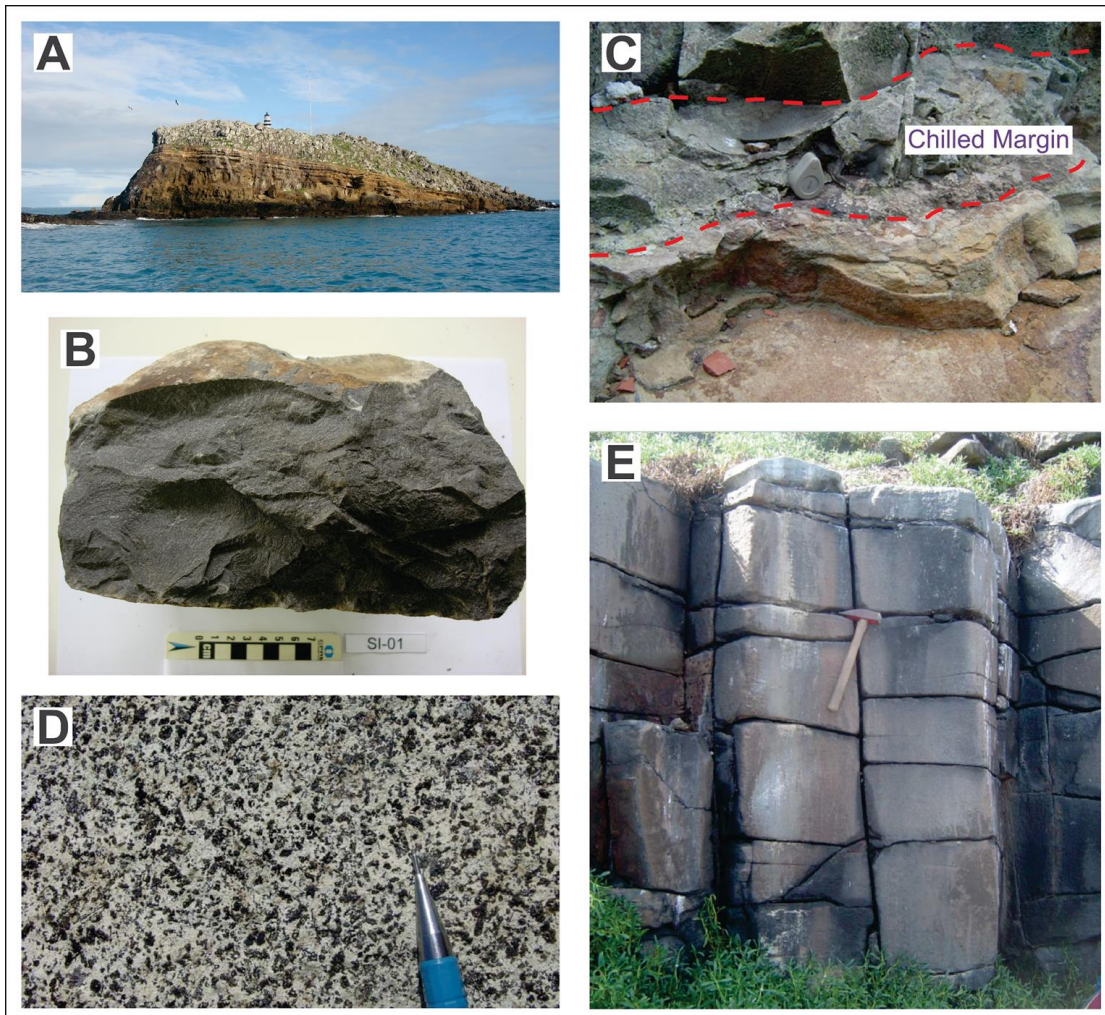


Fig. 5 –

Field, petrographic and structural features of magmatic rocks at Abrolhos islands. A) Landscape of Santa Bárbara with fractured rock layers of the magmatic succession overlapping sedimentary rocks; B) Equigranular fine grained phaneritic rock of the Pyroxene-Plagioclase-Olivine Diabase unit on Siriba island; C) Chilled margin at the lower contact between the diabase of the Pyroxene-Plagioclase Diabase unit and the rocks of the Sedimentary Unit below; D) Rock of the Porphyritic Diabase Unit; E) Columnar jointing of magmatic rocks on Siriba island.

4.2. Petrography

Samples from the Abrolhos Magmatic Succession were described under the optical microscope. Abbreviations used for the mineral names are those proposed by Whitney and Evans (2010).

4.2.1. Santa Bárbara Formation: Pyroxene-Plagioclase Diabase unit

Samples of the Pyroxene-Plagioclase Diabase unit that composes the Santa Bárbara Formation in the Santa Bárbara island are hypocrySTALLINE and microporphyritic fine-grained rocks. The groundmass contains plagioclase, clinopyroxene, and opaque mineral smaller than 0.2 mm in an intergranular texture (Fig. 6A). The groundmass commonly shows spherulites (Fig. 6B), chlorite, and felsitic texture (Winter, 2014; Fig. 6A) that are features typically attributed to devitrification. Despite the latter being commonly described in acid extrusive rocks, these devitrification products could be found in shallow-level intrusions (Cox et al., 1979). The phenocryst assemblage comprises plagioclase, occasionally olivine, and mostly pyroxene. Clinopyroxene phenocrysts vary from 0.1 mm to 2 mm in size and occur as subhedral to anhedral, fractured crystals, altered to chlorite (Fig. 6C) and locally embayed. Olivine is rare and occurs subordinately as anhedral crystals with approximately 1 mm and fractures filled by iddingsite. Plagioclase occurs as skeletal, fractured, and altered phenocrysts (0.3-1.2 mm) (Fig. 6A), locally as clusters, giving the rock a glomeroporphyritic texture (Fig. 6E). The opaque mineral occurs as anhedral crystals (0.5-1 mm) deeply embayed and encloses silicate groundmass, pointing to a *subsolidus* growth (Fig. 6D).

4.2.2. Porphyritic Diabase Unit

Samples of the Porphyritic Diabase unit from the top of the lithostratigraphic sequence in Santa Bárbara Island (Fig. 4) are hypocrySTALLINE rocks with ophitic and subophitic textures (Fig. 6F). The groundmass comprises grains smaller than 0.1 mm of clinopyroxene, opaque mineral, interstitial chlorite, and mainly plagioclase laths, the latter altered to sericite. The groundmass phases commonly show felsitic texture and interstitial chlorite and biotite, appearing to be glass alteration, thus suggesting the occurrence of devitrification (Fig. 6 G. The phenocrysts are represented by plagioclase and clinopyroxene. The plagioclase phenocrysts (0.5-1.6 mm) are scarce, skeletal, and altered to sericite (Fig. 6H). Clinopyroxenes phenocrysts (0.5-5 mm) occur fractured and display hourglass zoning (Fig. 6F). In most samples, they occur deeply embayed and enclose silicate groundmass phases (Fig. 6F), pointing to a possible resorption process. The opaque mineral occurs as anhedral to subhedral grains (0.3-2.5 mm) deeply embayed and enclosing silicate groundmass phases (Fig. 6I).

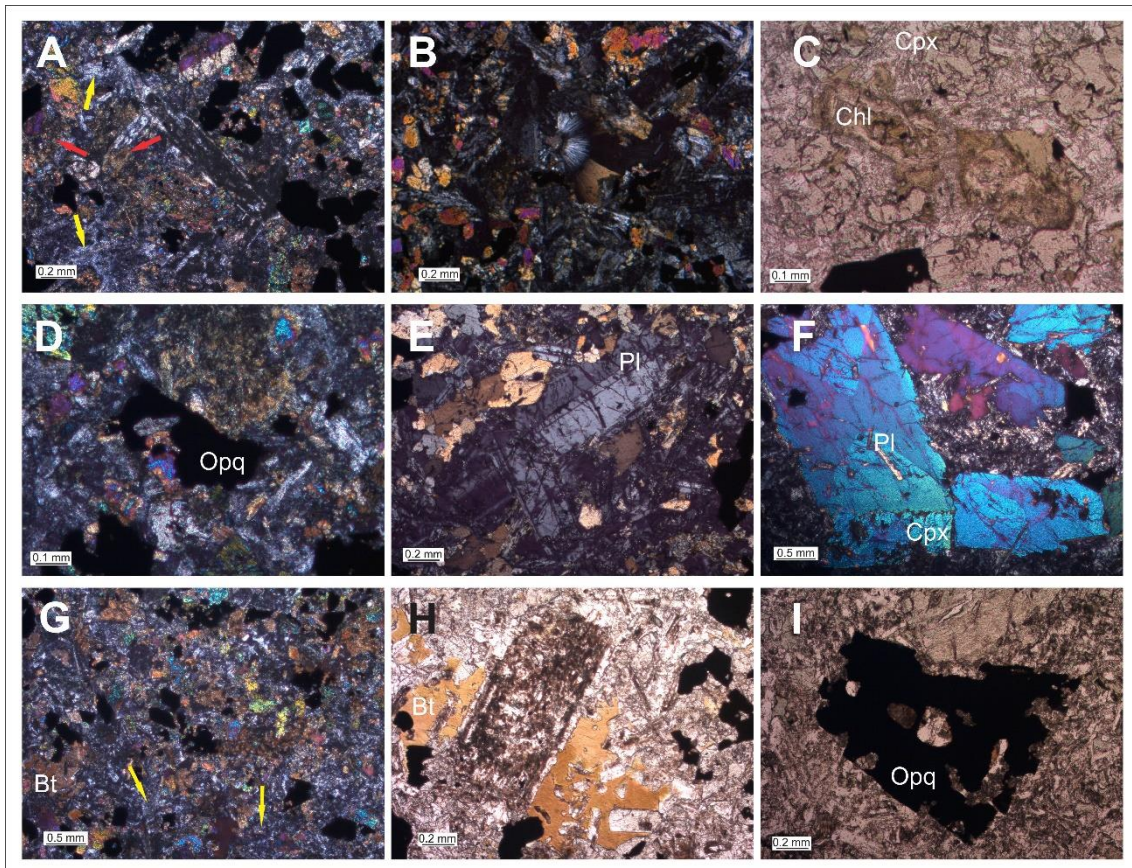


Fig. 6 – Photomicrographs of selected samples from the Pyroxene-Plagioclase Diabase and the Porphyritic Diabase units of the Santa Bárbara island under crossed (A, D, E, F, G) and parallel polarizers (B, C, H, I). The yellow arrow indicates the felsitic texture and the red one alteration to chlorite. See text for detailed descriptions. Bt = biotite, Chl = chlorite, Cpx = clinopyroxene, Opq = opaque mineral; Pl = plagioclase.

4.2.3. *Pyroxene-Plagioclase-Olivine Diabase unit*

Samples of the Pyroxene-Plagioclase-Olivine Diabase unit from Siriba and Redonda islands are porphyritic rocks with very fine (< 0.1 mm) groundmass with intergranular to intersertal textures (Fig. 7A) composed of plagioclase laths, clinopyroxene, opaque mineral, olivine, and interstitial chlorite. Samples from the Siriba island have a small amount of glass and two varieties of pyroxene grains, one being pleochroic pink and anhedral and the other being pleochroic green and subhedral (Fig. 7A). The phenocryst assemblage comprises plagioclase, occasionally olivine, and mostly pyroxene. Clinopyroxene microphenocrysts (about 0.5 mm) are pleochroic, pink, and display hourglass zoning (Fig. 7B). They are locally fractured and show subophitic texture on Redonda Island. Plagioclase phenocrysts occur as tabular grains (*ca.* 2 mm) with simple twinning, locally with compositional zoning, poikilitic texture (Fig. 7C), and forming a glomeroporphyritic texture together with pyroxene (Fig. 7D).

Olivine phenocrysts are scarce and occur as subhedral grains, fractured, and altered to iddingsite (Fig. 7E). Magmatic rocks in Siriba island show anhedral opaque mineral crystals deeply embayed, and enclosing silicate groundmass. Apatite occurs as an accessory mineral (Fig. 7A).

4.2.4. Olivine-Pyroxene-Plagioclase Diabase unit

Samples of the Olivine-Pyroxene-Plagioclase Diabase unit on Sueste Island holocrystalline and inequigranular. The groundmass shows intergranular texture with plagioclase, clinopyroxene, olivine, and opaque mineral smaller than 0.1 mm (Fig. 7F, G, H, I). The plagioclase occurs as laths with simple twinning slightly orientated around the phenocrysts (Fig. 7F, H). Clinopyroxene occurs as pleochroic, pink subhedral grains, and the olivine occurs as fractured anhedral crystals. The phenocrysts are olivine, clinopyroxene, and plagioclase. Clinopyroxene phenocrysts are fractured, commonly occurring as clusters giving the rock a glomeroporphyritic texture (Fig. 7F). The plagioclase occurs as euhedral grains about 0.5 mm in size with multiple twinning (Fig. 7G). Olivine phenocrysts occur as fractured, anhedral grains (about 2.5 mm) with compositional zoning showing an anhedral core followed by a resorbed and embayed rim (Fig. 7H). The opaque mineral occurs as anhedral grains (*ca.* 1 mm), deeply embayed, and encloses silicate groundmass, pointing to a *subsolidus* growth (Fig. 7I).

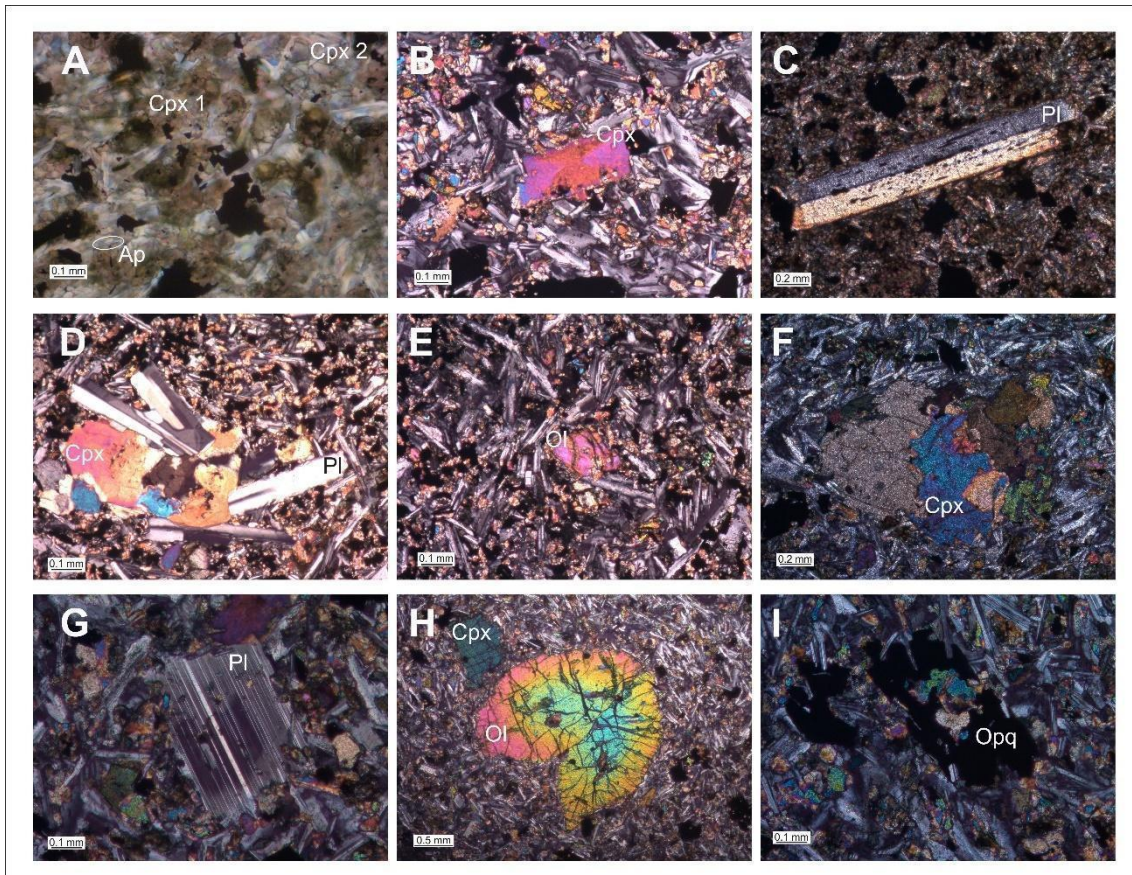


Fig. 7 – Photomicrographs of selected samples of the Pyroxene-Plagioclase-Olivine Diabase unit on Siriba and Redonda islands and of the Olivine-Pyroxene-Plagioclase Diabase unit on Sueste island under crossed (A, B, C, E, F, G, H, I) and parallel polarizers (D). See text for detailed descriptions. Ap = apatite, Cpx = clinopyroxene, Ol = olivine, Opq = opaque mineral; Pl = plagioclase.

All the analyzed samples display intergranular, porphyritic, poikilitic, and disequilibrium textures. Plagioclase, clinopyroxene, Fe-Ti oxide, and olivine are the main mineral phases in all units, sometimes showing embayment, resorbed rims, anhedral cores, and subhedral rims, and sieved textures. Previous works in Abrolhos (Fodor et al., 1989) also described fractured and zoned phenocrysts, devitrified and altered glass, chlorite, biotite, and iddingsite as secondary phases.

4.3. Whole-rock chemistry

Whole-rock geochemical data of the AVC rocks are given in Supplementary Material 2. These new data were compared with lithochemical data previously obtained for the VTR (Marques et al., 1999; Fodor and Hanan, 2000; Siebel et al., 2000; Skolotnev et al., 2011; Peyve and Skolotnev, 2014; Bongiorno et al., 2015; Santos, 2016; Santos et al., 2018b; 2022a,b; Jesus

et al., 2019; Maia et al., 2021; Santos and Hackspacher, 2021; Monteiro et al., 2022) and for the AVC (Fodor et al. 1989). The comparison was made with care since litho-geochemical data were obtained by either similar methods (ICP on fused samples) but at different laboratories (ACTLABS and ALS) or by different methods (X-ray fluorescence on pressed powder pellets; Fodor et al., 1989). It is reasonable to suppose that a few discrepancies observed during the comparative work may be due to the application of different analytical methods and, to a lesser extent, also same methods at different labs.

AVC samples have LOI values below 3.88 wt.%. Samples are chemically classified mostly as basalts and trachybasalts (Fig. 8a) and straddle the thermal divide in the TAS diagram, as typically seen in the transitional basaltic series. The newly analyzed samples from Santa Bárbara, Sueste, Siriba, and Redonda Islands are basic, relatively evolved rocks with SiO₂ content varying from 42.4 to 49.7 wt.%, MgO from 4.7 to 7.9 wt.%, and high TiO₂ contents (4.2 to 6.8 wt.%), as with previously published data by Fodor et al. (1989). A marked difference in the TAS diagram (Fig. 8a) when the new and compiled data of the AVC are compared concerns the Santa Bárbara basalts that plot either within the subalkaline field (compiled data) or in the alkaline field (this work). This may be due to the different analytical techniques used in those works. However, the alkaline affinity of the transitional basaltic series of the AVC rocks can be discriminated at the classification diagram based on immobile trace elements (Fig. 8b). This chemical classification is also supported by petrographic data since olivine is a groundmass phase in most of the studied rocks in Abrolhos islands, attesting to their alkaline affinity.

Variation diagrams for oxides and selected trace elements for the rocks of the Abrolhos Islands (*i.e.*, Santa Bárbara, Siriba, Sueste, and Redonda; Fig. 9) show a small compositional gap between approximately 5 and 8 MgO wt.%. It is difficult to observe a well-defined trend in most variation diagrams, and samples are unlikely to be related to a single liquid line of descent. However, silica is negatively correlated with MgO, whereas Ni and Sc are positively correlated with MgO (Fig. 9), which probably may reflect a role for olivine fractionation. Scattering in other variation diagrams makes it difficult to propose a role for the fractionation of clinopyroxene and plagioclase, although both phases are seen as phenocrysts in most AVC rocks. Although some scattering is observed in the trends of incompatible elements (*e.g.*, Rb, Ba, Ti) *versus* Zr, an increase in Nb, Y, La and Dy concentrations is observed with an increasing degree of differentiation (Zr; Fig. 9). This provides strong evidence in favor of their genetic relationship through different degrees of partial melting of a common mantle source. The

scattering of Rb and Ba may be due to the high mobility of these large-ion lithophile elements (LILE).

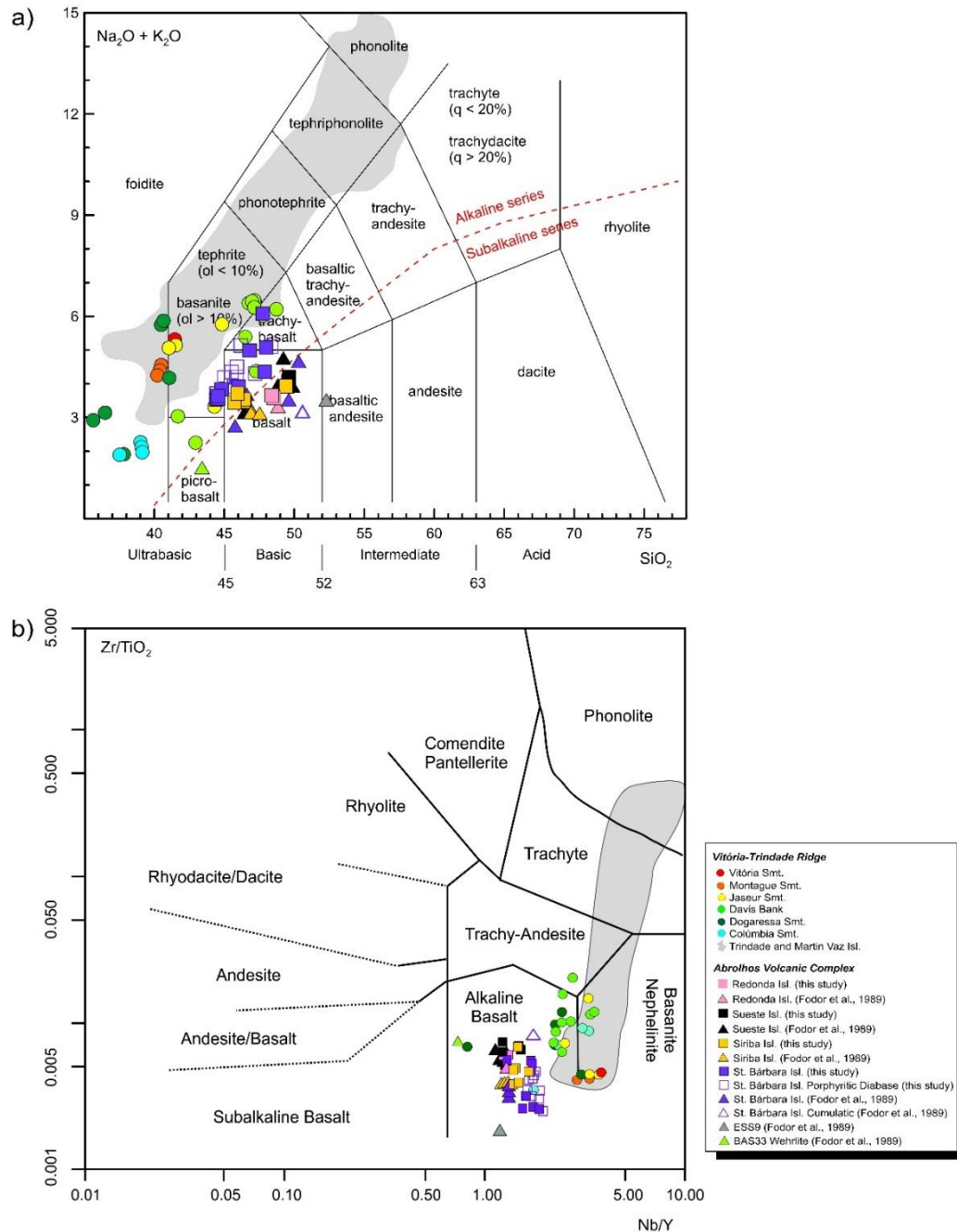


Fig. 8 – a) Total alkalis *versus* silica diagram (TAS – Le Bas et al., 1986) for the AVC and VTR samples. The AVC new analyzes were obtained by ICP but at different labs (ACTLABS ALS). Data compiled from Fodor et al. (1989) were obtained by XRF. Values recalculated to 100% on a volatile-free basis. Thermal divide curve between the alkaline and subalkaline fields from Irvine and Baragar (1971). b) Zr/TiO_2 *versus* Nb/Y diagram (Winchester and Floyd, 1977) for the AVC and VTR samples. VTR data are compiled from Marques et al. (1999), Fodor and Hanan (2000), Siebel et al. (2000), Skolotnev et al. (2011), Peyve and Skolotnev (2014), Bongiolto et al. (2015), Santos (2016), Santos et al. (2018b), Jesus et al. (2019) and Maia et al. (2021).

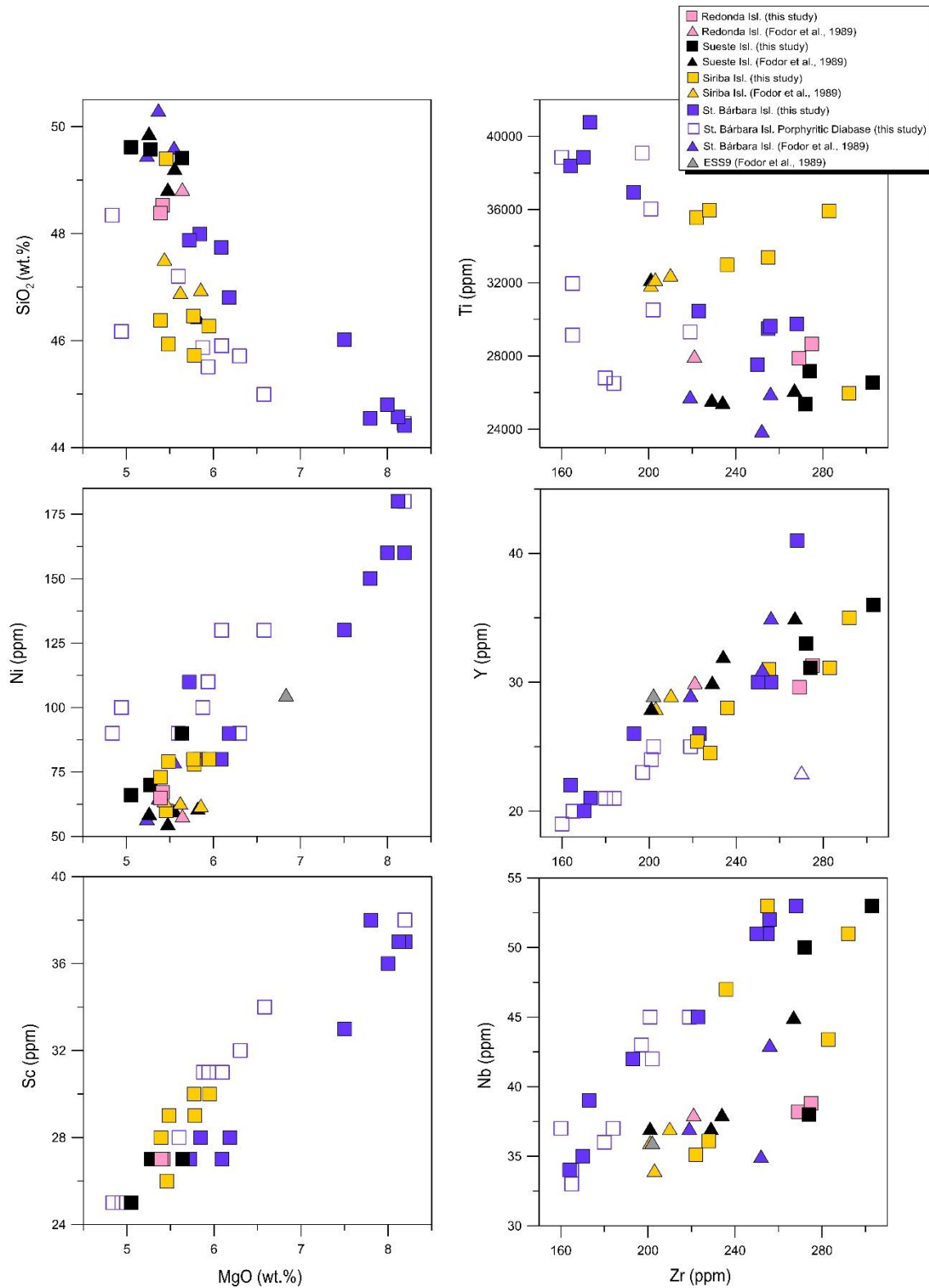


Fig. 9 – Samples from the Abrolhos islands plotted in variation diagrams. SiO₂, Ni and Sc *versus* MgO; Ti, Nb and Y *versus* Zr. Oxides values recalculated to 100% on a volatile-free basis.

Figure 10 shows chondrite-normalized trace element diagrams and rare earth elements (REE) patterns of AVC rocks, along with the VTR field for comparison. These patterns reveal similarities between the rocks from the AVC and the VTR, although the Abrolhos samples are more similar to the less enriched rocks in the VTR, especially in the case of the more incompatible elements. All chondrite-normalized REE patterns are strongly enriched in light REE (LREE) relative to heavy REE (HREE). The AVC rocks are characterized by having high abundances of U, Th, Ta, Nb, and Ti and depletions in Rb, K and P when normalized to the chondrite (Fig. 10a). In contrast to continental basalts (*e.g.*, Paraná-Etendeka; Peate, 1997), the trace element patterns of the AVC and VTR show a slight Nb-Ta positive anomaly typical of OIB and may indicate the presence of subducted crustal components recycled at the source of these magmatic events. The AVC rocks display a pronounced peak in Ti that lacks in the VTR lavas (Fig. 10a). The Abrolhos islands rocks show lower enrichment of the LREE (Fig. 10b), and higher values of the middle and HREE ones when compared with the VTR (La/Yb_N *avg.* 7.5 in Abrolhos; *ca.* 14.2-30 in VTR). Differences in La/Yb_N ratios may have resulted from either different degrees of partial melting in the presence of garnet from the same mantle source or derivation from distinct mantle sources, as it will be discussed in a further section of this paper. The Eu/Eu^* ratio of the AVC rocks varies from 0.96 to 1.11, although rocks of the Porphyritic Diabase Unit show a slight positive europium anomaly ($Eu/Eu^* = 1.53$).

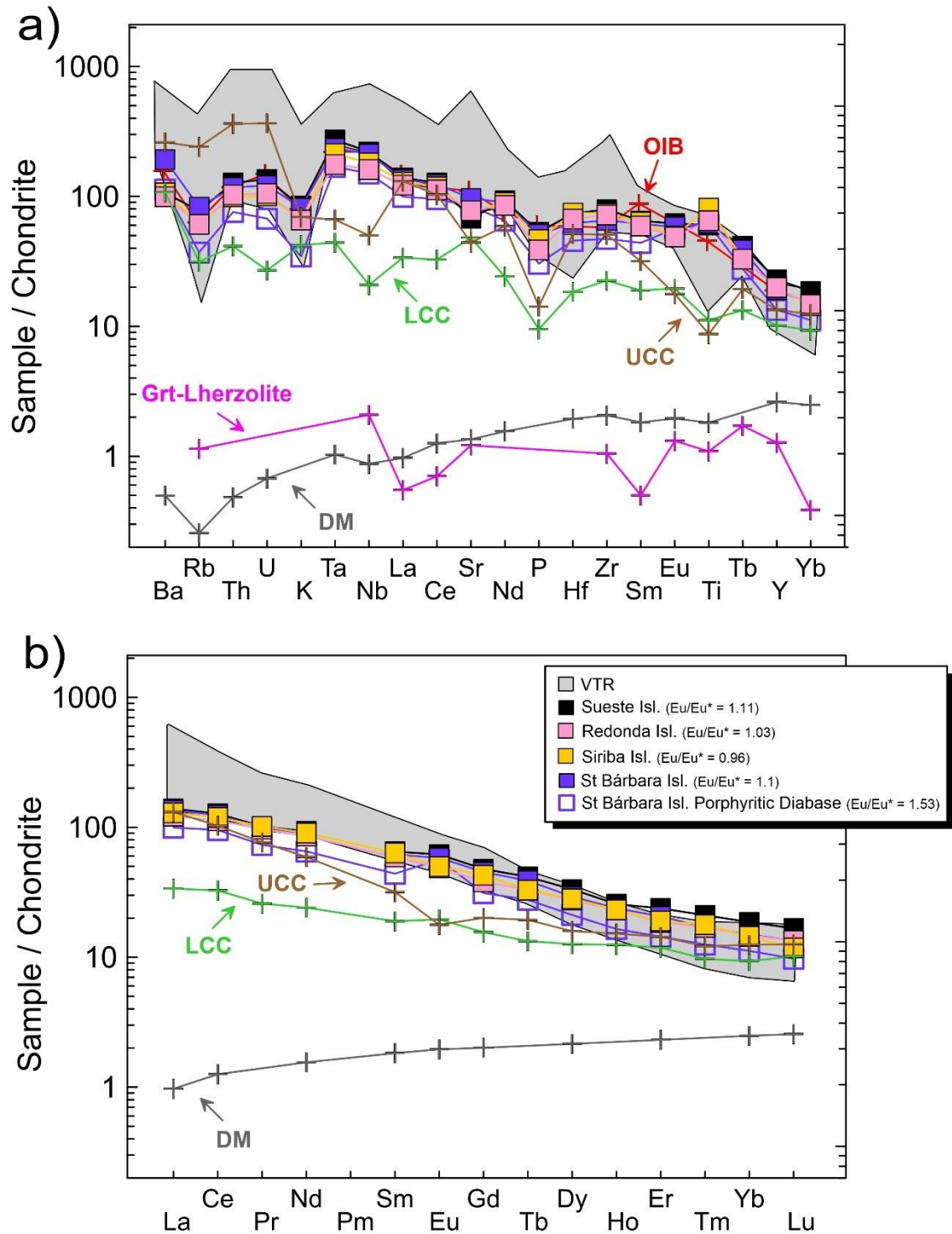


Fig. 10 – Normalized multielement diagrams for the VTR and AVC samples. (a) Chondrite-normalized trace element diagram and (b) Chondrite-normalized REE diagram. Normalization factors from McDonough and Sun (1995), except Rb, K and P (Sun, 1980). VTR data sources: Siebel et al. (2000); Bongioiolo et al. (2015); Santos (2016); Santos et al. (2018b); Jesus et al. (2019); Maia et al. (2021). OIB (Ocean Island Basalts; Weaver and Tarney, 1984), LCC (Lower Continental Crust; Rudnick and Gao, 2003), UCC (Upper Continental Crust; Rudnick and Gao, 2003), Grt-Lherzolite (Frey et al., 1985) and DM (Depleted Mantle; Salters and Stracke, 2004).

4.4. Sr and Nd isotopic compositions

Nine samples from the Abrolhos islands were analyzed for Sr and Nd isotopes (two from Santa Bárbara Island, two from Sueste Island, three from Siriba Island and two from Redonda Island; Table 1). Measured ratios rather than initial isotope ratios were used for comparison purposes since the AVC and the VTR have cenozoic ages, and age corrections resulted in differences only at 2σ values of isotope ratios.

Abrolhos Islands rocks have $^{143}\text{Nd}/^{144}\text{Nd}_{(m)}$ isotopic ratios ranging from 0.512818 to 0.512868, with ϵNd varying from + 3.85 to + 4.83, similar to the previously published data ($^{143}\text{Nd}/^{144}\text{Nd}_{(m)} = 0.512775 - 0.512841$; Fodor et al., 1989). The $^{87}\text{Sr}/^{86}\text{Sr}_{(m)}$ ratios obtained from the Abrolhos Islands samples range between 0.703691 and 0.705002, that are also in agreement with the early published data ($^{87}\text{Sr}/^{86}\text{Sr}_{(m)} = 0.703800 - 0.707330$; Fodor et al., 1983; 1989).

The more radiogenic Sr in the drill hole ESS9 and one sample from Santa Bárbara Island (FA-CV-02) could be due to alteration, as previously suggested for the wehrlite from drill hole BAS33 (0.7073; Fodor et al., 1989), despite the acid leaching of sample FA-CV-02. The Dogaressa Bank also shows more radiogenic Sr ratios justified by the active participation of seawater via fractures in the intermediate chamber (Peyve and Skolotnev, 2014). In addition, Quaresma et al. (*in press*) brought up the hypothesis of assimilation of anhydrite-rich, evaporitic sediments to explain Dogaressa radiogenic Sr ratios, which could also occur in Santa Bárbara Island. This evaporitic material would be found in the sedimentary sequences of the marginal basins (*e.g.*, Espírito Santo Basin) around the Abrolhos region.

The Sr-Nd isotope signatures of the Abrolhos islands overlap the main VTR range ($^{87}\text{Sr}/^{86}\text{Sr}_{(m)} 0.703607 - 0.704251$; $^{143}\text{Nd}/^{144}\text{Nd}_{(m)} 0.512622 - 0.512879$), pointing to a possible common mantle source(s) for these magmatism. The Sr-Nd isotope data (Fig. 11) would also be consistent with the involvement of a depleted mantle component (DMM) and an enriched component as EMI in the petrogenesis of the AVC and VTR, as proposed by previous works (Fodor et al., 1989; Marques et al., 1999; Siebel et al., 2000; Santos, 2013; 2016; Peyve and Skolotnev, 2014; Bongiolo et al., 2015; Pires and Bongiolo, 2016; Skolotnev and Peive, 2017; Maia et al., 2021; Quaresma et al., *in press*).

Table 1 – Sr and Nd isotope data for Santa Bárbara, Siriba, Sueste and Redonda Islands.

Island	Sample	$^{87}\text{Sr}/^{86}\text{Sr}$ (m)	Std. Err. Abs (2s)	$^{143}\text{Nd}/^{144}\text{Nd}$ d (m)	Std. Err. Abs (2s)	ϵ_{Nd}
Sueste	FACV13	0.703702	0.000012	0.512856	0.000002	+ 4.60
	FACV12b	0.703691	0.000011	0.512865	0.000005	+ 4.78
Siriba	FACV10a	0.703747	0.000009	0.512849	0.000006	+ 4.48
	SI-01	0.703763	0.000010	0.512841	0.000006	+ 4.32
	SB-13	0.703703	0.000011	0.512818	0.000005	+ 3.85
Redonda	IR-01A	0.703719	0.000009	0.512868	0.000005	+ 4.83
	IR-05	0.703962	0.000012	0.512864	0.000006	+ 4.77
Sta Bárbara	FACV02	0.705002	0.000013	0.512846	0.000006	+ 4.34
	FACV20	0.704079	0.000009	0.51286	0.000005	+ 4.69

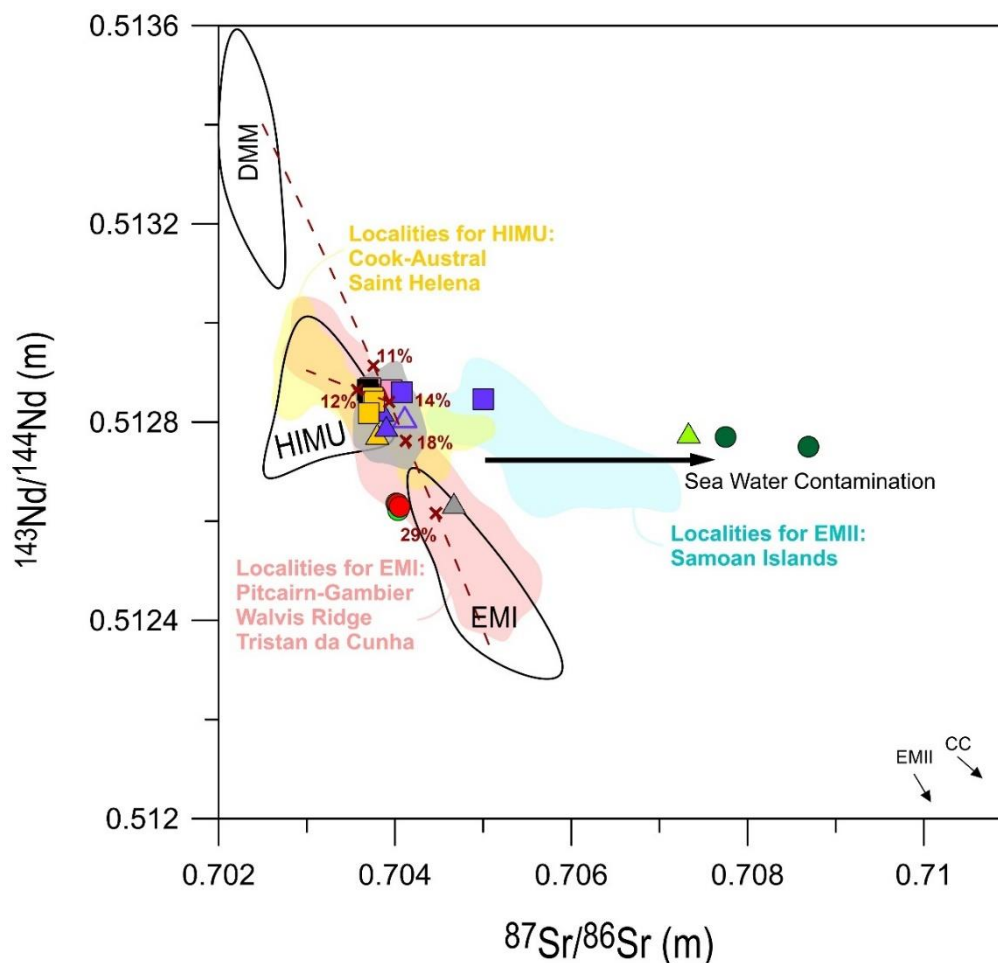


Fig. 11 – $^{143}\text{Nd}/^{144}\text{Nd}_{(m)}$ versus $^{87}\text{Sr}/^{86}\text{Sr}_{(m)}$ for Abrolhos islands and VTR lavas. Symbols such as in Fig. 8. The grey shaded area is the VTR compiled data from Halliday et al. (1992), Marques et al. (1999), Fodor and Hanan (2000), Siebel et al. (2000), Skolotnev et al. (2011), Bongiolo et al. (2015), Santos (2016), Peyve and Skolotnev (2014), Santos et al. (2018), with the exception of Vitória Seamount (Maia et al., 2021) e two samples from Davis Bank (Quaresma et al., *in press*). Abrolhos compiled data are from Fodor et al. (1983; 1989). Mantle components: DMM (Zindler and Hart, 1986; Hart et al., 1992; Rehkamper and Hofmann, 1997; Su and Langmuir, 2003; Salters and Stracke, 2004; Workman and Hart, 2005; Hofmann, 2014); EM I (Zindler and Hart, 1986; Eisele et al., 2002; Jackson and Dagsputa, 2008; Hofmann, 2014), EM II (Hart, 1988); HIMU (Zindler and Hart, 1986; Hart et al., 1992; Salters and White, 1998 and references therein; Stracke et al., 2005; Chan et al., 2008; Jackson and Dagsputa, 2008; Hofmann, 2014); CC (Continental Crust - Rollinson, 1993; Taylor and McLennan, 1985; Winter, 2014). Modeling assumes three-component mixing between DMM ($^{87}\text{Sr}/^{86}\text{Sr} = 0.7025$, $[\text{Sr}] = 7.66$ ppm, $^{143}\text{Nd}/^{144}\text{Nd} = 0.5134$ and $[\text{Nd}] = 0.58$ ppm; Zindler and Hart, 1986; Workman and Hart, 2005), EMI ($^{87}\text{Sr}/^{86}\text{Sr} = 0.705105$, $[\text{Sr}] = 495$ ppm, $^{143}\text{Nd}/^{144}\text{Nd} = 0.512333$, $[\text{Nd}] = 30.6$ ppm; Zindler and Hart, 1986; Eisele et al., 2002; Hoffman, 2014) and HIMU ($^{87}\text{Sr}/^{86}\text{Sr} = 0.7030$, $[\text{Sr}] = 589$ ppm, $^{143}\text{Nd}/^{144}\text{Nd} = 0.512904$, $[\text{Nd}] = 37.2$ ppm; Hanyu and Nakamura, 2000; Chan et al., 2008). The data from OIB localities for EMI, EMII and HIMU end-members are compiled from the GEOROC database (<http://georoc.mpch-mainz.gwdg.de/georoc/>). The Sr and Nd contents from the melt DMM were calculated considering a partial melting degree of *ca.* 10% (value from Stanton et al., 2022; $D_{\text{Sr}} = 0.0185$ and $D_{\text{Nd}} = 0.0317$).

5. Discussions

5.1. Intrusive *versus* Extrusive Character

The intrusive or extrusive character of the igneous rocks of the Abrolhos islands is rarely discussed in the literature and there is no consensus on the subject (Cordani, 1970; Cordani and Blazekovic, 1970; Fodor et al., 1989; Arena, 2008). Most of the igneous rocks that outcrop on the surface of the islands have their tops totally eroded, and the absence of an upper contact with sedimentary rocks hampers prompt discrimination of the intrusive or extrusive character of the magmatism. However, there are no textures and structures in Abrolhos islands that can be described as typical of extrusive rocks (*e.g.*, vesicular or amygdaloidal layers and pipes, cavities indicating volcanic degassing, flow structures, broken-like minerals, entablatures, among others). The columnar jointing in Siriba and Sueste islands cannot be exclusively attributed as an effusive feature since similar joints are also found in intrusive magmatic rocks and even in sedimentary rocks. Cordani and Blazekovic (1970) proposed that all the varieties present on the islands would be intrusive rocks based on the presence of chilled margins at both top and bottom of the units described in the wells and the surface samples. We also mapped chilled margins in Santa Bárbara and Redonda islands. In addition, seismic data reveal intrusive features, such as dykes and sills, which would have intruded sedimentary sequences and intervals containing older volcanic rocks (Sobreira, 1996, Sobreira et al., 2004; Stanton et al., 2021).

Furthermore, the magmatic unit mapped at the top of Santa Bárbara Island is an inequigranular porphyritic rock in which the phenocrysts make up more than 70% of the rock volume, with pyroxene and plagioclase phenocrysts up to 3 mm, showing subophitic and ophitic textures. The accumulation of phenocrysts would be difficult to explain by volcanic processes and would be more akin to an intrusive structure. Fodor et al. (1989) analyzed one sample from the drill hole SBST-1-BA on the Santa Bárbara island (573 m depth) that shows a planar arrangement of clinopyroxene and plagioclase grains (2-5 mm) with intergranular ilmenite crystals (1-2 mm), hence describing these crystals as cumulatic minerals, also typical of magmatic intrusions rather than flows. Altogether, the field and seismic data indicate that the igneous rocks of the Abrolhos islands are shallow intrusions, mostly sills. Thus, this work proposes that the mapped magmatic rocks in the Abrolhos Islands should be grouped into diabase units rather than basalt ones (Fig. 4).

5.2. Differentiation process involved in the Abrolhos Islands genesis

There is no discussion in the literature about the differentiation processes involved in the magmas of the submerged volcanic buildings of the VTR (*e.g.*, Vitória Seamount, Davis Bank, Colúmbia Seamount) possibly as a result of scarce sampling. In the case of the Trindade and Martin Vaz islands, several authors point out that the nephelinites/basanite-phonolite succession evolved via fractional crystallization (Marques et al., 1999; Siebel et al., 2000; Bongiolo et al., 2015; Santos, 2013; 2016; Santos et al., 2018a; 2021a,b; Oliveira et al., 2021; Monteiro et al., 2022). However, no previous published work has discussed possible differentiation processes in the case of the AVC in detail.

As mentioned in section 4.3, plots of major and trace element contents result in some scattering on variation diagrams (Fig. 9), indicating that the Abrolhos Islands samples probably did not evolve along a single liquid line of descent. The major and trace element variations suggest that the AVC rocks are not related to a differentiation process occurring in a single stage or in a single subvolcanic magma chamber. Perhaps, the islands represent distinct products of the same source through multiple magma chambers. The MgO range of the Santa Bárbara basalts (7.78 - 5.22 wt.%) can be used to test for possible differentiation processes. Basalts from Siriba, Sueste, and Redonda islands present less variable MgO contents (5.88 – 5.06 wt.%), which are also close to the concentration of the more evolved basalts in the Santa Bárbara island. Thus, it is also possible to test the hypothesis of a link by differentiation between the least evolved sample in Santa Bárbara and the more evolved samples in Santa Bárbara itself, as well as in the other three islands of the archipelago.

Trace element ratios of strongly incompatible elements vary within a narrow range as a result of fractional crystallization (Wood and Fraser, 1976). For instance, bulk partition coefficients for La and Nb between basaltic magmas and their respective typical fractionating assemblage (*i.e.*, olivine, clinopyroxene and plagioclase) are about 0.11 and 0.007, respectively (Rollinson, 1993). As such, variations in La/Nb ratios between less and more evolved basaltic compositions would hardly be greater than 10%. The same applies to variations in other strongly incompatible element ratios, such as La/Yb and Zr/Nb, for instance. Therefore, percentual variations of trace element ratios shown in Table 2 cannot be explained only by the fractional crystallization process. For example, variations in the La/Nb_N and La/Yb_N ratios between the least and more evolved samples from Santa Bárbara (FA-CV-02 and FA-CV-20) are about 50%, being between about 30% and 40% when the evolved samples of Siriba, Sueste and Redonda are taken into account (Table 2). It should be noted that there is little variation in

the Zr/Y ratio for the Abrolhos samples shown in Table 2. Bulk partition coefficients are strongly controlled by clinopyroxene during fractional crystallization of basaltic magmas. Therefore, a wider variation in Zr/Y ratio between less and more evolved basalts is to be expected, implying that differentiation processes more complex than simply fractional crystallization must have taken place during the petrogenesis of the Abrolhos basalts. One possibility would be assimilation concomitant to fractional crystallization (AFC; DePaolo, 1981) that could be coherent with the increasing values of trace element ratios observed between some samples shown in Table 2. However, some of the more evolved AVC magmas show the highest Nd isotopic ratios and the lowest Sr isotopic ratios (Table 2). It is the opposite trend expected from a fractional crystallization concomitant to the assimilation process (DePaolo, 1981).

The interpretation of elemental and isotopic data presented in these sections indicates no cogeneticity among diabases from all Abrolhos islands, neither by fractional crystallization nor by AFC. The nature of the magma flow (laminar or turbulent) in dyke-like conduits may control the amount of wall-rock assimilation (Thompson et al., 1986). As there are dike structures related to the Abrolhos magmatism (Stanton et al., 2021), magma may have assimilated crustal rocks during turbulent ascent (ATA; Kerr et al., 1995), implying that the less evolved, MgO-rich samples would bear the highest Sr isotope ratios and lowest Nd isotope ratios, for instance. However, such process is difficult to ascertain in the case of the AVC since there is some scatter in the Sr and Nd isotope data available. Besides possible assimilation by turbulent ascent, disequilibrium textures described in petrography (*e.g.*, embayment and resorption) indicate a possible magma recharge process (Lormand et al., 2021) that could be similar to the magma replenishment, tapping and fractionation (RTF) process (O'Hara and Mathews, 1981; Cox, 1988). In general, the lithochemical and isotope data of the AVC imply in the operation of differentiation processes more complex than simple fractional crystallization or AFC, such as ATA or RTF, for instance. Such complex evolution would be broadly consistent with the presence of a plumbing system below the Abrolhos archipelago.

Table 2 – Elemental and isotopic data for selected samples of the Abrolhos Archipelago. Initial isotope ratios (i) were calculated for 45.6 Ma. Normalization factors (N) from McDonough and Sun (1995). LOI stands for Loss on Ignition (wt.%).

Sample	FA-CV-02	FA-CV-20	IR-01A	IR-05	SI-01	FA-CV-12b
Islands	Santa Bárbara	Santa Bárbara	Redonda	Redonda	Siriba	Sueste
MgO	7.78	5.53	5.28	5.24	5.23	5.24
LOI	2.77	0.80	0.09	0.24	- 0.03	0.00
$^{87}\text{Sr}/^{86}\text{Sr}_{(i)}$	0.704971	0.704002	0.703652	0.703891	0.703690	0.703588
$^{143}\text{Nd}/^{144}\text{Nd}_{(i)}$	0.512803	0.512820	0.512827	0.512824	0.512800	0.512824
ϵNdi	+ 4.3	+ 4.7	+ 4.8	+ 4.8	+ 4.3	+ 4.8
La/Nb_N	0.4	0.6	0.7	0.8	0.7	0.6
La/Yb_N	5.9	9.0	8.1	8.2	8.8	7.3
Zr/Y	8.2	8.3	9.1	8.8	9.1	8.4
Zr/Nb	4.4	4.9	7.0	7.1	6.5	5.7

5.3. Plumbing system genetic model for the AVC magmatism

Stanton et al. (2021) mapped igneous structures with tabular and conical shapes as dykes and sills, which they believed to be associated with a shallow magmatic emplacement. The authors also mapped anomalies that demanded deeper and larger sources. As aforementioned, the AVC volcanism displays deep (> 5 km) central bodies (R1 and R2; Stanton et al., 2021) that feed radially seven smaller shallow elongated ones (E1-E7; Fig. 2). Following this, the AVC is probably related to a plumbing system (Stanton et al., 2021), from which the magma would be scattered through the upper and middle crust by interconnected dykes, sills, and other structures. The magma is stored at different crustal levels where it would be susceptible to different evolutionary processes (assimilation, magma mixing, fractional crystallization) and to eventually replenishment by magmatic pulses (Jerram and Bryan, 2015; Magee et al., 2018; and references therein). This model could be associated with the RTF process proposed here to explain the complex differentiation processes related with the AVC petrogenesis, despite the fact that it is still poorly known how those structures were connected and how the magma was stored in the crust through time below the Abrolhos archipelago. Indeed, a detailed analysis of the crystal population and a mineral chemistry study combined with higher resolution seismic data will be necessary to improve the characterization and definition of the AVC plumbing system. We further underline the difficulty of determining how magma was distributed and stored through the ancient system since magmatism is no longer active at present time in the area. Still, it would be possible to investigate it using, *e.g.*, *in situ* isotopic analyses in feldspar

and clinopyroxene grains in future works. Despite these drawbacks, we tried to illustrate a possible plumbing system related to the AVC magmatism (Fig. 12) by gathering models from different authors (Fodor et al., 1989; Jerram and Bryan, 2015; Magee et al., 2018; Stanton et al., 2021).

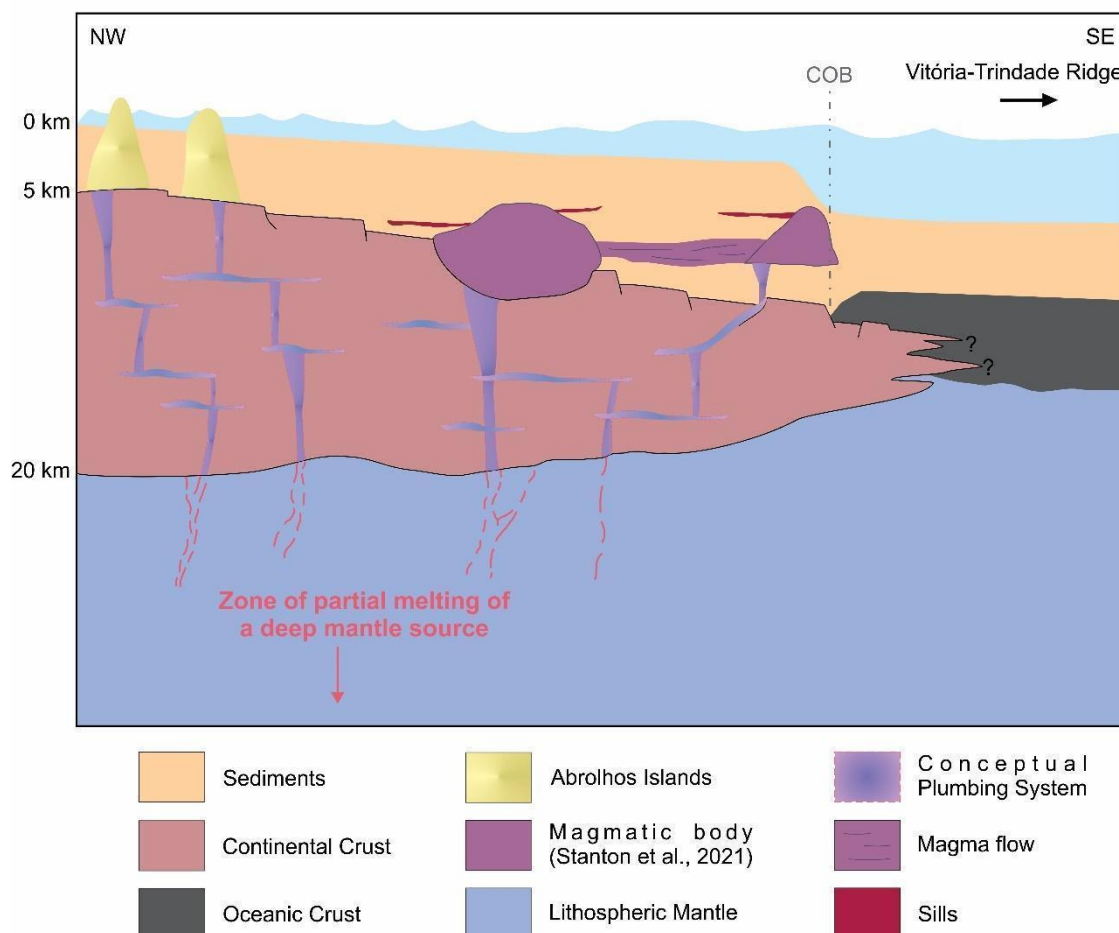


Fig. 12 – Schematic section illustrating the possible spatial relationships of some AVC igneous edifices. The conceptual plumbing system for AVC magmatism is based on models from different works (Fodor et al., 1989; Jerram and Bryan, 2015; Magee et al., 2018; Stanton et al., 2021). The distribution of most of the structures is speculative, as well as the connection between them.

5.4. Mantle source components involved in the AVC magmatism: results of geochemical modeling

The AVC and VTR isotopic data plot between the DMM and EMI end-members in the $^{87}\text{Sr}/^{86}\text{Sr}_{(m)}$ versus $^{143}\text{Nd}/^{144}\text{Nd}_{(m)}$ diagram (Fig. 11), which indicates possible mixture processes between depleted and enriched mantle components. The AVC shows slightly enriched values

of $^{206}\text{Pb}/^{204}\text{Pb}$ (18.9-19.33; Fodor et al., 1989) that cannot be explained by the DMM and EMI components alone, thus requiring a third component as a mantle source (Fig. 13). Besides the DMM and the EMI sources, the HIMU mantle component has been pointed out as a possible VTR source in previous works (Siebel et al., 2000; Peyve and Skolotnev, 2014; Pires and Bongiolo, 2016; Skolotnev and Peive, 2017; Quaresma et al., *in press*), and the latter may well be also involved in the AVC petrogenesis.

We modeled a mixture in variable proportions between an EMI component and a depleted asthenospheric source (DMM) with some incorporation of a HIMU-type end-member to test the hypothesis of the involvement of three different mantle sources in the petrogenesis of the AVC magmatism. To quantify the proportions of this mixture, we have performed model mixing calculations with these three components based on the mixing equation from DePaolo and Wasserburg (1979; and references therein). Although it is a ternary mixture, we perform the calculations in a binary way (based on the study by Rocha-Júnior et al., 2020; Quaresma et al., *in press*). Firstly, we calculated the mixture between the DMM and the EMI components and then the result with the HIMU end-member. In the absence of new Pb isotopic data, we selected the published data (Fodor et al., 1989) to elaborate our mixing calculations. We then recalculated the results of the two-step binary mixing modeling to 100%. As such, the Sr, Nd, and Pb isotopic compositions of the AVC can be explained by mixing between 3% to 21% of EMI with the depleted asthenospheric mantle (DMM) (Fig. 11 and 13). The diabase sample from the drill hole ESS9 would have the more significant contribution of the EMI component. Since the presence of a third component is necessary to explain the AVC slightly enriched Pb ratios, we added a HIMU-type component to the mixture. Thus, the ternary mix would have a contribution of 75% of DMM, <15% of EMI, and up to 10% of HIMU (Fig. 11 and 13).

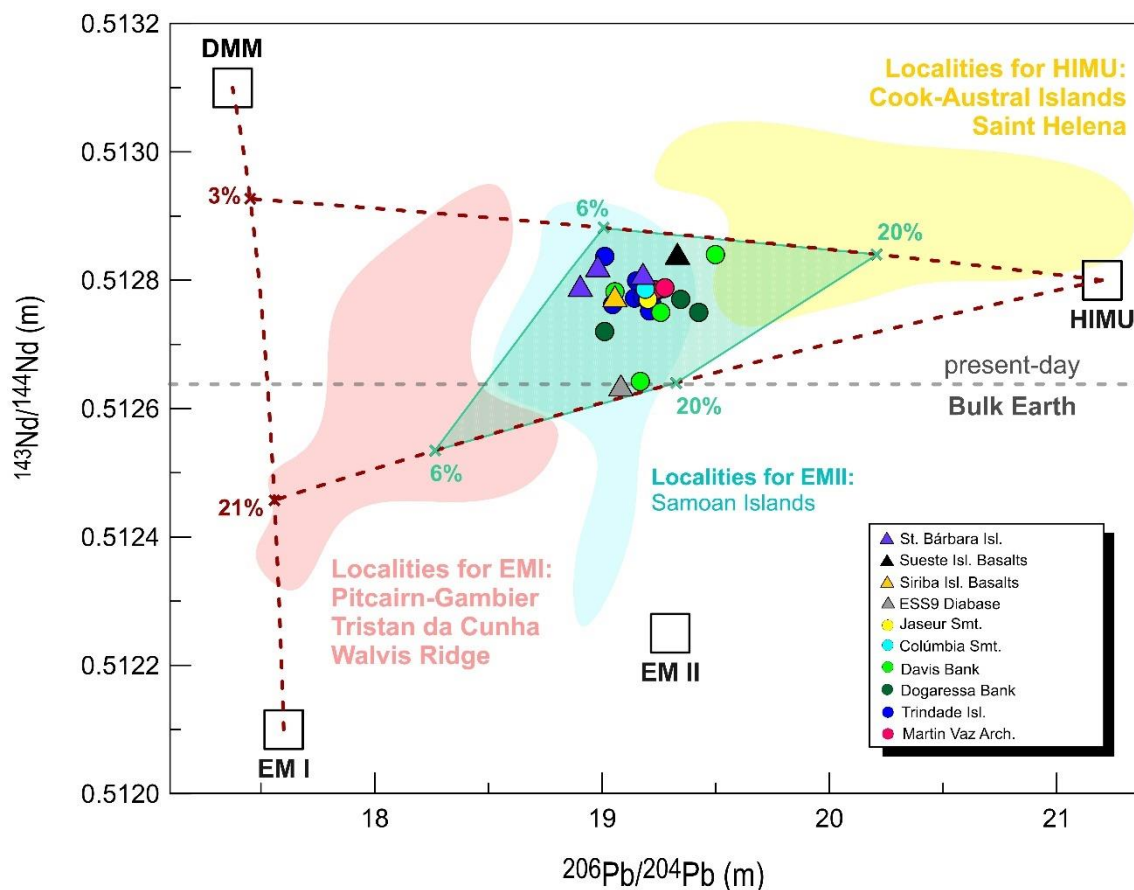


Fig. 13 – $^{143}\text{Nd}/^{144}\text{Nd}_{(m)}$ versus $^{206}\text{Pb}/^{204}\text{Pb}_{(m)}$ (modified from Quaresma et al., *in press*) for AVC (Fodor et al., 1989) and VTR rocks (Halliday et al., 1992; Fodor and Hanan, 2000; Siebel et al., 2000; Skolotnev et al., 2011; Peyve and Skolotnev, 2014; Quaresma et al., *in press*). Plot of mixing calculations between DMM, EMI and HIMU-type. Modeling assumes three-component mixing between DMM ($^{143}\text{Nd}/^{144}\text{Nd} = 0.5131$, $[\text{Nd}] = 9.6 \mu\text{g/g}$, $^{206}\text{Pb}/^{204}\text{Pb} = 17.375$, $[\text{Pb}] = 0.46 \mu\text{g/g}$), EMI ($^{143}\text{Nd}/^{144}\text{Nd} = 0.5121$, $[\text{Nd}] = 30.6 \mu\text{g/g}$, $^{206}\text{Pb}/^{204}\text{Pb} = 17.600$, $[\text{Pb}] = 2.82 \mu\text{g/g}$) and HIMU ($^{143}\text{Nd}/^{144}\text{Nd} = 0.5128$; $[\text{Nd}] = 45.7 \mu\text{g/g}$, $^{206}\text{Pb}/^{204}\text{Pb} = 21.200$, $[\text{Pb}] = 2.73 \mu\text{g/g}$). The parameters for the DMM, EMI, EMII and HIMU are from Zindler and Hart (1986), Salters and Stracke (2004), Workman and Hart (2005), Jackson and Dasgupta (2008), Gurenko et al. (2009), Hofmann (2014), Marques et al. (2018) and Rocha-Júnior et al. (2020). The data from OIB localities for EMI, EMII and HIMU end-members are compiled from the GEOROC database (<http://georoc.mpchmainz.gwdg.de/georoc/>). For the melt DMM, the Pb and Nd contents were calculated considering a partial melting degree of *ca.* 10% (value from Stanton et al., 2022; bulk $D_{\text{Nd}} = 0.0317$ and $D_{\text{Pb}} = 0.0092$).

5.5. Petrogenetic model for the AVC magmatism: origin of the AVC source components

As aforementioned, we suggest a mixture between a depleted asthenospheric source (DMM) with some incorporation of an EMI component and a HIMU-type end-member for the AVC magmatism. The EMI component has been associated with delaminated subcontinental lithospheric mantle (SCLM) (Eisele et al., 2002) and delamination of lower continental crust (LCC) (Tatsumi, 2000). Besides the Sr-Nd isotopic data, the incompatible trace element

signatures of the AVC also point to an involvement of an enriched mantle component probably associated with the lithospheric mantle (Fig. 14). The Th/Yb *versus* Ta/Yb plot suggests the presence of metasomatized lithospheric fragments since the AVC rocks are plotted subparallel to the mantle metasomatism trend (Fig. 14a; Etemadi et al., 2019). The Zr/Nb (<10) and Y/Nb (<5) ratios from AVC and VTR are low, which is a characteristic of OIB lavas (*e.g.* Xia and Li, 2019) and suggests an involvement of a shallow plume component (Wilson, 1989). Some authors suggested that the delaminated subcontinental lithosphere was incorporated into the local asthenosphere mantle during the Western Gondwana break-up (Bizzi et al., 1995; Marques et al., 1999; Peyve and Skolotnev, 2014; Skolotnev and Peive, 2017; Maia et al., 2021; Quaresma et al., *in press*). Later, the Trindade Plume would have thermally remobilized these fragments retained into shallower levels of the asthenosphere.

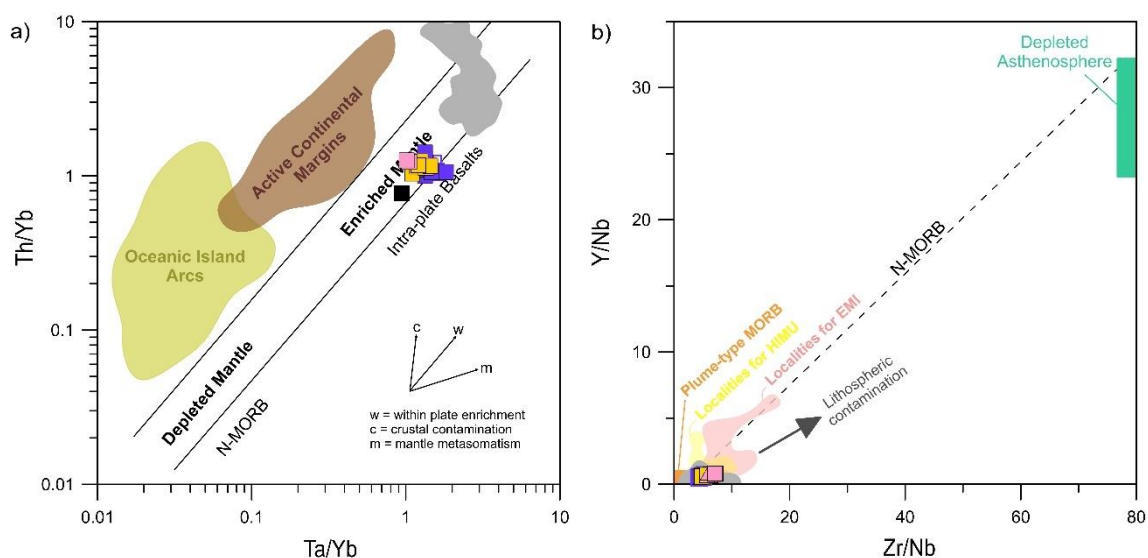


Fig. 14 – Discrimination diagram for mantle processes based on trace element ratios. a) Th/Yb *versus* Ta/Yb diagram (modified after Pearce, 1983; see Etemadi et al., 2019) for the AVC and VTR rocks. b) Y/Nb *versus* Zr/Nb diagram (modified after Wilson, 1989). Symbols and fields such as in Fig. 8. VTR data sources: Marques et al. (1999); Fodor and Hanan (2000); Siebel et al. (2000); Peyve and Skolotnev (2014); Bongiolo et al. (2015); Santos (2016); Santos et al. (2018b); Jesus et al. (2019); Maia et al. (2021). The data from OIB localities for EMI and HIMU end-members are compiled from the GEOROC database (<http://georoc.mpch-mainz.gwdg.de/georoc/>). The localities for EMI are Pitcairn-Gambier, Walvis Ridge and Tristan da Cunha, and for HIMU are Cook-Austral and Saint Helena.

Another alternative process that could explain the role of the SCLM in the VTR and AVC magmatism is the edge-driven convection (EDC; King and Anderson, 1995; 1998; King and Ritsema, 2000; King, 2007), which was also proposed by Quaresma et al. (*in press*) for the VTR. The EDC mechanism consists of small-scale convection cells originated by temperature and viscosity contrast in the upper mantle located at the edge of a continent or craton (King and

Anderson, 1998; King, 2007). These convection cells would be responsible for adding delaminated subcontinental lithosphere into the local mantle. The AVC is located at the Continent-Ocean Boundary (COB) southeast of the São Francisco craton, and the continent-ocean and craton boundaries are exactly the ideal sites to form this small-scale convection (King, 2007). The EDC has also been evoked to explain some of the South Atlantic magmatism (*e.g.*, Fernando de Noronha; Knesel et al., 2011; Perlingeiro et al., 2013). However, we highlight that the EDC model was brought up only as a potential explanation for the presence of an enriched mantle component (EMI).

The depleted mantle Nd model ages (T_{DMNd}) of the AVC and VTR range from 407 Ma to 767 Ma, and from 420 Ma to 640 Ma, respectively, matching the Brasiliano Event ages (790 – 490 Ma; *e.g.*, Brito Neves et al., 2014; Peixoto et al., 2017; Heilbron et al., 2020; and references therein). The Brasiliano-Pan-African Orogeny resulted in the consumption of oceanic lithosphere (the Adamastor Ocean) during the Neoproterozoic and the amalgamation of the Western Gondwana (Peixoto et al., 2017; Heilbron et al., 2020; Caxito et al., 2021; and references therein). The assimilation of subducted slabs of this Neoproterozoic oceanic plate in the local mantle may have contaminated it. The Brasiliano Orogeny introduced the oceanic lithosphere into the peridotitic mantle, possibly generating the eclogitization of the slab. The eclogite melt generates a high-Si liquid that, when reacting with the surrounding peridotite, produces a hybrid pyroxenite and mantle metasomatism (Sobolev et al., 2005, 2007; Gurenko et al., 2009). Indeed, the recycling of subducted oceanic crust has been linked to the HIMU endmember signatures (Hofmann and White, 1982; Zindler et al., 1982; Chauvel et al., 1992). Additionally, the AVC samples show lithogeochemical signatures that point out to the recycling of subducted crustal components at its source. During the subduction, the eclogite loses the LILE and becomes enriched in the HFSE (high-field strength elements), which would then explain the positive Nb-Ta and Ti anomalies (HSFE), and the depletion in Rb and K (LILE). It is noteworthy that metasomatized lithospheric mantle (Pilet et al., 2005; 2008; 2011; Niu, 2008; 2009; Niu et al., 2012) and mixtures of subducted oceanic crust (eclogite) and hybrid pyroxenite with peridotite (Sobolev et al., 2005, 2007; Mallik and Dasgupta, 2012) have been suggested as OIB and alkaline magma sources.

5.6. Petrogenetic correlation between the Abrolhos Volcanic Complex (AVC) and the Vitória-Trindade Ridge (VTR) magmatism

Several similarities between the geochemical signatures of the VTR and the AVC were highlighted along this work. The VTR rocks plot in the alkaline field in the TAS diagram (Fig. 8a). They are mostly ultrabasic rocks as opposed to the Abrolhos alkaline basalts, except for basanites and trachy-basalts from the Davis Bank. The latter are rocks as evolved as most of the Abrolhos basalts but display higher alkalis concentrations. VTR samples show a much wider range of lithochemical signatures than the Abrolhos samples, and comprise the less to more evolved compositions within the strongly undersaturated alkaline series of the Trindade and Martin Vaz islands. On the other hand, the AVC rocks comprise a discrete and different group compared with the VTR based on incompatible and immobile trace elements (Fig. 8b). Yet, the patterns of the AVC and VTR samples overlap in chondrite-normalized multielement and REE diagrams (Fig. 10), with less enrichment for AVC in the concentration of most trace elements, especially the more incompatible ones. This may be due to lower degrees of partial melting for the VTR lavas. We have observed pronounced negative anomalies for K and P, and Nb-Ta positive anomalies in both magmatism. The incompatible trace element patterns in the multielement diagrams are quite irregular among VTR volcanic edifices, while AVC shows a more regular arrangement. Obviously, differences may result from the scarce sampling. Nevertheless, both magmatism show geochemical signatures typical of OIB intraplate magmatic settings (Fig. 10a), such as the low Zr/Nb (AVC: 4.3-7.2; VTR: 2.1-10) and Y/Nb (AVC: 0.3-0.9; VTR: 0.1-1.2) ratios (Pearce and Norry, 1979; Niu et al., 2012; Xia and Li, 2019).

The Abrolhos islands rocks show lower contents of the LREE and slightly higher values of the middle and heavy REE when compared to the VTR (Fig. 10b). These differences in La/Yb_N ratios (*avg.* 7.5 in Abrolhos; *ca.* 14.2-30 in VTR) must have resulted from the different degrees of partial melting from the same mantle source. Considering batch melting as the melting process, Stanton et al. (2022) suggested a degree of partial melting ranging from 10% to 15% for AVC lavas derived from a garnet-lherzolite, while Siebel et al. (2000) suggested a smaller melt fraction (3.4–4.7%). VTR melting models suggest that its rocks were generated by a lower variable degree of partial melting (0.1 to 7%) from an enriched garnet-amphibole-phlogopite-spinel-lherzolite source enriched with minor amount of CO₂ (0.25 wt.%) with or without TiO₂ (Siebel et al., 2000; Santos and Marques, 2007; Peyve and Skolotnev, 2014;

Bongiolo et al., 2015; Skolotnev and Peive, 2017; Santos et al., 2018a; 2022a,b; Maia et al., 2021; Monteiro et al., 2022).

The VTR magmatism is also potentially related to a multiple-stage plumbing system. For Davis Bank magmatism, Rego et al. (2021) suggested a magma chamber located at depths of 12-30 km that probably experienced recharging processes, as it has been proposed here for the AVC. Other volcanic buildings (Colúmbia Seamount, Martin Vaz Archipelago, and Trindade Island) are apparently related to deeper magma chambers located 18–50 km deep, that linked Davis Bank magma chamber to a complex magma plumbing system.

Most Sr-Nd-Pb isotope signatures of the Arolhos islands overlap the main VTR range, pointing to a possible common mantle source for these magmatic events. The VTR and AVC Sr-Nd-Pb plot and model mixing calculations suggest the involvement of the enriched components EMI and HIMU incorporated in the depleted asthenospheric source (DMM). The slight differences in the VTR and AVC $^{87}\text{Sr}/^{86}\text{Sr}_{(m)}$, $^{143}\text{Nd}/^{144}\text{Nd}_{(m)}$, and $^{206}\text{Pb}/^{204}\text{Pb}_{(m)}$ ratios could be associated with different proportions in the mixture of the aforementioned mantle components. The calculated contributions of these three components (75% of DMM, <15% of EMI, and up to 10% of HIMU) for the AVC rocks resemble those proposed for the VTR magmatism. Quaresma et al. (*in press*) reported a contribution of 56% of DMM, 24% of EMI, and 20% of HIMU in the peridotitic source of the Davis Bank. For Vitória Seamount, Maia et al. (2021) calculated an EMI contribution on the depleted asthenospheric source (DMM) varying from 20% to 25%, while for other VTR volcanic edifices (*e.g.*, Jaseur Seamount, Dogaressa Bank, Colúmbia Seamount, Trindade and Martin Vaz Islands) the EMI involvement would vary from 10% to 20% (Monteiro et al., 2022; Santos et al., 2022a,b).

In section 5.5 we propose that the AVC source comprises a depleted asthenospheric mantle (DMM) enriched by detached fragments of the subcontinental lithospheric mantle probably associated with the Gondwana break up and recycled subducted oceanic crust consumed along the Brasiliano Orogeny. This petrogenetic model was also proposed for the VTR by Quaresma et al. (*in press*), thus pointing to a cogenetic relationship between these magmatic events. Furthermore, it is possible to observe a temporal continuation from the Arolhos magmatism ages (Paleocene-Eocene; 32-64 Ma; Cordani, 1970; Cordani and Blazekovic, 1970; Fodor et al., 1983; Sobreira and Szatmari, 2002; 2003; Sobreira et al., 2004) to the VTR ages (Oligocene-Pleistocene; 29.8-0.49 Ma; Cordani, 1970; Skolotnev et al., 2011; Geraldés et al., 2013; Santos, 2013; 2016; Pires et al., 2016; Santos et al., 2015; 2021; 2022a; Skolotnev and Peive, 2017; Monteiro et al., 2022; Quaresma et al., *in press*). Indeed, broad and accurate geochronological data is necessary, but the slight eastward age-progressive volcanism

from the AVC to the younger Martin Vaz and Trindade Islands supports a Trindade hotspot origin for these magmatic events.

6. Conclusions

Mapped magmatic rocks in the Abrolhos Islands (Santa Bárbara, Siriba, Sueste and Redonda) are shallow intrusions, mostly sills, and crop out into four units that compose the Abrolhos Magmatic Succession (AMS; from bottom to top): (i) Olivine-Pyroxene-Plagioclase Diabase unit on the Sueste island, (ii) Pyroxene-Plagioclase-Olivine Diabase unit on the Siriba and the Redonda islands, (iii) Pyroxene-Plagioclase Diabase unit (Santa Bárbara Formation), and (iv) Porphyritic Diabase unit on the Santa Bárbara island. The AVC rocks comprise a discrete and different group when compared with the VTR based on incompatible, immobile trace elements. The Abrolhos Islands include a transitional basalt series of alkaline affinity, with relatively evolved rocks with high TiO_2 contents. Santa Bárbara, Siriba, Sueste, and Redonda islands plots of major and trace element contents result in some scatter on variation diagrams indicating that the Abrolhos Islands samples probably did not evolve along a single liquid line of descent. Indeed, the litho-geochemical and isotope data of the AVC imply in the operation of differentiation processes more complex than simple fractional crystallization or AFC. Differentiation by magma replenishment, tapping, and fractionation (RTF) seems to have been the predominant process, potentially linked to the subvolcanic plumbing system evolution with interconnected dykes, sills, and other structures shapes.

We propose that the AVC source comprises a depleted asthenospheric mantle (represented by depleted MORB mantle - DMM) metasomatized by an enriched mantle I (EMI) component and a HIMU-type constituent. A viable mechanism for the influence of the EMI-like end-member could either be a physical detachment of the South American subcontinental lithospheric mantle during the breakup of the Gondwana or lithospheric delamination of the South American plate caused by edge-driven convection mechanism. The assimilation of subducted slabs of an oceanic crust, associated with the HIMU signatures, is possibly linked to the Brasiliano Event due to the depleted mantle Nd model ages ($T_{\text{DM Nd}}$) from AVC ranging from 407 Ma to 767 Ma. Our model mixing calculations suggest a mixture with 75% of DMM, <15% of EMI, and up to 10% of HIMU in the source of the AVC. The slight differences in the VTR and AVC Sr, Nd, and Pb ratios would be associated with different proportions in the mixture of the three mantle components aforementioned. Finally, the volcanic alignment between the VTR and AVC, along with the overlap of geochemical and isotopic data of their

different igneous rocks, cannot be a random circumstance but instead represent the sampling of a common shallow mantle source, thus suggesting a cogenetic relationship.

Funding

This work was supported by the CNPq (Pro Trindade Program) [Process N^o. 557,146/2009–7]; the MCT/CNPq project [n^o 26/2009]; the Universidade do Estado do Rio de Janeiro for PROCAD Program (Capacitation Program) leave and CAPES [Process 88.881.177228/2018–01] for the postdoctoral fellowship, to execute part of this research at Aveiro University, Portugal, and FAPERJ [APQ1 2019 n 210.179/2019].

Acknowledgments

We thank the LAGIR-UERJ staff (Carla Neto, Gilberto Vaz, João Ricardo Barcellos and Claudio Valeriano) for support and Sr-Nd isotope analyzes even during the COVID-19 pandemic. The first author thanks the student Lucas Guimarães P. Monteiro for the help in the geological map processing and the partnership in the research. Our many thanks to Prof. Dr. João Mata (Dom Luiz Research Group) and Prof^a. Dr^a. Leila Soares Marques (Universidade de São Paulo) for enlightening our discussions. Prof. Dr. Anderson Costa dos Santos would like to dedicate this manuscript to Prof. Ronald Viktor Fodor from NCSU (USA) for encouraging him in the Alkaline offshore volcanism and supporting his research and career. Dr. Fodor passed away on October 22, 2021. In the name of our research group, we pay this tribute to one of the greatest-known petrologists.

References

Alberoni, A.A.L., Jeck, I.K., Silva, C.G. 2020. The new Digital Terrain Model (DTM) of the Brazilian Continental Margin: detailed morphology and revised undersea feature names. *Geo-Marine Letters*, v. 40, p. 949–964. <https://doi.org/10.1007/s00367-019-00606-x>

Alberoni, A.A.L., Jeck, I.K. 2022. Chapter 3 - Brazilian Continental Margin morphology: ridges, rises, and seamounts. In: Santos, A.C., Hackspacher, P.C. Meso-Cenozoic Brazilian Offshore Magmatism: Geochemistry, Petrology and Tectonics. Elsevier Inc., 2021, p. 95-119. <https://doi.org/10.1016/B978-0-12-823988-9.00012-5>

Almeida, F.F.M. 2006. As ilhas oceânicas brasileiras e suas relações com a tectônica do Atlântico Sul. *Terra didática*, v. 2, p. 3-18.

Almeida, F.F.M., Carneiro, C.D.R., Mizusaki, A.M.P. 1996. Correlação do magmatismo das bacias da margem continental Brasileira com o das áreas emersas adjacentes. *Revista Brasileira de Geociências*, v. 26, p. 125-138.

Alves, E.C., Maia, M., Sichel, S.E., Campos, C.M.P. 2006. Zona de Fratura de Vitória-Trindade no Atlântico Sudeste e suas implicações tectônicas. *Revista Brasileira de Geofísica*, v. 24(1), p. 117–127.

Alves, E.C., Araujo, R.S., Ramos, E.C., Maia, M., Santos, A.C., Hackspacher, P.C. 2022. Chapter 2 - Ocean fracture zones: their evolution and impact on tectonic and magmatism of the South and Southeast Brazilian continental margin. In: Hackspacher, P.C., Santos, A.C. *Meso-Cenozoic Brazilian Offshore Magmatism: Geochemistry, Petrology and Tectonics*. Elsevier Inc., 2021, p. 47-94. <https://doi.org/10.1016/B978-0-12-823988-9.00012-5>

Arena, M.C. *Petrologia da Sucessão Magmática do Arquipélago de Abrolhos*. 2008. 113 fl. Dissertação (Mestrado em Geologia) – Faculdade de Geologia, Universidade do Estado do Rio de Janeiro, Rio de Janeiro, 2008.

Aulbach, S., O'Reilly, S.Y., Griffin, W.L., Pearson, N.J. 2008. Subcontinental lithospheric mantle origin of high Nb/Ta in eclogite xenoliths. *Nature Geoscience*, v. 1, p. 468–472. <https://doi.org/10.1038/ngeo226>

Barão, L.M., Trzaskos, B., Angulo, R.J., De Souza, M.C., Daufenbach, H.F., Santos, F.A., Vasconcellos, E.M.G. 2020. Deformational structures developed in volcanic sequences as a product of tectonic adjustments in the South Atlantic Ocean. *Journal of South American Earth Sciences*, v. 104, 102812. <https://doi.org/10.1016/j.jsames.2020.102812>

Bizzi, L.A., De Wit, M.J., Smith, C.B., McDonald, I., Armstrong, R.A. 1995. Heterogeneous enriched mantle materials and Dupal-type magmatism along the SW margin of the São

Francisco craton, Brazil. *Journal of Geodynamics*, v. 20 (4), p. 469–491. [https://doi.org/10.1016/0264-3707\(95\)00028-8](https://doi.org/10.1016/0264-3707(95)00028-8)

Bongiolo, E.M., Pires, G.L.C., Geraldés, M.C., Santos A.C., Neumann R. 2015. Geochemical modeling and Nd-Sr data links nephelinite-phonolite successions and xenoliths of Trindade Island (South Atlantic Ocean, Brazil). *Journal of Volcanology and Geothermal Research*, v. 306, p. 58–73. <https://doi.org/10.1016/j.jvolgeores.2015.10.002>

Brito Neves, B.B., Fuck, R.A., Pimentel, M.M. 2014. The Brasiliano collage in South America: a review. *Brazilian Journal of Geology*, v. 44 (3), p. 493–518. <https://doi.org/10.5327/Z2317-4889201400030010>

Caxito, F.A., Heilbron, M., Valeriano, C.M., Bruno, H., Pedrosa-Soares, A., Alkmim, F.F., Chemale, F., Hartmann, L.A., Dantas, E., Basei, M.A.S. 2021. Integration of elemental and isotope data supports a Neoproterozoic Adamastor Ocean realm. *Geochemical Perspectives Letters*, v. 17, p. 6-10. [10.7185/geochemlet.2106](https://doi.org/10.7185/geochemlet.2106)

Celli, N.L., Lebedev, S., Schaeffer, A.J., Ravenna, N., Gaina, C. 2020. The upper mantle beneath the South Atlantic Ocean. South America and Africa from waveform tomography with massive data sets. *Geophysical Journal International*, v. 221, p. 178–204. <https://doi.org/10.1093/gji/ggz574>

Chan, L.H., Lassiter, J. C., Hauri, E. H., Hart, S. R., Blusztajn, J. 2008. Lithium isotope systematics of lavas from the Cook–Austral Islands: Constraints on the origin of HIMU mantle. *Earth and Planetary Science Letters*, v. 277, p. 433–442. <https://doi.org/10.1016/j.epsl.2008.11.009>

Chauvel, C., Hofmann, A.W., Vidal, P. 1992. HIMU-EM: the French Polynesian connection. *Earth and Planetary Sciences Letters*, v. 110, p. 99-119. [https://doi.org/10.1016/0012-821X\(92\)90042-T](https://doi.org/10.1016/0012-821X(92)90042-T)

Colli, L., Fitcher, A., Bunge, H-P. 2013. Full waveform tomography of the upper mantle in the South Atlantic region: Imaging a westward fluxing shallow asthenosphere? *Tectonophysics*, v. 604, n. 24, p. 26-40. <https://doi.org/10.1016/j.tecto.2013.06.015>

Conceição, J.C.J., Mizusaki, A.M.P., Alves, D.B., Szatmari, P. 1996. Controle tectônico do magmatismo do Complexo Vulcânico de Abrolhos, Bacia do Espírito Santo. In: SBG, Congresso Brasileiro de Geologia, 39, Camboriú, Anais, v. 5, p. 384-387.

Cordani, U.G. 1970. Idade do vulcanismo do Oceano Atlântico Sul. *Boletim do Instituto de Geociências e Astronomia* (IGA-USP), v. 1, p. 9-75.

Cordani, U.G., Blazekovic, A. 1970. Idades radiométricas das rochas vulcânicas dos Abrolhos. In: 24º Congresso Brasileiro de Geologia, Brasília, Anais, p. 265-270.

Courtillot, V., Davaille, A., Besse, J., Stock, J. 2003. Three distinct types of hotspots in the Earth's mantle. *Earth and Planetary Science Letters*, v. 205, n. 3-4, p. 295-308. [https://doi.org/10.1016/S0012-821X\(02\)01048-8](https://doi.org/10.1016/S0012-821X(02)01048-8)

Cox, K.G., Bell, D., Pankhurst, R. 1979. *The Interpretation of Igneous Rocks*. George Allen and Unwin, London. <https://doi.org/10.1007/978-94-017-3373-1>

Cox, K.G. 1988. Numerical Modelling of a Randomized RTF Magma Chamber: A Comparison with Continental Flood Basalt Sequences. *Journal of Petrology*, v. 29, 3, p. 681-697. <https://doi.org/10.1093/petrology/29.3.681>

Day, J.M.D., Pearson, D.G., Macpherson, C.G., Lowry, D., Carracedo, J.C. 2010. Evidence for distinct proportions of subducted oceanic crust and lithosphere in HIMU-type mantle beneath El Hierro and La Palma, Canary Islands. *Geochimica et Cosmochimica Acta*, v. 74, p. 6565–6589. <https://doi.org/10.1016/j.gca.2010.08.021>

DePaolo, D.J. 1981. Trace element and isotopic effects of combined wallrock assimilation and fractional crystallization. *Earth and Planetary Sciences Letters*, v. 53 (2), p. 189-202. [https://doi.org/10.1016/0012-821X\(81\)90153-9](https://doi.org/10.1016/0012-821X(81)90153-9)

DePaolo, D.J., Wasserburg, G.J. 1979. Petrogenetic mixing models and Nd-Sr isotopic patterns. *Geochimica et Cosmochimica Acta*, v. 43(4), p. 615-627. [https://doi.org/10.1016/0016-7037\(79\)90169-8](https://doi.org/10.1016/0016-7037(79)90169-8)

Eisele, J., Sharma, M., Galer, S.J.G., Blichert-Toft, J., Devey, C.W., Hofmann, A.W. 2002. The role of sediment recycling in EM-1 inferred from Os, Pb, Hf, Nd, Sr isotope and trace element systematics of the Pitcairn hotspot. *Earth and Planetary Science Letters*, v. 196, p. 197-212. [https://doi.org/10.1016/S0012-821X\(01\)00601-X](https://doi.org/10.1016/S0012-821X(01)00601-X)

Etemadi, A., Karimpour, M.H., Malekzadeh Shafaroudi, A., Santos, J.F., Mathur, R., Ribeiro, S. 2019. U-Pb zircon geochronology, geochemistry and petrogenesis of the Hamech intrusions in the Kuh-e-Shah volcano-plutonic complex Eastern Iran. *Turkish Journal of Earth Sciences*, v. 28 (1), p. 38–59. <http://dx.doi.org/10.3906/yer-1710-5>

Fainstein, R., Summerhays, C.P. 1982. Structure and origin of marginal banks off eastern Brazil. *Marine Geology*, v. 46, p. 199-215. [https://doi.org/10.1016/0025-3227\(82\)90080-9](https://doi.org/10.1016/0025-3227(82)90080-9)

Fairhead, M.J., Wilson, M. 2005. Plate tectonic processes in the south Atlantic ocean: do we need deep mantle plumes? In: Foulger, G.R., Natland, J.H., Presnall, D.C., Anderson, D.L. (Eds.), *Plates, Plumes, and Paradigms*. Geological Society of America, p. 537–554. <https://doi.org/10.1130/0-8137-2388-4.537>

Ferrari, A., Riccomini, C. 1999. Campo de esforços Plio Pleistocênico na Ilha de Trindade (Oceano Atlântico Sul, Brasil) e sua relação com a tectônica regional. *Revista Brasileira de Geociências*, v. 29, n. 2, p. 195-202.

Fodor, R.V., Hanan, B.B. 2000. Geochemical evidence for the Trindade Hotspot trace: Columbia seamount ankaramite. *Lithos*, v. 51, p. 293–304. [https://doi.org/10.1016/S0024-4937\(00\)00002-5](https://doi.org/10.1016/S0024-4937(00)00002-5)

Fodor, R.V., Mckee, E.H., Asmus, H.E. 1983. K-Ar ages and the opening of the South Atlantic Ocean: basaltic rock from the Brazilian margin. *Marine Geology*, v. 54, M1-M8. [https://doi.org/10.1016/0025-3227\(83\)90002-6](https://doi.org/10.1016/0025-3227(83)90002-6)

Fodor, R.V., Mukasa, S.B., Gomes, C.B., Cordani, U.G. 1989. Ti-rich eocene basaltic rocks, abrolhos platform, Offshore Brazil, 18°S: Petrology with respect to South Atlantic magmatism. *Journal of Petrology*, v. 30, p. 763–786. <https://doi.org/10.1093/petrology/30.3.763>

França, R.L., Del Rey, A.C., Tagliari, C.V., Brandão, J.R., Fontanelli, P.R. 2007. Bacia do Espírito Santo. In: Milani, E.J., Rangel, H.D., Bueno, G.V., Stica, J.M., Winter, W.R., Caixeta, J.M., Pessoa Neto, O.C. (eds.). Bacias Sedimentares Brasileiras - Cartas Estratigráficas. *Boletim de Geociências da Petrobras*, Rio de Janeiro, v. 15, p. 501-509.

Frey, F.A., Sue, C.J., Stockman, H.W. 1985. The Ronda high temperature peridotite: Geochemistry and petrogenesis. *Geochimica et Cosmochimica Acta*, v. 49(11), p. 2469-2491. [https://doi.org/10.1016/0016-7037\(85\)90247-9](https://doi.org/10.1016/0016-7037(85)90247-9).

Geraldes, M.C., Motoki, A., Costa, A., Mota, C.E., Mohriak, W.U. 2013. Geochronology (Ar/Ar and K-Ar) of the South Atlantic post-break-up magmatism. *Geological Society London Special Publications*, v. 369, n. 1, p. 41-74. <http://dx.doi.org/10.1144/SP369.21>

Gibson, S.A., Thompson, R.N., Leonardos, O.H., Dickin, A.P., Mitchell, J.G. 1999. The limited extent of plume-lithosphere interactions during continental flood-basalt genesis: geochemical evidence from Cretaceous magmatism in southern Brazil. *Contributions to Mineralogy and Petrology*, v. 137, p. 147–169. <https://doi.org/10.1007/s004100050588>

Gomes, N.S., Borba, R.P., Cunha, E.M. 1992. Alteração hidrotermal em diabásios do Banco de Abrolhos, Bacia do Espírito Santo, Brasil: Resultados preliminares. In: XXXVII Congresso De Geologia. Sociedade Brasileira de Geologia, São Paulo, SP, p. 60-61.

Gomes, N.S., Suita, M.T. de F. 2010. Ocorrência de vulcanismo bimodal de idade terciária na Bacia de Mucuri. *Boletim de Geociências da Petrobras*, v. 18, p. 89-104.

Gurenko, A.A., Sobolev, A.V., Hoernle, K.A., Hauff, F., Schmincke, H.-U. 2009. Enriched, HIMU-type peridotite and depleted recycled pyroxenite in the Canary plume: a mixed-up mantle. *Earth and Planetary Sciences Letters*, v. 277, p. 514–524. <https://doi.org/10.1016/j.epsl.2008.11.013>

Halliday, A.N., Davies, G.R., Lee, D.C., Tommasini, S., Oaslick, C.R., Fitton, J.G., James D.E. 1992. Lead isotope evidence for young trace element enrichment in the oceanic upper mantle. *Nature*, v. 359, p. 623-627. <https://doi.org/10.1038/359623a0>

Hanyu, T., Nakamura, E. 2000. Constraints on HIMU and EM by Sr and Nd isotopes re-examined. *Earth Planets Space*, v. 52, p. 61–70. <https://doi.org/10.1186/BF03351614>

Hart, S.R. 1988. Heterogeneous mantle domains: Signatures, genesis and mixing chronologies. *Earth and Planetary Science Letters*, v. 90, p. 272–296. [https://doi.org/10.1016/0012-821X\(88\)90131-8](https://doi.org/10.1016/0012-821X(88)90131-8)

Hart, S.R., Hauri E.H., Oschmann, L.A., Whitehead, J.A. 1992. Mantle plumes and entrainment: isotopic evidence. *Science*, v. 256, p. 517–520. DOI: 10.1126/science.256.5056.517

Heilbron, M., Valeriano, C.M., Peixoto, C., Tupinambá, M., Neubauer, F., Dussin, I., Corrales, F., Bruno, H., Lobato, M., Almeida, J.C.H., Silva, L.G.E. 2020. Neoproterozoic magmatic arc systems of the central Ribeira belt, SE-Brazil, in the context of the West-Gondwana pre collisional history: A review. *Journal of South American Earth Sciences*, 102710. <https://doi.org/10.1016/j.jsames.2020.102710>

Hofmann, A.W. 2014. 3.3 - Sampling Mantle Heterogeneity through Oceanic Basalts: Isotopes and Trace Elements. In: Holland, H.D., Turekian, K.K (Eds.), *Treatise on Geochemistry* (Second Edition), v. 3, p. 67-101. <https://doi.org/10.1016/B978-0-08-095975-7.00203-5>

Hofmann, A.W., White, W.M. 1982. Mantle plumes from ancient oceanic crust. *Earth and Planetary Sciences Letters*, v. 57, p. 421–436. [https://doi.org/10.1016/0012-821X\(82\)90161-3](https://doi.org/10.1016/0012-821X(82)90161-3)

Irvine, T. N., Baragar, W. R. A. 1971. A guide to the chemical classification of the common volcanic rocks. *Canadian Journal of Earth Sciences*, v. 8, p. 523–548. <https://doi.org/10.1139/e71-055>

Jackson, M.G., Dasgupta, R. 2008. Compositions of HIMU, EM1, and EM2 from global trends between radiogenic isotopes and major elements in ocean island basalts. *Earth and Planetary Science Letters*, v. 276, p. 175–186. <https://doi.org/10.1016/j.epsl.2008.09.023>

Jerram, D.A., Bryan, S.E. 2015. Plumbing Systems of Shallow Level Intrusive Complexes. In: Breitkreuz, C., Rocchi, S. (Eds.), *Physical Geology of Shallow Magmatic Systems. Advances in Volcanology*. Springer, Cham. https://doi.org/10.1007/11157_2015_8

Jesus, J.V.M., Santos, A.C., Mendes, J.C., Santos, W.H., Rego, C.A.Q., Geraldés, M.C. 2019. Petrogênese do Banco Davis, Cadeia Vitória-Trindade, Atlântico Sul: o Papel de Voláteis (H₂O e CO₂) na Evolução Magmática do Banco Davis. *Anuário do Instituto de Geociências*, v.42, p. 3-19. http://dx.doi.org/10.11137/2019_3_03_19

Ker, A.C., Kempton, P.D., Thompson, R.N. 1995. Crustal assimilation during turbulent magma ascent (ATA); new isotopic evidence from the Mull Tertiary lava succession, N.W. Scotland. *Contributions to Mineralogy and Petrology*, v. 119, 142-154. <https://doi.org/10.1007/BF00307277>

King, S.D. 2007. Hotspots and edge-driven convection. *Geology*, v. 35, p. 223–226. <https://doi.org/10.1130/G23291A.1>

King, S.D., Anderson, D.L. 1995. An alternative mechanism for flood basalt formation. *Earth and Planetary Science Letters*, v. 136, p. 269–279. [https://doi.org/10.1016/0012-821X\(95\)00205-Q](https://doi.org/10.1016/0012-821X(95)00205-Q)

King, S.D., Anderson, D.L. 1998. Edge-driven convection. *Earth and Planetary Science Letters*, v. 160, p. 289–296. [https://doi.org/10.1016/S0012-821X\(98\)00089-2](https://doi.org/10.1016/S0012-821X(98)00089-2)

King, S.D., Ritsema, J. 2000. African hot spot volcanism: small-scale convection in the upper mantle beneath cratons. *Science*, v. 290, p. 1137–1140. DOI: 10.1126/science.290.5494.1137

Knesel, K.M., de Souza, Z.S., Vasconcelos, P.M., Cohen, B.E., Silveira, F.V. 2011. ⁴⁰Ar/³⁹Ar geochronology reveals the youngest volcanism in mainland Brazil and no evidence for a plume trace on the continent. *Earth and Planetary Science Letters*, v. 302, p. 38–50.

Koppers, A.A.P., Becker, T.W., Jackson, M.G., Konrad, K., Müller, R.D., Romanowicz, B., Steinberger, B., Whittaker, J.M. 2021. Mantle plumes and their role in Earth processes. *Nature*

Reviews Earth and Environment, v. 2, p. 382–401. <https://doi.org/10.1038/s43017-021-00168-6>

Le Bas, M.J., Le Maitre, R.W., Streckeisen, A., Zanettin, B. 1986. A Chemical Classification of Volcanic Rocks Based on the Total Alkali-Silica Diagram. *Journal of Petrology*, v. 27(3), p. 745-750. <https://doi.org/10.1093/petrology/27.3.745>

Le Roex, A.P., Class, C., O'Connor, J., Jokat, W. 2010. Shona and Discovery Aseismic Ridge Systems, South Atlantic: Trace Element Evidence for Enriched Mantle Sources. *Journal of Petrology*, v. 51, p. 2089–2120. <https://doi.org/10.1093/petrology/egq050>

Lormand, C., Zellmer, G.F., Sakamoto, N., Ubide, T., Kilgour, G., Yurimoto, H., Palmer, A., Németh, K., Iizuka, Y., Moebis, A. 2021. Shallow magmatic processes revealed by cryptic microantecrysts: a case study from the Taupo Volcanic Zone. *Contributions to Mineralogy and Petrology*, v. 176 (97), p. 1-24. <https://doi.org/10.1007/s00410-021-01857-7>

Magee, C., Stevenson, C.T.E., Ebmeier, S.K., Keir, D., Hammond, J.O.S., Gottsmann, J.H., Whaler, K.A., Schofield, N., Jackson, C. A-L., Petronis, M.S., O'Driscoll, B., Morgan, J., Cruden, A., Vollgger, S.A., Dering, G., Micklethwaite, S., Jackson, M.D. 2018. Magma plumbing systems: a geophysical perspective. *Journal of Petrology*, v. 59 (6), p. 1217–1251. <https://doi.org/10.1093/petrology/egy064>

Maia, T.M., Santos, A.C., Rocha-Júnior, E.R.V., Valeriano, C.M., Mendes, J.C., Jeck, I.K., Santos, W.H., Oliveira, A.L., Mohriak, W.U. 2021. First petrologic data for Vitória Seamount, Vitória-Trindade Ridge, South Atlantic: a contribution to the Trindade mantle plume evolution. *Journal of South American Earth Sciences*, v. 109, 103304. <https://doi.org/10.1016/j.jsames.2021.103304>

Mallik, A., Dasgupta, R. 2012. Reaction between MORB-eclogite derived melts and fertile peridotite and generation of ocean island basalts. *Earth and Planetary Science Letters*, v. 329-330, p. 97-108. <https://doi.org/10.1016/j.epsl.2012.02.007>

Matte, R.R. 2013. Sedimentologia e estratigrafia das ilhas de Santa Bárbara e Redonda, Arquipélago dos Abrolhos, sul da Bahia. *Boletim de Geociências da Petrobras*, v. 21, n. 2, p. 369-384.

Marques, L.S., De Min, A., Rocha-Júnior, E.R.V., Babinski, M., Bellieni, G., Figueiredo, A.M.G. 2018. Elemental and Sr-Nd-Pb isotope geochemistry of the Florianópolis Dyke Swarm (Paraná Magmatic Province): Crustal contamination and mantle source constraints. *Journal of Volcanology and Geothermal Research*, v. 355, p. 149-164. <https://doi.org/10.1016/j.jvolgeores.2017.07.005>

Marques, L.S., Ulbrich, M.N.C., Ruberti, E., Tassinari, C.G. 1999. Petrology, geochemistry and Sr-Nd isotopes of the Trindade and Martin Vaz volcanic rocks (Southern Atlantic Ocean). *Journal of Volcanology and Geothermal Research*, v. 93, p.191–216. [https://doi.org/10.1016/S0377-0273\(99\)00111-0](https://doi.org/10.1016/S0377-0273(99)00111-0)

McDonough, W.F., Sun, S.S. 1995. The composition of the Earth. *Chemical Geology*, v. 120, p. 223-253. [https://doi.org/10.1016/0009-2541\(94\)00140-4](https://doi.org/10.1016/0009-2541(94)00140-4)

Meibom, A., Anderson, D.L. 2003. The statistical upper mantle assemblage. *Earth and Planetary Science Letters*, v. 217, p. 123-139. [https://doi.org/10.1016/S0012-821X\(03\)00573-9](https://doi.org/10.1016/S0012-821X(03)00573-9)

Mohriak, W.U. 2006. Interpretação geológica e geofísica da Bacia do Espírito Santo e da região de Abrolhos: petrografia, datação radiométrica e visualização sísmica das rochas vulcânicas. *Boletim de Geociências da Petrobras*, v. 14, n. 1, p. 133-142.

Mohriak, W.U. 2020. Genesis and evolution of the South Atlantic volcanic islands offshore Brazil. *Geo-Marine Letters*, v. 40, p. 1–33. <https://doi.org/10.1007/s00367-019-00631-w>

Mohriak, W. U., Paula, O., Szatmari, P., Sobreira, J. F., Parsons, M., Macqueen, J., Undli, T. H., Berstad, S., Weber, M., Horstad, I. 2003. Volcanic provinces in the Eastern Brazilian margin: geophysical models and alternative geodynamic interpretations. In: International Congress of The Brazilian Geophysical Society, v. 8, 2003, Rio de Janeiro. Rio de Janeiro: Sociedade Brasileira de Geofísica, 2003. 1 CD-ROM, 4f

Monteiro, L.G.P., Santos, A.C., Pires, G.L.C., Barão, L.M., Rocha-Júnior, E.R.V., Biancini, J.R.C., Hackspacher, P.C., Júnior, H.I.A., Jeck, I.K., Santos, J.F. 2022. Chapter 10 - Trindade Island: evolution of the geological knowledge. In: Hackspacher, P.C., Santos, A.C. Meso-Cenozoic Brazilian Offshore Magmatism: Geochemistry, Petrology and Tectonics. Elsevier Inc., 2021, p. 337-390. <https://doi.org/10.1016/B978-0-12-823988-9.00015-0>

Motoki, A., Novais, L.C.C., Sichel, S.E., Neves, J.L., Aires, J.R. 2007. Felsic pyroclastic rock originated from subaqueous eruption in the Espírito Santo sedimentary basin: an association with the tectonic-sedimentary model. *Geociências*, v. 26(2), p. 151–160.

Negredo, A.M., Van Hunen, J., Rodríguez-González, J., Fullea, J. 2022. On the origin of the Canary Islands: Insights from mantle convection modelling. *Earth and Planetary Science Letters*, v. 584, 117506. <https://doi.org/10.1016/j.epsl.2022.117506>

Neto, C.C.A., Valeriano, C.M., Vaz, G.S., Medeiros, S.R, Ragatky, C.D. 2009. Composição Isotópica do Sr no padrão NBS987 e nos padrões de rocha do USGS BCR-1, AGV-1, G-2 e GSP-1: Resultados Preliminares Obtidos por TIMS no Laboratório de Geocronologia e Isótopos Radiogênicos – LAGIR – UERJ, RIO DE JANEIRO. In: Boletim de Resumos Expandidos do Simpósio 45 Anos de Geocronologia no Brasil, IGc–USP, CPGeo –Centro de Pesquisas Geocronológicas, CD-ROM.

Niu, Y. 2008. The Origin of Alkaline Lavas. *Science*, v. 320, p. 883-884. DOI: 10.1126/science.1158378

Niu, Y. 2009. Some basic concepts and problems on the petrogenesis of intra-plate ocean island basalts. *Chinese Science Bulletin*, v, 54, p. 4148-4160. <https://doi.org/10.1007/s11434-009-0668-3>

Niu, Y., Wilson, M., Humphreys, E.R., O’Hara, M.J. 2012. A trace element perspective on the source of ocean island basalts (OIB) and fate of subducted ocean crust (SOC) and mantle lithosphere (SML). *Episodes*, v. 35, p. 310-327. <https://doi.org/10.18814/epiugs/2012/v35i2/002>

Niu, Y.L., O'Hara, M.J. 2003. Origin of ocean island basalts: A new perspective from petrology, geochemistry, and mineral physics considerations. *Journal of Geophysical Research: Solid Earth*, v. 108, 2209. <https://doi.org/10.1029/2002JB002048>

Novais, L.C.C., Zelenka, T., Szatmari, P., Motoki, A., Aires, J.R., Tagliari, C.V. 2008. Ocorrência de rochas vulcânicas ignimbríticas na porção norte da Bacia do Espírito Santo: evolução do modelo tectono-sedimentar. *Boletim de Geociências da Petrobras*, v. 16(1), p. 139-156.

O'Connor, J.M., Duncan, R.A. 1990. Evolution of the Walvis Ridge–Rio Grande Rise Hot Spot System: Implications for African and South American plate motions over plumes. *Journal of Geophysical Research*, v. 95, 17475–17502. <https://doi.org/10.1029/JB095iB11p17475>.

O'Hara, M.J., Mathews, R.E. 1981. Geochemical evolution in an advancing, periodically replenished, periodically tapped, continuously fractionated magma chamber. *Journal of the Geological Society*, v. 138, p. 237-277. <http://dx.doi.org/10.1144/gsjgs.138.3.0237>

De Oliveira, A.L., Dos Santos, A.C., Nogueira, C.C., Maia, T.M., Geraldes, M.C. 2021. Green core clinopyroxenes from Martin Vaz Archipelago Plio-Pleistocene alkaline rocks, South Atlantic Ocean, Brazil: A magma mixing and polybaric crystallization record. *Journal of South American Earth Sciences*, v. 105, 102951. <https://doi.org/10.1016/j.jsames.2020.102951>

Oliveira, L.C, Oliveira R.M.A.G., Pereira, E. 2018. Seismic characteristics of the onshore Abrolhos magmatism, East-Brazilian continental margin. *Marine and Petroleum Geology*, v. 89, p. 488-499. <https://doi.org/10.1016/j.marpetgeo.2017.10.016>

Pearce, J.A. 1983. Role of the sub-continental lithosphere in magma genesis at active continental margins. In: Hawkesworth, C.J., Norry, M.J., editors. *Continental Basalts and Mantle Xenoliths*. Nantwich, UK: Shiva Publisher, pp. 230-249.

Pearce, J.A., Norry, M.J. 1979. Petrogenetic implications of Ti, Zr, Y and Nb variations in volcanic rocks. *Contributions to Mineralogy and Petrology*, v. 69, p. 33–47. <https://doi.org/10.1007/BF00375192>

Peate, D.W. 1997. The Parana-Etendeka province. In: J.J.Mahoney and M.F. Coffin (eds.) Large igneous provinces: continental, oceanic and planetary flood volcanism. American Geophysical Union, 100, Geophysical Monograph Series, p. 217-245.

Peixoto, C.A., Heilbron, M., Ragatky, D., Armstrong, R., Dantas, E., Valeriano, C.M., Simonetti, A. 2017. Tectonic evolution of the Juvenile Tonian Serra da Prata magmatic arc in the Ribeira belt, SE Brazil: Implications for early west Gondwana amalgamation. *Precambrian Research*, v. 302, p. 221–254. <https://doi.org/10.1016/j.precamres.2017.09.017>

Perlingeiro, G., Vasconcelos, P.M., Knesel, K.M., Thiede, D.S., Cordani, U.G. 2013. $^{40}\text{Ar}/^{39}\text{Ar}$ geochronology of the Fernando de Noronha Archipelago and implications for the origin of alkaline volcanism in the NE Brazil. *Journal of Volcanology and Geothermal Research*, v. 249, p. 140-154. <http://dx.doi.org/10.1016/j.jvolgeores.2012.08.017>

Peyve, A.A., Skolotnev, S.G. 2014. Systematic variations in the composition of volcanic rocks in tectono-magmatic seamount chains in the Brazil Basin. *Geochemistry International*, v. 52, p. 111–130. <https://doi.org/10.1134/S0016702914020062>

Pfänder, J.A., Jung, S., Münker, C., Stracke, A., Mezger, K. 2012. A possible high Nb/Ta reservoir in the continental lithospheric mantle and consequences on the global Nb budget – Evidence from continental basalts from Central Germany. *Geochimica et Cosmochimica Acta*, v. 77, p. 232–251.

Pilet, S., Baker, M.B., Stolper, E.M. 2008. Metasomatized lithosphere and the origin of alkaline lavas. *Science*, v. 20, p. 916-919. <https://doi.org/10.1126/science.1156563>

Pilet, S., Hernandez, J., Sylvester, P., Poujol, M. 2005. The metasomatic alternative for ocean island basalt chemical heterogeneity. *Earth and Planetary Science Letters*, v. 236, p. 148-166. <https://doi.org/10.1016/j.epsl.2005.05.004>

Pilet, S., Baker, M.B., Müntener, O., Stolper, E.M. 2011. Monte Carlo Simulations of Metasomatic Enrichment in the Lithosphere and Implications for the Source of Alkaline Basalts. *Journal of Petrology*, v. 52, p. 1415-1442. <https://doi.org/10.1093/petrology/egr007>

Pires, G.L.C., Bongiolo, E.M. 2016. The nephelinitic–phonolitic volcanism of the Trindade Island (South Atlantic Ocean): Review of the stratigraphy, and inferences on the volcanic styles and sources of nephelinites. *Journal of South American Earth Sciences*, 72, 49-62. <https://doi.org/10.1016/j.jsames.2016.07.008>

Pires, G.L.C., Bongiolo, E.M., Geraldés, M.C., Renac, C., Santos, A.C., Jourdan, F., Neumann, R. 2016. New $^{40}\text{Ar}/^{39}\text{Ar}$ ages and revised $^{40}\text{K}/^{40}\text{Ar}^*$ data from nephelinitic–phonolitic volcanic successions of the Trindade Island (South Atlantic Ocean). *Journal of Volcanology and Geothermal Research*, v. 327, p. 531-538. <https://doi.org/10.1016/j.jvolgeores.2016.09.020>

Quaresma, G.O.A., Santos, A.C., Rocha-Júnior, E.R.V., Bonifácio, J., Rego, C.A.Q., Mattielli, N., Mata, J., Jourdan, F., Geraldés, M.C. *In press*. Isotopic Constraints on Davis Bank, Vitória-Trindade Ridge: A Revisited Petrogenetic Model. *Journal of South American Earth Sciences*.

Rego, C.A.Q., Quaresma, G.O., Santos, A.C., Mohriak, W.U., Jesus, J.V.M., Rodrigues, S.W.O. 2021. Davis Bank geodynamic context, South Atlantic Ocean: Insights into the Vitória-Trindade Ridge evolution. *Journal of South American Earth Sciences*, v. 112, 103620. <https://doi.org/10.1016/j.jsames.2021.103620>

Rehkamper, M., Hofmann, A.W. 1997. Recycled Ocean Crust and sediment in Indian Ocean MORB. *Earth and Planetary Science Letters*, v. 147, p. 93-106. [https://doi.org/10.1016/S0012-821X\(97\)00009-5](https://doi.org/10.1016/S0012-821X(97)00009-5)

Rocha-Júnior, E.R.V., Marques, L.S., Babinski, M., Machado, F.B., Petronilho, L.A., Nardy, A.J.R. 2020. A telltale signature of Archean lithospheric mantle in the Paraná continental flood basalts genesis. *Lithos*, v. 364-365, p. 364-365, 105519. <https://doi.org/10.1016/j.lithos.2020.105519>

Rollinson, H.R. 1993. *Using Geochemical Data: Evaluation, Presentation, Interpretation*. New York, USA, Longman Science and Technical. ISBN 978-0-582-06701-1

Rudnick, R.L., Gao, S. 2003. 3.01 - Composition of the continental crust. In: Rudnick, R.L., Holland, H.D., Turekian, K.K. (Eds.), *The Crust. Treatise of Geochemistry*, v. 3. Elsevier - Pergamon, Oxford, p. 1–64. <https://doi.org/10.1016/B0-08-043751-6/03016-4>

Salters, V.J.M., Stracke, A. 2004. Composition of the depleted mantle. *Geochemistry, Geophysics, Geosystems*, v. 5, Q05B07. <https://doi.org/10.1029/2003GC000597>

Salters, V.J.M., White, W.M. 1998. Hf isotope constraints on mantle evolution. *Chemical Geology*, v. 145, p. 447-460. [https://doi.org/10.1016/S0009-2541\(97\)00154-X](https://doi.org/10.1016/S0009-2541(97)00154-X)

Santos, A.C. 2013. Petrography, Litho geochemistry and $^{40}\text{Ar}/^{39}\text{Ar}$ dating of the seamounts and Martin Vaz Islands - Vitória-Trindade Ridge. Dissertation, Universidade do Estado do Rio de Janeiro, Brazil.

Santos, A.C. 2016. Petrology of Martin Vaz Island and Vitoria-Trindade Ridge seamounts: Montague, Jaseur, Davis, Dogaressa and Columbia. Trace elements, $^{40}\text{Ar}/^{39}\text{Ar}$ dating and Sr and Nd isotope analysis related to the Trindade Plume evidence. Ph.D. Thesis, Universidade do Estado do Rio de Janeiro, Brazil.

Santos, A.C., Geraldés, M.C., Vargas, T., Willians, S. 2015. Geology of Martin Vaz, South Atlantic, Brazil. *Journal of Maps*, v. 11, p. 314–322. <https://doi.org/10.1080/17445647.2014.936913>

Santos, A.C., Geraldés, M.C., Siebel, W., Mendes, J., Bongiolo, E., Santos, W.H., Garrido, T. C.V., Rodrigues S.W.O. 2018a. Pleistocene alkaline rocks of Martin Vaz volcano, South Atlantic: low-degree partial melts of a CO₂-metasomatized mantle plume. *International Geology Review*, v. 61, p. 296–313. <https://doi.org/10.1080/00206814.2018.1425921>

Santos, A.C., Hackspacher, P.C. 2021. Meso-Cenozoic Brazilian Offshore Magmatism: Geochemistry, Petrology and Tectonics. Elsevier Inc. Academic Press, 512 p. <https://doi.org/10.1016/C2019-0-05400-3>

Santos, A.C., Mata, J., Jourdan, F., Rodrigues, S.W. De O., Monteiro, L.G.P., Guedes, E., Benedini, L., Geraldés, M.C. 2021. Martin Vaz Island geochronology: Constraint on the Trindade Mantle Plume track from the youngest and easternmost volcanic episodes. *Journal of South American Earth Sciences*, v. 106, 103090. <https://doi.org/10.1016/j.jsames.2020.103090>

Santos, A.C., Mohriak, W.U., Geraldés, M.C., Santos, W.H., Ponte-Neto, C.F., Stanton, N. 2018b. Compiled potential field data and seismic surveys across the Eastern Brazilian continental margin integrated with new magnetometric profiles and stratigraphic configuration for Trindade Island, South Atlantic, Brazil. *International Geology Review*, v. 61, p. 1728-1744. <https://doi.org/10.1080/00206814.2018.1542634>

Santos, A.C., Oliveira, O.L., Bevilaqua, L.A., Rocha-Júnior, E.R.V., Rodrigues, S.W.O., Mendes, J.C., Jeck, I.K. 2022a. Chapter 11 - Martin Vaz Archipelago: the youngest magmatism in the Brazilian Territory. In: Santos, A.C., Hackspacher, P.C. *Meso-Cenozoic Brazilian Offshore Magmatism: Geochemistry, Petrology and Tectonics*. Elsevier Inc., 2021, p. 391-432. <https://doi.org/10.1016/B978-0-12-823988-9.00013-7>

Santos, A.C., Rocha-Júnior, E.R.V., Quaresma, G.O.A., Maia, T.M., Jesus, J.V.M., Rego, C.A.Q., Jeck, I.K. 2022b. Chapter 9 - Vitória-Trindade seamounts: undersaturated alkaline series evolution from an enriched metasomatized source. In: Santos, A.C., Hackspacher, P.C. *Meso-Cenozoic Brazilian Offshore Magmatism: Geochemistry, Petrology and Tectonics*. Elsevier Inc., 2021, p. 293-336. <https://doi.org/10.1016/B978-0-12-823988-9.00004-6>

Santos, R.N., Marques, L.S. 2007. Investigation of ^{238}U - ^{230}Th - ^{226}Ra and ^{232}Th - ^{228}Ra - ^{228}Th radioactive disequilibria in volcanic rocks from Trindade and Martin Vaz Islands (Brazil; Southern Atlantic Ocean). *Journal of Volcanology and Geothermal Research*, v. 161, p. 215–233. <https://doi.org/10.1016/j.jvolgeores.2006.11.010>

Siebel, W., Becchio, R., Volker, F., Hansen, M.A.F., Viramonte, J., Trumbull, R.B., Haase, G., Zimmer, M. 2000. Trindade and Martin Vaz Islands, South Atlantic: Isotopic (Sr, Nd, Pb) and trace element constraints on plume related magmatism. *Journal of South American Earth Science*, v. 13, p. 79–103. [https://doi.org/10.1016/S0895-9811\(00\)00015-8](https://doi.org/10.1016/S0895-9811(00)00015-8)

Skolotnev, S.G., Bylinskaya, M.E., Golovina, L.A., Ipatova, I.S. 2011. First Data on the Age of Rocks from the Central Part of the Vitória-Trindade Ridge (Brazil Basin, South Atlantic). *Doklady Earth Sciences*, v. 437, p. 316–322. <https://doi.org/10.1134/S1028334X11030093>

Skolotnev, S.G., Peive, A.A. 2017. Composition, structure, origin, and evolution of off-axis linear volcanic structures of the Brazil Basin, South Atlantic. *Geotectonics*, v. 51, p. 53–73. <https://doi.org/10.1134/S001685211701006X>

Skolotnev, S. G., Peyve, A.A., Turko, N.N. 2010. New Data on the Structure of the Vitoria Trindade Seamount Chain (Western Brazil Basin, South Atlantic). *Doklady Earth Sciences*, v. 431, n. 2, p. 435-440. <https://doi.org/10.1134/S1028334X10040057>

Sobolev, A.V., Hofmann, A.W., Sobolev, S.V., Nikogosian, I.K. 2005. An olivine-free mantle source of Hawaiian shield basalts. *Nature*, v. 434 (7033), p. 590-597. <https://doi.org/10.1038/nature03411>

Sobolev, A.V., Hofmann, A.W., Kuzmin, D.V., Yaxley, G.M., Arndt, N.T., Chung, S.L., Danyushevsky, L.V., Elliott, T., Frey, F.A., Garcia, M.O., et al. 2007. The amount of recycled crust in sources of mantle-derived melts. *Science*, v. 316 (5823), p. 412–417. DOI: 10.1126/science.1138113

Sobreira, J.F.F., França R.L. 2006. Um modelo tectono-magmático para a região do Complexo Vulcânico de Abrolhos. *Boletim de Geociências da Petrobras*, v. 14, p. 143-147.

Sobreira, J.F.F., Szatmari, P., Mohriak, W.U., Valente, S.C., York, D. 2004. Recorrência, em diferentes escalas, do magmatismo paleogênico no Arquipélago de Abrolhos, Complexo Vulcânico de Abrolhos. XLII Congresso Brasileiro de Geologia, Araxá, Minas Gerais, Anais.

Sobreira, J.F.F., Szatmari, P. 2002. Datações Ar-Ar Das Rochas Vulcânicas De Abrolhos E Implicações para a Evolução da Margem Continental Leste Brasileira No Terciário. XLI Congresso Brasileiro de Geologia, João Pessoa, Pernambuco, Anais, p. 395.

Sobreira, J.F.F., Szatmari, P. 2003. Idades Ar-Ar para as rochas ígneas do Arquipélago de Abrolhos, margem sul da Bahia. In: Simpósio Nacional De Estudos Tectônicos, 9, 2003, Búzios. Boletim de Resumos, p. 382-383.

Stanton, N., Gordon, A., Cardozo, C., Kuszniir, N. 2021. Morphostructure, emplacement and duration of the Abrolhos Magmatic Province: A geophysical analysis of the largest post-

breakup magmatism of the South-Eastern Brazilian Margin. *Marine and Petroleum Geology*, v. 133, 105230. <https://doi.org/10.1016/j.marpetgeo.2021.105230>

Stanton, N., Gordon, A.C., Valente, S.C., Mohriak, W.U., Maia, T.M., Arena, M. 2022. Chapter 6 - The Abrolhos Magmatic Province, the largest postbreakup magmatism of the Eastern Brazilian margin: a geological, geophysical, and geochemical review. In: Santos, A.C., Hackspacher, P.C. Meso-Cenozoic Brazilian Offshore Magmatism: Geochemistry, Petrology and Tectonics. Elsevier Inc., 2021, p. 189-230. <https://doi.org/10.1016/B978-0-12-823988-9.00014-9>

Stracke, A., Hofmann, A.W., Hart, S.R. 2005. FOZO, HIMU, and the rest of the mantle zoo. *Geochemistry, Geophysics, Geosystems*, v. 6, n. 5, p. 1-20. <https://doi.org/10.1029/2004GC000824>

Sun, S.-S. 1980. Lead isotopic study of young volcanic rocks from mid-ocean ridges, ocean islands and island arcs. *Philosophical Transactions of the Royal Society of London*, v. 297, p. 409-445. <https://doi.org/10.1098/rsta.1980.0224>

Szatmari, P., Mohriak, W.U. 1995. Plate model of post-breakup tectono-magmatic activity in the adjacent Atlantic. In: SBG/Núcleo Rio grande do Sul, Simpósio Nacional de Estudos Tectônicos, 5, Gramado, Anais, 1, p. 213-214.

Su, Y., Langmuir, C.H. 2003. Global MORB chemistry compilation at the segment scale, PhD Thesis, Department of Earth and environmental Sciences, Columbia University.

Tanaka, T., Togashi, S., Kamioka, H., Amakawa, H., Kagami, H., Hamamoto, T., Yuhara, M., Orihashi, Y., Yoneda, S., Shimizu, H., Kunimaru, T., Takahashi, K., Yanagi, T., Nakano, T., Fujimaki, H., Shinjo, R., Asahara, Y., Tanimizu, M., Dragusanu C. 2000. JNdi-1: a neodymium isotopic reference in consistency with LaJolla neodymium. *Chemical Geology*, v. 168, p. 279–281. [https://doi.org/10.1016/S0009-2541\(00\)00198-4](https://doi.org/10.1016/S0009-2541(00)00198-4)

Tatsumi, Y. 2000. Continental crust formation by crustal delamination in subduction zones and complementary accumulation of the enriched mantle I component in the mantle. *Geochemistry, Geophysics, Geosystems*, v. 1. <https://doi.org/10.1029/2000GC000094>

Taylor, S.R., McLennan, S.M. 1985. *The Continental Crust: Its Composition and Evolution*. Oxford, UK: Blackwell. ISBN 978-0632011483

Thompson, R.N., Gibson, S.A., Mitchell, J.G., Dickin, A.P., Leonardos, O.H., Brod, J.A., Greenwood, J.C. 1998. Migrating Cretaceous–Eocene Magmatism in the Serra do Mar Alkaline Province, SE Brazil: Melts from the Deflected Trindade Mantle Plume? *Journal of Petrology*, v. 39, p. 1493–1526. <https://doi.org/10.1093/petroj/39.8.1493>

Thompson, R.N., Morrison, M.A., Dickin, A.P., Gibson, I.L., Harmon, R.S. 1986. Two contrasted styles of interaction between basic magmas and continental crust in the British Tertiary Volcanic Province. *Journal of Geophysical Research*, v. 91, 5985–5997. <https://doi.org/10.1029/JB091iB06p05985>

Valeriano, C.M., Medeiros, S.R., Vaz, G.S., Neto, C.C.A. 2009. Sm-Nd isotope dilution TIMS analyses of BCR-1, AGV-1 and G-2 USGS rock reference materials: first results from the LAGIR laboratory at UERJ, Rio de Janeiro. In: Boletim de Resumos Expandidos do Simpósio 45 Anos de Geocronologia no Brasil, IGc–USP, CPGeo –Centro de Pesquisas Geocronológicas, CD-ROM.

Valeriano, C.M., Vaz, G.S., Medeiros, S.R., Neto, C.C.A., Ragatky, C.D., Geraldés, M.C. 2008. The Neodymium isotope composition of the JNdi-1 oxide reference material: results from the LAGIR Laboratory, Rio de Janeiro. Proceedings of the VI South American Symposium on Isotope Geology, San Carlos de Bariloche - Argentina – 2008 (CD-ROM), pp. 1-2

Veloso, J.A.V., Machado, D.L. 1986. Estudos sismológicos na ilha da Trindade desenvolvidos pela estação sismológica da UnB. In: Cong. Bras. Geol., 34, Goiânia. 1986. Anais Goiânia SBG, 6, 2.608-2.613.

Vieira, V.S., Novais, L.C.C., da Silva, M.A., Corrêa, T.R., Lopes, N.H.B. 2014. Caracterização geoquímica das rochas ignimbríticas no noroeste do estado do Espírito Santo. In: CONGRESSO BRASILEIRO DE GEOLOGIA, 47., 2014, Salvador. Anais. Salvador: SBG Núcleo Bahia, 2014. 1CD-ROM.

Weaver, B., Tarney, J. 1984. Empirical approach to estimating the composition of the continental crust. *Nature*, v. 310, p. 575-57. <https://doi.org/10.1038/310575a0>

Wilson, M. 1989. *Igneous Petrogenesis*. Springer, First Edition.

Winchester, J.A., Floyd, P.A. 1977. Geochemical discrimination of different magma series and their differentiation products using immobile elements. *Chemical Geology*, v. 20, p. 325-343. [https://doi.org/10.1016/0009-2541\(77\)90057-2](https://doi.org/10.1016/0009-2541(77)90057-2)

Winter, J.D. 2014. *Principles of Igneous and Metamorphic Petrology*. Pearson Education Limited, Second Edition.

Whitney, D.L., Evans, B.W. 2010. Abbreviations for names of rock-forming minerals. *American Mineralogist*, v. 95, p. 185–187. <https://doi.org/10.2138/am.2010.3371>

Wood, B.J., Fraser, D.G. 1976. *Elementary thermodynamics for geologists*. Oxford: Oxford University Press. 303pp.

Workman, R.K., Hart, S.R. 2005. Major and trace element composition of the depleted MORB mantle (DMM). *Earth and Planetary Science Letters*, v. 31, p. 53-72. <https://doi.org/10.1016/j.epsl.2004.12.005>

Xia, L., Li, X. 2019. Basalt geochemistry as a diagnostic indicator of tectonic setting. *Gondwana Research*, v. 65, p. 43–67. <https://doi.org/10.1016/j.gr.2018.08.006>

Zindler, A., Hart, S.R. 1986. Chemical geodynamics. Annual reviews: *Earth and Planetary Science Letters*, v. 14, p. 493–571.

Zindler, A., Jagoutz, E., Goldstein, S. 1982. Nd, Sr and Pb isotopic systematics in a three-component mantle: a new perspective. *Nature*, v. 58, p. 519-523. <https://doi.org/10.1038/298519a0>

APPENDIX C – Abrolhos Volcanic Complex petrography compilation

Reference	Litotype	Island	Textures	Groundmass	Grain Sizes	Phenocrysts	Phenocrysts sizes	Alteration minerals	Observations	Modal
Fodor et al., 1989	Basalt	Redonda (AB4); Santa Bárbara (AB20, 22, T6); Sueste (AB23, 24, 25, 27); Siriba (AB29, 30, 32)	Intergranular; plagic	Plag + Cpx + Fe-Ti oxides ± Ol	0.1-0.5 mm	Plag + Cpx + Fe-Ti oxides ± Ol	1 mm	Smectite	Cpx with compositional zoning	45% Cpx (+Ol); 46-32% Plag
Arena, 2008	Px-Plag Basalt	Santa Bárbara (FA-CV-02, FA-CV-01 c, FA-CV-20, FA-CV-16, FA-CV-01)	Hypocrystalline; Inequigranular; Porphyritic; Ophitic; Subophitic	Cpx + Plag + Op	< 1 mm	Cpx (augite) + Plag	1-2.5 mm	Chlorite, saussurite, biotite, carbonate	Cpx phenocrysts with poikilitic texture, compositional zoning and corrosion	Phenocrysts: 80% Cpx, 20% Plag
Arena, 2008	Px-Plag Basalt (chilled margin)	Santa Bárbara (FA-CV-01)	Hypocrystalline; Inequigranular; Porphyritic	Plag + Op + Glass		Plag	0.2- 0.3 mm	Saussurite		
Arena, 2008	Px-Plag-Ol Basalt	Siriba (FA-CV-10a, FA-CV-10b, FA-CV-11); (Redonda)	Holocrystalline; Inequigranular; Porphyritic	Cpx + Plag + Ol	0.1-0.5 mm	Cpx (augite) + Plag + Ol	0.5-1 mm		Apatite and opaque minerals as accessory mineral; Plagioclase phenocrysts with poikilitic texture, compositional zoning, fractures and opaque minerals inclusions	Phenocrysts: 80% Cpx, 15% Plag, 5% Ol
Arena, 2008	Ol-Plag Basalt	Sueste (FA-CV-12a, FA-CV-13)	Holocrystalline; Inequigranular; Porphyritic	Cpx + Plag + Ol + Op	0.1-0.3 mm	Ol + Plag	0.5-3 mm	Iddingsite	Fractured and zoned phenocrysts; apatite as accessory mineral	Phenocrysts: 80% Ol, 20% Plag
Fodor et al., 1989	Diabase	Santa Bárbara (T4 620 m; AB17; T3 670 m)		Plag	0.2-1 mm	Cpx + Fe-Ti oxides	2-4 mm	Biotite, chlorite, sericite	Px with irregular and jagged margins, some oxides show resorption features	27-43% Cpx, 14-11% Oxd
Fodor et al., 1989	Diabase	ESS9 (120 km from Abrolhos Archipelago)	Intergranular			Cpx + Fe-Ti oxides + Qtz	1-3 mm	Smectite; plagioclase alterations		58% Plag, 26% Cpx; 6-5% Oxd; 8% Smc, 1-5% Qtz
Cordari, 1970	Diabase	SEST-1-BA (620 m and 709 m)	Holocrystalline; Porphyritic; Ophitic	Labradorite + Mag + Ap		Augite		Alterations phases		
Cordari, 1970	Diabase	Redonda	Holocrystalline; Porphyritic	Labradorite + Augite + Mag + Bt + Ap		Labradorite + Ol				
Cordari, 1970	Diabase	Sueste	Holocrystalline; Ophitic	Labradorite + Augite + Mag + Bt + Ap + Ol		-				
Cordari, 1970	Diabase	Siriba	Holocrystalline; Subophitic	Labradorite + Augite + Mag + Ap		-				
Gomes et al., 1992	Diabase	2-SEST-1-BA	Holocrystalline (some Hypocrystalline); Hypidiomorphic; Inequigranular; Seriate; Ophitic; Subophitic; Poikilitic	Anorthite + Cpx (augite or diopside) + Ol + Op + Tit + Bt				Saussurite; prehnite; argillomaterials; biotite; amphibole; chlorite; epidote	Symplectite titanite rims in opaque minerals; spinel inclusions in the olivine; apatite as accessory mineral Mineral paragenesis of metabasalts	
Fodor et al., 1989	Cumulate	SE-1-BA (T3 573 m)	Intergranular			Cpx + Plag + Ilm	1-5 mm	Smectite and chlorite	Px altered to smectite and chlorite; plagioclase converted to albite	
Arena, 2008	Cumulate	Santa Bárbara (FA-CV-03a,b)	Hypocrystalline; Inequigranular; Porphyritic	Plag + Cpx + Op	0.1-1 mm	Cpx (augite) ± Plag	1-4 mm	Saussurite; chlorite; biotite	Cpx phenocrysts with compositional zoning and corrosion	
Fodor et al., 1989	Wehrite	BAS33 (11 m) (60 km from Abrolhos Archipelago)	Intergranular; Poikilitic; intercumulus			Cpx + Ol + Plag + Opx + Ilm + Cr-Mag	0.2-3 mm		Cpx in a poikilitic relationship with subrounded Ol	50% alteration phases; 21% Ol; 13% Cpx; 3% Plag (+ Opx); 4% Oxd